The Influence of Stress Conditions on Intracellular Dimethylsulphoniopropionate (DMSP) and Dimethylsulphide (DMS) Release in *Emiliania huxleyi*

Michelle Fernandes

A thesis submitted to the School of Environmental Sciences, at the University of East Anglia, United Kingdom, for the degree of Doctor of Philosophy

March 2012

Abstract

Blooms of *Emiliania huxleyi* are responsible for the long-term trapping of carbon in coccolith plates, which sink to the ocean floor. In addition, *E. huxleyi* contains high concentrations of dimethylsulphoniopropionate (DMSP) the precursor of dimethylsulphide (DMS). In the atmosphere, DMS enhances cloud formation influencing climate. Thus *E. huxleyi* may play a significant role on global climate and the oceanic carbon cycle. Recently, the antioxidant function of DMSP and its breakdown products has been proposed. Increases in intracellular DMSP concentration (DMSPp) under stress conditions are documented in various phytoplankton species and strains, but results are not always consistent. A study on how nitrate and phosphate limitation, UV light, solar radiation, light deprivation and herbicide-induced oxidative stress affect DMSP metabolism in *E. huxleyi* CCMP 370, 373 and 1516 was conducted. A decrease in DMSPp was seen with exposure to UV radiation in all strains and under N- and P-limitation in *E. huxleyi* 370 and 373 with no change in *E. huxleyi* 1516, whereas it increased in solar radiation and light-deprived cells in all strains. Also higher number of cells with compromised membranes (SYTOX Green staining) was noted in solar radiation and light-deprived conditions (50% in *E. huxleyi* 373, 70% in *E. huxleyi* 370 and 1516 after 72 h exposure to solar radiations, while 40%, 50% and 20% in *E. huxleyi* 370, 373 and 1516 respectively after 10 days of light-deprivation). Flow cytometry revealed two cell sub-populations in paraquat-treated cells on the basis of red fluorescence and were sorted in *E. huxleyi* 1516, but no increase in DMSPp was seen. In all stress treatments, a decrease in DMSPp culture concentrations and total DMSP with increasing dissolved DMSP and DMS concentrations was observed although cells had intact membranes. The data suggest that stress does not always result in increased DMSPp concentration in *E. huxleyi*.

Acknowledgements

Dedicated to my loving parents,

Edgar and Maria Fernandes

List of Contents

List of Figures

15

List of Tables

Chapter 1

General Introduction

Chapter 1: General Introduction

1.1 Overview

On most occasions, the oceans and other water bodies present a rather challenging environment for phytoplankton. They are exposed to stress on varying temporal and spatial scales with constant changing physico-chemical factors. The response to stress imposed on marine algae permits us to gain information on the mechanisms that organisms use to exploit environmental resources or cope with environmental stress. This thesis is a study of the influence of stress conditions on intracellular dimethylsulphoniopropionate (DMSP) and dimethylsulphide (DMS) release in *Emiliania huxleyi*.

In this chapter, I will commence with the general definitions of stress, followed by a brief account of various cellular responses to stress in phytoplankton. I will then introduce the concept of oxidative stress in the marine environment, followed by stress-induced cell death. Next is an overview of the climatic importance of DMS, biological importance of its precursor DMSP and a review on the current literature focusing on the influence of stress conditions on the physiological role of intracellular DMSP and DMS release. And finally this chapter will introduce *E. huxleyi* the species under investigation and conclude with goals and objectives of this research project.

1.2 Stress

Stress is a term commonly used but is challenging to define in biological systems. It was first introduced in physics but in 1926, Walter Cannon was the first to use it in a biological context to refer to external factors disrupting homeostasis – that is an organism's optimal condition for living (Cannon 1926). Selye continued to define stress as a state 'manifested by a specific syndrome which consists of all the non-specifically induced changes within a biological system' based on its physiological effects on mammals (Selye 1956). Modifying Selye's broad definition, Bayne (1975) defined stress

as 'a measurable alteration of a physiological (or behavioural, biogeochemical or cytological) steady state which is induced by an environmental change and which renders the individual (or the population or the community) more vulnerable to further environmental change'. In plants, Grime (1979) defined stress as 'environmental constraints, shortages and excesses in the supply of solar energy, water and mineral nutrients' and 'sub- or supra- optimal temperatures and growth inhibiting toxins'.

The definitions of stress used above, encompass a broad physical range of conditions that include climatic variables such as temperature and humidity, as well as radiation, food shortage, pollutants, pesticides and other environmental toxins. In the marine system, this would mean that all organisms are stressed most of the time because survival and reproduction would probably never achieve their maximum under the constantly changing natural conditions. Nonetheless the term 'stress' in ecology refers to circumstances where there is high mortality (or the potential for high mortality) or a drastic reduction in reproductive output because of changed environmental conditions.

Changes in the physical and biotic environmental conditions such as mixing, temperature fluctuations, light availability, varying pH and salinity, exposure to ultraviolet radiation, nutrient limitation, bacterial or viral attack, zooplankton grazing and exposure to pollutants can often affect normal processes within a phytoplankton cell (Fig. 1.1). Unless a cell can cope with the constantly altering environments to which they are exposed, extinctions will follow. But what is fascinating in the marine world is the tendency for adaptation and survival of the unicellular organisms as documented by the geological records of the long history of life on earth, so much so that for almost a century, phytoplankton were believed to exist perpetually by binary fission unless consumed by heterotrophic zooplankton or sedimentation (Walsh 1983). However, recent studies have highlighted the fact that severe environmental conditions can cause stress and stress beyond a cell's tolerance will induce cell death. For example, six-day dark stress induced chlorophyte *Dunaliella tertiolecta* underwent catastrophic cell death (Berges and Falkowski 1998). Also cell death events by lysis, independent of grazing heterotrophs were documented in field populations especially after blooms when growth

conditions became suboptimal (Agusti et al. 1998; Brussaard et al. 1995; Van Boekel et al. 1992).
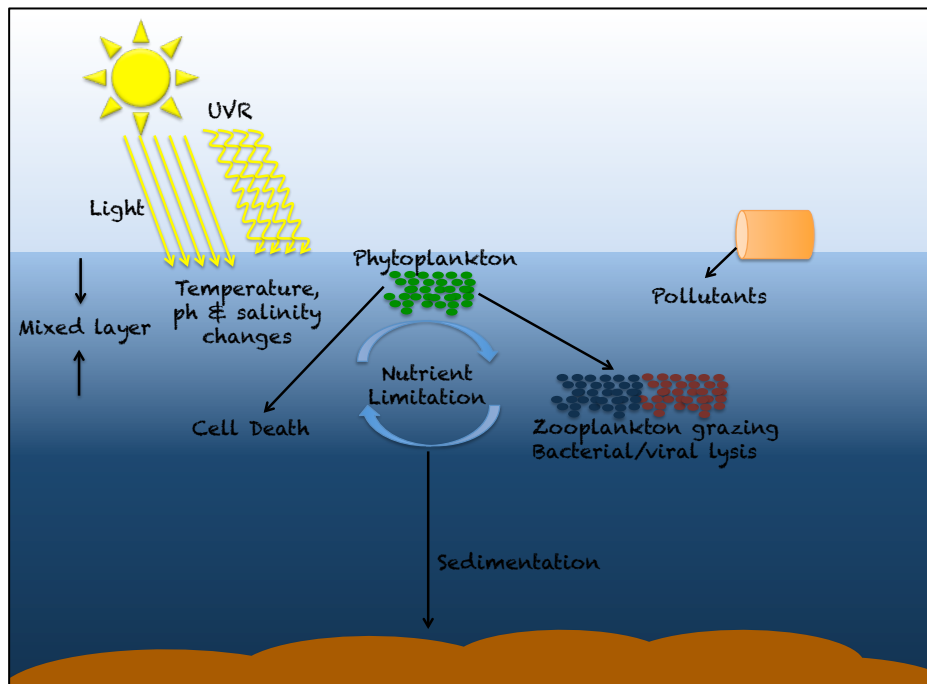
Figure 1.1 Factors affecting normal processes within a phytoplankton cell. Extreme changes in the physical and biotic environmental conditions such as mixing, temperature fluctuations, light availability, varying pH and salinity, exposure to ultraviolet radiation, nutrient limitation and exposure to pollutants can result in cell death. Zooplankton grazing, bacterial and viral attack and sedimentation are also processes by which phytoplankton cell losses occur.

1.2.1 Cellular stress responses

A cell's preliminary response to a stressful stimulus is counteracting it by the activation of survival pathways thus helping the cell to defend against and recover from the injury (Fulda et al. 2010). However, if the stressful conditions continue to persist beyond the limits of the resistance of the cell, then cells activate death-signaling pathways eventually eliminating damaged cells (Bidle and Falkowski 2004; Fulda et al. 2010). In response to environmental stress including changes in temperature, salinity, light and nutrients, phytoplankton will alter their cell physiology to cope with the change.

In the following sections, more emphasis will be given to cellular responses to light-, ultraviolet radiation (UVR-) and nutrient-induced stress, these being the kinds of stress examined in this study.

1.2.1.1 Response to temperature and salinity stress

Recent studies based on decades of satellite data show that the increasing sea surface temperatures (about 0.2°C per decade) (Doney 2006) seem to correlate with decreasing phytoplankton productivity (Behrenfeld et al. 2006; Boyce et al. 2010). These findings though arguable (Mackas 2011; McQuatters-Gollop et al. 2011; Rykaczewski and Dunne 2011) can raise specific concerns about increasing temperature-induced stress, as temperature is a very important ecological parameter that affects the phase transition of lipids, the conformation of macromolecules and the kinetics of physicochemical reactions in phytoplankton. Some of the cellular stress responses observed in marine algae to cope with varying temperature conditions are changes made to carbon allocation within the cell, particularly lipids (Kakinuma et al. 2006; Ventura et al. 2008) and an increase in fatty acid unsaturation is an accepted mechanism for low-temperature acclimation (Al-Hasan et al. 1991; Dawes et al. 1993). Furthermore, the capacity to tolerate changes in salinity is also an important factor to determine vertical and horizontal phytoplankton distributions. In response to salinity changes, a characteristic tolerance mechanism in marine algae is the maintenance of constant cell turgor by altering its osmotic potential, which is regulated by concentrations of internal inorganic ions and organic osmolytes (Kirst 1990; Liu et al. 2000).

1.2.1.2 Response to light stress

Light is one of the major limiting factors affecting phytoplankton growth due to its seasonal, diurnal fluctuations and varying intensity and spectral distribution with depth in the natural environment. Growth rate in phytoplankton increases linearly with increasing irradiances but at harmful supra-optimal levels of irradiance, growth rate and photosynthetic rate decrease. This light-induced reduction in photosynthetic capacity in phytoplankton is referred to as 'photoinhibition' and affects the photosystem II (PSII)

more than any other component of the photosynthetic apparatus, by generating harmful reactive oxygen intermediates (ROI's) (Osmond 1994). So also, in very low light conditions, cellular metabolic activity is affected due to lack of energy generated via suppressed photosynthesis (Falkowski and LaRoche 1991). Thus in both low- and high-light conditions, algal growth is limited due to effects on photosynthesis.

Microalgae have evolved over many generations with protective mechanisms and strategies to cope with varying light stress. Some of the cellular stress responses observed in microalgae to date are changes in growth rate and dark respiration rate, alteration of pigment and fatty acid content. Cells also alter cellular proteins as a strategy to cope with light-induced stress. For example, the rate of protein synthesis in the marine diatom *Phaeodactylum tricornutum* increased on exposure to low-light intensity (Bohlin) (Morris et al. 1974), while at light saturating intensities, the marine algae *Nannochloropsis sp.* reached its maximal protein content (30% of the organic content) (Fábregas et al. 2004). Light stress also results in the adjustment of the cellular lipid content (Fábregas et al. 2004; Mock and Gradinger 2000; Mock and Kroon 2002). Khotimchenko and Yakovleva (2005) suggested that variations in the lipid composition of *Tichocarpus crinitus* can be considered as one of the mechanisms of adaptation to varying incident light intensity. The degree of tolerance to different light intensities varies with algal species. For example, slight photoinhibition occurred in *Emiliania huxleyi* at extremely high intensities between 1000-1500 μmol photons $m^{-2}s^{-1}$ (Nanninga and Tyrrell 1996) in comparison with other algal species that are photoinhibited at light intensities between 500-1000 μmol photons $m^{-2}s^{-1}$.

To cope with high-light stress, it has been established that phytoplankton initiate signal transduction pathways like photoacclimation, photoprotection and photorepair (Niyogi 2009; Ragni et al. 2008) as discussed below.

Photoacclimation is a phenotypic modification in the components of the photosynthetic apparatus to varying light irradiances, which involves adjustments of the light and dark reactions to harvest and utilize light in order to optimize photosynthesis for growth changes (Falkowski and LaRoche 1991; MacIntyre et al. 2002; Moore et al. 2006). Photoacclimation to high irradiances is generally indicated by changes in the

macromolecular composition and ultrastructure of the photosynthetic apparatus (Durnford and Falkowski 1997; Falkowski and Raven 1997); for example, in the size of the PSII antenna (Suggett et al. 2007), and size and/or number of the reaction centers (Falkowski and Owens 1980) (RCs; Falkowski and Owens 1980), decrease in the photosynthetic pigment content, e.g. the chlorophyll content (Anning et al. 2000; MacIntyre et al. 2002), decrease in chlorophyll to carbon ratio (Geider et al. 1997; MacIntyre et al. 2002) and decrease in photosynthetic to non-photosynthetic pigment ratios (Leonardos and Harris 2006; MacIntyre et al. 2002).

Photoacclimation can be a short-term or a long-term survival strategy (Humby and Durnford 2006). Short-term photoacclimation (seconds to minutes) involves the dissipation of excess light energy via carotenoids in the xanthophyll cycle (Demmig-Adams and Adams 1996). Thus, state transitions of the light harvesting complex proteins in the chloroplast within the photosynthetic apparatus can aid the excitation energy distribution between photosystem I and II (PSI, PSII) (Haldrup et al. 2001; Wollman 2001). When the short-term photoacclimation responses fail to improve the damage caused by photoinhibition, the cells initiate long-term photoacclimation responses that can last from hours to days. Long-term photoacclimation involves extensive changes in enzyme activity and gene expression leading to reduction in the cell's light-harvesting capacity via alterations in the light-harvesting antenna size, concentration of photosynthetic complexes and photosystem stoichiometry (Falkowski and LaRoche 1991; Niyogi 1999; Niyogi 2009). On the whole, photoacclimation serves to sustain a constant photosynthetic efficiency in varying light conditions by regulating the competence of the cell to harvest and utilize light.

Photoadaptation in contrast to photoacclimation (which is a temporary phenotypic response to the varying light field), is a genotypic response to light at an evolutionary level to adapt to the particular photic environment (Falkowski and LaRoche 1991). Photoadaptation of phytoplankton can occur on a timescale of less than a day and is an effective permanent response against high irradiances and UVB radiation (Davidson 1998).

Photoprotection is used to describe all mechanisms that protect the cells from photodamage caused by high light irradiances. *Non-photochemical quenching* (NPQ) is a well-known photoprotective mechanism in marine photoautotrophs (Falkowski and Raven 1997) and involves dissipation of excess light energy in the form of heat. In many phytoplankton groups such as prymnesiophytes and dinoflagellates, this thermal dissipation of light energy results in the decrease in PSII activity (Gorbunov et al. 2001; Moore et al. 2006) and can operate in both light-harvesting antennae via the xanthophyll cycle (Arsalane et al. 1994; Olaizola et al. 1994) and in the reaction centers (RCs) even if they are temporarily inactivated or damaged (Gorbunov et al. 2001). Alternative electron transport pathways can also help to remove excess absorbed light energy from the photosynthetic apparatus: the *Assimilatory Linear Electron Transport pathway,* the *Oxygen-Dependent Electron Transport* and the *Cyclic Electron Transport pathway* as described below.

The *Assimilatory Linear Electron Transport pathway* involves utilization of the excess light energy absorbed by the light harvesting complexes (LHC's) in the process of photochemistry that drives linear electron transport from H_2O to NADPH, resulting in O_2 evolution and reduction of CO_2, NO_3^-, and SO_4^{-2}.

The *Oxygen-Dependent Electron Transport* involves the consumption of the excess excitation energy by the non-assimilatory electron transport to oxygen. Oxygen can function as an electron acceptor either through the oxygenase reaction catalyzed by Rubisco (photorespiration) or by direct reduction of oxygen by electrons on the photosystem I (PSI) (Mehler 1951) which has been defined by various terms including the pseudocyclic electron transport, the Mehler-ascorbate peroxidase reaction, and the water-water cycle (Asada 1999).

The *Cyclic Electron Transport pathway* involves the dissipation of excitation energy absorbed by PSII and PSI and thus plays a very important role as a photoprotection pathway (Niyogi 1999). This pathway is also responsible for the downregulation of PSII.

Photorepair of the photodamaged PSII in the photosynthetic apparatus is highly important to decide the fate of the cell and the rate of this process must match the rate of

damage to avoid photoinhibition resulting from net loss of functional PSII centres. Photorepair involves a selective degradation of damaged proteins and incorporation of the newly synthesized chloroplast-encoded proteins to rebuild an operative PSII (Aro et al. 1993).

1.2.1.3 Response to ultraviolet radiation (UVR) stress

At the sea surface, sunlight will also be contain ultraviolet radiation (UVR), which can affect bacterial activity (Buma et al. 2003; Kaiser and Herndl 1997), primary productivity (Häder 2011) and photochemical degradation of dissolved organic matter (DOM) (Mopper and Kieber 2002). UVR is also known to cause photoinhibition in phytoplankton, particularly on exposure to the UVB waveband (Balseiro et al. 2008; Garbayo et al. 2008). In contrast to high-light photoinhibition, which is caused by down-regulation of the PSII, UVB-induced photoinhibition is caused by protein damage and the recovery from UVB stress would take longer than recovery from high-light stress (Franklin and Forster 1997). UVR-stress causes DNA damage in both bacteria and phytoplankton (Häder and Sinha 2005) but photosynthetic cells have the ability to activate repair processes and synthesize UV-absorbing compounds to prevent severe damages (Boelen et al. 1999). Thus marine phytoplankton are not entirely defenceless against UVR stress.

Marine plankton are recognized to have four UVR defence mechanisms, namely avoidance, screening, quenching and repair as discussed below. All of these mechanisms are noted mainly in zooplankton (Rautio and Tartarotti 2010) and motile phytoplankton species (Davidson 1998; Gerbersdorf and Schubert 2011).

Avoidance is the mechanism by which plankton move vertically to a protected environment. This may involve changes in cell size, shape, outer covering and buoyancy. However, by this mechanism, the photosynthetic cells may experience a reduction in light exposure (Davidson 1998).

Screening involves the production of UV-absorbing compounds including mycosporin-like amino acids (MAA's), flavonoids and sheath pigments (Sinha et al. 1998). These

compounds aid to reduce intracellular UV exposure, photodamage and support normal metabolic activity; however, the synthesis of the UV-absorbing compounds would involve utilization of the cell's metabolic energy of production and maintenance (Davidson 1998).

Quenching involves the upregulation of antioxidants, radical trapping enzymes and carotenoids, which protect the intracellular organelles from the toxic effects of the reactive oxygen intermediates (ROI's). However, the mechanism of quenching involves utilization of the cell's metabolic energy of production and maintenance (Davidson 1998).

Repair processes against UVR-induced damage in phytoplankton are the last line of defence mechanisms and are of four types depending on the environment (Davidson 1998; Diffey 1991). *Photoreactivation* (PR) is one of the most important DNA repair mechanisms and is activated by exposure to UVA and photosynthetically active radiation (PAR) and is therefore light-dependent. *Excision* mechanisms (ER) (eg. nucleotide excision 'dark' repair) can be triggered for UVR-induced DNA damage (Karentz et al. 1991; Martínez et al. 2012) and these mechanisms are mainly dark-dependent. *Post-replication repair* is another mechanism sorted for cell survival, where UV-damaged DNA can replicate. *Resynthesis* (RS) is a slow mechanism and involves repairs to the UV-damaged DNA and the permanently damaged photosystems. These repair mechanisms are reported in cyanobacteria (Ehling-Schulz and Scherer 1999; Sinha and Häder 2008).

1.2.1.4 Response to nutrient stress

Phytoplankton growth is often nutrient limited in surface seawaters mainly due to lack of macronutrients particularly nitrogen and phosphorous but extensive investigations have shown that other trace nutrients can also be limiting. For example, iron is the limiting nutrient in the equatorial Pacific and Southern ocean (Boyd et al. 1999; Timmermans et al. 1998), while zinc is limiting in the central North Pacific (Bruland 1989; Morel et al. 1994).

Studies suggest that appropriate levels of nitrogen and phosphorus are fundamental for cell photosynthesis (Hu and Zhou 2010) and, in response to nutrient stress, phytoplankton are known to alter their cellular carbon forms. For example, in response to nitrogen deficiency, lipid storage is enhanced (Mutlu et al. 2011; Shifrin and Chisholm 1981) and protein content is reduced (Heraud et al. 2005; Lynn et al. 2000). Under Phosphorus starvation, the carbohydrate content in algal cells is increased and it has been suggested that increased carbohydrate:protein ratios are an indication of phosphorus deficiency (Beardall et al. 2005; Dean et al. 2008). So also, lipid content is increased under phosphorus limiting conditions (Heraud et al. 2005; Lynn et al. 2000; Sigee et al. 2007). In contrast, no significant differences in cellular carbon forms were detected in several algal species in phosphate-depleted conditions (Cade-Menun and Paytan 2010). They explained that phytoplankton in a phosphorus-limiting environment can re-adjust their internal cellular phosphorus needs and transfer the cellular phosphorus pool to maintain growth rate (Cembella et al. 1984; Ji and Sherrell 2008) until the cell runs out of its internal phosphorus content. This would then force it to elevate its rate of carbohydrate synthesis (Dean et al. 2008; Sigee et al. 2007). Under phosphorus-enriched conditions, algae have been reported to uptake and store the excess phosphorus in the form of polyphosphate (Cade-Menun and Paytan 2010; Stevenson and Stoermer 1982). Interestingly, phosphorus stress can also vary the response of algae to light and temperature stress (Gauthier and Turpin 1997; Sterner et al. 1997).

1.2.2 Oxidative stress in marine phytoplankton

In the marine environment the process of photosynthesis in plankton that takes place in the chloroplast and results in the production of oxygen, is the backbone of their existence. However, during the processes of photosynthesis and respiration, highly reactive intermediates of reduced oxygen, usually referred to as reactive oxygen intermediates (ROI's) or reactive oxygen species (ROS), are formed (Apel and Hirt 2004). They are generally toxic (Gerschman et al. 2005) and are scavenged by the various enzymatic and non-enzymatic defences of the cell (Apel and Hirt 2004; Mallick and Mohn 2000).

Molecular oxygen (O_2) in its ground state does not react with organic molecules unless the molecule is 'activated' (Cadenas 1989). However, either by energy transfer or electron transfer reactions, the ground state oxygen molecule can be activated to its reactive forms. Energy transfer would lead to the formation of singlet oxygen ($^1O_2$), while electron transfer reactions would result in successive univalent reduction of the molecular oxygen to produce a series of reactive intermediates including superoxide radicals (O_2^-), hydrogen peroxide (H_2O_2) and hydroxyl radical (HO•) and finally water (H_2O) (Fridovich 1998; Klotz 2002) (Fig. 1.2).
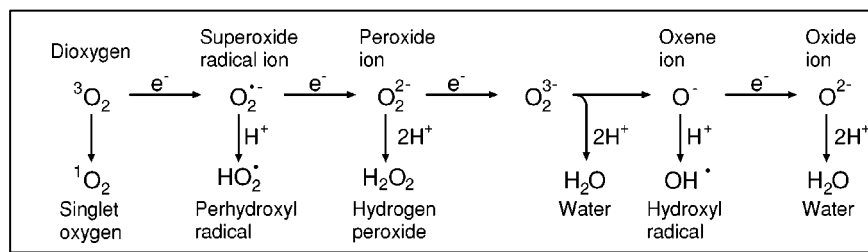
Figure 1.2 Activation of ground state triplet oxygen by energy transfer or electron transfer reactions to produce highly reactive intermediates of oxygen (ROI's) or also known as reactive oxygen species (ROS) (from Apel and Hirt (2004))

The common underlying setback encountered by marine phytoplankton is oxidative stress (Lesser 2006). This is mainly because in the marine environment phytoplankton are constantly exposed to varying environmental conditions such as high light irradiance, UV radiation, temperature fluctuation, salinity change, nutrient depletion, grazing, viral attack and toxic pollutants that would result in the excess production of ROS and accumulation beyond the cell's capacity to quench it (Latifi et al. 2009; Xue et al. 2005).

In seawater, phytoplankton and bacteria can be affected by the photochemical production of ROS, caused by the interaction between the UV radiation with dissolved organic matter (DOM) (Mopper and Kieber 2000), dissolved oxygen and trace metals (Yocis et al. 2000). Also during wet precipitation, atmospheric peroxides get deposited in surface seawater increasing the ROS abundance (Gerringa et al. 2004). These transient species readily react with cellular macromolecules, affect cell membranes and inhibit photosynthesis. In phytoplankton, singlet oxygen ($^1O_2$) is continuously produced by the photosystem II (PSII) during photosynthesis and is less stable than dioxygen ($^3O_2$;

ground state triplet molecular oxygen) and hence readily reacts with cellular macromolecules. In aqueous media, the lifetime of singlet oxygen is ~ 3.7 μs (Lesser 2006). Superoxide radicals (O_2^-) which undergo spontaneous dismutation to produce H_2O_2 and O_2, which is sometimes catalyzed by the antioxidant enzyme superoxide dismutase (SOD) (Asada and Takahashi 1987; Moffett and Zafiriou 1990) has a lifetime of 50 μs in the cell (Asada and Takahashi 1987; Cadenas 1989; Fridovich 1998; Lesser 2006) and a reported half-life in seawater ranging from seconds to minutes (Millero 2006; Zafiriou 1990). Superoxides have a significant damaging potential (Fridovich 1986) and can diffuse across membranes at a very slow rate (Asada and Takahashi 1987; Cadenas 1989; Fridovich 1998; Halliwell and Gutteridge 1999; Lesser 2006). Hydrogen peroxide (H_2O_2) an uncharged molecule, is a more stable ROS with a half-life ranging from hours to days (Petasne and Zika 1997; Yuan and Shiller 2001; Yuan and Shiller 2005) and readily diffuses across biological membranes. H_2O_2 damages various cellular constituents like DNA and enzymes involved in carbon fixation and is also an important signaling molecule in programmed cell death (Halliwell and Gutteridge 1999). Further reduction of H_2O_2 results in the much more destructive hydroxyl radical ($HO^\bullet$) with a lifetime of 10^{-7} s (Lesser 2006) that can initiate a damaging chain reaction of lipid peroxidation in the unsaturated lipids within cell membranes and causes denaturation of proteins and nucleic acids.

Phytoplankton are known to have an effective protection against the harmful effects of ROS in the form of antioxidant defence systems classified as *scavenging enzymes* and *antioxidant molecules*. The scavenging enzymes include *superoxide dismutase* (SOD), which occurs as a metalloprotein and is found as Cu-, Zn- or Fe- SOD in unicellular eukaryotic algae especially dinoflagellates (Dufernez et al. 2008; Lesser and Shick 1989; Okamoto et al. 2001). Another scavenging enzyme is *catalase*, which is a heme-containing group involved in the catalytic conversion of hydrogen peroxide to water and oxygen. *Peroxidases* are also like catalases that catalyze the reduction of hydrogen peroxide to water and are of two kinds: Ascorbate peroxidase (APX) and Glutathione peroxidase. The major non-enzymatic antioxidant molecules are *Ascorbate*, *Glutathione*, *Tocopherol* and *Carotenoids*. The soluble antioxidant ascorbate has been measured in marine microalgae like the diatoms, prymnesiophytes, prasionophytes, chlorophytes and

in other species (Brown and Miller 1992). It scavenges not only hydrogen peroxide, but also singlet oxygen, superoxide and hydroxyl radicals, and lipid hydroperoxides without enzyme catalysts. Glutathione (GSH) is another soluble antioxidant involved in the rapid quenching of singlet oxygen, superoxide and hydroxyl radicals and is known to be produced in marine phytoplankton in response to stress (Dupont et al. 2004; Kawakami et al. 2006). Tocopherol can quench singlet oxygen, superoxide and hydroxyl radicals and occurs as α-tocopherol in phytoplankton (Durmaz 2007). Phytoplankton also contain carotenoids, as an accessory pigment in photosynthesis for light-harvesting, but these lipid-soluble molecules can also act as ROS scavengers when the photosynthetic apparatus is stressed by high photon flux density. In the event of photoprotection, carotenoids are known to dissipate the excess excitation energy via the xanthophyll cycle (Demmig-Adams and Adams 1996).

Besides the damaging effects on cellular components and macromolecules caused by the enhanced production of ROS during stress, there are growing indications that the antioxidant systems of the cell regulate intracellular levels of ROS. Thus, they play an important role as signaling molecules for the activation of stress-response and defence pathways (Apel and Hirt 2004; D'Autreaux and Toledano 2007; De Pinto et al. 2006; Foyer and Noctor 2003; Foyer and Noctor 2005; Torres et al. 2006). Furthermore, there is growing evidence that phytoplankton cells can undergo programmed cell death (PCD) in response to environmental stress (Berman-Frank et al. 2007; Bidle and Bender 2008; Bidle and Falkowski 2004; Bidle et al. 2007; Franklin et al. 2006; Jiménez et al. 2009; Okamoto and Hastings 2003; Segovia et al. 2003; Zuppini et al. 2007). This has therefore meant a large significance for the involvement of oxidative stress in the induction of PCD. Reports of oxidative stress-driven cell death were documented in the cyanobacterium *Microcystis aeruginosa* with a simultaneous increase of a toxic discharge of hydrogen peroxide into the media when stressed (Ross et al. 2006) and in an abrupt bloom-termination of *Peridinium gatunense* mediated by CO_2 limitation (Vardi et al. 1999). There is evidence that oxidative stress-driven cell death occurs despite the upregulation of antioxidants in the algal cells of *Chlamydomonas reinhardtii* and *Peridinium gatunense* (Butow et al. 1997; Murik and Kaplan 2009) suggesting the influence of oxidative stress in programmed cell death in marine phytoplankton.

1.2.3 Stress-induced cell death

Stress beyond a cell's tolerance can induce molecules and processes that function in normal cell signaling and survival responses, to play a dual role in inducing cell death. This has been documented in oxidative stress-induced cell death with cells possessing high antioxidant activity but not in cells with low antioxidant activity (Murik and Kaplan 2009). Cell death was also augmented in cells possessing low antioxidant activity with the addition of the antioxidant dehydroascorbate, a product of ascorbate peroxidase (APX), but not by the addition of other antioxidant molecules like ascorbate or reduced glutathione (Murik and Kaplan 2009), suggesting the influence of the antioxidant molecule of APX in triggering the cell death pathway in phytoplankton.

For a long time, cell death mechanisms were not established in phytoplankton as compared with other organisms like bacteria, protozoa, fungi, plants and animals. However, studies of algal bloom dynamics to identify the mechanisms controlling the abrupt termination of natural blooms led to the identification of mass cell lysis, a kind of loss process besides grazing and sedimentation (Agusti et al. 1998; Brussaard et al. 1995). Cell lysis is a process of phytoplankton mortality and is determined by the dissolved esterase method. Cell lysis results in the rupture of the cell membrane with subsequent discharge of the cell contents into the surrounding medium. This represents a significant source of nutrient rich dissolved organic compounds in the water column, loss of the primary production that is directly available to herbivores and reduction in the total possible particulate sinking flux. Reports show that enhanced cell lysis results from two major factors, which include parasitic attack by viruses (Bidle and Falkowski 2004; Brussaard 2004; Suttle 2005) and bacteria (Imai et al. 1993; Ohki 1999) and environmental stress like light deprivation (Berges and Falkowski 1998; Segovia and Berges 2009; Segovia et al. 2003), high light stress (Berman-Frank et al. 2004), UV exposure (Moharikar et al. 2006), high temperature (Zuppini et al. 2007), high salinity (Affenzeller et al. 2009), nutrient limitation (Bidle and Bender 2008) and CO_2 limitation (Vardi et al. 1999).

Intensive research on the factors inducing phytoplankton cell lysis led to the discovery of the autocatalytic cell death pathway. Analogous to programmed cell death (PCD) in multicellular organisms, the autocatalytic cell death pathway is a cellular self-destruction mechanism (autolysis) and is independent of viral attacks. The term *programmed cell death* (PCD) refers to a genetically controlled or regulated form of cell death and is linked with a series of biochemical and morphological changes (Bidle and Falkowski 2004). Apoptosis (Moharikar et al. 2006), paraptosis (Franklin and Berges 2004; Sperandio et al. 2000) and autophagy (Berg et al. 2005) are essentially programmed forms of cell death, while necrosis is a mode of cell death that does not involve gene expression and occurs when the cell cannot adapt to the changing environment. PCD involves a biochemical stimulation of a specialized cellular machinery which consists of receptors, adapters, signal-kinases, proteases and nuclear factors (Aravind et al. 2001). A PCD response is induced by environmental stress associated with enhanced oxidative stress. Evidence for PCD-like cell death or the autocatalytic cell death pathway in phytoplankton was found in the aging cultures of the cyanobacterium *Trichodesmium* sp. exposed to high irradiance, combined phosphorus and iron depletion (Berman-Frank et al. 2004), in the dinoflagellate *Peridinium gatunense* under CO_2 limitation (Vardi et al. 1999), in light deprived unicellular chlorophyte *Dunaliella tertiolecta* (Segovia et al. 2003) and in nutrient-limited diatoms *Ditylum brightwellii* (Brussaard et al. 1997) and *Thalassiosira weissflogii* (Berges and Falkowski 1998).

In multicellular eukaryotes, PCD is mediated by a group of protein-splitting enzymes of a specific class of proteases, called caspases (**c**ysteinyl **asp**artate-specific prote**ases**) that do not exist in prokaryotes and unicellular eukaryotes. However, an increase in caspase-like activity and expression of caspase-like enzymes were reported in stressed cyanobacteria and microalgae (Lane 2008; Segovia et al. 2003). Genome sequencing has revealed two families of caspase-like proteins – paracaspases and metacaspases that mediate PCD (Tsiatsiani et al. 2011; Uren et al. 2000). Of the two caspase orthologues, metacaspases, though characterized *in silico* are found in prokaryotic and eukaryotic phytoplankton genomes (Bidle and Falkowski 2004). A number of metacaspase orthologues providing evidence for caspase-like activity (Bozhkov et al. 2010; Carmona-Gutierrez et al. 2010; Enoksson and Salvesen 2010; Vercammen et al. 2007) are reported

in the model phytoplankton such as the unicellular chlorophyte *Chlamydomonas reinhardtii* (Murik and Kaplan 2009) and other marine species like the diatom *Thalassiosira pseudonana* (Bidle and Bender 2008) and the unicellular coccolithophore *Emiliania huxleyi* (Bidle and Falkowski 2004; Bidle et al. 2007).

The process of PCD usually expected in metazoans, may have developed in phytoplankton cells as a strategy to eliminate specific stress-induced damaged cells (Bidle and Falkowski 2004). As a result of PCD, organic matter and cellular nutrients released into the water, are available to the surviving cells, thereby benefitting the phytoplankton population by increasing the chances of survival of the healthier cells under nutrient stress (Bidle and Falkowski 2004). PCD is also thought to play a role in the defence against viral infection of clonal populations (Georgiou et al. 1998) and in regulating cellular differentiation (Bidle and Falkowski 2004).

1.3 Overview of the importance of DMS and DMSP

In the following sections, this chapter will introduce a climatically and biologically significant sulphur compound and focus on the influence of stress conditions on its physiological role and release in marine phytoplankton.

1.3.1 Role of DMS in the global sulphur cycle

Dimethylsulphide (DMS) is a gas mainly produced in the ocean surface layers by marine phytoplankton. It was first revealed to be produced by marine algae by Challenger (1951) and based on his findings, the first measurements of DMS in a cruise over the Atlantic and the discovery of its abundance in surface ocean waters was the pioneering work of Lovelock (1972). At that time, studies of the global sulphur cycle consistently suggested that in order to achieve the sulphur balance there must be a substantial flux of volatile sulphur from the oceans into the atmosphere. The earlier sulphur budgets attributed this flux to hydrogen sulphide (H_2S) from coastal areas. But later, it became clearer that H_2S was highly reactive to oxygen and so with the discovery and measurements of DMS in the ocean and atmosphere, it was then accepted that most of

the flux of sulphur was from DMS with a small contribution from carbonyl sulphide (COS) that was formed photochemically in seawater (Ferek and Andreae 1984). Subsequent measurements of DMS were made throughout the Pacific (Andreae and Raemdonck 1983; Barnard et al. 1984; Bates and Quinn 1997; Cline and Bates 1983; Marandino et al. 2009; Turner et al. 1988), the Atlantic (Iverson et al. 1989; Marandino et al. 2008; Turner et al. 1988) and the Southern Oceans (Yang et al. 2011). Estimates of global sulphur emissions to the atmosphere in the late 90's showed that out of the total 100 Tg S yr^{-1}, 65.6 Tg S yr^{-1} were of anthropogenic origin, 13.7 Tg S yr^{-1} originated from volcanoes, 18.2 Tg S yr^{-1} from DMS, while only 2.5 Tg S yr^{-1} was from biomass burning (Graf et al. 1997). Recently estimated DMS emissions from the ocean to the atmosphere reveals a higher input of ~ 28 Tg S yr^{-1} (Lana et al. 2011a). Thus in todays world, the sulphur compound DMS accounts for ~ 50% of the total natural sulphur flux to the atmosphere, confirming a significant role of DMS in the global sulphur cycle (Fig. 1.3).
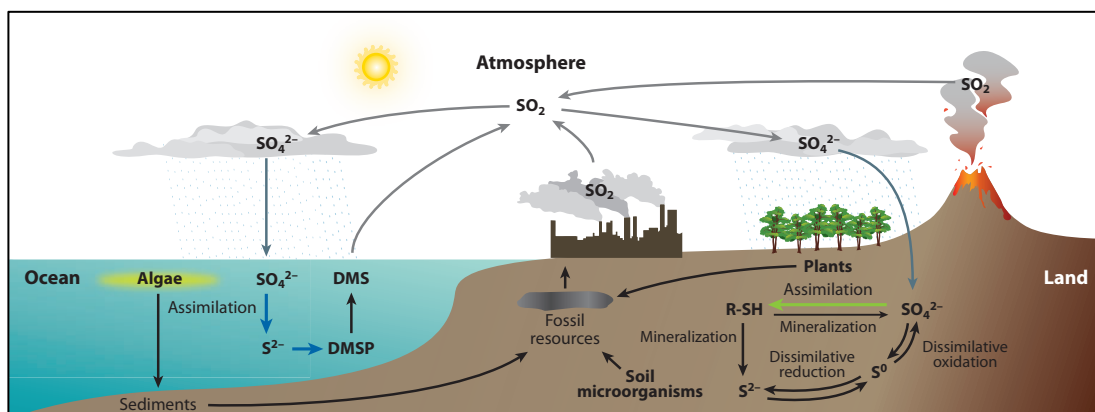
Figure 1.3 Biogeochemical Sulphur cycle with oceanic DMS playing a significant role. Volatile compounds of Sulphur are released to the atmosphere from natural sources such as volcanoes and oceans and via anthropogenic activity. In the atmosphere, the volatile sulphur compounds are oxidized to sulphur dioxide, which are subsequently rained out (wet deposition) or fall back (dry deposition) to the earth's surface. Plants assimilate sulphur in various forms from the soil (green arrow on land) and when they die or are consumed by animals, these organic compounds are returned to land or water where they are then dissimilated by soil microorganisms that mineralize S-compounds to sulphate. In the ocean, sulphur assimilation occurs in algae (blue arrows in the ocean) that release sulphur in the form of DMS, which is fluxed into the atmosphere (Takahashi et al. 2011).

1.3.2 Role of DMS in the radiation balance of the earth

DMS is usually found at several orders of magnitude higher concentration in the ocean than in the atmosphere (Andreae 1990). This concentration gradient causes it to escape into the atmosphere (Andreae 1990). Once there, DMS has a short life span of about one day (Kloster 2006) as DMS is oxidised by hydroxide and nitrate radicals to yield acidic species such as sulphur dioxide, sulphuric acid and methane sulphonic acid (MSA) (Plane 1989). In this way, DMS influences the pH of aerosols and rainwater, especially in remote open oceans like the Southern ocean and the polar seas (Charlson and Rodhe 1982). In the atmosphere, these oxidation products of DMS exist as tiny submicron size particles called aerosols, which reflect back the incoming solar radiation. They also act as cloud condensation nuclei (CCN) and are responsible for cloud formation. This process enhances albedo and increases rainfall. Thus DMS not only plays a role in the biogeochemical sulphur cycle but also plays an important role in the radiation balance of the earth (Fig. 1.4 A). However, recently it is suggested that there are many potential aerosol-cloud-rainfall interactions but many are non-linear. This means that an increase in particle number can lead to a different effect on rainfall if the increase occurs under high or low pre-existing particle loading. This is sometimes called the cloud lifetime indirect aerosol effect. This would therefore imply that if oxidation of DMS to produce CCN results in a larger number of smaller particles, then there could be some evidence that DMS produces less rainfall (Denman et al. 2007; Stevens and Feingold 2009). So also, DMS may play another contrasting role in the atmosphere in the form of a hypothetical 'halogen activation' autocatalytic cycle. Sulphuric acid derived from DMS oxidation in the atmosphere might catalase the release of highly reactive halogens (like Br and Cl) from sea salt particles into the air and destroy the ozone (Ayers and Gillett 2000; Vogt et al. 1996).
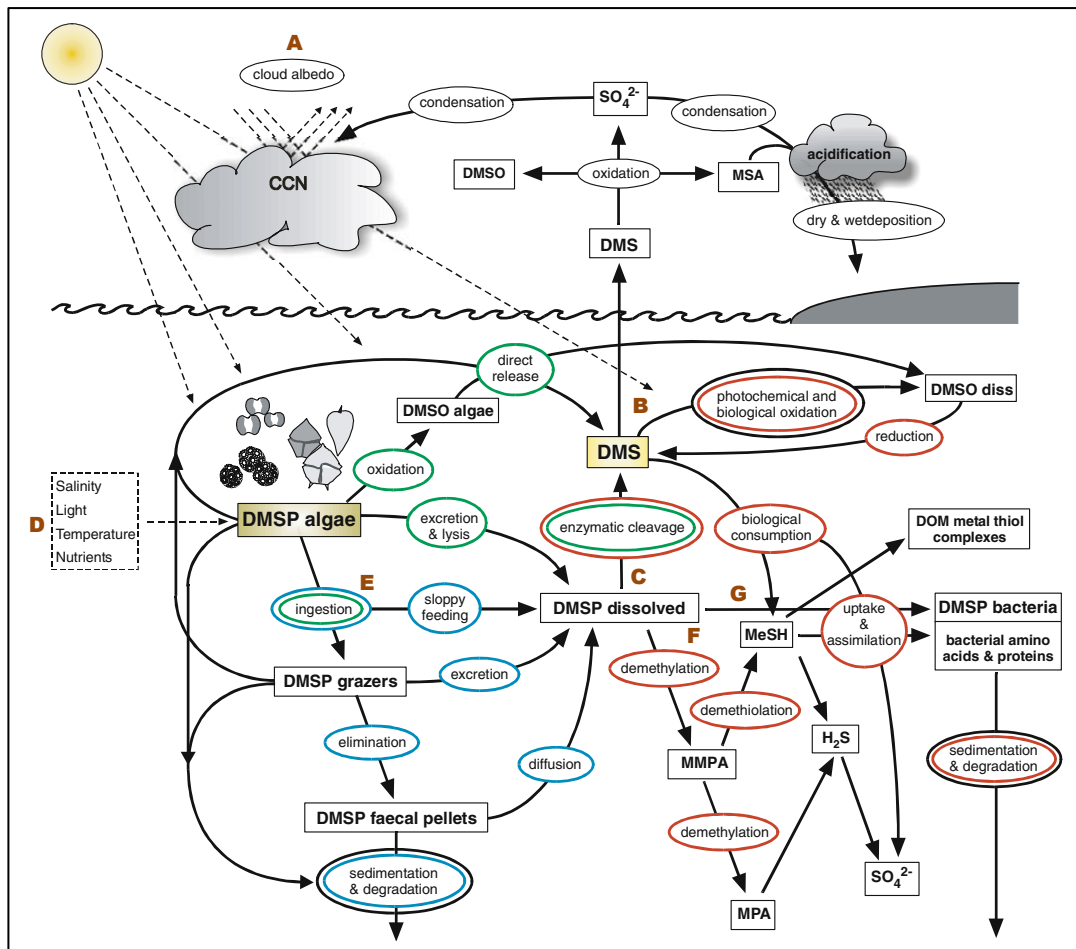
Figure 1.4 Fate of oceanic DMSP and DMS controlled by biotic and abiotic factors indicated by the coloured ellipses; red-bacteria, green-phytoplankton, blue-zooplankton and black-abiotic. (A) DMS plays an important role in the radiation balance of the earth. (B) DMS from the surface seawaters, escapes into the atmosphere and in the seawater it undergoes bacterial and abiotic degradation to produce dimethyl sulphoxide (DMSO) and other molecules. (C) Dissolved DMSP in seawater is available for DMSP lyase activity by bacteria and phytoplankton, which results in the cleavage of DMSP to DMS and acrylic acid. (D) Environmental factors such as salinity, light, temperature and nutrients influence the amount of DMSP produced by phytoplankton, at the species level. (E) DMSP released into seawater under grazing pressure. (F) Bacterial activity on dissolved DMSP to produce methylmercaptopropionate (MMPA), mercaptopropionate (MPA) and methanethiol (MeSH). (G) Bacterial assimilation of dissolved DMSP, leading to no formation of DMS (Diagram modified from Stefels et al. (2007)).

1.3.3 Climatic importance of DMS

In the 1970's, James Lovelock put forward a thought-provoking hypothesis, known as the 'Gaia Hypothesis' suggesting that life moderated the planet by the fact that the whole process between the biotic and abiotic systems, could create a 'Self-Regulating Global Thermostat' (Lovelock 1979; Lovelock 1972; Lovelock and Margulis 1974). Since then, a mechanism was proposed to imply that the natural sulphur cycle altered global climate (Shaw 1983). Using Lovelock's hypothesis and Shaw's idea of the sulphur cycle, a paper was published in Nature by Charlson, Lovelock, Andreae and Warren which until now remains the cornerstone for all research in this area and is known as the CLAW hypothesis (acronym taken from the authors names) (Charlson et al. 1987). The CLAW hypothesis states that an increase in sea surface temperature by the penetration of sunlight through the earths atmosphere thus increasing the light penetration within the water column would lead to an increase in overall primary productivity, resulting in an increase in DMS production. This in turn would increase the flux of DMS across the sea surface and so raise the number of cloud condensation nuclei (CCN) in the atmosphere. The resulting enhanced cloudiness would tend to cool the atmosphere, countering the warming effects, and thus, DMS would work in reverse of the greenhouse gases (Fig. 1.5).
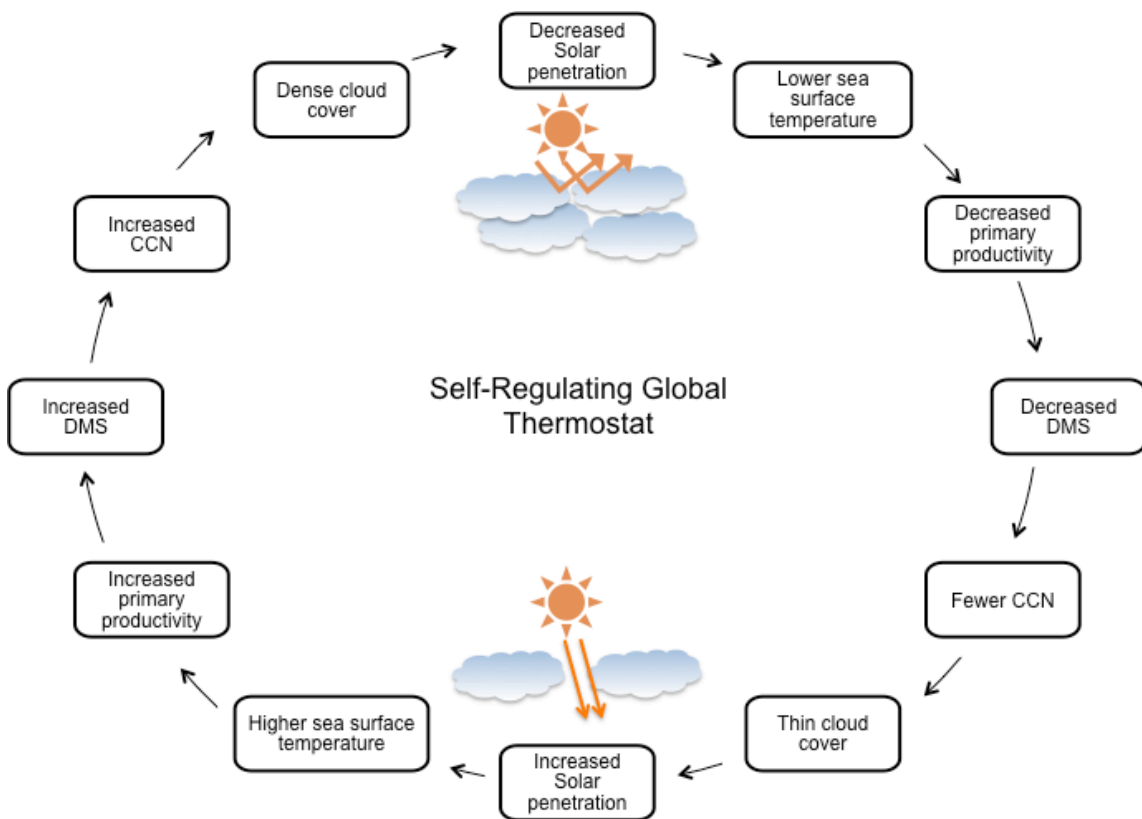
Figure 1.5 Lovelock's 'Self-regulating Global thermostat' based on the Gaia hypothesis suggesting that life moderated the planet.

1.3.4 Challenges facing the CLAW hypothesis

The ocean surface layer influences climate through the exchange of greenhouse gases such as carbon dioxide and water vapour (Kiene et al. 1999). These gases absorb the outgoing longwave radiation and keep the average surface temperature of the earth ~ 15°C. If not for these gases, the surface temperature of the earth would be -19°C (Halmann and Steinberg 1999). But, with the onset of industrialization and intense anthropogenic activities, there have been overwhelming emissions of the greenhouse gases leading to 'Global Warming'; in effect the earth has already warmed by 0.75°C since 1900. It would be ground-breaking research to arrive at any conclusion pointing to the fact that DMS from the ocean is regulating the warming effect of the greenhouse gases. At present, intense research is ongoing to explore the climatic importance of DMS before coining DMS with the term of 'the anti-greenhouse gas'. But the challenges

involved in estimating DMS flux to the atmosphere, intricacy of the interconnected processes involved in the climatic feedback mechanisms, the complications created as a result of increasing anthropogenic activity and the increasing significance of the non-DMS sources of CCN in the marine boundary layer (Ayers and Cainey 2007; Quinn and Bates 2011) have delayed confirmation or denial of the simplistic CLAW hypothesis. Indeed the CLAW hypothesis has spun interdisciplinary research for decades improving our understanding of the link between ocean-derived CCN and cloud formation and that algae have an important role in the climate system. But at some point, unless we fully understand the complex biogeochemistry and cloud physics with global climate change affecting the marine environment, we would be unable to understand the relevance or correctness of the CLAW hypothesis (as originally stated or modified).

1.3.5 Global distribution of DMS

Several attempts have been made to study the global distribution of DMS in seawater and the biogeochemical processes that control its concentration and emission to the atmosphere (Cline and Bates 1983; Gibson et al. 1990; Iverson et al. 1989; Kiene 1992; Putaud and Nguyen 1996; Turner et al. 1989; Wakeham et al. 1987). DMS concentrations are found to be highly variable on a regional and seasonal basis (Bates et al. 1987; Cooper and Matrai 1989). Open ocean surface seawater DMS concentrations generally range from 0.5 to 5.0 nM and are lowest during the winter months in high latitudes (Bates et al. 1987). In general, upwelling regions appear to have the highest mean DMS concentration, coastal and continental waters intermediate levels and the oligotrophic ocean waters the lowest (Andreae 1990; Andreae and Barnard 1984; Holligan et al. 1987; Simó et al. 1997; Turner et al. 1996; Watanabe et al. 1995).

Although DMS in seawater is believed to be produced mainly by marine phytoplankton (Andreae 1986; Barnard et al. 1984; Baumann et al. 1994; Holligan et al. 1987; Keller et al. 1989), some studies suggest that DMS can also be produced in sediments from the degradation of detritus settled on the bottom sediment (Andreae 1985). The concentration of DMS in seawater is the net result of the interplay of production and consumption processes. After production in seawater, the lifetime of DMS in surface

waters is of the order of one day (Kiene and Bates 1990) as it is degraded both microbially (Suylen et al. 1986; Taylor and Kiene 1989) and photochemically to dimethyl sulphoxide (DMSO) (Brimblecombe and Shooter 1986; Brugger et al. 1998; Kieber et al. 1996) and is lost to the atmosphere via air-sea exchange (Kieber et al. 1996) (Fig. 1.4 B).

Attempts are ongoing to establish global relations between chlorophyll *a* and DMS so as to facilitate mapping of DMS through satellite imagery (Kettle et al. 1999; Lana et al. 2011a; Lana et al. 2011b; Liss et al. 1993). This has gained momentum since many studies have found correlations between DMS and chlorophyll *a* concentration (Andreae and Barnard 1984; Liss et al. 1994; Malin et al. 1994; Malin et al. 1993; McTaggart and Burton 1993; Turner et al. 1989; Turner et al. 1988; Vallina et al. 2008). On the other hand, other studies show no such correlations on larger regional scales (Andreae and Barnard 1984; Holligan et al. 1987; Watanabe et al. 1995).

1.3.6 Dimethylsulphoniopropionate (DMSP) the precursor of DMS

Prior to the work of Lovelock (1972), Haas (1935) reported methyl sulphide emissions from the seaweed *Polysiphonia fastigiata*. Subsequently, dimethylsulphoniopropionate (DMSP), the precursor of DMS was isolated from this species (Challenger and Simpson 1948) and Greene (1962) demonstrated the biosynthesis of DMSP from its precursor methionine. The occurrence of DMSP in marine phytoplankton was documented by Ackman et al. (1966). DMS is produced by the enzymatic cleavage of DMSP (Cantoni and Anderson 1956), producing equimolar amounts of DMS and acrylic acid (Greene 1962) (Equation 1; Fig. 1.4 C).

$$(H_3C)_2 S^+ - CH_2 - CH_2 - COO^- \text{ (aq)} \rightarrow (CH_3)_2S \text{ (g)} + CH_2 = CH - COOH \text{ (aq)}$$

$$\text{DMSP} \qquad\qquad \text{DMS} \qquad \text{Acrylic acid}$$
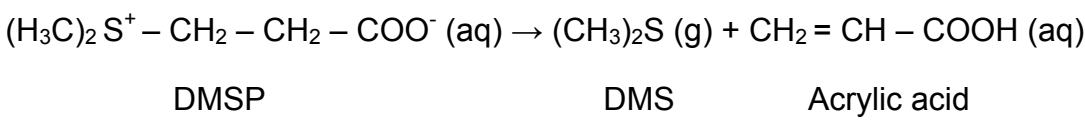
Equation 1 Cleavage reaction of DMSP producing equimolar amounts of DMS and acrylic acid.

Acrylic acid is known for its anti-bacterial properties, which protects the cell against bacterial attack (Sieburth 1960) especially during grazing (Van Alstyne et al. 2001). This grazer deterrent mechanism of acrylic acid was based on several studies highlighting the dominance of the DMSP producer *Phaeocystis* species during bloom conditions (Estep et al. 1990; Wolfe et al. 1997).

1.3.7 Species-specific occurrence of DMSP

DMSP concentration within phytoplankton cells is observed to be extremely species specific (Keller et al. 1989) and heterotrophs are also known to contain DMSP. In addition, environmental factors such as salinity, temperature, physical disturbances, tidal exposure and nutrients may also influence the amount of DMSP produced by phytoplankton, even at the species level (Andreae and Barnard 1984; Leck et al. 1990; Turner et al. 1989; Watanabe et al. 1995) (Fig. 1.4 D). So far, studies have revealed the importance of certain phytoplankton groups as major contributors to DMS and its precursor DMSP. According to Keller, the major phytoplankton groups producing DMS and DMSP is in the following order:

Prymnesiophytes > Prasinophytes > Pelagophytes (ex chrysophytes) > Chlorophytes

Barnard et al. (1984) carried out DMS measurements in the South Eastern Bering Sea and have attributed the high DMS concentrations to the abundances of the prymnesiophyte *Phaeocystis pouchetti* rather than with total chlorophyll concentration or primary production during the diatom-dominated spring phytoplankton bloom. The analyses of phytoplankton species composition in nearshore waters around mainland Britain in summer indicated the coccolithophores (in particular *Cyclococcolithus leptoporus*), various dinoflagellates including the bloom species *Gyrodinium aureolum* and certain unidentified taxa of small flagellates (Turner et al. 1988) as the main sources of DMS. In another study on the monsoon-driven tropical estuarine waters of Zuari (Goa), a mixed bloom of diatoms and dinoflagellates were found to be the chief producers of DMSP and DMS (Shenoy and Patil 2003).

Charlson et al. (1987) previously recognized that there is no direct relationship between the abundance of phytoplankton and the concentration of DMS. The concentration of DMS in the water, which largely determines the flux of DMS to the atmosphere, is a complex function of production and consumption processes. The antagonism between DMSP production, consumption and DMS volatilization depends on the environmental conditions and thereby determines the net flux of DMS to the atmosphere.

1.4 Physiological roles of DMSP in response to cell stress

1.4.1 DMSP as a compatible solute

The physiological function of DMSP in phytoplankton is receiving considerable attention in order to try to understand the biological importance of DMS and DMSP. DMSP production involves successive S-methylation, deamination and decarboxylation (Andreae 1986) in algae containing methionine (Andreae 1990) and it is found in a variety of marine phytoplankton as an osmolyte (Keller 1988) and as a cryoprotectant (anti-freeze) in ice algae (Karsten et al. 1992; Kirst et al. 1991; Nishiguchi and Somero 1992; Vairavamurthy et al. 1985). Algae accumulate compatible solutes to regulate osmotic balance. Glycine betaine (GBT) acts as part of the group of osmolytes (like the photosynthetic products-sugars, polyols and hetrosides) maintaining osmotic balance and turgor pressure (difference between the cellular and external hydrostatic pressures) within cells. DMSP being a tertiary sulfonium analogue of the quaternary ammonium compound GBT provides evidence to suggest that DMSP may also help to maintain intracellular isotonic or hypertonic conditions (Stefels 2000; Welsh 2000). Phytoplankton intracellular DMSP concentration increases with high salinity conditions (Dickson and Kirst 1987; Vairavamurthy et al. 1985), although this may not always be the case (Colmer et al. 1996; Otte and Morris 1994; Van Diggelen et al. 1986). Interestingly, it is observed that when there is a sudden drop in salinity, DMSP can be released from the cell as a response to stress (Niki et al. 2007).

1.4.2 DMSP as a carbon source for bacteria

Phytoplankton cells release DMSP under conditions of grazing pressure (Fig. 1.4 E) (Belviso et al. 1990; Dacey and Wakeham 1986; Leck et al. 1990; Morales et al. 1991), viral infection (Bratbak et al. 1995; Malin et al. 1992), leakage from ageing cells (Turner et al. 1988), bacterial activity (Ledyard and Dacey 1994; Ledyard et al. 1993) and during senescence (Leck et al. 1990; Nguyen et al. 1988) increasing the amount of dissolved DMSP in the water and making it available for DMSP-lyase activity. However, DMSP concentrations in seawater are usually found to be low 1–50 nM (Kiene and Slezak 2006), but its turnover is rapid ranging from 1–129 nMd^{-1} (Kettle et al. 1999; Kiene and Linn 2000; Turner et al. 1988). The chemical half-life of DMSP at the pH of seawater is about 8 years (Dacey and Blough 1987) but its conversion to DMS is not the only fate of DMSP in seawater. Recent works suggest that a large fraction of DMSP is demeythylated and demethiolated by bacterioplankton to produce methanethiol which is then used for methionine and eventually protein synthesis (Kiene 1996) (Fig. 1.4 F). Simo and Pedros-Alio (1999) have reported two major pathways of DMSP degradation. The first one leads to DMS production and is carried out by both algal and bacterial enzymes (DMSP cleavage) and the second one in which bacteria play a major role and utilize DMSP (DMSP assimilation) for other purposes, does not result in DMS formation (Fig. 1.4 G). Bacteria are important DMSP and DMS degraders (Matrai and Keller 1994).

1.4.3 DMSP as an anti-grazing compound and infochemical

DMSP and its cleavage products DMS and acrylic acid have been proposed to act as chemical deterrents to grazing. Dacey and Wakeham (1986) were the first to report that grazing on phytoplankton enhanced DMS concentration. Further, increased release rates of DMS and DMSP were observed when the ciliate microzooplankton *Strombidium sulcatum* grazed on the prymnesiophyte *Isochrysis galbana* (Christaki et al. 1996). A laboratory study involving the ingestion of *Emiliania huxleyi* by the heterotrophic dinoflagellate *Oxyrrhis marina* resulted in the rapid cleavage of DMSP to DMS and presumably also acrylic acid (Wolfe and Steinke 1996). Acrylic acid is suggested to act

as a toxin (Wolfe and Steinke 1996) and is shown to reduce bacterial production (Slezak et al. 1994). It was further observed that the microzooplankton grazers preferred *E. huxleyi* strains with lower DMSP lyase activity compared to strains with higher activity (Wolfe and Steinke 1996; Wolfe et al. 1997).

Strom et al. (2003) showed that DMSP reduced grazing rates on phytoplankton and Strom and Wolfe (2001) suggested that DMSP may serve as a warning infochemical to grazers within the phycosphere, permitting them to identify harmful acrylate-producing phytoplankton and reject them. Steinke et al. (2002) suggested that DMSP acts as an infochemical in a tritrophic interaction, whereby under microzooplankton grazing pressure, phytoplankton release DMSP signaling the mesozooplankton of its prey location thereby decreasing the grazing pressure on the phytoplankton. At higher trophic levels, the DMS generated from grazing can influence the migration pattern of zooplankton and thus help predators such as seabirds and marine mammals to easily locate zooplankton-rich areas (Bonadonna et al. 2006; Nevitt 2008; Nevitt and Bonadonna 2005; Nevitt and Haberman 2003; Nevitt et al. 1995).

1.4.4 DMSP as an overflow mechanism

It has been suggested that the production of DMSP and glycine betaine (GBT) are related to nitrogen availability (Andreae 1986). In nitrogen replete conditions, GBT is produced, while under nitrogen deplete conditions DMSP is produced, due to its lower nitrogen requirement. DMSP has been observed to increase in nitrogen depleted cells of the coccolithophore *Emiliania huxleyi* (Turner et al. 1988), the diatom *Thalassiosira pseudonana* (Bucciarelli and Sunda 2003) and *Tetraselmis subcordiformis* (Gröne and Kirst 1992), in addition to other phytoplankton species (Keller and Bellows 1996). However, there are studies suggesting a down-regulation of cellular DMSP under nitrogen limiting conditions in batch and continuous cultures (Keller et al. 1999a; Keller et al. 1999b). The results from the batch and continuous culture experiments also did not show a reciprocal relationship between GBT and DMSP production, although coupling of GBT production and nitrogen availability was observed. Simó (2001) proposed that various phytoplankton species evolve to produce DMSP according to the N-availability

such that short-term fluctuations of nitrogen would have a much less effect on DMSP and GBT production. So those phytoplanktons like the diatoms, evolved to inhabit nitrogen replete environments which would favour GBT production and would end up being low DMSP producers, while those that thrive under nitrogen limitation would produce more DMSP, for example the haptophytes and small dinoflagellates which are high DMSP producers.

Stefels (2000) proposed an alternative theory for increased DMSP production under nitrogen depleted conditions, suggesting that DMSP represents an overflow mechanism for excess reduced sulphur and perhaps carbon and also a way of dissipating surplus energy under unbalanced growth conditions. Nitrogen depletion would result in an unbalanced cell growth due to the increase in the ratio of S:N within the cell, thereby increasing the cellular concentrations of cysteine and methionine. Conversion of these excess sulphur compounds into DMSP would provide an explanation for the upregulation of DMSP in the cell and excretion of DMSP into the surrounding medium would thus help maintain cellular balance (Stefels 2000). Furthermore, it was suggested that the DMSP overflow mechanism could be involved in protein turnover mechanisms and amino acid reallocation as an adaptation to stress (Stefels 2000). Earlier, it was pointed out that methionine availability controls DMSP production (Gröne and Kirst 1992) and the transamination pathway leads to the production of DMSP from methionine, which is beneficial to a cell in nitrogen depleted conditions (Gage et al. 1997). Nitrogen deficient cells would breakdown existing proteins with proteases to redistribute nitrogen to other amino acids, thereby increasing the methionine concentration and subsequently increasing DMSP production (Gröne and Kirst 1992).

DMSP is also proposed as an overflow for excess carbon when the cell produces more carbohydrate than it requires (Stefels 2000). Under high light conditions, CO_2 fixation increases relative to nitrate assimilation, leading to an excessive production of carbohydrates (Turpin 1991). In iron deficient conditions, nitrogen deficiency is induced relative to carbon assimilation, causing DMSP production to increase. In support of this theory, increased intracellular DMSP concentrations were observed in *Phaeocystis* sp.

exposed to high light irradiances and in iron depleted conditions (Stefels and Van Leeuwe 1998).

1.4.5 DMSP as an antioxidant system

It has been proposed that DMSP and its breakdown products may act as an antioxidant system (Sunda et al. 2002) when the production of reactive oxygen species (ROS) exceeds the cell's capacity to detoxify them. In support of the antioxidant hypothesis, DMS production via DMSP lyase activity increases in response to oxidative stress induced by CO_2 and Fe limitation, exposure to UV radiation, H_2O_2 and high concentrations of Cu^{+2} ions (Sunda et al. 2002). Culture studies of the diatom *Thalassiosira pseudonana* revealed a similar upregulation in cellular DMSP under N, P, Si and CO_2 limitation (Bucciarelli and Sunda 2003). In addition, increased activity of the DMSP system in response to CO_2 and Fe limitation and increased solar UV radiation was also observed in *E. huxleyi* (Sunda et al. 2002). Further, Fe limitation was shown to increase the DMSP to carbon ratio in the diatom *Skeletonema costatum* (Sunda et al. 2002), a similar result also observed in the Antartic prymnesiophyte *Phaeocystis* sp. (Stefels and Van Leeuwe 1998). Exposure to high light irradiances also causes oxidative stress and has resulted in an increase in DMSP concentrations in some Antarctic macro- and micro-algae (Karsten et al. 1992; Stefels and Van Leeuwe 1998).

Furthermore, Sunda and co-workers (2002) demonstrated that DMSP can scavenge hydroxyl radicals and proposed that the enzymatic cleavage of DMSP enhances antioxidant protection, as DMS and acrylate are respectively 60 and 20 times more effective in scavenging hydroxyl radicals than DMSP itself. DMS is highly reactive towards singlet oxygen groups (Wilkinson et al. 1995) and since it is an uncharged molecule, it could potentially serve as an antioxidant within photosynthetic membranes where lipid peroxidation reactions occur. Further, oxidation of DMS would result in DMSO, a substance already credited for its antioxidant properties (Lee and De Mora 1999) and being hydrophilic, DMSO would accumulate in the cell making it a more effective antioxidant. Finally, reaction of DMSO with hydroxyl radicals produces methane sulphinic acid (MSNA), which is an effective scavenger of the harmful

hydroxyl radicals (Scaduto 1995). Besides DMSP and its derived S products, there are other S-containing amino acids like cysteine and methionine involved in ROS quenching especially of the harmful singlet oxygen and hydroxyl radicals (Moller et al. 2007). Noctor and Foyer (1998) have also demonstrated that glutathione (GSH) is an effective scavenger of hydrogen peroxide.

The antioxidant theory is further supported by the summer increase in DMS to chlorophyll ratios due to the oxidative stress induced by increased solar radiation (Sunda et al. 2002). This implies that DMS released by the activation of the DMSP antioxidant system would act as a negative feedback mechanism on UV oxidative stress by enhancing cloud albedo and thereby decreasing the incoming solar radiation (Charlson et al. 1987; Sunda et al. 2002).

1.5 *Emiliania huxleyi*

Research presented in this thesis, on the influence of stress conditions on intracellular DMSP and DMS concentration, is focused mainly on the photosynthetic unicellular eukaryote *Emiliania huxleyi* (Fig. 1.6). The fossil records of this coccolithophore species belonging to the class of prymnesiophytes, reveals its appearance on earth around 268,000 years ago (Raffi et al. 2006; Thierstein et al. 1977), about the same time as *Homo sapiens*, and is common in the world oceans since 70,000 years ago (Brown and Yoder 1994) making this microalgae an intriguing subject of study in response to stress. *Emiliania huxleyi* (namely the CCMP1516 strain) was the first genome to be sequenced in phylum haptophyceae, broadening our understanding of the biology and evolution of the members in this group and this makes it a model organism for research.
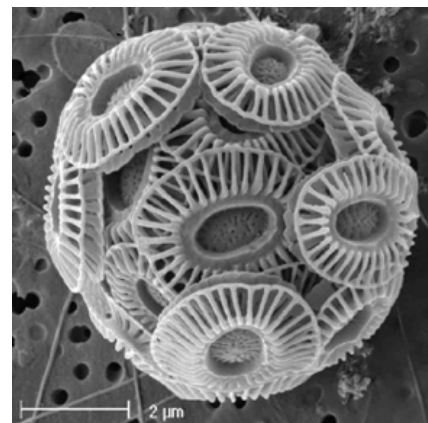
Figure 1.6 *Emiliania huxleyi* from the western Mediterranean (image courtesy of Markus Geisen / The Natural History Museum, London).

1.5.1 Cell structure, reproduction and life-cycle

The cell structure of *E. huxleyi* (Fig. 1.7) is that of a typical algal cell comprising the cell membrane, chloroplast, nucleus, endoplasmic reticulum, golgi body and mitochondria. In addition, this algal cell possesses a coccolith vesicle on the inside of the cell responsible for the formation of the coccolith. After generating the coccolith, the vesicle migrates to the edge of the cell and fuses with the cell membrane to constantly extrude the coccolith being produced within the cell, into the coccosphere (Westbroek et al. 1993).
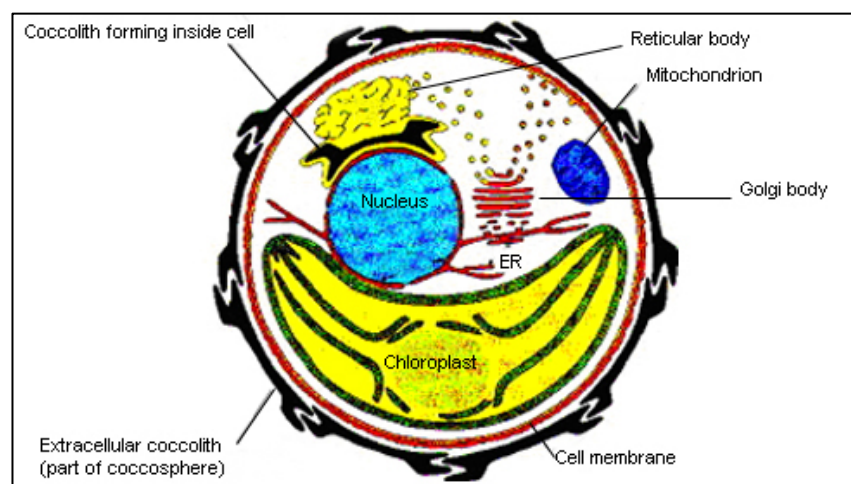
Figure 1.7 Cell structure of *Emiliania huxleyi* (Diagram from the Natural History Museum, London, modified from the original in Westbroek et al. (1993))

Reproduction in *E. huxleyi* is mainly by the asexual binary fission method, where one parent cell divides into two identical daughter cells by the process of mitosis. Cell division in *E. huxleyi* generally occurs up to once a day depending on the environmental conditions (Paasche 2001). However, if light and nutrients are not at optimum levels, this can hamper the cellular reproduction process.

An interesting feature of *E. huxleyi* is its dimorphic haplo-diploid life-cycle (Fig. 1.8), wherein it can switch phases via the processes of meiosis and syngamy to maintain genetic diversity with asexual reproduction in either phase (Green et al. 1996; Paasche 2001). The diploid phase (2N), containing two copies of each chromosome, is the non-motile stage bearing coccoliths. The haploid phase (N) containing one copy of each chromosome is the motile stage bearing two flagellae for swimming, with the absence of coccoliths but the formation of cellulosic scales. It also has one more cell type in its life-cycle known as the naked non-motile cell, which has been the type of cells used in this study.
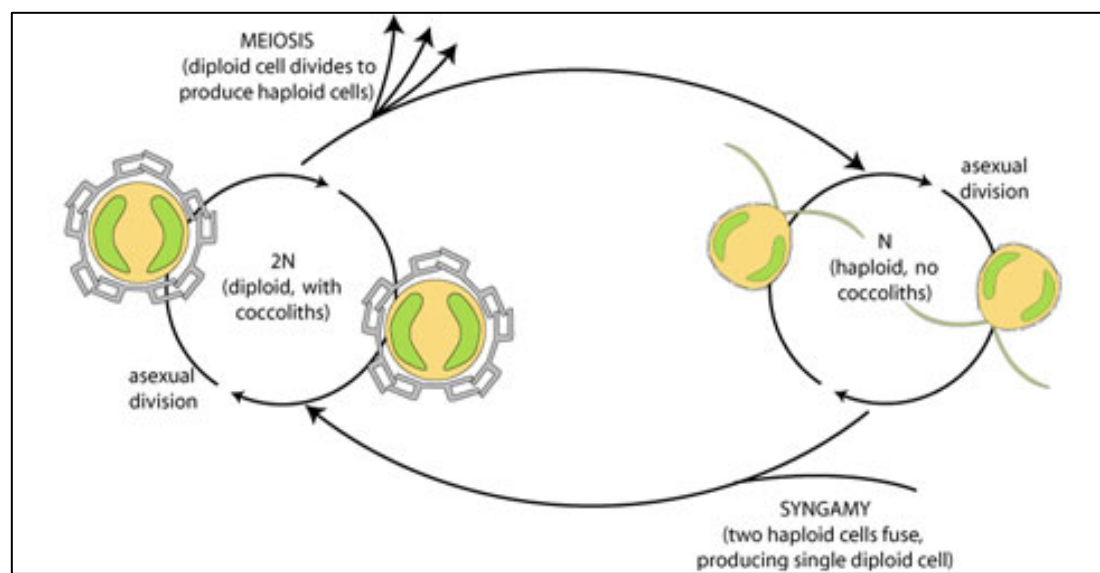
Figure 1.8 Life-cycle of *Emiliania huxleyi* (Diagram from the Natural History Museum, London)

1.5.2 Distribution and ecology

E. huxleyi, one of the most eurythermal (temperature-tolerant) and euryhaline (salinity-tolerant) of all species (Winter et al. 1994), is widely distributed in the freezing and nutrient-rich waters of the subarctic, in equatorial waters and along the borders of the subtropical oceanic gyres and in upwelling zones (Flores et al. 2010; Okada and Honjo 1975; Okada and McIntyre 1979; Winter et al. 2008). It is vertically distributed in the 50-100 m of the water column to carry out photosynthesis. It is capable of fixing atmospheric carbon into both photosynthetic and biomineralized product ($CaCO_3$, calcite). Further, its unique calcifying ability of over-producing coccoliths results in the formation of multilayered coccospheres or the release of excess coccoliths into the water column, when compared to the other coccolithophore species regularly producing a single coccolith layer. Hence, *E. huxleyi* may play an important ecological role in the carbon dioxide sink (Westbroek et al. 1993) and in the marine carbon cycle via the export of calcite to the seabed; sedimentation (Baumann 2004). Apart from global carbon cycling, *E. huxleyi*, being a major DMSP producer and containing DMSP lyase (Keller et al. 1989; Steinke et al. 1998), also plays an important role in the sulphur cycle, thus playing a significant role in global climate change.

E. huxleyi can also have a significant impact on the local environment by its periodic bloom formation covering large areas of the sea surface (Fig. 1.9). These blooms are categorized by a dense cell population of 1 to 10 million cells L^{-1} with the loose floating coccoliths giving the water a milky-white appearance, in contrast to green or red coloration produced by other phytoplankton species. *E. huxleyi* blooms typically occur in the North sea (Holligan et al. 1993b), the Black sea (Oguz and Merico 2006), the Bering Sea (Sukhanova and Flint 1998), the North Atlantic ocean (Holligan et al. 1993a; Malin et al. 1993), the Patagonian shelf around the Falklands and Argentina, in the North Pacific and the seas west of Great Britain (by SeaWiFS, satellite observations). Several hypotheses and supporting evidence brought forward for the environmental conditions that facilitate *E. huxleyi* blooms are high light (Nanninga and Tyrrell 1996), low silicate, phosphate more limiting than nitrate, low dissolved CO_2 concentrations, high carbonate ion concentrations and types of grazers in the area.

Figure 1.9 LANDSAT Satellite image of *Emiliania huxleyi* bloom in the English Channel (Latitude 50°11′1″N and longitude 0°31′52″W) off the coast of Plymouth (Cornwall) 24, July 1999 (Photo: NASA, image courtesy of Andrew Wilson and Steve Groom).

Development of *E. huxleyi* blooms are either prevented or terminated by viral infestation (Bratbak et al. 1993; Martinez et al. 2007; Wilson et al. 2002b). Based on the 'Red Queen evolutionary dynamics' originally proposed by Van Valen (1973), named after the Red Queen in Alice in Wonderland who said, "It takes all the running you can do, to keep in the same place", it has been suggested that coccolithoviruses are responsible for the rapid evolution shown by *E. huxleyi* (Emillani 1993; Smetacek 2001). However, a recent study by Frada et al. (2009) proposed an alternative model, called the 'Cheshire Cat dynamics' after the cat in Alice in Wonderland, which escaped execution by gradually turning invisible. This study demonstrated that under viral attack, the diploid phase cells could switch to the more virus-resistant haploid phase and by this mechanism a proportion of the population could escape viral attack at the end of the bloom period. The alternate non-coccolith bearing motile haploid phase cells of the life-cycle appear to be immune to viral attack, possibly because it has a very different cell-surface and so is in effect invisible to the viruses.

The coccolithoviruses increase the ROS production in the infected cells (Evans et al. 2006) thereby causing rapid degradation of cellular components, a drastic drop in photosynthetic efficiency, an upregulation of metacaspase protein expression associated with the induction of caspase-like activity and subsequently activating the autocatalytic programmed cell death (PCD) pathway (Bidle et al. 2007). Mesocosm experiments have

shown DMS accumulation in response to viral-induced decline of *E. huxleyi* blooms (Darroch 2003; Evans 2004) and a culture study on viral infected axenic strains of *E. huxleyi* resulted in the cleavage of DMSP to DMS (Evans et al. 2007). In addition, there are several field studies reporting high DMS levels associated with blooms (Holligan et al. 1993a; Malin et al. 1993; Matrai and Keller 1993). In contrast, other investigations on *E. huxleyi* blooms under viral attack in the Norwegian coastal waters and in seawater mesocosm experiments, did not result in increased DMSP nor DMS concentrations due to bacterial degradation or assimilation of the sulphur compounds released during cell lysis in the natural environment. So also the bloom size was relatively less dense with maximum cell concentration of $11 \times 10^6 \, L^{-1}$ (Bratbak et al. 1995). There is also evidence to suggest that the process of grazing is more accountable for increased DMSP and DMS concentrations than viral lysis (Archer et al. 2001; Evans et al. 2007; Wilson et al. 2002a).

E. huxleyi is usually adapted to a wide range of aquatic environments. However, there are serious concerns over the potential ecological threats posed by ocean acidification. How *E. huxleyi* has evolved to be a dominant and abundant species despite the varying environment is of great importance. Its response to stress permits us to gain information on the mechanisms that organisms use to exploit environmental resources or cope with environmental stress.

1.6 Goals, objectives and thesis overview

The goals and objectives of this research project evolved over time. However, the main goal of the research was to determine natural ways in the environment that induce cell lysis and cell death and whether this would trigger effects on DMSP and DMS release from the cells, especially because DMSP and DMS are proposed to act as an effective antioxidant system under stress conditions.

To achieve this goal, I firstly had to decide on a DMSP-producing phytoplankton to work with, out of the rich and diverse marine phytoplankton community. Having possessed and read the book '*The Ages of Gaia: A biography of our living earth*',

written by James Lovelock, the proposer of the '*Gaia Hypothesis*', the large image of the coccolithophore *Emiliania huxleyi,* pictured in the book at the very beginning of the introduction chapter on page 2 inspired me. As explained earlier in this chapter (section 1.5), there is no doubt of the biogeochemical importance of the *E. huxleyi* species.

Various studies document changes in intracellular DMSP concentration under stress conditions for several phytoplankton species and strains, but results are not always consistent. To understand how the environment, with its ongoing natural processes, drives intracellular DMSP and DMS concentrations in *E. huxleyi* and how *E. huxleyi* may modify itself as the environment changes, it was necessary to examine the organisms cellular stress response patterns under a specified set of laboratory conditions. For this, *E. huxleyi* cells were subjected to a range of environmental stress conditions simulated in the laboratory. Natural conditions were also tested where appropriate.

Besides the general layout of a thesis that includes an Introduction (Chapter 1) providing a comprehensive literature review on the subject; Methodology (Chapter 2) accounting for the culturing techniques and analytical methods used within the study; this thesis also contains four chapters revealing the kinds of stress induced in *E. huxleyi*, its physiological cellular stress response and the influence of the stress factors on DMSP and DMS release from the cells. Each of the four result chapters was treated as an objective to accomplish the research goal reviewed in the final discussion and conclusions (Chapter 7).

In Chapter 3 an investigation of nutrient-limitation on *E. huxleyi* is reported. The investigation was handled in two different ways and this was the only chapter that included a silicifying phytoplankton group of diatoms, *Thalassiosira pseudonana*, besides the calcifying, *E. huxleyi*. So firstly, batch cultures of *E. huxleyi* and *T. pseudonana* were monitored under gradual nutrient-exhaustion over a period of 28 days and an add-back experiment was performed to identify the limiting nutrient in both cases. The results from this first part are published in Limnology and Oceanography. The second highlight in this chapter is the effect of N-free media and P-free media followed by the add-back of the nutrient on the growth and DMSP concentrations and DMS

release in the three strains of *E. huxleyi*, namely CCMP370, CCMP373 and CCMP1516. Changes in membrane permeability were related to cell lysis and cell death.

In Chapter 4 a study of UV-induced stress on *E. huxleyi* is reported. In this chapter, the aforementioned three strains of *E. huxleyi* were monitored for physiological responses, cell death and changes in DMSP concentrations in different light conditions and under various UV treatments in artificial set-ups and in natural light conditions i.e. solar radiation. Recovery experiments under normal light conditions were also conducted.

In Chapter 5 an examination of light-deprivation or dark stress on the three strains of *E. huxleyi* is reported. In this chapter, physiological responses to cell stress, cell lysis, cell death and changes in DMSP and DMS concentrations were recorded over a period of 10 days in *E. huxleyi* 370 and 373 and 18 days in *E. huxleyi* 1516 placed in continuous darkness. At the end of the monitoring period, the cultures were re-illuminated and re-growth tested. In addition, at various points within the prolonged darkness-monitoring period, the cells were re-exposed to the light-dark cycle and tested for re-growth.

Chapter 6 covers a study on the herbicide-induced oxidative stress in *E. huxleyi*. This particular treatment, though not a natural form of stress, was used as a guaranteed way to induce oxidative stress. Previously many experiments have shown that exposure to paraquat or methyl viologen enhances the production of ROS in plants and algae (Bray et al. 1993; Broadbent et al. 1995; Okamoto and Hastings 2003). This treatment also broadens our understanding of the potential effects of pollutants that induce oxidative stress, on intracellular DMSP and DMS release in *E. huxleyi*. In this chapter, a 48, 72 and 120 h time-series exposure to 1 mM paraquat was carried out on *E. huxleyi* 1516 and a 72 h time-series exposure was conducted on *E. huxleyi* 370 and 373 to monitor the physiological responses to cell stress, cell lysis, cell death and changes in DMSP and DMS concentrations. This artificially-induced oxidative stress in *E. huxleyi* 1516 was verified by hydrogen peroxide excretion. A novel method of cell sorting on the Cytopeia influx was developed and optimized for the first time to sort cell populations based on fluorescence. The sorted cell populations were then analyzed for intracellular DMSP concentrations.

This work has been a sincere attempt to understand the biological role of DMSP and DMS within *E. huxleyi* cells and the results from the study are essential to explain how biology and atmosphere linked in the CLAW hypothesis, may not always respond consistently to environmental changes.

1.7 Hypothesis

In view of the above, the following hypothesis was put to the test:

"If DMSP acts as an antioxidant system, then under stress conditions that induce oxidative stress in Emiliania huxleyi, DMSP will increase".

Chapter 2

General Methods

Chapter 2: General Methods

2.1 Algal cultures

Axenic cultures of *Emiliania huxleyi* CCMP370, CCMP373 and CCMP1516 (Table 2.1) were procured from the Provasoli-Guillard National **C**enter for the **C**ultivation of **M**arine **P**hytoplankton (CCMP, Maine, USA) recently renamed as the **N**ational **C**enter for **M**arine **A**lga and Microbiota (NCMA). These phytoplankton strains were maintained as batch cultures in two kinds of media (see section 2.2) and were grown in 100 ml Erlenmeyer flasks with 50 mls of media and capped with a cotton-filled muslin bungs, covered with aluminium foil. The cultures were incubated in a MLR-351 Plant Growth Chamber (Sanyo, Loughborough, UK) at 17°C under a light:dark cycle of 14:10 h at an illumination of 100 μmol photons m^{-2} sec^{-1} (Scalar PAR Irradiance Sensor QSL 2101, Biospherical Instruments Inc., San Diego, USA) and the flasks were gently swirled once a day, to keep the cells in suspension. Under these culture conditions, the *E. huxleyi* cells did not produce coccoliths and remained as naked cells.

Table 2.1 Strain information for *Emiliania huxleyi*. Origin and isolation information obtained from Steinke et al. (1998). Additional information derived from the homepages of the National Center for Marine Alga and Microbiota (NCMA; https://ncma.bigelow.org/).

Emiliania huxleyi			
Strain	370	373	1516
Synonyms	451 B	BT 6	2090
	F451	CSIRO-CS-57	
Origin	North Sea	Sargasso Sea	North Pacific
Collector	Passche	Guillard	Polans
Year of Isolation	1959	1960	1991

An inoculum of the stock culture was transferred to fresh media every 8 days to maintain exponential growth using the aseptic technique, in the sterile environment of a Walker Class II laminar flow cabinet. The aseptic technique involved wiping the interior of the cabinet with 70% ethanol and flaming the neck of the glassware with a gas burner before

and after the culture transfers. Glassware and culture media were autoclaved at 120°C for 30 minutes. Axenicity of the cultures was monitored regularly for bacterial contamination especially before and at the end of an experiment, by DAPI staining and epifluorescence microscopy (see section 2.3).

2.2 Media preparation

All three strains of *E. huxleyi* were successfully grown in two kinds of media: ESAW-Si (Enriched Seawater, Artificial Water) and f/2-Si. Silicate was omitted, as it is not needed by *Emiliania*. The cultures were used according to the need and objective of the experiment; for example, the nutrient limitation work was carried out with cultures growing in ESAW so that the nitrate and phosphate concentrations could be easily controlled and all the other stress experiments were conducted in the f/2-Si media.

2.2.1 ESAW-Si (Enriched Seawater, Artificial Water) medium

The original ESAW medium was proposed by Harrison et al. (1980) and was later modified for a wider range of coastal and open ocean phytoplankton (Berges et al. 2001; Berges et al. 2004) (Table 2.2).

Seawater Base: The seawater base is composed of two parts: the anhydrous salt solution and the hydrated salt solution, which were prepared separately to avoid formation of any precipitates. The anhydrous salt solution was made by dissolving the anhydrous salts in 600 ml distilled water and the hydrated salt solution was made by dissolving the hydrated salts in 300 ml distilled water. The two salt solutions were autoclaved, cooled to room temperature and combined in a sterile environment with the addition of sterile distilled water to make a final volume of 1 L of the seawater base. The pH was noted as 8.2 and the salinity (hand-held conductivity meter WTW LF340-B/SET) was in the range of 30-33.

Macronutrients, metals and vitamins: Stock solutions of macronutrients, iron, trace metals and vitamins were individually prepared and stored at 4°C, except the vitamin solution, stored at -20°C.

The seawater base was enriched just before cell transfers, with 1 ml L^{-1} of the above stock solutions using a syringe filter to avoid bacterial contamination.

Table 2.2 Recipe for ESAW-Si media (without silicate, dH$_2$O is distilled water).

Compounds	Stock Solution (gL^{-1}dH$_2$O)	Quantity in 1L	Final concentration in the medium (M)
Anhydrous salts			
NaCl		21.194 g	3.63 x 10^{-1}
Na$_2$SO$_4$		3.550 g	2.50 x 10^{-2}
KCl		0.599 g	8.03 x 10^{-3}
NaHCO$_3$		0.174 g	2.07 x 10^{-3}
KBr		0.0863 g	7.25 x 10^{-4}
H$_3$BO$_3$		0.0230 g	3.72 x 10^{-4}
NaF		0.0028 g	6.67 x 10^{-5}
Hydrated salts			
MgCl$_2$.6H$_2$O		9.592 g	4.71 x 10^{-2}
CaCl$_2$.2H$_2$O		1.344 g	9.14 x 10^{-3}
SrCl$_2$.6H$_2$O		0.0218 g	8.18 x 10^{-5}
Macronutrients			
NaNO$_3$	46.670	1 mL	5.49 x 10^{-4}
NaH$_2$PO$_4$.H$_2$O	3.094	1 mL	2.24 x 10^{-5}
Iron solution		1 mL	
Na$_2$EDTA.2H$_2$O		2.44 g	6.56 x 10^{-6}
FeCl$_3$ 6H$_2$O		1.77 g	6.55 x 10^{-6}
Trace Metal solution		1 mL	
Na$_2$EDTA.2H$_2$O		3.090 g	8.30 x 10^{-6}
ZnSO$_4$.7H$_2$O		0.073 g	2.54 x 10^{-7}
CoSO$_4$.7H$_2$O		0.016 g	5.69 x 10^{-8}
MnSO$_4$.4H$_2$O		0.540 g	2.42 x 10^{-6}
Na$_2$MoO$_4$.2H$_2$O	1.48	1 mL	6.12 x 10^{-9}
Na$_2$SeO$_3$	0.173	1 mL	1.00 x 10^{-9}
NiCl$_2$.6H$_2$O	1.49	1 mL	6.27 x 10^{-9}
Vitamins solution		1 mL	
Thiamine HCL		0.1 g	2.96 x 10^{-7}
Biotin	1 g	1 mL	4.09 x 10^{-9}
B12	2 g	1 mL	1.48 x 10^{-9}

2.2.2 f/2-Si medium

The f/2 formulation is a modification of the original f medium by Guillard and Ryther (1962) and is represented as f/2 as it is prepared at half the strength of the f medium. The f/2 medium usually always contains macronutrients like nitrogen, phosphorus, and silicates and micronutrients such as trace metals and vitamins. The macro- and micro-nutrient solutions were stored at 4°C and the vitamin solution was stored at -20°C.

The f/2-Si medium (Table 2.3) was prepared with natural seawater sampled from the North Atlantic open ocean or the North Sea that was aged in the dark at 12°C for at least a year. The seawater was filtered through a 0.2 μm pore size cellulose acetate filter to remove any particles. The medium was made using 97.5% filtered seawater and 2.5% distilled water to avoid precipitation in the medium (Mc Lachlan 1973). One drop of concentrated hydrochloric acid (HCl) was added to lower the pH to 7 or 7.5 to balance the increase of pH due to loss of CO_2 during the sterilising process. The medium was sterilised by heating to 120°C for 30 minutes in a Priorclave autoclave. It was then left to cool and enriched just before cell transfers, with 1 ml L^{-1} of the above macro- and micro-nutrients, trace metal solution and vitamin solution using a syringe filter to avoid bacterial contamination.

Table 2.3 Recipe for f/2-Si media (without silicate, dH_2O is distilled water).

Compounds	Stock solution (g L^{-1} dH_2O)	Quantity in 1 L	Final concentration in the medium (M)
Macronutrients			
$NaNO_3$	75	1 mL	8.83×10^{-4}
$NaH_2PO_4H_2O$	5	1 mL	3.63×10^{-5}
Trace Metals solution		1 mL	
Fe/EDTA	6.25		11.87×10^{-6}
$CuSO_47H_2O$	9.8	1 mL	4×10^{-8}
$Na_2MoO_42H_2O$	6.3	1 mL	3×10^{-8}
$ZnSO_47H_2O$	22	1 mL	8×10^{-8}
$CoCl_26H_2O$	10	1 mL	5×10^{-8}
$MnCl_24H_2O$	180	1 mL	9×10^{-7}
Vitamin Solution		1 mL	
Vitamin B12 (cyanocobalamin)	1	1 mL	4×10^{-10}
Biotin	0.1	10 mL	2.1×10^{-9}
Thiamine HCl		200 mg	3×10^{-7}

2.3 Culture axenicity by DAPI staining

The blue-fluorescent DAPI nucleic acid stain was used to verify the axenicity of the *E. huxleyi* cultures. DAPI (4',6-diamidino-2-phenylindole) is a fluorochrome that binds to DNA forming a stable fluorescent complex which when excited with UV light (360 nm), fluoresces by emitting blue light (450 nm) which can be observed under a fluorescent microscope (Kapuscinski 1995; Porter and Feig 1980).

Depending on the cell density of the culture, a sample of 1–4 ml was transferred in a sterile environment in a sterile screw-capped bijou vial and made up to 4 ml with 0.2 μm syringe filtered seawater. The culture sample was then fixed in a fume cupboard, with 3 μl ml^{-1} of Lugol's iodine (a mixture of 10% w/v aqueous KI and 5% w/v iodine) and 50 μl ml^{-1} of neutralised formalin (20% aqueous formaldehyde with 100 g l^{-1} hexamine) and finally 1 μl ml^{-1} of sodium thiosulphate solution (3% w/v, stored at 4°C) was added to discolour the iodine colouration from the Lugol's solution that would interfere with the DAPI fluorescence. All of the above reagents were syringe filtered before adding to the culture sample. Finally, 10 μl ml^{-1} of DAPI solution (1 mg ml^{-1} stock solution, Sigma Aldrich, stored at -20°C) was added and the sample was incubated in the dark at room temperature for 15 minutes. The DAPI stained sample was filtered under vacuum through two filters: a 0.2 μm pore black polycarbonate filter of 25 mm diameter placed on a 0.45 μm pore white cellulose nitrate backing filter, rinsed with sterile seawater. The black polycarbonate filter was carefully placed onto a glass slide bearing a drop of immersion oil, followed by another drop of the immersion oil on the filter itself and covered with a coverslip. The glass slide was examined under a fluorescence microscope (Olympus BX40, Essex, UK) at 100-fold magnification objective with epifluorescence light and a UV light filter. The *E. huxleyi* cells appear fluorescent blue and if bacteria are present, small bright dots or elongated sticks appear in the background and the black background also appears cloudy.

2.4 Cell density and cell volume using the particle counter

Cell density (cells ml^{-1}), cell diameter (µm) and the volume per ml (µm^3 ml^{-1}) from which the cell volume (µm^3) was derived, were measured using an automated particle counter (Beckman Multisizer 3 Coulter Counter, High Wycombe, UK).

The Coulter counter instrument contains two electrodes: one inside a tube with a small aperture and another just on the outside. Both of these are immersed into a plastic cuvette that contains particles suspended in a low concentration electrolyte (in this case the diluted culture sample) that provides a current path when an electric field is applied. The particle counter is based on the Coulter principle, which is a change in the electric field when a particle from a sample passes through the aperture. Every electrical pulse recorded is equivalent to a particle passing through the aperture and the amplitude of a pulse is proportional to the volume of the particle, which is processed to give the particle diameter and other particle characteristics, assuming the particle is spherical.

Prior to cell counting, the culture samples were diluted to 1:10 or for denser cultures, 1:20 with filtered seawater that acts as the electrolyte and this was done to prevent coincidence so that one cell could pass through the 100 µm aperture at a time. Samples were analysed in triplicate. Data was collected and interpreted using the Coulter Multisizer software.

2.5 Fluorescence and photosynthetic capacity using the phyto-PAM

Photosynthetic pigment fluorescence and photosynthetic capacity (also known as the 'quantum yield of photosynthesis', or 'photosynthetic yield' or photosynthetic efficiency (F_V:F_M); terminology discussed in Maxwell and Johnson (2000)) were monitored on a phyto-PAM fluorometer, which is a pulse amplitude modulated (PAM) chlorophyll fluorometer. The phyto-PAM fluorometer is able to excite at four different wavelengths: 470 nm (blue), 520 nm (green), 645 nm (light red) and 665 nm (dark red) and measure the corresponding fluorescence emission and also has the ability to apply saturating pulses of light to assess cell photosynthetic capacity.

The phyto-PAM fluorometer is based on the quantitative relationship between chlorophyll fluorescence and the efficiency of photosynthetic energy conversion and works on the fundamental character of this relationship. It relies on the principle that fluorescence originates from the same excited states created by light absorption, which alternatively can be photochemically converted (via photochemistry) or also dissipated into heat (via fluorescence quenching). Hence, the relationship between fluorescence and photosynthesis is a result of the first law of thermodynamics and simple calculus, from which an index indicating how well the cells are channelling light or excitation energy to photochemistry, and hence the 'capacity' of the cells for photosynthesis can be obtained.

$$Fluorescence\ +\ photochemistry\ +\ heat\ =\ 1$$

This is done by 'switching off' photochemistry and measuring fluorescence and heat, which are determined as relative values by two fluorescence measurements. The two fluorescence measurements take place shortly before and during a pulse of saturating light i.e. within less than a second at the photosystem II reaction centre (PSII RC; on the thylakoid membranes of the chloroplasts), which represents the physical site of the measurement. Light will excite chlorophyll a into its excited state where it can then transfer an electron into the electron transport chain (ETC) for the production of ATP, the reduction of NADP and the ultimate production of glucose. As the electron is transferred through the ETC, the initial electron acceptor becomes open to accept a new electron. Under high light, this system saturates because all the reaction centers are closed (occupied by electrons). When the reaction centers are closed, new electrons cannot be accepted at the rate the chlorophyll is being excited and this results in the emission of the excess excitation energy in the form of fluorescence.

The efficiency, with which light energy is utilized, is a function of how "healthy" the cell is. When cells are under stress, the system becomes saturated more easily and the system does not process light as efficiently. To measure photosynthetic efficiency, it is necessary to dark-adapt the culture sample for 30 minutes so that all of the electron acceptors in the reaction centers are "open" and able to accept electrons resulting in

maximum quantum yield. Measuring cells without dark-adaptation gives the effective quantum yield, since quenching is operating and the cells are adapted to their current light regime. The PAM fluorometer shines a weak light at the sample, called the measuring light (Grasshoff et al. 1976). The pulse modulated measuring light was generated by a light-emitting diode (LED) and does not have much actinic effect (i.e. it does not cause any reduction of the electron acceptors downstream of PSII). Fluorescence is measured at this point when most light energy can be accepted into the ETC for photochemistry. This is the minimal fluorescence yield F_t (initial fluorescence). When the F_t signal on the PAM stabilises, the sample is then given a saturating pulse of actinic light until all of the electron acceptors are saturated and the reaction centers are closed. The PAM uses more LEDs at a higher frequency to quickly saturate PSII (<1 s). Saturation is the complete reduction of the electron acceptors downstream of PSII and causes an immediate increase in fluorescence to a maximal level called F_M (F max). All absorbed light energy at this point will then be given off as fluorescence. The difference between the initial fluorescence (F_t) and the maximum fluorescence (F_M) is known as the variable fluorescence ($F_V = F_M - F_t$). F_V normalized to F_M (F_V/F_M) is a measure of the photosynthetic efficiency of photosystem II. This is the yield, or photosynthetic capacity. This will range between 0 and around 0.7. The lower the yield, the more PSII reaction centres (RCs) are closed (this could be due to photoinhibition, or nutrient limitation). The higher the yield, the more RCs are open. Under stress, changes in $F_V:F_M$ will occur rapidly in cells and so this parameter is often one of the preliminary and most sensitive indicators of physiological stress (Suggett et al. 2009).

A culture sample of 3 ml was dark-adapted for 30 minutes and then transferred gently into a clean quartz cuvette (washed with ethanol, followed by distilled water and oven dried at 30°C) avoiding bubbles. The cuvette was immediately placed in the emitter-detector unit, with a light-proof hood. Since chlorophyll is the dominating pigment, fluorescence emission was recorded at 470 nm at gain 5. The autogain was commenced on the phyto-PAM to find the best gain setting when the fluorescence reading was below 300. A saturating pulse was applied and the F_V/F_M was noted from the PHYTO-WIN software.

2.6 DMSP and DMS analyses using gas chromatography

DMSP measured as particulate DMSP (DMSPp), dissolved DMSP (DMSPd) and total DMSP (DMSPt) along with DMS concentrations were determined in the culture samples. DMSPp, DMSPd and DMSPt were subjected to an overnight alkali hydrolysis to DMS and the headspace technique (see section 2.6.1.1) was used to acquire the DMS. The headspace technique involves the equilibration of liquid samples with a headspace of air and the partition coefficient for DMS is temperature-controlled. To measure the DMS dissolved in the culture sample, it was first extracted and pre-concentrated using the purge-and-trap system (see section 2.6.2.1). The resulting DMS was analysed using gas chromatography, an analytical technique used to separate, detect and quantify compounds that can be vaporised without chemical decomposition (see section 2.6.5).

2.6.1 DMSPp analyses

Five ml of the culture was sampled with a gas-tight syringe and gently filtered through a glass-fibre filter (25 mm, Whatman GF/F, nominal pore size 0.7 μm) using a swinnex unit. The filter was then placed into a 5 ml vial containing 3 ml of 0.5 M NaOH and immediately closed with a gas-tight screw cap containing a PTFE/silicone septa (Alltech), stored in the dark and later analysed by the headspace technique (see section 2.6.1.1). The amount of DMSPp on the filter was then calculated with reference to calibration curves (see section 2.6.6.1) and expressed as a concentration (DMSPp) in the cells (Steinke et al. 2000). When DMS and DMSPd concentrations in the culture were not being determined, 3 ml of the culture was sufficient for DMSPp analyses. In such a case, 3ml of the culture was gently filtered using the hand-held vacuum pump (< 10 cm Hg) through a 25 mm Whatman GF/F (nominal pore size 0.7 μm) on a small-size filtration set-up unit and the filter was treated as explained above.

2.6.1.1 Headspace technique

The vials were kept in the dark and placed in a constant temperature heating block at 30°C overnight to ensure complete hydrolysis of DMSP to DMS. The headspace of the vial was then analysed for DMS by piercing the septum with a gas-tight microlitre

syringe and removing 50 µl from the headspace for direct injection onto the gas chromatograph column (Shimadzu GC-2010 with FPD detection) (see section 2.6.5). The gas chromatography (GC) settings associated with this method are detailed in Table 2.4 (section 2.6.5).

2.6.2 DMS analyses

The above filtrate (see section 2.6.1) was purged with an inert gas to analyse the culture DMS concentration. The filtrate was purged for 15 minutes (N_2, 60 ml min^{-1}) in a cryogenic purge-and-trap system (see section 2.6.2.1); DMS was trapped in a Teflon loop (-150°C), flash evaporated by immersing the loop in boiling water and then swept into the GC (Turner et al. 1990). The amount of DMS in the purge tube was then calculated with reference to calibration curves (see section 2.6.6.2) and expressed as a concentration (DMS) from the culture.

2.6.2.1 Purge-and-Trap system

The purge-and-trap system (Fig. 2.1) was made up of a glass tube (for purging DMS out of the culture) with (a) a sample injection port at the top of the purge tube that was used to introduce the filtered culture sample via a two-way Luer valve (b) a needle valve at the bottom of the purge tube to receive the purging gas (N_2 1, oxygen-free grade, purified through an activated charcoal filter; flow rate of 60 ml min^{-1}) through a fine glass frit which generated streams of small bubbles and monitored by a flow meter (m). When not in use, the purge gas to the system was switched off using a two-way valve at the bottom of the purge tube. An elongated purge tube was used to increase the path length for nitrogen bubbles and thus enhance the purging efficiency. The outlet at the top of the purge tube was connected by a 1/8-inch-o.d. PTFE (polytetrafluoroethylene) tubing to a series of moisture traps in order to remove water vapour from the gas extract, thus preventing ice formation and blockages in the cryotrap (f). The first moisture trap was a (c) glass tubing packed with glass wool followed by (d) a Dry-Perm (Nafion) drier (72 inches length; MD-050, Perma Pure) as the second moisture trap. The water vapour was promptly carried out of the system by a counterflow of N_2 (N_2 2, flow rate of 150 ml

min^{-1}). The sample gas containing the DMS extract is carried through the cryotrap (f, 25 cm 1/8 inch-o.d. PTFE Teflon tubing wound halfway in a double loop), where DMS was collected and N$_2$ gas passed to the flow meter (k) to monitor the counter flow rate. The cryotrap was suspended in the headspace of a Dewar flask (g) containing liquid nitrogen and the headspace temperature was maintained at -150°C ± 5°C by an automated temperature control unit (j, designed and built at the Environmental Sciences Workshop, UEA). The temperature control unit (j) consisted of a temperature sensor (i) attached to the cryotrap; a resistor (h) immersed in liquid N$_2$, and an electronic control box. When the temperature of the headspace increased, the resistor began to heat increasing the vapour pressure of the liquid N$_2$ thus generating a cooling vapour and lowering the temperature of the headspace to -150°C. The purge-and-trap system was prepared for sample analysis by immersing the cryotrap loop in liquid N$_2$ to rapidly cool the loop and then suspended in the headspace of the Dewar flask, where the temperature was maintained at -150°C. With a sample volume of 5 ml, purging was achieved for 15 minutes. At the end of the purging time, the cryotrap was then promptly immersed in boiling water while the DMS was flushed by the He carrier gas into the GC (l) by switching a six-port valve (e) to connect the cryotrap with the GC. The gas flow settings of the purge and trap system and the GC settings associated with this method are detailed in Table 2.4 (section 2.6.5).
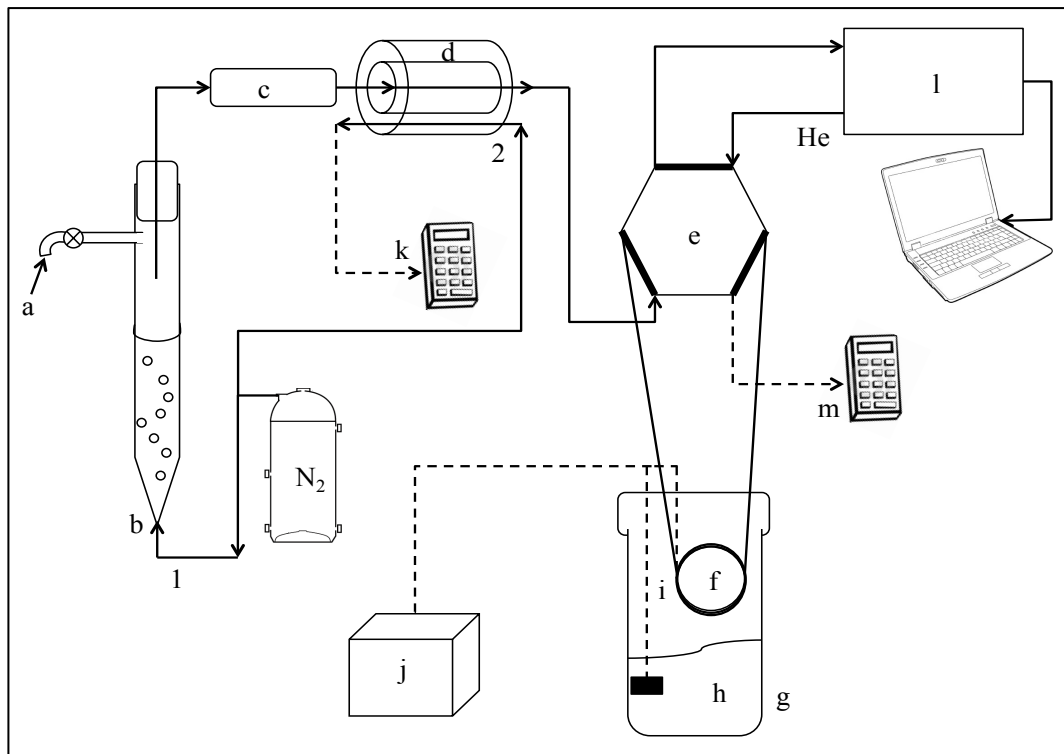
Figure 2.1 Purge and Trap system used to extract and pre-concentrate the dissolved DMS in the culture. (a) sample injection port, (b) entry for purge gas N_2, (c) glass wool moisture trap, (d) nafion drier, (e) manual six-port valve, (f) cryotrap, (g) Dewar Flask, (h) heating resistor immersed in liquid N_2, (i) temperature sensor, (j) temperature control unit, (k) flow meter to monitor the flow rate of the counter flow gas, (l) gas chromatograph (GC), (m) flow meter to monitor the flow rate of purge gas. There were two points of entry for N_2, 1 - purging gas that carries DMS and 2 - drier gas in counter flow direction (Diagram modified from Caruana (2010)).

2.6.3 DMSPd analyses

After purging the DMS out from the filtrate (obtained from section 2.6.2), the concentration of dissolved DMSP (DMSPd) was determined by transferring 4 ml of the purged filtrate into a 20 ml crimp vial, to which 10 ml distilled water and then 1 ml of 10 M NaOH was added (Dacey and Blough 1987) ensuring a constant analytical volume of 15 ml. The vial was immediately crimped with an aluminium seal with a Pharma-Fix liner (Alltech Associates Inc.) to create a gas-tight seal and stored in the dark at room temperature to promote hydrolysis to DMS. Later the samples were analysed by the headspace technique (see section 2.6.1.1). The amount of DMSPd in the filtrate was then

calculated with reference to calibration curves (see section 2.6.6.1) and expressed as a concentration (DMSPd) from the culture.

2.6.4 DMSPt analyses

Total DMSP (DMSPt = DMSPp + DMSPd + DMS) was measured in an unfiltered volume of culture (2.5 ml) hydrolysed in 0.5 ml of 10 M NaOH in a PTFE/silicone septa vial and later analysed by the headspace technique (see section 2.6.1.1). The amount of DMSPt (see section 2.6.6.1) in the culture was then calculated with reference to calibration curves and expressed as a concentration (DMSPt) in the culture.

2.6.5 Gas chromatography for DMS analyses

A gas chromatograph (Shimadzu GC-2010, Milton Keynes, UK) equipped with a capillary column of fused-silica (30 m × 0.53 mm CP-SIL 5CB; Varian, Oxford, UK) and a flame photometric detector (FPD) was used. Helium (flow rate of 35 ml min^{-1}) was used as the carrier gas to deliver the injected DMS sample through the column, which is then eluted from the column at a specific retention time (RT). A mix of hydrogen (flow rate of 60 ml min^{-1}) and air (flow rate of 70 ml min^{-1}) supplied the flame, which burned the sulphur compound subsequently emitting a light signal perceived by the FPD. A peak appears on the computer interface and when this peak is higher than the background noise of the chromatograph, the software automatically integrates the peak. The RT and the kind of the peak (sharp and narrow) are dependent on the gas chromatograph (GC) settings including column temperature, gas flow rate and temperature. Different GC settings were used for DMS measurements via the headspace technique and the purge-and-trap system (Table 2.4) because the methods involved in the introduction of the DMS gas into the column varied.

Table 2.4 Gas chromatograph settings for the headspace and purge-and-trap methods of introduction of DMS into the column and flow settings for N_2 gas through the purge-and-trap system.

GC Components	Temperature (°C)	Gas	Flow rate (ml min^{-1})	Pressure (kPa)
GC settings for the headspace technique				
Injector	200	Helium	Total Flow 35 Purge Flow 3	68.4
Column	120			
Detector	250	Hydrogen	60	
		Air	70	
GC and flow settings for the purge-and-trap system				
Injector	200	Helium	Total Flow 28.4 Purge Flow 3	45.6
Column	60			
Detector	250	Hydrogen	60	
		Air	70	
Purge and Trap Components				
Purge flow		Nitrogen	60	
Nafion drier flow		Nitrogen	150	

Within the optimum range of the detector, the response in terms of the peak is non-linear but is approximately a square root function. Thus, the square roots of peak areas (SQRT Peak area) are used for the DMS quantification by comparison with a concentration range of standards with which a calibration curve is obtained.

2.6.6 Calibrations

Individual calibrations were conducted for DMSPp, DMSPd, DMSPt and DMS because of the variations in the methodology (vial set-ups, concentration ranges and different GC settings for headspace and purge-and-trap methods) and based on the calibration curves, the concentrations of DMSP and DMS were acquired in the culture sample. The gas chromatograph (GC) was calibrated using commercially available DMSP (Centre for Analysis, Spectroscopy and Synthesis, University of Groningen laboratories, The Netherlands) that is converted to DMS by cold hydrolysis. DMSP stocks were prepared by dilution of the purchased commercial stock DMSP in distilled water to a

concentration of 0.025 moles S (equivalent to 0.8 g S ml^{-1}) and stored at -20°C. The stocks were then defrosted and diluted again with distilled water to solutions of concentrations ranging from 0.000125 to 0.0005 moles S (equivalent to 0.004 to 0.016 g S ml^{-1}).

2.6.6.1 DMSP calibration with the headspace technique

To calibrate the DMSP parameters like DMSPp, DMSPd and DMSPt obtained with the headspace technique, a series of known concentration (0.1-100 μM) of DMSP standards were prepared in triplicate vials identical to those used for experimental samples. To prepare the DMSPp and DMSPt standards, 5 ml vials were used while DMSPd standards were made in 20 ml vials. In each case, the appropriate volume (1-10 μl for DMSPp and DMSPt and 1-50 μl for DMSPd) of the DMSP working stock solution (75 μM, 7.5 mM and 30 mM) was pipetted on the septum inside the cap. Very carefully and rapidly, the cap was inverted to seal the vial for the DMSPp and DMSPt standards while the DMSPd standard vials were tightly crimped. Every vial for the DMSPp standards contained 3 ml of 0.5 M NaOH + DMSP working stock solution, for the DMSPt standards it contained 2.5 ml distilled water + 0.5 ml of 10 M NaOH + DMSP working stock solution and for the DMSPd standards, the vial contained 14 ml distilled water + 1 ml of 10 M NaOH + DMSP working stock solution. The vials were closed and agitated to mix the solutions and left in the dark to promote DMSP cleavage. Later they were analysed by the headspace technique (see section 2.6.1.1). The calibration was obtained by relating the detection signal as the square root of the peak area (y) to DMSP concentration (x) (Fig. 2.2). The linear relationship y = mx + c, where 'm' is the slope and 'c' is the intercept, was used to quantify the DMSPp or DMSPd or DMSPt concentration in each sample. The limit of detection was calculated to be 0.035 μM based on the three standard deviation of the blank.
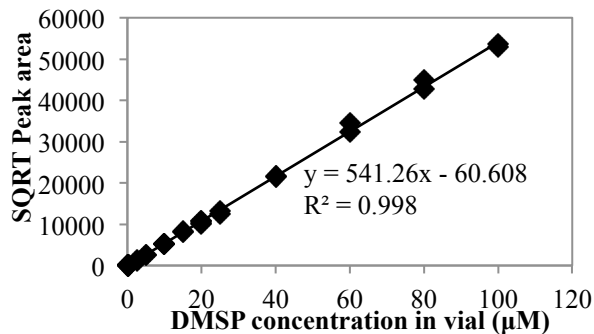
Figure 2.2 Calibration curve obtained via headspace technique for DMSP measurements in duplicate standards (ranging from 0.1 to 100 μM) by gas chromatography (example shown is from DMSPp calibrations; SQRT Peak area is square root of the peak area). The linear regression curve is shown with its correlation coefficient R^2.

2.6.6.2 DMSP calibration with the purge-and-trap system to acquire DMS

DMS acquired via the purge and trap system was calibrated with DMSP standard solutions directly loaded into the purge tube. A known concentration of DMSP stock solution + 1 ml of 10 M NaOH and a top up of distilled water to make a total volume of 5 ml in the purge tube is then tightly shut with the top of the purge tube. The purge gas is then bubbled into the standard for 15 minutes and the procedure is continued as described for DMS analysis via purge-and-trap (see section 2.6.2.1). The calibration was obtained by relating the detection signal as the square root of the peak area (y) to DMSP concentration (x) (Fig. 2.3). The linear relationship $y = mx + c$, where 'm' is the slope and 'c' is the intercept, was used to quantify the DMSP, which is in actual the DMS concentration in each sample. The limit of detection was calculated to be 0.0007 μM based on the three standard deviation of the blank.
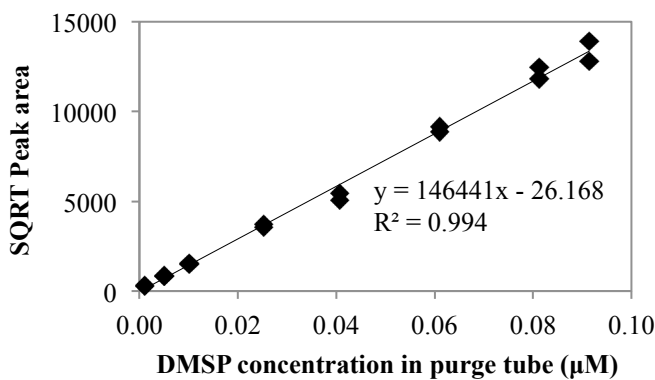
Figure 2.3 Calibration curve obtained with the purge-and-trap system for DMS measurements in duplicate DMSP standards (ranging from 0.001 to 0.091 μM) by gas chromatography (SQRT Peak area is square root of the peak area). The linear regression curve is shown with its correlation coefficient R^2.

2.7 Membrane integrity using flow cytometry

Membrane integrity, as a proxy for cell viability (Brussaard et al. 2001; Veldhuis et al. 2001), was investigated in *E. huxleyi* cultures during the various stress experiments using the nucleic acid stain SYTOX Green, in combination with flow cytometry. Flow cytometry is based on the optical properties of single particles or cells at high speed, being analysed as they move with a liquid stream and a beam of laser light of single wavelength is directed on to the liquid stream. In algal cells, fluorescence emissions are associated with the photosynthetic pigments within the cells or labelled cells with cytoplasmic or nuclear dyes. SYTOX Green, a membrane impermeable DNA-binding dye is recommended as an indicator of dead cells as it does not cross the membranes of live cells and only stains cells with compromised plasma membranes. Thus compromised cells are easily detected by the large increase in green fluorescence as the fluorophore binds with the DNA while viable cells remain unstained. This approach is recently in wide use to assess the viability of phytoplankton and bacteria (Brussaard et al. 2001; Franklin et al. 2012; Lebaron et al. 1998; Roth et al. 1997; Vardi et al. 1999; Veldhuis et al. 2001; Veldhuis et al. 1997).

SYTOX Green (Invitrogen S7020; excitation 504 nm, emission 523 nm) was diluted from the commercial stock supplied at 5 mM in dimethylsulphoxide (DMSO) solution to 0.1 mM in Milli-Q water. The commercial stock was stored frozen at -80°C and the

working stock at -20°C and was thawed in the dark prior to use, as SYTOX Green degrades when exposed to light. Prior to use, some initial tests were carried out to determine the optimum stain concentration and the optimum staining period for all the three strains of *E. huxleyi*. Cells in the mid-exponential phase were heat-killed cells (80°C, 5 min) and the 'maximum fluorescence ratio' approach was taken (Brussaard et al. 2001; Franklin et al. 2012). On the basis of these results, SYTOX Green was applied at a final concentration of 0.5 μM and the cells were left in the dark for 10 minutes. The SYTOX Green stained cells were compared with unstained controls via flow cytometry (BD FACScalibur equipped with an air-cooled argon ion laser, 15 mW; 488 nm and a 530/30 band pass filter) (Fig. 2.4).
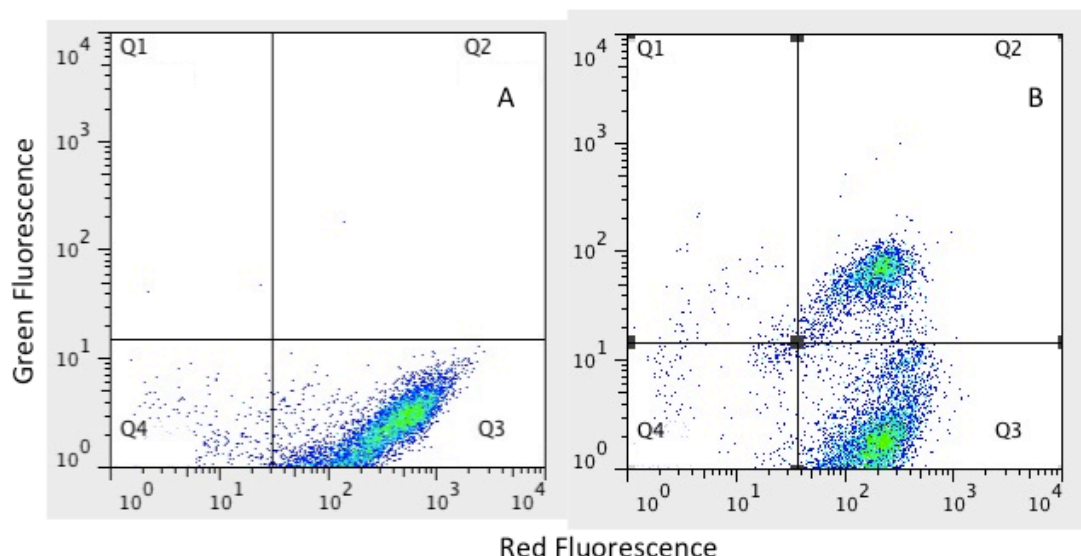
Figure 2.4 Example of a biparametric plot of red fluorescence (650 nm) versus green fluorescence (530 nm) showing membrane integrity using SYTOX Green staining in combination with flow cytometry during light deprivation in *Emiliania huxleyi*. (A) shows live cells in exponential growth phase before SYTOX Green addition (B) shows cells after SYTOX Green addition. Note that Q1 + Q2 = stained or cells with compromised membranes; Q3 = unstained normal or viable cells; Q4 = unstained debris and low-red cells.

The FACScalibur flow cytometer was set up with Milli-Q water as the sheath fluid. The analyses were triggered on red fluorescence and performed at ''lo'' flow rate (~ 20 μl min^{-1}) and 10,000 events were collected. To avoid coincidence, an event rate between 100 and 400 cells s^{-1} was used for every culture sample (Brussaard et al. 2001).

Depending on the cell density, the culture samples were diluted in sterile f/2-Si medium prior to analysis. At the start of each experiment, Flowset beads (Beckman-Coulter) were analyzed and the bead fluorescence was used to normalize stain fluorescence (Marie et al. 2005); these were used as instrument controls. Cells were discriminated based on their autofluorescence (650 nm) versus the green fluorescence of the SYTOX-Green stain (522 – 523 nm).

2.8 Cell sorting using the Cytopeia influx cell sorter

Cell sorting using the Cytopeia influx high-speed cell sorter (BD Biosciences) was exclusively carried out with *E. huxleyi* cells of strain CCMP1516 under herbicide-induced oxidative stress (see Chapter 6, section 6.2.5). Singlet droplet sorting combined with flow cytometry has been a novel approach to study DMSP concentrations in cell populations having common light scattering and fluorescent characteristics.

The most common method of sorting cells is by electrostatic deflection of charged droplets (Fig. 2.5). In this, the sample passes through a fluorescence measuring station where the fluorescent character of interest of each cell is measured. A gate is placed around the cells of interest in the cytogram displayed on the computer screen during acquisition, so that the cytometer identifies which cells to sort. Using a conductive sheath fluid, as the sample flows through a narrow central path, a vibrating mechanism causes the stream of fluid emerging from the exit nozzle to break into individual droplets containing one or more cells of interest. The system is adjusted so that there is a low probability of more than one cell per droplet, for high purity recovery of cells. The resulting stream of electrically-charged droplets passes through a pair of charged plates and are then deflected based upon their charge and collected into tubes. The uncharged droplets are collected separately as waste.

Using the droplet-based cell sorting technique on the Cytopeia influx high-speed cell sorter, the method was optimised for sorting the cells of *E. huxleyi* 1516 cultures and the sub-populations were analysed for cell volume changes and changes in DMSPp concentrations (results shown in Chapter 6, section 6.2.5).
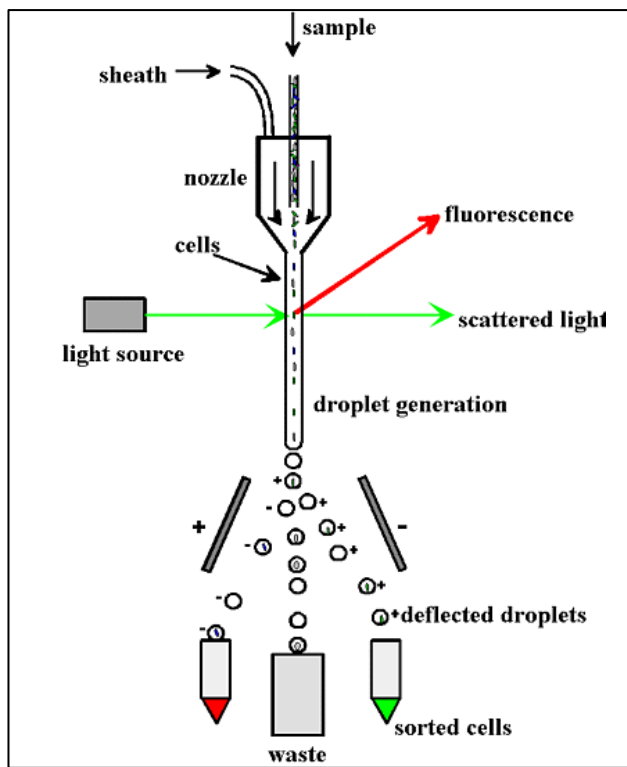
Figure 2.5 A single droplet-based cell sorter involves the selection of individual cells of interest by applying an electrical charge to a fluid stream (containing the sample). The resulting electrically-charged droplet containing a cell travels through an electric field between two high voltage deflection plates of opposite polarities. These droplets (containing the cells of interest) are eventually deflected into a collection tube for further use (diagram modified from http://www.appliedcytometry.com).

2.9 Hydrogen peroxide measurements using fluorometry

DMSP is proposed to serve as an effective antioxidant system protecting cells from the harmful effects of oxidative stress. This would imply that examining the activity of antioxidant enzymes such as superoxide dismutase (SOD) or other antioxidant molecules like ascorbate may not be effective methods to determine oxidative stress in DMSP-producing phytoplankton. Furthermore, quantifying the products of ROS damage to membranes, lipids and proteins may result in underestimated levels of oxidative stress with an effective antioxidant system (Collén and Davison 1997). Thus a more reliable method to determine oxidative stress in DMSP-producing phytoplankton would be the direct measurements of the reactive oxygen species (ROS) concentration like hydrogen peroxide (H_2O_2).

81

Hydrogen peroxide (H_2O_2) excreted in both micro-and macro-algae culture medium has been previously measured using enzymatic methods (Evans et al. 2006) or chemiluminescence (Collén and Pedersén 1996; Collén et al. 1995).

Here, H_2O_2 excreted into the media was measured by an enzymatic assay based on the catalytic reduction of H_2O_2 by horseradish peroxidase in the presence of the H-donor molecule p-hydroxyphenyl acetic acid (POHPAA) to the fluorescent dimer 6,6'-dihydroxy-3,3'-biphenyldiacetic acid (excitation 320 nm, emission 400 nm). H_2O_2 concentration is directly proportional to the fluorescence intensity, as one molecule of the fluorescent dimer is produced for every H_2O_2 molecule (Guilbault et al. 1967). The emitted fluorescence was measured using a simple fluorometer comprising of a phosphor coated mercury lamp (Jelight) as the excitation source, a monochromator to filter out the undesired wavelengths and a photomultiplier tube (Hamamatsu R268) for fluorescence detection. The output of the fluorescence measurements were noted off a digital voltmeter attached to the instrument.

A working stock of fluorescent reagent solution was made with 255 μM POHPAA (Aldrich), 0.25 M Tris and 50 units ml^{-1} of horseradish peroxidase (Aldrich) in distilled water. The pH was adjusted to 8.8 with hydrochloric acid and the fluorescent reagent was stored in the dark at 4°C. For the experimental assay, 0.2 ml of the fluorescent reagent solution was mixed with 3.8 ml of the culture sample and allowed to react for 15 minutes in a plastic cuvette covered with a piece of aluminium foil. The background concentrations of H_2O_2 in the media were determined by measuring fluorescence with and without, the addition of catalase and very low levels of H_2O_2 were noted. A working stock of catalase (Aldrich) was made up to 500 units ml^{-1} in distilled water. For catalase additions, 0.1 ml of the working stock was added to 3.7 ml of the culture sample and allowed to react for 10 minutes before the addition of 0.2 ml fluorescent reagent solution with the additional waiting time of 15 minutes for the reaction to occur. Fluorescence measurements were conducted at exactly at the end of 15 minutes to note the H_2O_2 excretions in the medium.

The assay was calibrated using H_2O_2 standards made up in f/2-Si medium from a 500 nM H_2O_2 stock solution (Fig. 2.6). The standards prepared contained 0, 25, 50 and 100%

of the stock solution (i.e. 0, 125, 250 and 500 nM H_2O_2). The calibration was obtained by relating the voltage signal (in Volts) (y) to H_2O_2 concentration (in nM) (x) (Fig. 2.6). The linear relationship y = mx + c, where 'm' is the slope and 'c' is the intercept, was used to quantify the H_2O_2 concentration in each sample. The limit of detection was 1.63 V based on the lowest concentration used in the calibration, which in this case was a blank (distilled water).
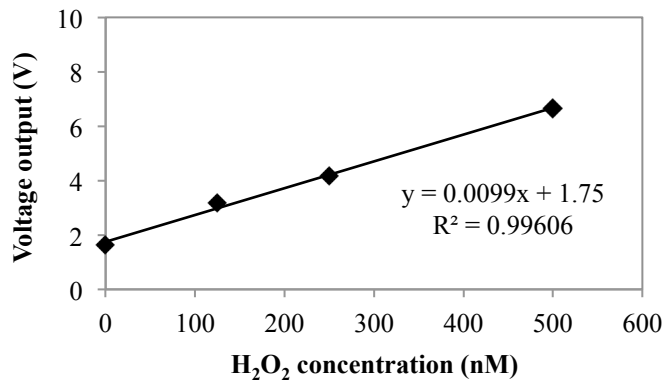
Figure 2.6 Calibration for H_2O_2 measurements using the fluorometer equipped with a digital voltmeter for the output signal. The linear regression curve is shown with its correlation coefficient R^2.

Chapter 3

The Influence of Nutrient Limitation on Intracellular DMSP and DMS Release

Chapter 3: The Influence of Nutrient Limitation on Intracellular DMSP and DMS Release

Some of the data in this chapter are from Franklin et al. 2012 on which I am a co-author. I contributed the DMSP and DMS data and to the nutrient add-back experiments. Other data from the paper will be included in this chapter for context and this will be clearly indicated by appropriate citation. Alterations have been made to fit with the thesis.

Franklin DJ, Airs RL, Fernandes M, Bell TG, Bongaerts RJ, Berges JA, Malin G. 2012. Identification of senescence and death in *Emiliania huxleyi* and *Thalassiosira pseudonana*: Cell staining, chlorophyll alterations, and dimethylsulfoniopropionate (DMSP) metabolism. Limnology and Oceanography 57: 305-317.

Abstract

We measured membrane permeability, hydrolytic enzyme, and caspase-like activities using fluorescent cell stains to document changes caused by nutrient exhaustion in the coccolithophore *Emiliania huxleyi* and the diatom *Thalassiosira pseudonana*, during batch-culture nutrient limitation. We related these changes to cell death, pigment alteration, and concentrations of dimethylsulfide (DMS) and dimethylsulfoniopropionate (DMSP) to assess the transformation of these compounds as cell physiological condition changes. *E. huxleyi* persisted for 1 month in stationary phase; in contrast, *T. pseudonana* cells rapidly declined within 10 d of nutrient depletion. *T. pseudonana* progressively lost membrane integrity and the ability to metabolize 5-chloromethylfluorescein diacetate (CMFDA; hydrolytic activity), whereas *E. huxleyi* developed two distinct CMFDA populations and retained membrane integrity (SYTOX Green). Caspase-like activity appeared higher in *E. huxleyi* than in *T. pseudonana* during the post-growth phase, despite a lack of apparent mortality and cell lysis. Photosynthetic pigment degradation and transformation occurred in both species after growth; chlorophyll *a* (Chl *a*) degradation was characterized by an increase in the ratio of methoxy Chl *a* : Chl *a* in *T. pseudonana* but not in *E. huxleyi*, and the increase in this ratio preceded loss of membrane integrity. Total DMSP declined in *T. pseudonana* during cell death and DMS increased. In contrast, and in the absence of cell death, total DMSP and DMS increased in *E. huxleyi*. Our data show a novel chlorophyll alteration product associated with *T. pseudonana* death, suggesting a promising approach to discriminate nonviable cells in nature.

3.1 Background and significance

Marine primary productivity is fundamentally dependent on the availability of nutrients and many studies have considered nutrient limitation. Several growth experiments on various phytoplankton species have been able to assertively isolate the limiting nutrient using the 'add-back' experimental approach (Franklin et al. 2012) or nutrient addition bioassay experiments on natural phytoplankton populations (Hinz et al. 2012; Moore et al. 2008). In many cases, nitrogen (N) is thought to be the macronutrient most frequently limiting marine phytoplankton growth (Downing et al. 1999; Franklin et al. 2012; Glibert 1988; Gruber 2004) as with the exception of N-fixing marine cyanobacteria, most phytoplankton require combined forms of N like ammonium, nitrate, or nitrite. However, there are findings that imply phosphorus, silica, iron or other factors limiting phytoplankton growth (Bertrand et al. 2011; Murrell et al. 2002; Sylvan et al. 2006; Wu and Chou 2003). Iron (Fe) has received much attention as the limiting nutrient in open ocean areas because it is sometimes only available in extremely low amounts. Fe derives mainly from leaching from rocks and can be delivered to the ocean in dust storms. N-fixing organisms generally have a high Fe requirement and so Fe-limitation also limits nitrogen fixation (Moore et al. 2009).

In near-shore and temperate waters in spring, most of the N in seawater is present as nitrate. During the growth season, autotrophic organisms use nitrate for growth and convert it into other forms of N, especially organic N and ammonium. In summer, nitrate is depleted in large parts of the surface waters (Glibert 1988) leading to higher concentrations of dissolved organic N compounds than the concentration of inorganic N (Antia et al. 1991; Braven et al. 1984). Affected by such conditions, it would be beneficial for phytoplankton to have the ability to use organic N sources in addition to inorganic N (Flynn and Butler 1986). *Emiliania huxleyi* has been shown to take up organic N species, such as some amino acids, purines, amides, and urea (Palenik and Henson 1997), although the use of dissolved organic N differs among *E. huxleyi* strains (Strom and Bright 2009). The uptake of ammonium and urea during blooms has also been reported from field observations in Norwegian fjords and the North Sea (Lessard et al. 2005).

Phosphorus (P) can be limiting primary producers in marine, freshwater and terrestrial environments (Elser et al. 2007) like the Chesapeake Bay which receives large amounts of freshwater (Fisher et al. 1999) and tropical coastal regions where sequestration of P in calcareous sediments is thought to initiate P limitation (Smith 1984). Interestingly, the North Pacific subtropical gyre which was previously thought to be N-limited is gaining attention due to recent evidence for P-limitation. It has been suggested that this change may have led to the dominance of the prokaryotic picophytoplankton in these oligotrophic waters (Karl et al. 2001). Phosphorus in the form of orthophosphate is also known to be limiting in the eastern Mediterranean sea (Krom et al. 2004; Thingstad et al. 2005) and the Sargasso Sea (Cotner et al. 1997)

In temperate regions, *E. huxleyi* blooms often occur after a diatom spring bloom as the water column becomes stratified and macronutrients such as nitrate, phosphate, and silicate are low (Iglesias-Rodríguez et al. 2002; Tyrrell and Taylor 1996). Several studies have shown that *E. huxleyi* outcompetes other phytoplankton at high N:P rather than low N:P ratios (Riegman et al. 1992), but *E. huxleyi* blooms have also been observed in both low- and high-N:P waters (Tyrrell and Merico 2004). A modelling study in the north east Atlantic indicated that low phosphate concentrations in combination with high light were most likely to cause *E. huxleyi* blooms (Tyrrell and Taylor 1996), whereas a modelling study for the Black Sea found low nitrate concentrations combined with high light most likely to trigger *E. huxleyi* blooms (Oguz and Merico 2006). Lessard et al. (2005) examined the environmental conditions associated with several *E. huxleyi* blooms in the North Atlantic and North Sea from 1991-1997 and concluded that most blooms occur in NO_3-limited waters. These observations reveal the competitive nature of *E. huxleyi* strains to exploit conditions when either nitrogen or phosphorus are in short supply.

In aerobic organisms reactive oxygen species (ROS) are products of normal metabolism and in photosynthetic organisms the chloroplasts are a major source of ROS. Primary producers can increase the production of antioxidants and antioxidant enzymes to deal with ROS (Lesser and Shick 1989), but oxidative stress occurs when a cell's capacity for dealing with them is exceeded. Nutrient limitation can disrupt photosynthesis and

enhance oxidative stress. It also decreases in the synthesis of nitrogen-rich antioxidant enzymes like ascorbate peroxidase (Logan et al. 1999) and reduces the activity of enzymes that repair oxidative damage (Litchman et al. 2002). The D1 and D2 proteins are critical components of the photosystem II reaction centre. During photosynthesis these proteins, especially D2, turn over very rapidly due to light-induced damage and are constantly replaced. When the rate of repair cannot keep up with the damage due to photo-inactivation the result is photo-inhibition (Allakhverdiev and Murata 2004; Nishiyama et al. 2006; Ragni et al. 2008) and a reduction in variable to maximum photosystem II fluorescence (F_V/F_M) (Berges and Falkowski 1998).

Sunda et al. (2002) proposed that phytoplankton may produce the N-free compound dimethylsulphoniopropionate (DMSP) as an antioxidant under N-limited conditions. Their calculations show that DMSP and its enzymatic cleavage products have high reaction rate constants with hydroxyl radicals and they suggested that these compounds would scavenge these harmful radicals under conditions of oxidative stress. Some studies have shown that nitrogen limitation leads to increased DMSP concentration (Keller and Bellows 1996; Stefels et al. 2007; Turner et al. 1988). For example, a 2.6-fold increase in intracellular DMSP (from 1.6-4.3 mM) was observed in the nitrogen-replete diatom *Thalassiosira pseudonana* CCMP 1335 cultures at the onset of nitrogen starvation (Hockin et al. 2012) and a further 3 days into the stationary phase resulted in an increase in concentration to about 18 mM (Nicola Hockin, personal communication). Another study on the same diatom species and strain under N-limitation, also reported an increase in intracellular DMSP (Bucciarelli and Sunda 2003). In addition, Harada et al. (2009) found that when the diatom *T. oceanica* grown in low-nitrate conditions approached stationary phase, intracellular DMSP concentration increased from 2.1 to 15 mM in 60 h and previously a study on the unicellular alga *Tetraselmis subcordiformis* (prasinophyceae) showed a 75% increase in DMSP within 24 h, in response to nitrogen deficiency (Gröne and Kirst 1992). Batch cultures of *Hymenomonas carterei* and *Skeletonema costatum* also show increased DMS concentrations during the stationary phase (Vairavamurthy et al. 1985; Vetter and Sharp 1993). Also, *E. huxleyi* grown in low nitrate showed a 31% higher DMSP per cell (Turner et al. 1988). It was also seen that the average intracellular DMSP concentration (95 mM) in natural phytoplankton

from low nitrate (NO_3 < 0.2 μM) coastal seawater samples was higher than in the nearby high nitrate waters (DMSP = 37 mM), even though there was no pronounced difference in phytoplankton species composition (Turner et al. 1988).

Phosphate is an important component of DNA, RNA, phospholipids and ATP. A significant decrease in RNA and ATP per cell was observed in P-deficient diatoms (Sakshaug and Holm-Hansen 1977) and decreases in membrane phospholipids under P-limitation have been observed in the diatom *Ditylum brightwellii* (Brussaard et al. 1997). P-limitation hampers the synthesis of RNA and ATP, leading to an overall decrease in the rate of protein synthesis. In the case of the proteins present in the photosynthetic apparatus and active in the Calvin-Benson cycle, P-limitation results in a decrease in the rates of light utilization and carbon fixation (Falkowski and Raven 1997). The inhibition of protein synthesis under P-limitation may therefore lead to effects on cell metabolism and, whilst oxidative stress can occur, the effect is indirect and slower than that seen with N-limitation. P-limitation appears to cause a smaller increase in cellular DMSP than limitation by other nutrients (Bucciarelli and Sunda 2003). Besides under N- and P-limitation, Sunda et al. (2002) also observed that intracellular DMSP concentration increases in *Emiliania huxleyi*, *Thalassiosira pseudonana* and *Skeletonema costatum* when growth is limited due to CO_2 or Fe limitation.

Nutrient limitation can often affect normal processes within a phytoplankton cell, thereby enhancing oxidative stress and as mentioned above, some studies suggest DMSP up-regulation, which has led to the proposed antioxidant role of DMSP. Here an attempt is made to examine cellular physiological responses to N- and P-limitation and how DMSP and DMS concentrations alter with nutrient limitation in three strains of *E. huxleyi* and to examine the relationship between cell death and DMSP and DMS content. The nutrient-limitation experiments carried out in Franklin et al. 2012 presented me with the challenge and the opportunity to work on, as well as compare the responses of another major bloom-forming silicifying phytoplankton species, namely the diatom *T. pseudonana* with a rather different ecology and intracellular DMSP concentration, with that of the calcifying *E. huxleyi* species.

3.2 Methodology

3.2.1 Nutrient-limitation and nutrient add-back conditions for experiments with *Emiliania huxleyi* and *Thalassiosira pseudonana* (Franklin et al. 2012)

3.2.1.1 Culture conditions and growth measurements

Franklin, D. grew duplicate unialgal cultures of *E. huxleyi* 1516 (CCMP; calcifying) and *T. pseudonana* 1335 (CCMP) in 500 mL of ESAW/5 media (enriched seawater, artificial water; Harrison et al. 1980) in 1 L borosilicate conical flasks and carried out the sub-sampling and most measurements. ESAW/5 is enriched with $NaNO_3$, NaH_2PO_4, Na_2SiO_3 etc). Silicate was omitted in the medium for *E. huxleyi*. Light was supplied at 100 μmol photons m^{-2} s^{-1} (Biospherical Instruments QSL 2101) from cool white fluorescent tubes, on a 14:10 h light:dark cycle (08:00 h to 22:00 h) at a constant temperature of 17°C. To minimize the presence of dead cells and debris in the cultures at the beginning of the experiment, cultures were grown in semi-continuous mode and closely monitored before measurements commenced. Each day at 10:00 h biomass was quantified as cell volume, or coccosphere volume in the case of *E. huxleyi*, (Coulter multisizer) and fluorescence (Phyto-PAM). The efficiency of Photosystem II (F_V:F_M; 30-min dark acclimation) was measured at the same time.

3.2.1.2 Fluorescent cell staining and flow cytometry

Franklin, D. also did the fluorescent staining analyses with three molecular probes: SYTOX Green a 'dead' cell indicator (Veldhuis et al. 1997) (also see Chapter 2.7), 5-chloromethylfluorescein diacetate (CMFDA) a 'live' cell indicator, that undergoes enzymatic cleavage indicating the hydrolytic enzymatic activity (Garvey et al. 2007) and a fluorescein isothiocyanate conjugate of carbobenzoxy-valyl-alanyl-aspartyl-[O-methyl]-fluoromethylketone to label cells containing activated caspases (CaspACE; Promega G7462) and detect caspase-like activity. CMFDA (Invitrogen C2925) was diluted to 1 mM in acetone prior to use (Peperzak and Brussaard 2011) and aliquoted

and stored at -20°C. It was added to a final concentration of 10 µM and incubated for 60 min under the culture temperature and light conditions. SYTOX Green and CMFDA final concentration and incubation time were optimized prior to use with heat-killed cells (80°C, 5 min) and the maximum fluorescence ratio approach (Brussaard et al. 2001). Franklin, D. used an adaptation of the protocol of Bidle and Bender (2008) to detect caspase-like activity: CaspACE was added to cells at a final concentration of 0.5 µM and incubated for 30 min at culture temperature in the dark, before flow cytometric analysis. Working stocks of all stains were stored at -20°C before use. Milli-Q water was used as the sheath fluid, analyses were triggered on red fluorescence using lo flow (~ 20 µL min^{-1}) and 10,000 events were collected. An event rate between 100 and 400 cells s^{-1} was used to avoid coincidence and when necessary samples were diluted in 0.1-µm-filtered artificial seawater prior to analysis. Flowset beads (Beckman-Coulter) were analyzed at the beginning of each set of measurements, and bead fluorescence was used to normalize stain fluorescence (Marie et al. 2005).

3.2.1.3 Other analyses

In the nutrient-limitation growth experiment described in section 3.2.1 above, photosynthetic pigments were measured by Airs, R. L. (methods detailed in Franklin et al. 2012) while I carried out the DMSP and DMS measurements (methods detailed in Chapter 2.6). In addition, nutrient add-back experiments to establish the limiting nutrient were carried out by Bell, T. and I (detailed below in section 3.2.1.4).

3.2.1.4 Nutrient add-back conditions

In the nutrient add-back experiment, duplicate unialgal cultures of *E. huxleyi* 1516 (CCMP; calcifying) and *T. pseudonana* 1335 (CCMP) were grown as described in section 3.2.1.1 At the onset of stationary phase when the biomass was approximately 2.5 x 10^6 cells ml^{-1} for both species, the cultures were diluted 1 in 20. This was repeated twice before starting the experiment. Filter sterilised nutrients were added (see below) when cell density was at about 2 x 10^6 cells ml^{-1} to bring the nitrate, phosphate and/or silicate (*T. pseudonana* only) concentration back to that of standard ESAW/5 medium.

For each treatment, duplicate 500 ml cultures were set-up in 1 L flasks and 5 ml samples were drawn daily for the duration of both experiments and cell density, cell volume and photosynthetic capacity were monitored.

3.2.2 Nitrate-free (N_0), Phosphate-free (P_0) and nutrient add-back conditions for experiments with three *Emiliania huxleyi* strains

Triplicate cultures of *E. huxleyi* 370, 373 and 1516 were grown to mid-log phase in ESAW medium (silicate-free) in 2 L conical flasks. The cells were pre-concentrated by centrifugation (5000 rpm or 5310 g; 17°C for 5 mins) to reduce carry-over of nutrients in the ESAW medium. Coulter counter analysis showed that only about 2000 cells per ml remained in the supernatant which represented only ~ 3% of the original cells. The cell pellets were resuspended in N_0 and P_0 media and aliquots (10 ml) were used to innoculate triplicate 250 ml flasks with 140 ml of (a) standard ESAW medium (control), (b) nitrate-free ESAW (N_0) and (c) phosphate-free ESAW (P_0). The initial cell density was ~ 65,000. Cell counts measurements verified that cells were transferred quantitatively and F_V:F_M and fluorescence were not affected after the transfer.

Cells were acidified to check whether the cell volume increases observed were due to coccolith formation during N- and P-limitation. For this, concentrated HCl was added to the culture sample to get a final concentration of 3.6 mM (Buitenhuis et al. 2008). The sample was left for one minute for the coccoliths to dissolve and immediately cell volume and cell diameter measurements were carried out using the Coulter multisizer and the cells were also examined under the microscope.

After three days growth in the N- and P-free media, the respective nutrient was added back to the culture flasks to bring the media back to the 549 μM nitrate and 22.4 μM phosphate concentration of standard ESAW medium.

Throughout the experiment all cultures were monitored daily for cell density, cell volume, fluorescence, photosynthetic capacity, membrane permeability using SYTOX Green staining and DMS and DMSP content (see Chapter 2 for methods).

3.3 Results

3.3.1 *E. huxleyi and T. pseudonana* in nutrient-limited and add-back conditions (Franklin et al. 2012)

3.3.1.1 Cell culture growth measurements

Under the culture conditions used, *E. huxleyi* 1516 and *T. pseudonana* 1335 both achieved a specific growth rate (μ; d^{-1}) of 0.6 and a final cell density of $\sim 2.5 \times 10^6$ cells ml^{-1}. Stationary phase commenced around day 8. *E. huxleyi* cell number remained constant for 20 d after this, whereas *T. pseudonana* cell number began to decline after 5 d into stationary phase, and by day 28, had declined by 65% (Fig. 3.1A). The coccosphere volume of *E. huxleyi* increased from a mean of about 35 μm^3 during the growth phase to almost 80 μm^3 at the end of the stationary phase. *T. pseudonana* also increased in cell volume, but by less than *E. huxleyi* coccosphere volume and the increase in cell volume stabilized after the growth phase at about 50 μm^3 (Fig. 3.1A). Dark-acclimated $F_V:F_M$ (maximum Photosystem II efficiency [PSII efficiency] or photosynthetic capacity) declined from a maximum of 0.6 in early log-phase to zero in *T. pseudonana* at day 11 in stationary phase while dark-acclimated $F_V:F_M$ remained in the range of 0.48-0.58 in *E. huxleyi* (Fig. 3.1B). In both species, cell fluorescence dropped after the onset of stationary phase (Fig. 3.1C).
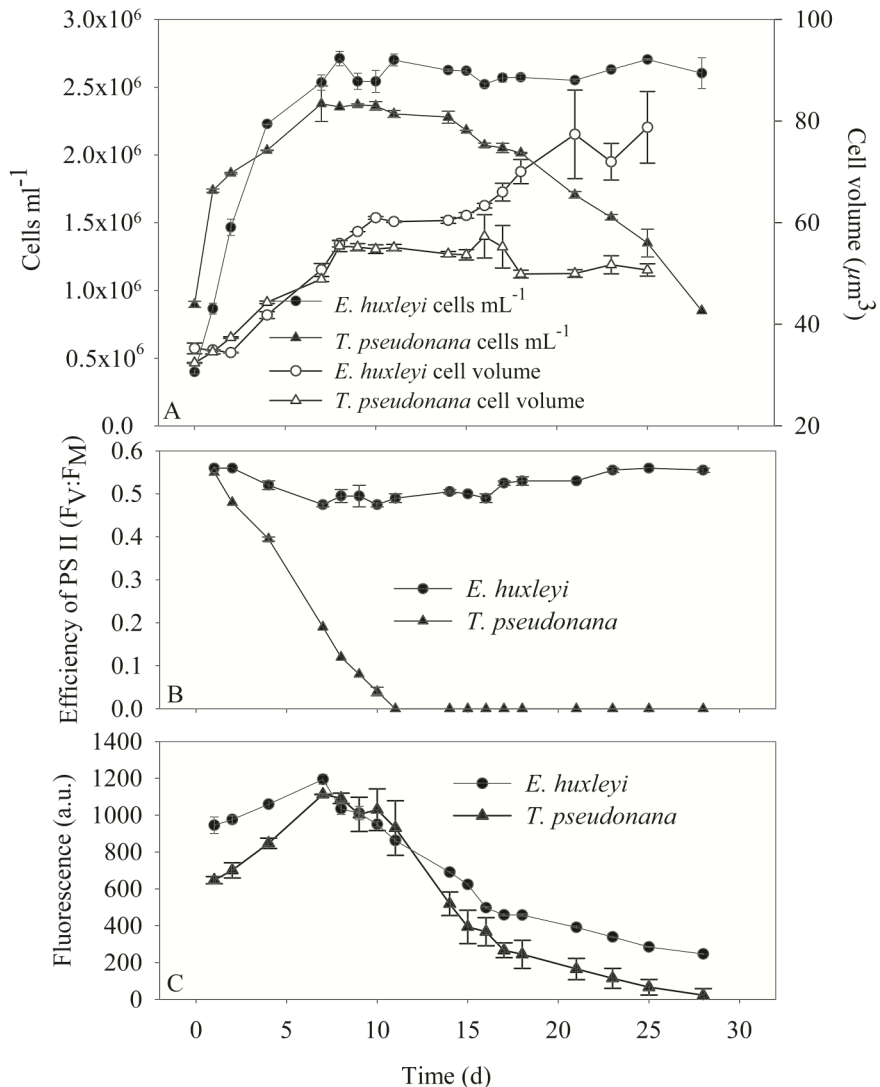
Figure 3.1 (A) Cell density and cell volume, (B) efficiency of photosystem II (F_V:F_M) and (C) in vivo fluorescence in *Emiliania huxleyi* 1516 and *Thalassiosira pseudonana* 1335 batch cultures (duplicate cultures, mean and standard error shown during 28 days in batch culture from Franklin et al. (2012)).

3.3.1.2 SYTOX Green staining

Throughout the whole experiment, *E. huxleyi* showed < 5% SYTOX labeled cells; signifying that almost all cells had undamaged plasma membranes. In contrast, the *T. pseudonana* cultures had low levels of labeled cells (< 2%) until the stationary phase, and then promptly increased to a maximum of 25% by the end of the monitoring period (Fig. 3.2B).
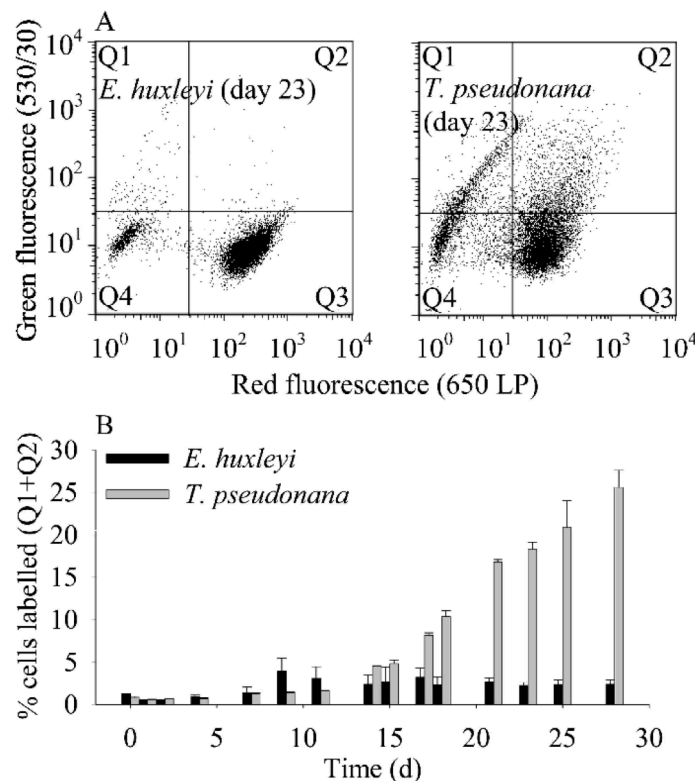
Figure 3.2 SYTOX Green staining for membrane permeability in *Emiliania huxleyi* and *Thalassiosira pseudonana* during nutrient depletion in batch culture over 28 days (A) representative flow cytometry plots (day 23). (B) % of SYTOX-stained cells (mean and standard error; two replicates). In (A) and (B) Q1 + Q2 = stained cells, where Q1 = stained debris and cells with low red fluorescence, and Q2 = stained normal cells, Q3 = unstained normal cells, and Q4 = unstained debris and low-red cells (from Franklin et al. (2012)).

3.3.1.3 CMFDA and CaspACE staining

Results from the CMFDA and CaspACE staining have been discussed at length by Franklin et al. (2012). Over the 28 d monitoring period, CMFDA staining resulted in two distinct cell populations in *E. huxleyi*: one with high red and high green fluorescence, progressively increasing their CMFDA metabolism in the stationary phase and the other was about 20% of cells with high red but low green fluorescence which did not metabolize the probe and was comparable to the unstained cells. *T. pseudonana* showed a single cell population of high red and high green fluorescence involved in metabolizing the probe. These cells showed a decline in CMFDA fluorescence during the 28 d monitoring period. CaspACE fluorescence staining increased with time in *E. huxleyi*, while no obvious trend was seen in *T. pseudonana*.

3.3.1.4 Photosynthetic pigments

Data from the photosynthetic pigment analyses is detailed in Franklin et al. (2012). *T. pseudonana* exhibited a steady increase in the ratios of methoxychlorophyll *a* : Chl *a,* hydroxychlorophyll *a* : Chl *a* and carotenoid : Chl *a* during the transition from active growth to stationary phase. No increase in the ratios of methoxychlorophyll *a* : Chl *a* and hydroxychlorophyll *a* : Chl *a* was observed in *E. huxleyi,* however the carotenoid : Chl *a* ratio remained constant.

3.3.1.5 DMSP and DMS

As anticipated, *E. huxleyi* displayed a higher intracellular DMSP content (DMSPp per cell volume; Fig. 3.3a) ranging between 100 to 120 mM, whereas in *T. pseudonana* there was a prominent increase in DMSPp per cell volume from days 0 to 10 from 0.7 to 35 mM. Within the stationary or death phase, consistent concentrations of DMSPp per cell volume of ~ 120 mM in *E. huxleyi* and 35 mM in *T. pseudonana* were seen. DMSPp per cell displayed a definite increasing trend from 4 to 10 fmol per cell in *E. huxleyi* and a distinct increase of 0 to 2 fmol per cell from days 0 to 10 in *T. pseudonana,* followed by a very gradual increase from 2 to 3 fmol per cell in the stationary or death phase (Fig. 3.3b). Over the whole timecourse the DMSPp concentration in the *E. huxleyi* culture
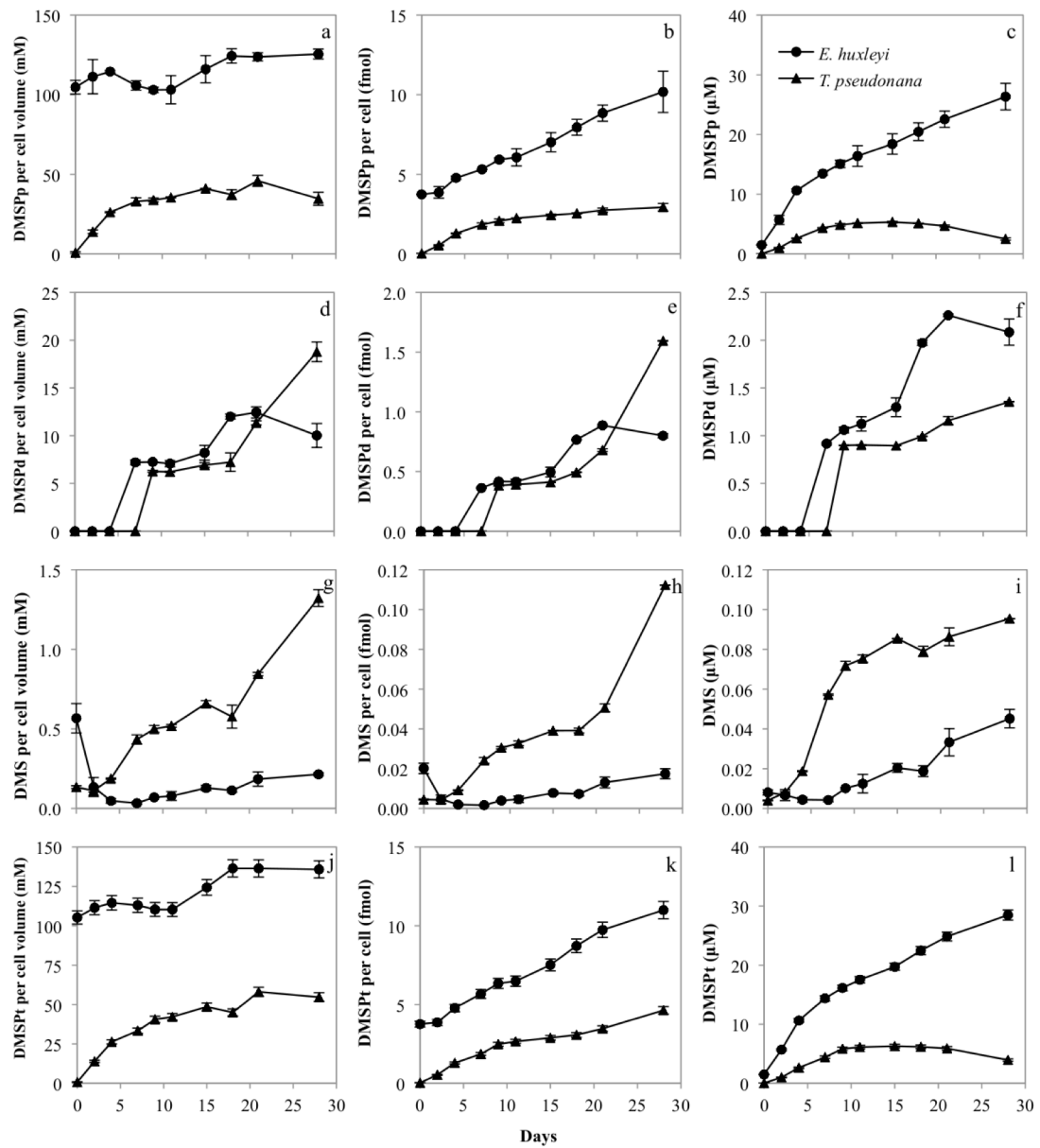
Figure 3.3 Effect of nutrient exhaustion in duplicate batch cultures of *E. huxleyi* 1516 and *T. pseudonana* 1335 on (a) DMSPp per cell volume (mM), (b) DMSPp per cell (fmol), (c) DMSPp (µM) (d) DMSPd per cell volume (mM), (e) DMSPd per cell (fmol), (f) DMSPd (µM) (g) DMS per cell volume (mM), (h) DMS per cell (fmol), (i) DMS (µM) (j) DMSPt per cell volume (mM) (k) DMSPt per cell (fmol) and (l) DMSPt (µM). The average value and range of data is shown (n=2). Where no range bars are visible, the data range was smaller than the symbol size.

showed an increasing trend from 2 to 25 µM, while for *T. pseudonana* a distinct increase from 0 to 5 µM was seen in the log phase of growth, the concentration remained

consistent at 5 μM in the stationary phase and then decreased in the death phase to 3 μM on the last day of the monitoring period (Fig. 3.3c).

Dissolved DMSP (DMSPd) increased in both species after the growth phase, reaching a maximum of 2.26 μM in *E. huxleyi* and 1.36 μM in *T. pseudonana* (Fig. 3.3f). DMSPd per cell volume was below detection in *T. pseudonana* in the log-phase, increased to a consistent value of 6 mM in the stationary phase and increased further still to a concentration of 19 mM on day 28 (Fig. 3.3d). DMSPd per cell volume was also non-detectable in the *E. huxleyi* cultures in the log phase, but it increased to 7 mM by day 7 and then again increased to 12.5 mM at day 21 before decreasing to 10 mM in the late stationary phase (Fig. 3.3d). DMSPd per cell also increased after the growth phase to about 0.4 fmol in both species, but a more distinctive increase to 1.6 fmol per cell was seen in *T. pseudonana*, while in contrast, a decrease to 0.8 fmol per cell was observed in *E. huxleyi* in the late stationary phase (Fig. 3.3e).

A distinct increasing trend was seen in the concentration of DMS in both cultures over the course of the experiment. Higher DMS concentrations increasing from 0.004 μM to 0.095 μM were observed in *T. pseudonana* with a substantial jump in concentration between days 4 and 7, whereas in the *E. huxleyi* cultures, DMS exhibited an increase from 0.008 μM to 0.045 μM (Fig. 3.3i). DMS per cell volume was also higher in *T. pseudonana* displaying an increasing pattern from 0.1 to 1.3 mM compared to a low but gradual increase from 0.04 to 0.2 mM in *E. huxleyi* (Fig. 3.3g). The DMS per cell patterns displayed in both species followed the same trend as of DMS per cell volume. In *T. pseudonana*, DMS per cell increased from 0.004 to 0.11 fmol and in *E. huxleyi* from 0.002 to 0.02 fmol per cell (Fig. 3.3h).

Over the course of the experiment, total DMSP (DMSPt) increased with time in *E. huxleyi* cultures, whereas *T. pseudonana* showed no substantial relationship with time (Fig. 3.3l). Within the *T. pseudonana* data set, however, a decline in DMSPt is suggested within the stationary or death phase (Fig. 3.3l). DMSPt per cell volume (Fig. 3.3j) as expected, followed a similar trend as seen in DMSPp per cell volume (Fig. 3.3a), with an increase from 100 to 130 mM in *E. huxleyi* and from below detection to 60 mM in *T. pseudonana*. DMSPt per cell (Fig. 3.3k) in both species, as expected, followed a similar

trend as seen in DMSPp per cell (Fig. 3.3b), with an increase from 4 to 11 fmol in *E. huxleyi* and from 0 to 4.5 fmol per cell in *T. pseudonana*.

The increasing trend in DMSPp (Fig. 3.3c) or DMSPt (Fig. 3.3l) is not reflected in DMSPp per cell volume (Fig. 3.3a) in *E. huxleyi* perhaps due to the increasing coccosphere volume in stationary phase (Fig. 3.1A). Thus DMSPp per cell volume although observed to be constant, may be masked by the coccosphere volume increase.

3.3.1.6 Nutrient add-back to *E. huxleyi* and *T. pseudonana*

Bell, T. and I performed nutrient 'add-back' experiments to test what controlled limitation (Fig. 3.4; data not shown in Franklin et al. 2012). These experiments indicated that for *T. pseudonana,* nitrogen caused growth limitation; when nitrate was added back, cell numbers increased from 1.6 to 2.8 x 10^6 cells ml^{-1} (Fig. 3.4b). The pattern for *E. huxleyi* was less clear with cell numbers increasing from 2.15 to 2.25 x 10^6 cells ml^{-1} on adding back nitrate and 2.03 to 2.09 x 10^6 cells ml^{-1} on adding back phosphate (Fig. 3.4a). By calculation, nitrogen should have been limiting in both species at this point assuming cells were using nutrients in the Redfield ratio (Franklin et al. 2012). Importantly, fluorescence increased for both species upon nitrate addition indicating nitrate as the limiting nutrient. There was a very slight increase in fluorescence when phosphate was added back to *E. huxleyi*, but no increase above the control when phosphate or silicate were added back to *T. pseudonana* (Fig. 3.4 e, f). Photosynthetic capacity did not show any differentiating trends between the control versus the nitrate or phosphate add-backs in *E. huxleyi* (Fig. 3.4c). In contrast, nitrate add-back in *T. pseudonana* delayed the decrease in cell photosynthetic capacity by 2 days compared with the control, phosphate and silicate addition cultures (Fig. 3.4d).
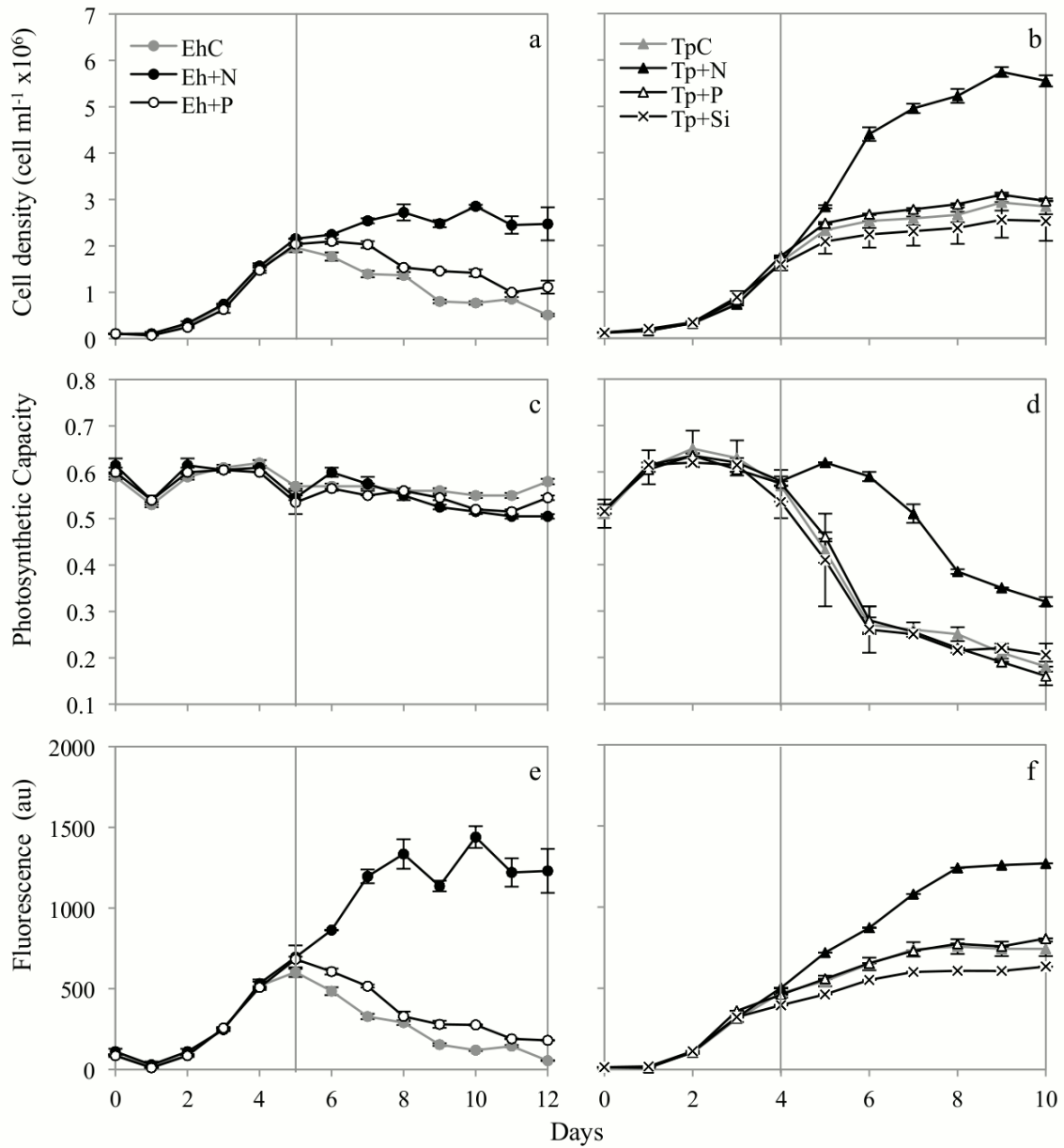
Figure 3.4 Examining the consequences of nutrient add-back to *E. huxleyi* 1516 (circles) and *T. pseudonana* 1335 (triangles) on cell density (a, b), photosynthetic capacity (c, d) and fluorescence (e, f) (au = arbitrary unit). The grey circles/triangles denote control cultures (no nutrient add-back); the black solid symbols denote nitrate add-back; the hollow symbols denote phosphate add-back and the cross symbols (x) denote silicate add-back (only to *T. pseudonana*). The nutrients were added back on day 5 in *E. huxleyi* and on day 4 in *T. pseudonana*, as shown by the vertical grey lines. The average value and range of data is shown (n=2). Where no range bars are visible, the data range was smaller than the symbol size.

3.3.2 Three *E. huxleyi* strains in Nitrate-free (N_0), Phosphate-free (P_0) media and add-back conditions

3.3.2.1 Cell culture and growth measurements

During the exponential growth phase, the specific growth rate ($\mu;d^{-1}$, n = 3) was 0.65 for all the three control strains (Fig. 3.5d, e, f and Fig. 3.6d, e, f) although the final cell density (Fig. 3.5a, b, c and Fig. 3.6a, b, c) varied as follows: *E. huxleyi* 370 = 4 x 10^6 cells ml^{-1}, *E. huxleyi* 373 = 3 x 10^6 cells ml^{-1} and *E. huxleyi* 1516 = 7 x 10^6 cells ml^{-1}. In both N_0 and P_0 media, the cell density increased for a few days and then remained constant (Fig. 3.5a, b, c and Fig. 3.6a, b, c), more visibly reflected in the log plots (Fig. 3.5d, e, f and 3.6d, e, f). This continued increase in cell density was probably due to utilisation of residual nutrients in the media or cell reserves. On day 7, following the nutrient add-back on day 6, only a minimal increase was seen in cell numbers after nitrate was added (Fig 3.5a, b, c): from 0.65 to 0.69 x 10^6 cells ml^{-1} in *E. huxleyi* 370; from 0.16 to 0.23 x 10^6 cells ml^{-1} in *E. huxleyi* 373 and from 0.7 to 0.93 x 10^6 cells ml^{-1} in *E. huxleyi* 1516, but there was a more marked increase with phosphate addition (Fig 3.6a, b, c): from 0.45 to 1.06 x 10^6 cells ml^{-1} in *E. huxleyi* 370; from 0.15 to 0.36 x 10^6 cells ml^{-1} in *E. huxleyi* 373 and from 0.47 to 1.06 x 10^6 cells ml^{-1} in *E. huxleyi* 1516.

Cell volume was affected differently under limitation by the two different nutrients. Cell volume increased in N_0 and P_0 cultures but this was more marked for *E. huxleyi* 373 under both treatments (Fig 3.5h, 3.6h) and for phosphate across all 3 strains (Fig 3.6g, h and i). Under P_0 conditions, cell volume in *E. huxleyi* 370 and 373 increased from ~ 30 to 100 μm^3 but only from ~ 25 to 60 μm^3 in *E. huxleyi* 1516 (Fig. 3.6g, h, i). By naked eye, the *E. huxleyi* cultures turned milky-white in the P_0 conditions whereas there was more colouration in the N_0 cultures suggesting coccolith formation under P_0 conditions. Microscopic observations confirmed this and the increase in cell diameter was seen with the Coulter Multisizer. Brief acidification of the P-limited cells showed a characteristic drop in cell volume whereas such a drop was not observed in the N-limited cells. However, even after the coccolith removal the P-limited cells were still bigger than those in the control cultures (Fig. 3.6g, h, i). Again the difference was substantial for *E.*

huxleyi 373 (Fig 3.6h). The increase in cell volume seen after acidification of the P-limited cells was similar to the increase seen in the N-limited cells without acidification, indicating that nutrient limitation causes increase in cell volume. Ignoring such increases in cell volume when nutrients are in short supply would make a substantial difference when computing intracellular DMSP concentrations. The add-back of the limiting nutrient led to a notable decrease in cell volume in both the N_0 and P_0 cultures. In *E. huxleyi* 370 and 1516 cell volumes returned to those in the control cultures by day 10 (Fig. 3.5g, i and 3.6g, i).
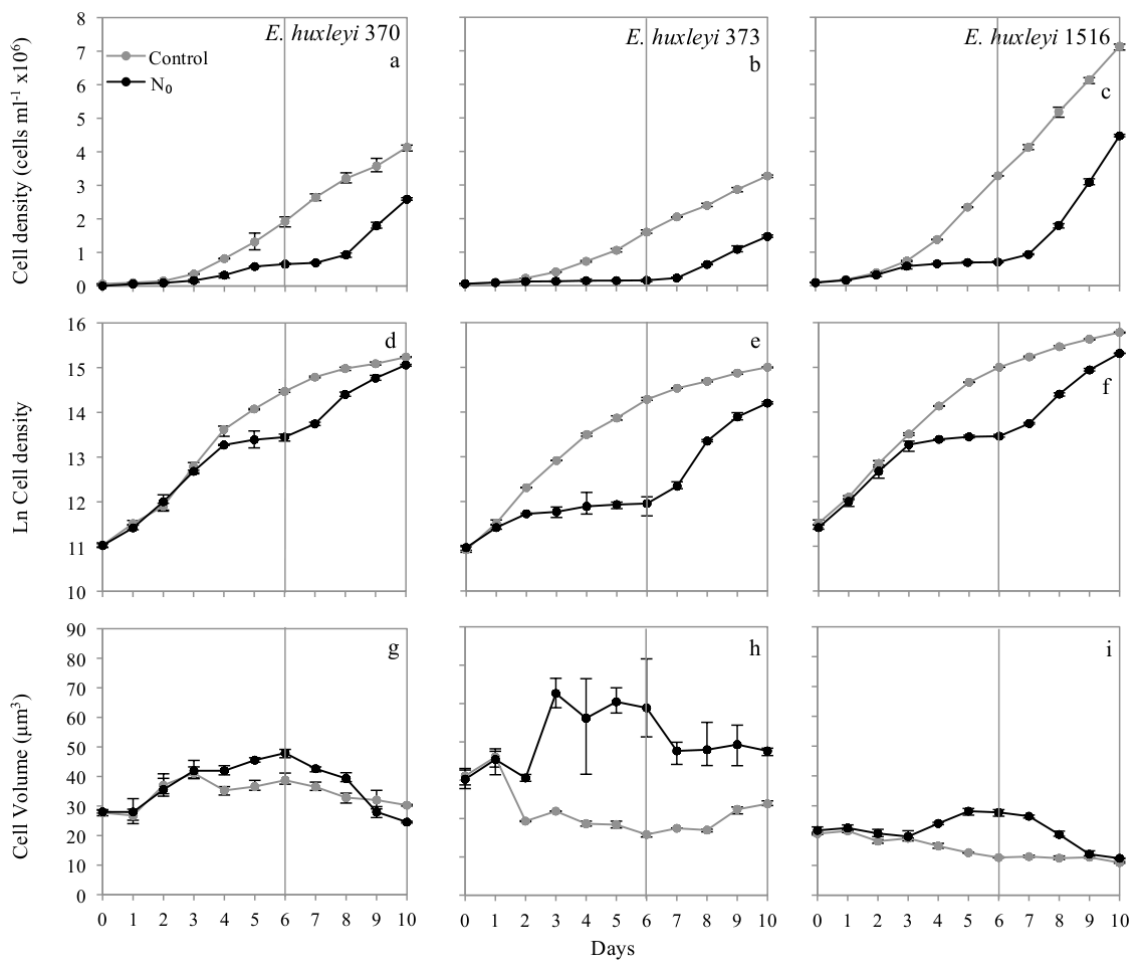
Figure 3.5 Impact of nitrogen limitation (N_0) on *E. huxleyi* 370, 373 and 1516 on cell density (a, b, c), growth curve (d, e, f) and cell volume (g, h, i). The grey symbols represent the control culture and the black symbols represent the culture growing in N-free media. On day 6 (vertical grey line), nitrate was added back to the N-free flasks. The average value and range of data is shown (n=3). Where no range bars are visible, the data range was smaller than the symbol size.
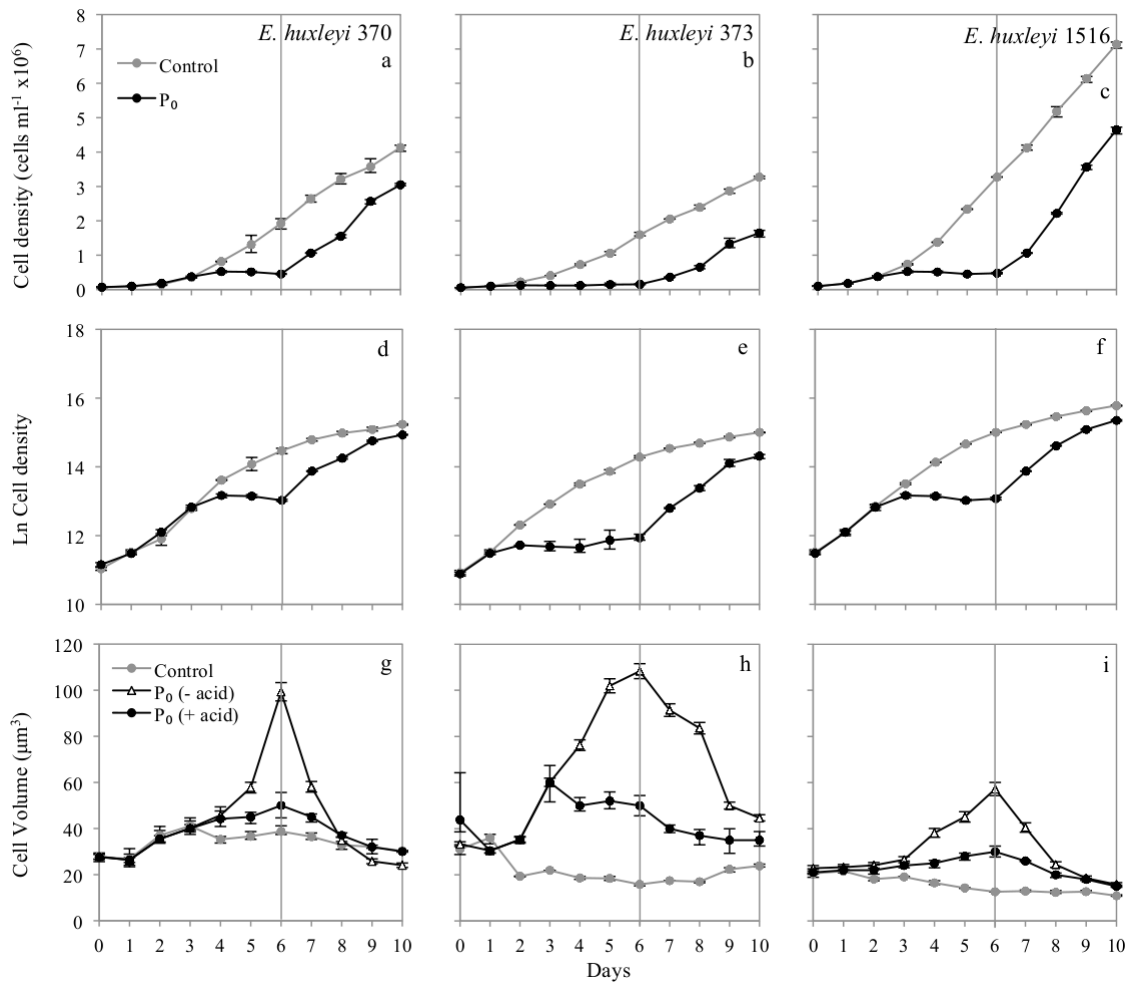
Figure 3.6 Impact of phosphate limitation (P_0) on *E. huxleyi* 370, 373 and 1516 on cell density (a, b, c), growth curve (d, e, f) and cell volume (g, h, i). The grey symbols represent the control culture and the black symbols represent the culture growing in P-free media. In the cell volume data plots (g, h, i) triangles denote standard cell volume measurements and the solid circles show cell volumes after the addition of acid to dissolve the coccoliths. On day 6 (vertical grey line), phosphate was added back to the P-free media. The average value and range of data is shown (n=3). Where no range bars are visible, the data range was smaller than the symbol size.

Fluorescence in N_0 and P_0 cultures followed a similar trend as that of the cell density plots. Note that on days 9 and 10 of the experiment some of the cultures appeared to enter stationary phase, but this was due to fluorescence detection being saturated on the phyto-PAM instrument (Fig. 3.7b, c and Fig. 3.8b, c). The add-back of the respective nutrient led to a renewed increase in the fluorescence of the N_0 and P_0 cultures (Fig. 3.7a, b, c and Fig. 3.8a, b, c).

Photosynthetic capacity (or photosynthetic efficiency of the photosystem II; F_V/F_M) in N_0 and P_0 cultures did not display a definite trend but remained almost in the range of 0.5 to 0.6 throughout the deprivation period (Fig. 3.7d, e, f and Fig. 3.8d, e, f). The add-back of N and P into the media, resulted in higher photosynthetic capacity of the previously-deprived cells compared to the cells of the control cultures of *E. huxleyi* 370 and 1516, however, a decrease in photosynthetic capacity up to 0.4 was noted in *E. huxleyi* 373 (Fig. 3.7d, e, f and Fig. 3.8d, e, f).

3.3.2.2 SYTOX Green staining

On days 1 and 2, up to 17% of the control cells of all three strains were SYTOX Green labeled (Fig. 3.7j, k, l and 3.8j, k, l) and up to 20% cells of all three strains were labeled in the P_0 condition while in the N_0 condition, 23% cells had compromised membranes in *E. huxleyi* 370, 17% in *E. huxleyi* 373 and up to 26% in *E. huxleyi* 1516. Mirroring the labeled cells on days 1 and 2, the percentage of viable cells was low at about 70% increasing to over 90% by day 10 (Fig. 3.7g, h, i and Fig 3.8g, h, i) in both N_0 and P_0 conditions. At the first two time points, the high number of labeled cells and low number of viable cells may have been due to the combined effects of centrifugation during the transfer of the cells to N- and P-free media and the initial shock from the change in media.

Throughout the 10 days of the experiment this stain indicated similar trends in the percentage of viable cells for control and N_0 cultures of all three *E. huxleyi* strains (Fig. 3.7g, h, i). However, such a similarity was not observed between the control and P_0 cultures in either of the three *E. huxleyi* strains (Fig. 3.8g, h, i). The percentage of viable P-deprived cells followed the control, but later decreased in comparison to the viable
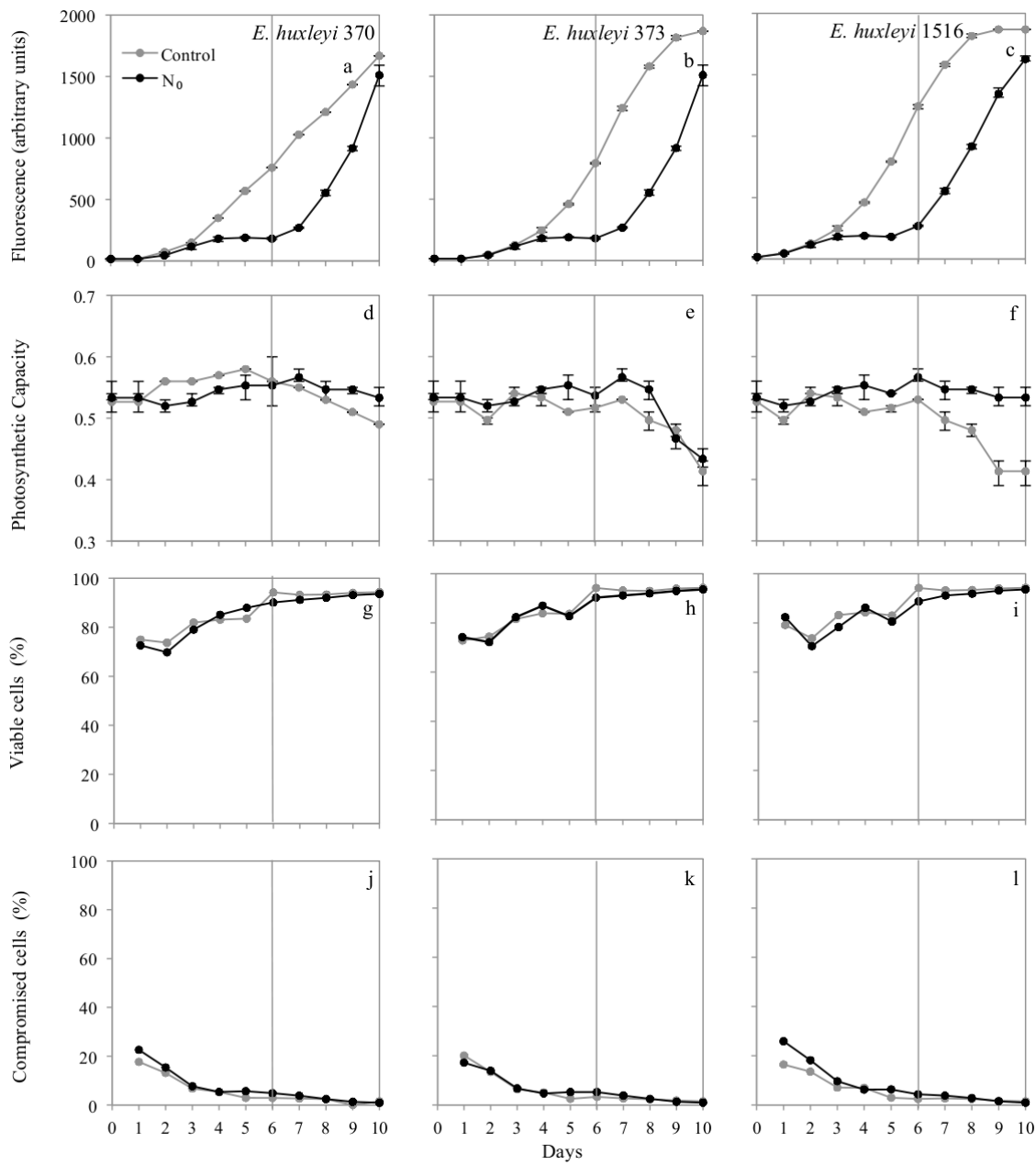
Figure 3.7 Impact of nitrogen limitation (N_0) in *E. huxleyi* 370, 373 and 1516 on fluorescence (a, b, c), photosynthetic capacity (d, e, f) and membrane permeability assessed with SYTOX Green (percentage of viable cells - g, h, i and percentage of compromised cells - j, k, l). The grey symbols represent the control cultures and the black symbols the cultures in N-free medium. On day 6 (vertical grey line), nitrate was added back to the N-free cultures. The average value and range of data is shown (n=3). Where no range bars are visible, the data range was smaller than the symbol size.
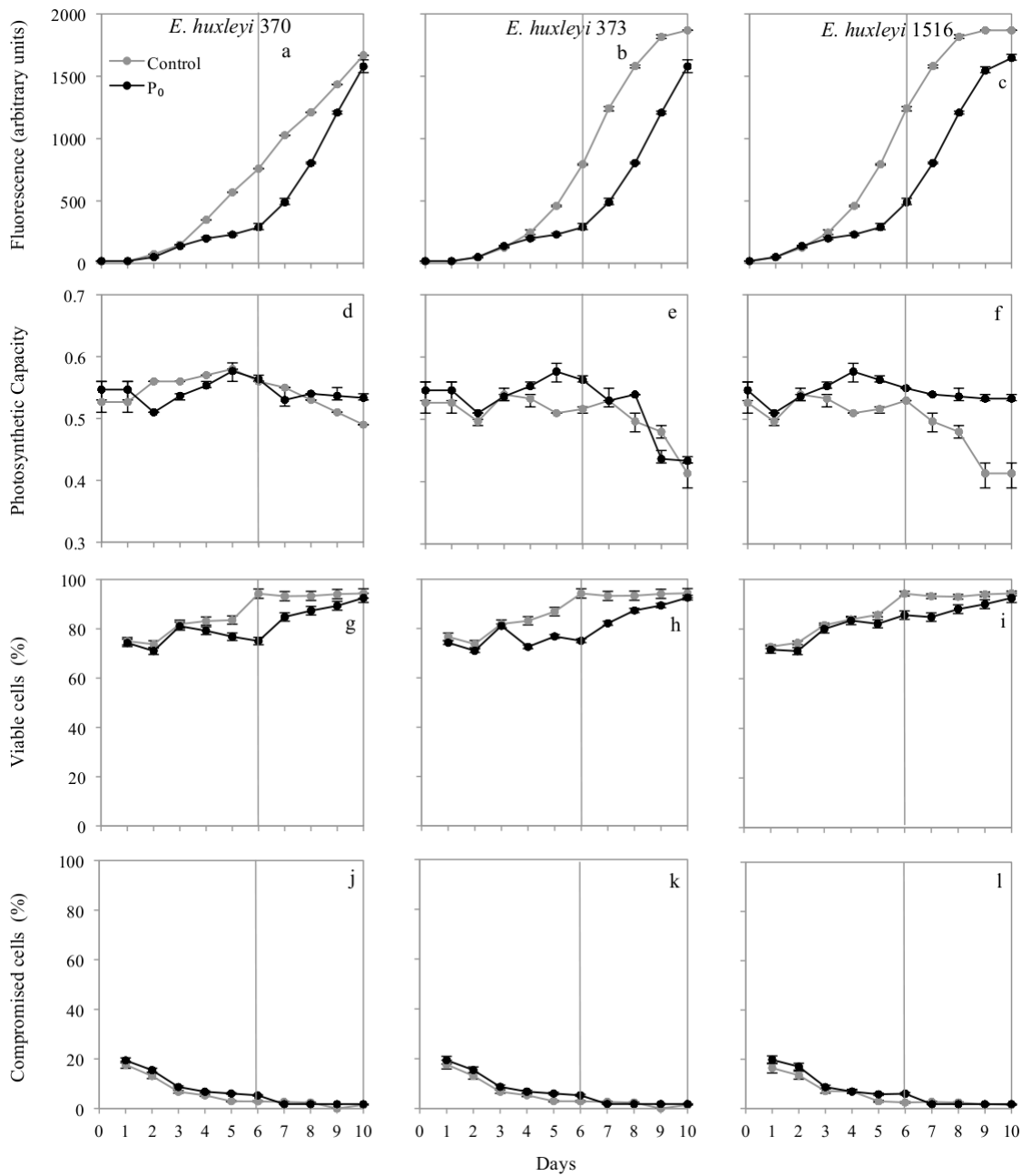
Figure 3.8 Impact of phosphate limitation (P_0) in *E. huxleyi* 370, 373 and 1516 on fluorescence (a, b, c), photosynthetic capacity (d, e, f) and membrane permeability (percentage of viable cells - g, h, i and percentage of compromised cells - j, k, l). The grey symbols represent the control culture and the black symbols represent the culture growing in P-free media. On day 6 (vertical grey line), phosphate was added back to the P-free media. The average value and range of data is shown (n=3). Where no range bars are visible, the data range was smaller than the symbol size.

cells in the control. This decrease was strain-specific: from days 3 to 6, an 80-75% drop in viable cells was seen in *E. huxleyi* 370 and 373, while from days 3 to 6, *E. huxleyi* 1516 stabilized at ~ 82%. The decrease seen in percentage viable cells was more distinct when compared to the control viable cells, which was at 94% for all three strains on day 6.

The percentage of compromised cells of all three *E. huxleyi* strains in N_0 and P_0 media were similar in trends through the 10 days of the monitoring period (Fig. 3.7j, k, l and Fig. 3.8j, k, l). However, there were differences in percentage of compromised cells between the control and N_0 cultures and also between the control and P_0 cultures. The percentage of compromised cells in the N_0 and P_0 media reached a maximum on day 5. In N_0 cultures, it was 6% in *E. huxleyi* 370, 5% in *E. huxleyi* 373 and 6.3% in *E. huxleyi* 1516 while in the control cultures it was 3% in *E. huxleyi* 370, 2.5% in *E. huxleyi* 373 and 3% in *E. huxleyi* 1516. In P_0 cultures, the percentage of compromised cells was 6% while in control cultures it was 3% for all the three strains of *E. huxleyi*.

3.3.2.3 DMSP and DMS

3.3.2.3.1 DMSPp per cell volume

Intracellular DMSP (DMSPp per cell volume) concentration decreased relative to the control between days 3 and 6 in N-free *E. huxleyi* 370 from 195 to 160 mM and between days 3 and 5 in *E. huxleyi* 373 from 234 to 217 mM (Fig. 3.9a, b), but in *E. huxleyi* 1516 the N_0 and control culture showed similar DMSPp per cell volume concentrations up to day 5 (Fig. 3.9c). Over the same timescale there was little difference in DMSPp per cell volume concentration between the control and P_0 cultures of *E. huxleyi* 370 and 1516, though *E. huxleyi* 373 displayed a small decrease in DMSPp per cell volume between days 3 and 5 from 228 to 209 mM (Fig. 3.10a, b, c). The N add-back resulted in an increase in DMSPp per cell volume concentration in all three strains (Fig. 3.9a, b, c) and whilst it also increased in *E. huxleyi* 373 and 1516 with P add-back, a decrease back to the day 0 value was seen in *E. huxleyi* 370.
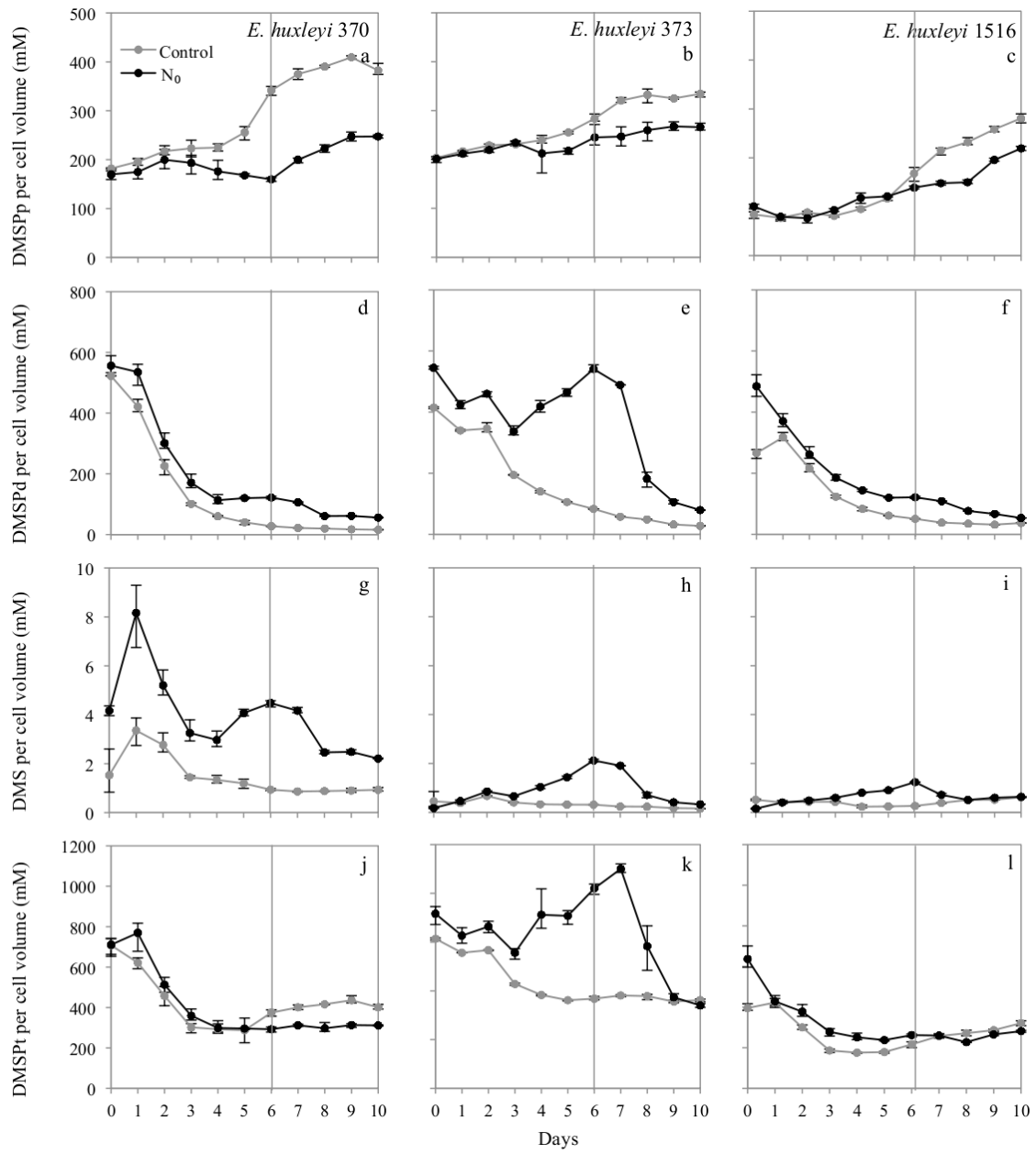
Figure 3.9 Impact of nitrogen limitation (N_0) in *E. huxleyi* 370, 373 and 1516 on per cell volume concentrations (mM) of DMSPp (a, b, c), DMSPd (d, e, f), DMS (g, h, i) and DMSPt (j, k, l). The grey symbols represent the control culture and the black symbols represent the culture growing in N-free media. On day 6 (vertical grey line), nitrate was added back to the N-free media. The average value and range of data is shown (n=3). Where no range bars are visible, the data range was smaller than the symbol size.
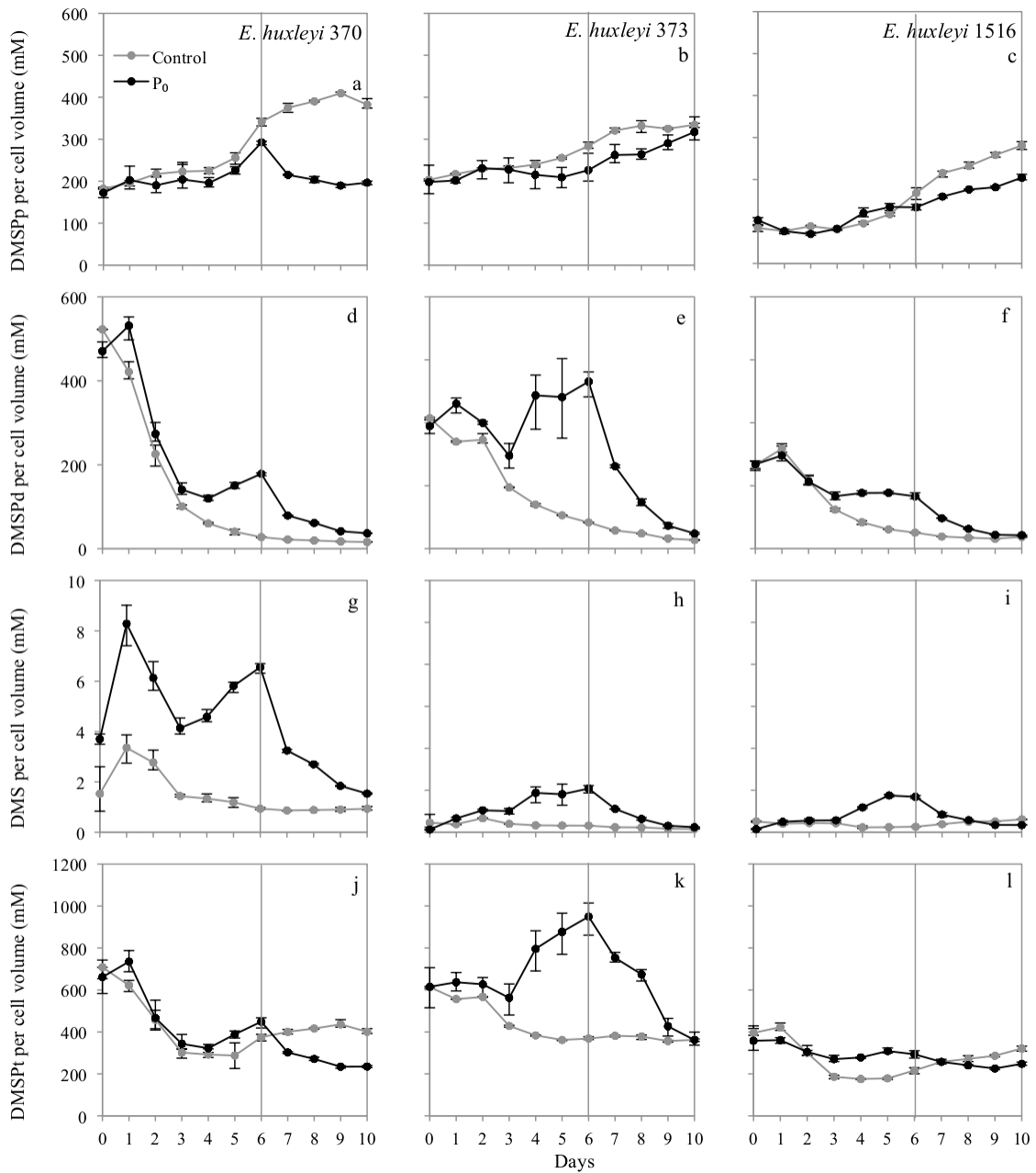
Figure 3.10 Impact of phosphate limitation (P_0) in *E. huxleyi* 370, 373 and 1516 on per cell volume concentrations (mM) of DMSPp (a, b, c), DMSPd (d, e, f), DMS (g, h, i) and DMSPt (j, k, l). The grey symbols represent the control culture and the black symbols represent the culture growing in P-free media. On day 6 (vertical grey line), phosphate was added back to the P-free media. The average value and range of data is shown (n=3). Where no range bars are visible, the data range was smaller than the symbol size.

109

3.3.2.3.2 DMSPd per cell volume

At the start of the experiment, DMSPd per cell volume values were high in all the three strains in the control, N_0 and P_0 cultures (Fig. 3.9d, e, f and Fig. 3.10d, e, f). This could have been due to the centrifugation step in the preparation of the inoculum and the higher percentage compromised cells seen with SYTOX Green in samples taken on days 1 and 2 also suggest this (Fig. 3.8j, k, l and Fig. 3.9j, k, l). Over the 10 days of the monitoring period, DMSPd per cell volume in the control cultures showed a decreasing trend from 523 to 15 mM in *E. huxleyi* 370, 415 to 28 mM in *E. huxleyi* 373 and 266 to 37 mM in *E. huxleyi* 1516. Relative to the control concentrations, N_0 and P_0 cultures showed higher concentrations in all the three strains from days 1 to 6. On day 6 in N_0 cultures, a maximum of 122 mM in *E. huxleyi* 370 and 1516 and 541 mM in *E. huxleyi* 373 whereas in P_0 cultures, a maximum of 178 mM in *E. huxleyi* 370, 167 mM in *E. huxleyi* 1516 and 531 mM in *E. huxleyi* 373 was observed relative to the control concentrations of 27 mM in *E. huxleyi* 370, 50 mM in *E. huxleyi* 1516 and 83 mM in *E. huxleyi* 373 on the same day. The N and P add-back resulted in a decrease in DMSPd per cell volume concentration in all three strains. A decrease to control value was seen by day 10 in all three strains with P add-back and in *E. huxleyi* 1516 with the N add-back.

3.3.2.3.3 DMS per cell volume

DMS per cell volume followed strain specific trends in control as well as both N- and P-free conditions (Fig 3.9g, h, i and Fig 3.10g, h, i). From days 0 to 6, *E. huxleyi* 373 and 1516 increased from 0.17 to 2.12 mM and from 0.15 to 1.24 mM in N_0 cultures while from 0.12 to 2.08 mM and from 0.14 to 1.69 mM in P_0 cultures. However under N deprivation, *E. huxleyi* 370 increased from 4.2 mM on day 0 to 8.2 mM on day 1 then decreased to 3 mM on day 4 and increased again to 4.5 mM on day 6, while under P-deprivation, the concentration increased from 3.7 mM on day 0 to 8.3 mM on day 1 and then decreased to 4.1 mM on day 3 and increased again to 6.6 mM on day 6. Following the N- and P- add-back, DMS per cell volume concentration decreased in all three strains. But despite the decreasing trend observed in *E. huxleyi* 370, by day 10, DMS per cell volume concentration remained higher (2.2 mM in N_0 culture and 1.5 mM in P_0 culture) than the control culture of 0.9 mM. By day 10, a decrease equal to control value

110

was seen in *E. huxleyi* 373 and 1516 (0.3 mM and 0.6 mM respectively) in N add-back culture and *E. huxleyi* 373 (0.2 mM) in P add-back culture. While the decrease was lower than the control in *E. huxleyi* 1516 (0.3 mM) in P add-back culture.

3.3.2.3.4 DMSPt per cell volume

At the start of the experiment, DMSPt per cell volume values were high in all the three strains in the control, N_0 and P_0 cultures (Fig 3.9j, k, l and Fig. 3.10j, k, l) similar to the observation in DMSPd per cell volume (Fig. 3.9d, e, f and Fig. 3.10d, e, f). This may be again attributed to the centrifugation step in the preparation of the inoculum. DMSPt per cell volume concentrations showed very strain specific behaviour especially relating N_0 and P_0 cultures to the control. The N-free *E. huxleyi* 370 (Fig. 3.9j) followed the control up to day 5 and then remained at 292 mM on day 6 while the control increased to 375 mM; the P-free *E. huxleyi* 370 (Fig. 3.10j) also followed the control up to day 4 and then increased to 450 mM on day 6 compared to the control value of 375 mM. Following the add-back, N-free *E. huxleyi* 370 continued to remain constant in the range of 292 mM to 313 mM lower than the control (375 mM to 436 mM). N-free *E. huxleyi* 373 decreased from 716 mM on day 0 to 556 mM on day 3 and later increased to 820 mM on day 6, while P-free *E. huxleyi* 373 decreased from 615 mM on day 0 to 562 mM on day 3 and later increased to 950 mM on day 6 (Fig. 3.9k and Fig. 3.10k). After the N add-back DMSPt per cell volume continued to increase to 900 mM for a day while P add-back showed a rapid decrease to 753 mM the next day. By day 10, the N and P add-back to *E. huxleyi* 373 cultures followed the control concentration of 360 mM. In both N- and P-free *E. huxleyi* 1516 (Fig. 3.9l and Fig. 3.10l) DMSPt per cell volume remained higher than the control with the exception of the first three days in P-free *E. huxleyi* 1516. In the N-free media between days 0 and 6 the concentration dropped from 636 to 262 mM while in the P-free media it remained in the range of 358 to 293 mM. Following the N add-back *E. huxleyi* 1516 showed a low of 281 mM, while the P add-back showed a clear decrease to 248 mM compared to the control at 321 mM for both.

3.3.2.3.5 DMSPp per cell

DMSP has been previously expressed on a per cell basis in culture studies (Turner et al. 1988; Vairavamurthy et al. 1985), thus variations in DMSP per cell were also derived to understand the data from a different perspective.

DMSPp per cell for all the three strains increased under N- and P-free conditions from days 0 to 6 (Fig. 3.11a, b, c and Fig. 3.12a, b, c). However from days 0 to 6, N-free *E. huxleyi* 373 and 1516 showed a higher increase of 6 to 12 fmol and 2.2 to 3.9 fmol per cell respectively (Fig. 3.11b, c) and P-free *E. huxleyi* 373 and 1516 also showed a higher increase of 8.7 to 11.3 fmol and 2.2 to 4 fmol respectively from days 0 to 6 (Fig. 3.12b, c) compared to the *E. huxleyi* 373 control cultures (6 to 4.5 fmol) and *E. huxleyi* 1516 control cultures (1.7 to 2.1 fmol). But, the N-free *E. huxleyi* 370 showed a very less increase of 4.8 fmol on day 0 to 7.7 fmol on day 6 while the P-free *E. huxleyi* 370 showed an increase of 4.8 fmol on day 0 to 14.6 fmol per cell on day 6, following the control culture of 5 fmol on day 0 to 13 fmol per cell on day 6. In *E. huxleyi* 370, N add-back increased upto 8.8 fmol followed by a decrease to 6 fmol by day 10 while P add-back rapidly reduced the DMSPp per cell levels to 6 fmol by day 10. However, in *E. huxleyi* 373 N and P add-back did not follow any clear pattern (Fig. 3.11b and Fig. 3.12b) and the N and P add-back in *E. huxleyi* 1516 resulted in a decrease to 3 fmol in DMSPp per cell levels similar to that in the control culture.

3.3.2.3.6 DMSPd per cell

Dissolved DMSP (DMSPd) per cell in N_0 and P_0 cultures decreased at first and subsequently increased by day 6 in all three strains, excluding the continued decrease in N-free *E. huxleyi* 1516. In N-free *E. huxleyi* 370, DMSPd per cell dropped from 15.6 to 4.7 fmol on day 4 and increased to 5.8 fmol on day 6; in N-free *E. huxleyi* 373 the value dropped from 16.5 to 14 fmol on day 2 and increased to 26.5 fmol by day 6; and in N-free *E. huxleyi* 1516 the value dropped from 10.5 to 3.4 fmol on day 6. In P-free *E. huxleyi* 370, DMSPd per cell decreased from 13 to 5.6 fmol on day 3 and increased to 8.9 fmol on day 6; in P-free *E. huxleyi* 373 the value dropped from 17 to 14.1 fmol on day 2 and increased to 26.5 fmol on day 6; and in P-free *E. huxleyi* 1516 the value dropped from 5.6 to 4 fmol on day 3 and increased to 5 fmol on day 6. Under nutrient

deprivation the cultures showed higher DMSPd per cell values when compared to the control values. The N and P add-back decreased the DMSPd per cell values in all three
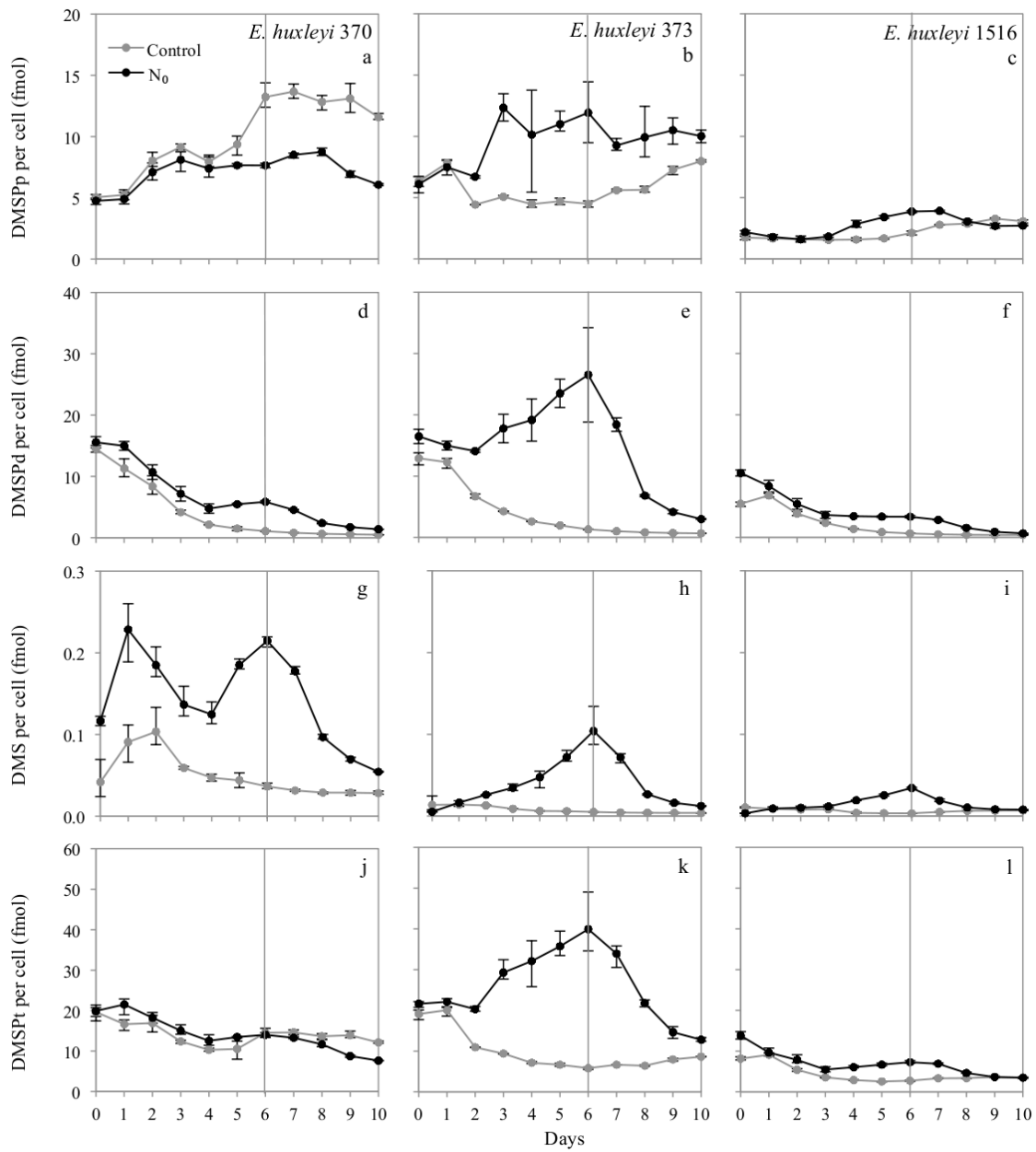
Figure 3.11 Impact of nitrogen limitation (N_0) in *E. huxleyi* 370, 373 and 1516 on per cell levels (fmol) of DMSPp (a, b, c), DMSPd (d, e, f), DMS (g, h, i) and DMSPt (j, k, l). The grey symbols represent the control culture and the black symbols represent the culture growing in N-free media. On day 6 (vertical grey line), nitrate was added back to the N-free media. The average value and range of data is shown (n=3). Where no range bars are visible, the data range was smaller than the symbol size.
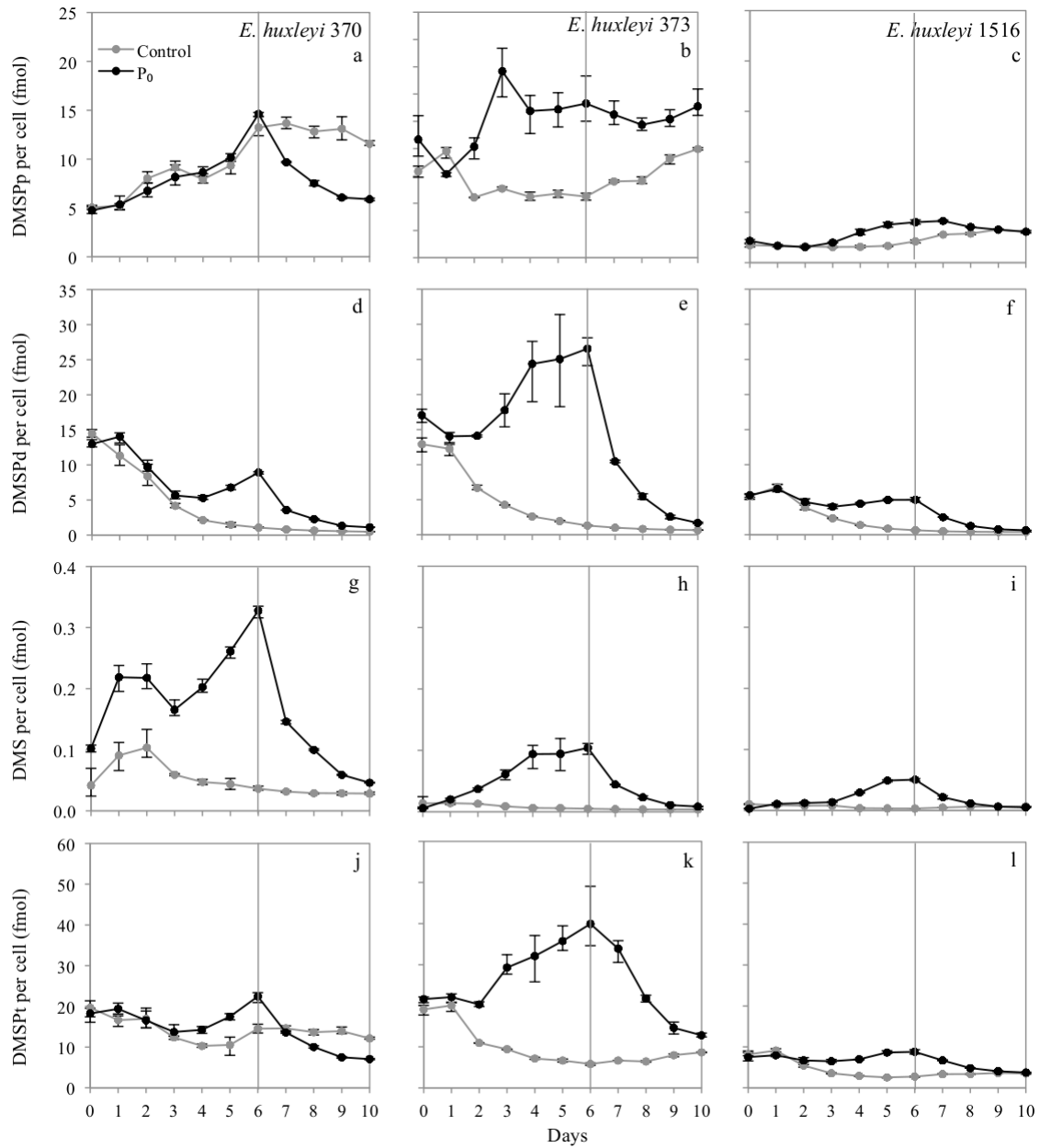
Figure 3.12 Impact of phosphate limitation (P_0) in *E. huxleyi* 370, 373 and 1516 on per cell levels (fmol) of DMSPp (a, b, c), DMSPd (d, e, f), DMS (g, h, i) and DMSPt (j, k, l). The grey symbols represent the control culture and the black symbols represent the culture growing in P-free media. On day 6 (vertical grey line), phosphate was added back to the P-free media. The average value and range of data is shown (n=3). Where no range bars are visible, the data range was smaller than the symbol size.

strains and by day 10 the values leveled off with the control cultures (Fig. 3.11d, e, f and 3.12d, e, f) except in N add-back to *E. huxleyi* 373 where the value was as high as 3 fmol compared to the 0.66 fmol in the control culture.

114

3.3.2.3.7 DMS per cell

In N_0 and P_0 cultures, DMS per cell was high and exhibited strain-specific patterns (Fig. 3.11g, h, i and 3.12g, h, i). N-deprived *E. huxleyi* 370 showed continued variations; DMS per cell rose from 0.11 to 0.22 fmol on day 1, followed by a decrease to 0.12 fmol on day 4 with an increase again to 0.21 fmol on day 6. While P-free *E. huxleyi* 370 rose from 0.1 to 0.22 fmol on day 1, followed by a decrease to 0.17 fmol on day 3 with an increase again to 0.33 fmol per cell on day 6. N- and P-free *E. huxleyi* 373 increased from 0.005 to 0.11 fmol by day 6. N- and P-free *E. huxleyi* 1516 followed the control till day 3 then rose to 0.04 and 0.05 fmol respectively compared to control at 0.003 fmol on day 6. After the N and P add-back, a decrease was observed in all the three strains. It matched the control in *E. huxleyi* 1516 and 373 by day 10. However, although N and P add-back to *E. huxleyi* 370 showed a decrease in DMS per cell, the values still remained higher at 0.05 fmol than the control at 0.03 fmol on day 10.

3.3.2.3.8 DMSPt per cell

Total DMSP (DMSPt) per cell in N_0 and P_0 cultures decreased at first and subsequently increased by day 6 in all three strains (Fig. 3.11j, k, l and Fig. 3.12j, k, l). In N-free *E. huxleyi* 370, the value dropped from 20 to 12.5 fmol on day 4 and increased to 14 fmol by day 6; in N-free *E. huxleyi* 373, the drop was from 21.6 to 20.3 fmol on day 2 and increased to 40 fmol by day 6; and in *E. huxleyi* 1516 the value dropped from 13.8 to 5.5 fmol on day 3 and increased to 7.3 fmol by day 6. In P-free *E. huxleyi* 370, DMSPt per cell dropped from 18.3 to 13.7 fmol on day 3 and increased to 22.4 fmol by day 6; in P-free *E. huxleyi* 373 the value dropped from 21.6 to 20.3 fmol on day 2 and increased to 40 fmol by day 6; and in *E. huxleyi* 1516 the value dropped from 7.5 to 6.5 fmol on day 3 and increased to 8.8 fmol on day 6. Under N and P deprivation the cultures showed higher DMSPt per cell values when compared to the control except in the P-deprived *E. huxleyi* 370 and 1516. The N and P add-back decreased the DMSPt per cell values in all the three strains and *E. huxleyi* 1516 values leveled off with the control cultures by day 10. In *E. huxleyi* 370 values dropped lower than the control (14.6 fmol) by day 7 and reached 7.6 fmol in N_0 culture and 7.1 fmol in P_0 culture by day 10.

3.3.2.3.9 DMSPp in the culture

In N- and P-deprived cultures, DMSPp concentration followed the control for 3 days in *E. huxleyi* 370 and 373, and for 4 days in *E. huxleyi* 1516 (Fig. 3.13a, b, c and Fig. 3.14a, b, c). It then lagged and remained low till day 6 in N_0 cultures at 5.3 μM in *E. huxleyi* 370, 1.8 μM in *E. huxleyi* 373 and 2.7 μM in *E. huxleyi* 1516 and in P_0 cultures at 6.6 μM in *E. huxleyi* 370, 1.7 μM in *E. huxleyi* 373 and 1.9 μM in *E. huxleyi* 1516 when compared to the control culture at 25.4 μM in *E. huxleyi* 370, 7.2 μM in *E. huxleyi* 373 and 6.9 μM in *E. huxleyi* 1516. N add-back resulted in an increase to 21 μM in *E. huxleyi* 370, 14.7 μM in *E. huxleyi* 373 and 12.1 μM in *E. huxleyi* 1516 while P add-back resulted in an increase to 18 μM in *E. huxleyi* 370, 18.2 μM in *E. huxleyi* 373 and 14.2 μM in *E. huxleyi* 1516 but despite this increase, the N- and P-deprived culture concentration remained lower than the control on day 10.

3.3.2.3.10 DMSPd in the culture

High DMSPd concentration was observed across all the three N and P-deprived strains that rose to 4 μM in *E. huxleyi* 370 and 373 and 2.4 μM in *E. huxleyi* 1516 (Fig. 3.13d, e, f and 3.14d, e, f). An increase was seen in the N add-back for all the three strains; *E. huxleyi* 370 and 373 showed higher concentrations (4.8 and 4.4 μM respectively) while *E. huxleyi* 1516 showed similar concentrations when compared to the control cultures (3 μM) on day 10. The P add-back led to a decrease in *E. huxleyi* 370 and 373 but *E. huxleyi* 1516 continued to show an increase and similar concentrations when compared to the control at 3 μM.

3.3.2.3.11 DMS in the culture

In N_0 and P_0 cultures of *E. huxleyi* 373 and 1516, DMS concentration followed the control culture initially but later increased to 0.015 μM and 0.024 μM when compared to the control on day 6 (Fig. 3.13g, h and Fig. 3.14g, h). While *E. huxleyi* 1516 showed a continuous increase of 0.007 to 0.148 μM from days 1 to 6 in both the cultures (Fig. 3.13i and Fig. 3.14i). On adding back P, *E. huxleyi* 370 and 1516 showed a steady release of DMS at 0.14 μM and 0.02 μM respectively but when N was added back to *E. huxleyi* 370 a gradual increase to 0.18 μM and in *E. huxleyi* 1516, an initial decrease to 0.017 μM on day 7 and then a gradual increase to 0.035 μM by day 10 was observed.
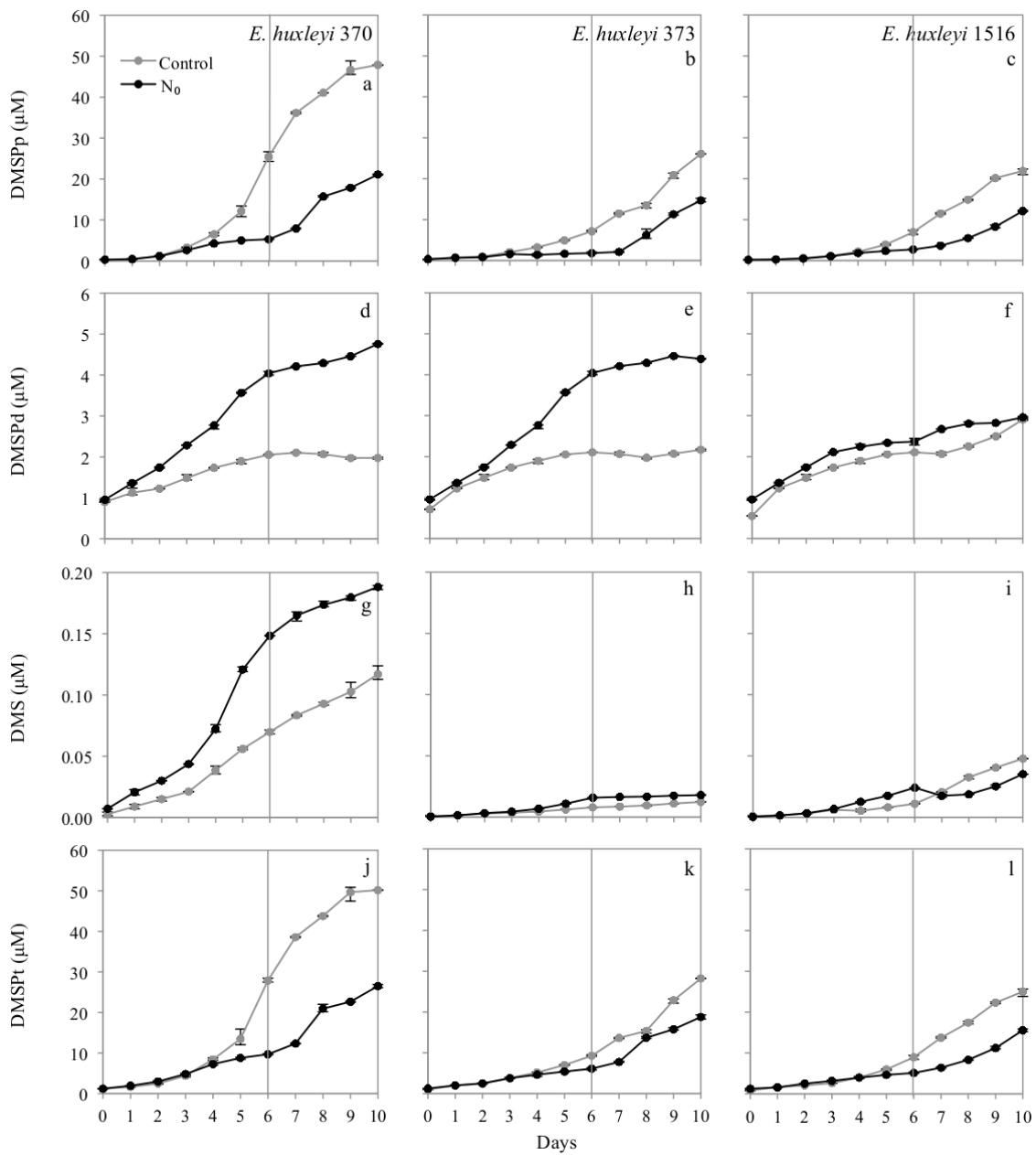
Figure 3.13 Impact of nitrogen limitation (N_0) in *E. huxleyi* 370, 373 and 1516 on DMSPp (a, b, c), DMSPd (d, e, f), DMS (g, h, i) and DMSPt (j, k, l) in the culture (μM). The grey symbols represent the control culture and the black symbols represent the culture growing in N-free media. On day 6 (vertical grey line), nitrate was added back to the N-free media. The average value and range of data is shown (n=3). Where no range bars are visible, the data range was smaller than the symbol size.
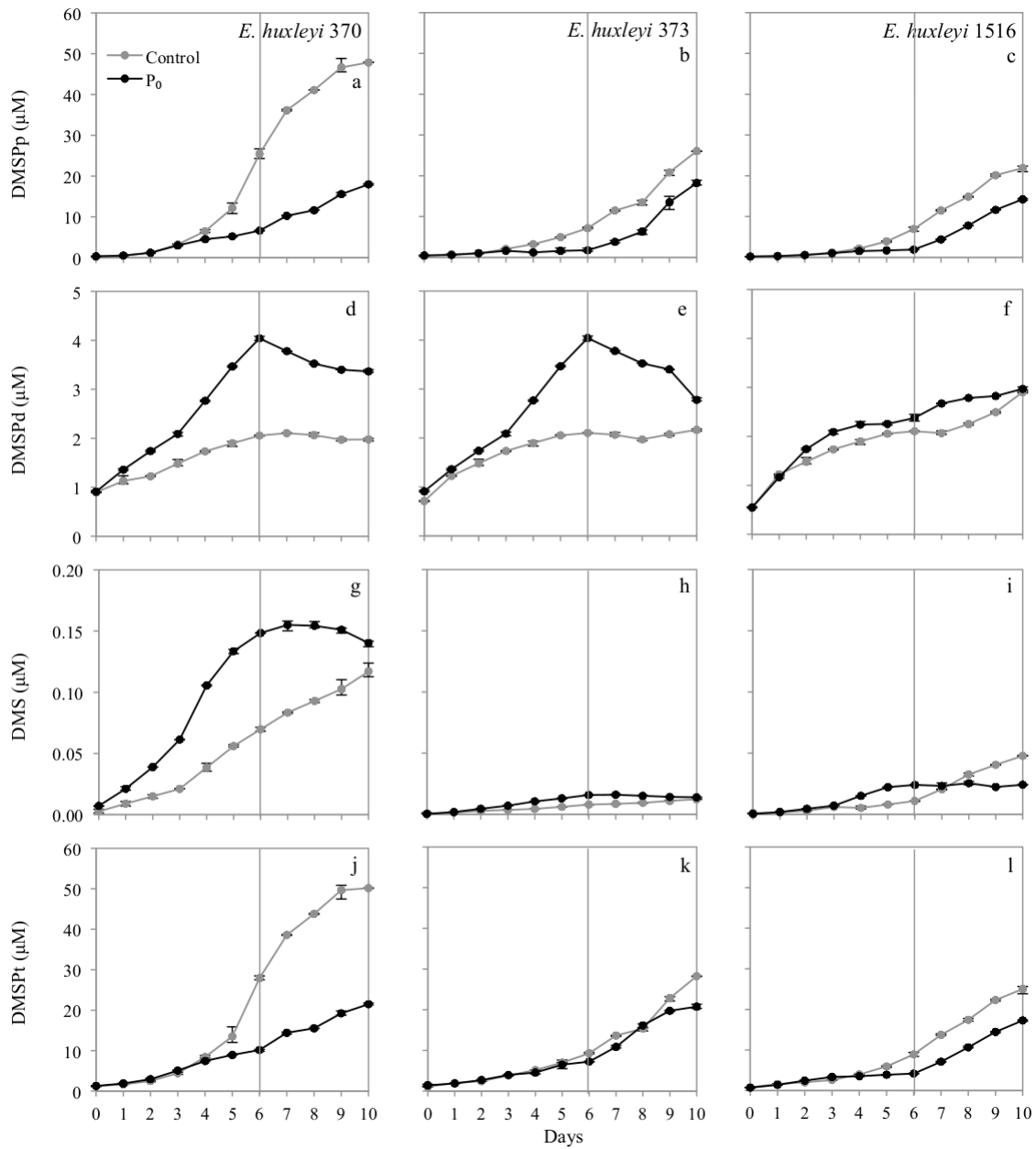
Figure 3.14 Impact of phosphate limitation (P_0) in *E. huxleyi* 370, 373 and 1516 on DMSPp (a, b, c), DMSPd (d, e, f), DMS (g, h, i) and DMSPt (j, k, l) in the culture (μM). The grey symbols represent the control culture and the black symbols represent the culture growing in P-free media. On day 6 (vertical grey line), phosphate was added back to the P-free media. The average value and range of data is shown (n=3). Where no range bars are visible, the data range was smaller than the symbol size.

Meanwhile *E. huxleyi* 373 showed a very steady DMS release at 0.1 μM in both the N and P add-back conditions.

3.3.2.3.12 DMSPt in the culture

A slow and gradual increase in total DMSP (DMSPt) was seen in all the three strains (Fig. 3.13j, k, l and Fig. 3.14j, k, l). On day 6 an increase in DMSPp in N-free *E. huxleyi* 370 to 9.7 μM, in *E. huxleyi* 373 to 6.13 μM and *E. huxleyi* to 5.1 μM and in P-free *E. huxleyi* 370 to 10.2 μM, in *E. huxleyi* 373 to 7.2 μM and in *E. huxleyi* 1516 to 4.2 μM was less compared to the control. N and P add-back showed continued increase in DMSPt though the increase remained lower than the control for all the three strains.

3.4 Discussion

In this chapter, two different approaches were taken to study the effect of nutrient limitation on cell growth and DMSP metabolism; (1) cultures of *E. huxleyi* 1516 and *T. pseudonana* 1335 were grown through to nutrient exhaustion (Franklin et al. 2012) (2) cultures of three strains of *E. huxleyi* 370, 373 and 1516 were transferred to medium without nitrate or phosphate. In both cases nutrients were added back to confirm the nutrient limitation observed. Alongside DMS and DMSP measurements, cell density, cell volume, the efficiency of PSII (F_V/F_M), fluorescence and membrane permeability were analysed to give an indication of the physiological state of the cultures.

The results from the 1st approach (Franklin et al. 2012) established the fact that the coccolithophore *E. huxleyi* is a higher DMSP producer than the diatom *T. pseudonana*. Maximum intracellular DMSP concentration seen in *E. huxleyi* was 120 mM and 35 mM in *T. pseudonana* (Fig. 3.3a). The results also highlighted the dissimilar responses between the two species under prolonged nutrient deprivation. In the 28 d monitoring period, *E. huxleyi* continued in stationary phase (Fig. 3.1A), with only < 5% cells having lost their cell membranes (Fig. 3.2B), while *T. pseudonana* demonstrated all the three phases of growth: exponential stationary and senescence (Fig. 3.1A) with only < 2% cells having lost their cell membrane in the stationary phase rising to about 25% by the end of the monitoring period (Fig. 3.2B). *E. huxleyi* developed two distinct cell populations with CMFDA staining unlike the single cell population seen in *T. pseudonana* indicating a difference between the two species in hydrolytic activity. Also, caspase-like activity emerged higher in *E. huxleyi* than in *T. pseudonana* although there

were no obvious signs of cell lysis or mortality during nutrient depletion. The concentration of methoxychlorophyll *a* and hydroxychlorophyll *a* relative to Chlorophyll *a* increased in *T. pseudonana* during senescence which was marked by the decline in PSII efficiency from 0.6 to 0.1 and the rise in the percentage of cells labeled with SYTOX Green. In contrast to *T. pseudonana*, the concentration of methoxychlorophyll *a* and hydroxychlorophyll *a* relative to Chlorophyll *a* remained constant in *E. huxleyi*, just as the consistency seen in PSII efficiency and the percentage of cells labeled with SYTOX Green. DMS increased and Total DMSP decreased in *T. pseudonana* during cell death while in *E. huxleyi* total DMSP and DMS increased in the absence of cell death. The add-back data indicated N as the limiting nutrient to the growth of *T. pseudonana* while it was not very clear in *E. huxleyi* perhaps due to the timing of the add-back.

The results from the 2nd approach highlighted the general variation in growth, DMSP and DMS responses between different *E. huxleyi* strains that has been observed in other studies (e.g. Steinke et al 1998). This sort of variation is not unique to *E. huxleyi*; a recent study on symbiotic dinoflagellates of the genus *Symbiodinium* also showed strain-specific differences in DMSP concentrations and sensitivity to temperature-induced oxidative stress (Steinke et al. 2011).

In this study, the absence of external inorganic nitrogen and inorganic phosphates in *E. huxleyi* resulted in cell growth arrest (Fig. 3.5a, b, c and Fig. 3.6a, b, c), which was observed after a few days when the cells must have exploited the stored nutrients within the cells. Such an observation is commonly noted when cells growing in batch cultures are faced with nutrient exhaustion after the onset of the stationary phase. In this situation, the viable cells compromise on the use of energy and other cellular resources by arresting cell division and divert resources towards cell survival strategies. Loebl et al. (2010) used a similar type of experimental manipulation (centrifugation of cells and re-suspension in nitrogen-free media) with *E. huxleyi* (isolated from the North Sea coast at Bergen, Norway), to induce nitrogen limitation and also observed an increase in cell number for several days followed by cell growth arrest.

In N- and P-free media cells increased in cell volume (Fig. 3.5g, h, i and Fig. 3.6g, h, i). The increase recorded in the P-limited condition was substantial though strain specific. This increase observed in cell volume may be explained by the inability to produce nucleic acids under phosphate limitation which would inhibit cell division (Bucciarelli and Sunda 2003). Acidification of the samples resulted in no change in cell volume to the N-limited cells but a substantial decrease in cell volume of P-limited cells due to the removal of coccoliths, but even after acidification the naked cell volume was higher than that of cells in the control medium. Various studies examining the roles of nitrogen and phosphorus in coccolith formation in *E. huxleyi* have shown that calcification is stimulated in P-deficient conditions and suppressed in P-sufficient conditions (Kayano and Shiraiwa 2009; Paasche 1998; Paasche and Brubak 1994). We also reported an increase in coccosphere volume in batch cultures of *E. huxleyi* 1516 under nutrient exhaustion conditions in Franklin et al. (2012). In contrast, Stefels et al. (2007), observed cell volume reduction in batch cultures of the Antarctic prymnesiophyte *Phaeocystis* sp. under nitrate and iron limitation, while cell volume remained constant under phosphate-limitation. However, this conclusion was drawn from sonicated (to break up colonies) acid Lugol's iodine fixed samples cultured under combined iron and light stress (Stefels and Van Leeuwe 1998). Several studies have reported that preservatives like Lugol's iodine minimize cell loss but cause cells to shrink (Stoecker et al. 1994) thereby reducing cell volume (Montagnes et al. 1994). Bucciarelli and Sunda (2003) observed a decrease in cell volume in *T. pseudonana* (CCMP1335) under nitrate-limitation, in agreement with our data for the same species and identical-strain (Franklin et al. 2012).

In general, any process that impedes the proper functioning of the cellular components involved in the transfer of excitation energy or electrons within the photosynthetic apparatus and metabolic activity would increase the production of reactive oxygen species (ROS) and have the potential to increase oxidative stress within the cell. The formation of active oxygen species increases under stress conditions, such as low temperature, high salinity and CO_2 limitation (Butow et al. 1998; Noctor and Foyer 1998). Nitrogen limitation should increase oxidative stress within algal cells because of decreased photosynthetic efficiency, as evidenced by lower variable to maximum

photosystem II fluorescence (F_V/F_M) (Berges and Falkowski 1998). However, in the data presented here *E. huxleyi* maintained PSII activity over at least 28 d of nitrogen depletion, as indicated by maintenance of $F_V:F_M$, whereas it declined in *T. pseudonana* (Fig 3.1 B). Loebl et al. 2010 found that $F_V:F_M$ dropped to marginal levels after 7–10 d in *T. pseudonana* and *Coscinodiscus sp* suggesting that this might be common in diatoms. This capacity of *E. huxleyi* to sustain photosynthetic function under nitrogen-depleted conditions relative to the diatoms may explain its ability to form large blooms under low-nitrogen, high-light conditions (Loebl et al. 2010). Under phosphorus depletion, Loebl et al. (2010) reported that PSII function declined sharply within 7 d in *E. huxleyi* and within 3 d in *T. pseudonana*, indicating that *E. huxleyi* is adapted to maintain PSII function under long-term nitrogen depletion but not under phosphorus depletion. However in contrast, my data for *E. huxleyi* 1516 show increasing $F_V:F_M$ levels in late log phase under phosphate-limiting conditions in *E. huxleyi* (Fig. 3.8f). These results combined with the add-back data from Franklin et al. (2012) suggest that N-limitation and P-limitation may not consistently have adverse effects on the photosynthetic apparatus of *E. huxleyi*. Another key point supporting the above observations was that SYTOX Green labeling (Fig. 3.7j, k, l and Fig. 3.8j, k, l) suggested intact cell membranes; < 20% cells lost their membrane integrity on transfer to N- and P-limited media and < 5% lost integrity with prolonged nutrient deprivation (Fig. 3.2B) (Franklin et al. (2012). This might suggest that *E. huxleyi* can tolerate oxidative stress associated with nutrient-limited conditions.

A number of enzymes and small molecules like ascorbic acid and glutathione are involved in antioxidant protection, either in preventing the over-reduction of the photosynthetic apparatus or in scavenging harmful ROS. Among important antioxidant enzymes are superoxide dismutase and ascorbate peroxidase, which remove superoxide radicals and hydrogen peroxide (Asada 1999). Under increased oxidative stress, antioxidants and antioxidant systems are generally up-regulated. For example, under CO_2 limitation the cellular activities of catalase (Butow et al. 1998) and ascorbate peroxidase (Sunda et al. 2002) increase. Similarly under nitrogen limitation, ascorbic acid concentrations increase relative to chlorophyll (Logan et al. 1999). An up-regulation of intracellular DMSP concentration or of enzymatic conversion of DMSP to

DMS also occurs under increased oxidative stress linked to solar ultraviolet radiation exposure or to CO_2 and Fe-limitation (Sunda et al. 2002). Very few studies have been carried out on the effect of phosphate limitation on the production of DMSP and DMS. A seawater mesocosm experiment in a Norwegian fjord (June 1995) concluded that phosphate limitation did not affect the production of DMSP and DMS (Wilson et al. 1998). In another study, phosphate-limited batch cultures of the coastal diatom *T. pseudonana* showed a very small increase in intracellular DMSP concentrations (Bucciarelli and Sunda 2003).

In 2002, Sunda et al. reported that the enzymatic cleavage of DMSP could theoretically enhance antioxidant capacity, as DMS and acrylate are 60 and 20 times respectively more effective in scavenging hydroxyl radicals than DMSP itself. They also showed that the putative DMSP/DMS antioxidant system is up-regulated in increased oxidative stress situations (Sunda et al. 2002). There have been reports of increased intracellular DMSP concentrations under N-limitation like in the diatom *Thalassiosira pseudonana* (Bucciarelli and Sunda 2003; Keller et al. 1999b). DMSP increased from ~ 2 mM to 50 mM in nitrogen limited conditions (Bucciarelli and Sunda 2003) and in N-limited chemostat cultures of *E. huxleyi* CCMP 378, an 88% increase in intracellular DMSP concentration (from 59 to 111 mM) was reported (Keller et al. 1999b). However in contrast to the above, the data presented here shows a decrease in intracellular DMSP, though strain specific. In both N_0 and P_0 conditions, *E. huxleyi* 370 and 373 showed a decrease in intracellular DMSP (Fig. 3.9a, b and Fig. 3.10a, b) while no change was observed in *E. huxleyi* 1516 (Fig. 3.9c and Fig. 3.10c). The variations seen in intracellular DMSP (DMSPp per cell volume) may be due to the cell volume variations seen between the *E. huxleyi* strains. The DMSPp concentrations in both the N_0 and P_0 cultures (µM; Fig. 3.13a, b, c and 3.14a, b, c) clearly show evidence for a decrease in DMSP concentration in all three strains. However under both N- and P-free conditions, an increase in DMS (Fig. 3.13g, h, i and Fig. 3.14g, h, i) and the DMSPd (Fig. 3.13d, e, f and Fig. 3.14d, e, f) fraction was observed in all three *E. huxleyi* strains even with its cell membranes intact suggesting active transport. A similar kind of result was observed in an investigation on the effect of nitrogen limitation on intracellular DMSP and its enzymatic cleavage to DMS in semi-continuous cultures of *E. huxleyi* (CCMP 374), no

increase in DMSP was observed, but DMSP lyase activity increased which resulted in a 20-fold increase in the quantity of DMS in the culture per unit cell volume, and a 40- to 80- fold increase in the DMS:chl *a* ratio (Sunda et al. 2007). Assuming enough stress being produced to *E. huxleyi* cells growing in N_0 and P_0 media resulting in enhanced DMSPd and DMS, it can be proposed that the photosynthetic efficiency of PSII was constantly repaired thereby keeping the ROS production under control and maintaining cell membrane integrity.

Sunda et al. (2002) proposed the antioxidant hypothesis based on the elevated concentrations of intracellular DMSP observed under stress conditions. But, it can be reasoned that in the process of mopping up radicals, DMSP would be converted into one of its breakdown products resulting in a loss of DMSP, unless the stress reaction results in increased de novo synthesis (up-regulation) of DMSP. In such cases, a consequent excess production may lead to increased intracellular concentrations of DMSP and/or one of the breakdown products or a decrease in DMSP as it is cleaved in the absence of new synthesis (Stefels et al. 2007). Until now, there is no study to suggest a definite link between increased DMSP and oxidative stress or that DMSP reduces oxidative stress.

3.5 Conclusions

Considering the two different approaches to study the impact of nutrient limitation on cell growth and DMSP metabolism, this study highlights the observation that the response to stress conditions may be species-specific and strain-specific. The relative importance of the different DMSP functions in phytoplankton cells may thus vary among species and be highly dependent on environmental conditions. In Franklin et al. (2012) we concluded that *E. huxleyi* is much better able to cope with nutrient deprivation than *T. pseudonana*, through a cellular reorganization that may involve caspase-like activity and DMSP production. In response to nitrogen limitation, *T. pseudonana* showed a substantial increase in DMSP concentration and died and lysed rapidly. The differences in the responses in the two species suggest the ecological importance of their groups in nature.

In addition, the experiments reported here involving the growth of *E. huxleyi* 370, 373 and 1516 in N-free and P-free media, showed strain-specific responses but showed a decrease in intracellular DMSP concentrations accompanied by an increase in DMSPd and DMS release. A key point to raise here is that examining cell volume is a very important parameter to be considered while comparing intracellular concentrations. Here, naked cells of *E. huxleyi* increased in cell volume in N-deprived and in P-deprived conditions. Also, coccolith formation occurred in response to P-deprivation, which was not encountered in N-deprived conditions.

It is critical to assess the linkage between nutrient limitation and oxidative stress in order to determine DMSP and its breakdown products competing for the role in an antioxidant system within a phytoplankton cell. However, nutrient limitation may play an important role in regulating the dynamics of DMSP and DMS in marine surface waters.

Chapter 4

The Influence of Ultraviolet Light on Intracellular DMSP in *Emiliania huxleyi*

Chapter 4: The Influence of Ultraviolet Light on Intracellular DMSP in *Emiliania huxleyi*

4.1 Background and significance

Ultraviolet radiation (UVR, 100-400 nm) is the most photochemically reactive component of solar radiation. It is generally subdivided into 3 wavebands: UVA 320-400 nm, UVB 280-320 nm and UVC < 280 nm (Fig. 4.1). UVC radiation is absorbed by the Earth's atmosphere and is not generally considered to be of biological relevance (Holzinger and Lutz 2006; McKenzie et al. 2003), although some experimental lighting systems do include a small quantity of the UVC waveband (Hannen and Gons 1997).

With the exception of a small portion in the UVA region, UVR is not photosynthetically active but it impedes phytoplankton growth and photosynthetic activity (Davidson et al. 1994; Gao et al. 2007a; Gao and Ma 2008). UVR can damage and/or alter the composition of cell membranes (Llabres and Agusti 2006) and intracellular macromolecules like proteins and DNA (Bouchard et al. 2005; Goes et al. 1995). Various reports suggest that UVB radiation causes DNA damage, lipid peroxidation, inhibition of carbon fixation and photosystem II damage in phytoplankton (Garde and Cailliau 2000; Van De Poll et al. 2001) and that UVB is more detrimental than UVA (Häder 1997; Vernet 2000). UVR stress can also promote the production of reactive oxygen species (ROS) in photosynthetic cells (Beardall et al. 2009; Häder et al. 2007; He and Häder 2002a; He and Häder 2002b).

Algae and cyanobacteria have evolved various mechanisms to protect and repair themselves against the damage caused by UVB and can adjust or acclimate to tolerate enhanced UVB doses (Xue et al. 2005). It has also been recognized that UVA can stimulate photo repair of UVB-induced DNA damage in algae (Karentz et al. 1991) and enhance photosynthetic carbon fixation (Gao et al. 2007b). In plants, UVR may help secondary metabolite formation like flavonoids which is needed especially for pathogen resistance (Holzinger and Lutz 2006).
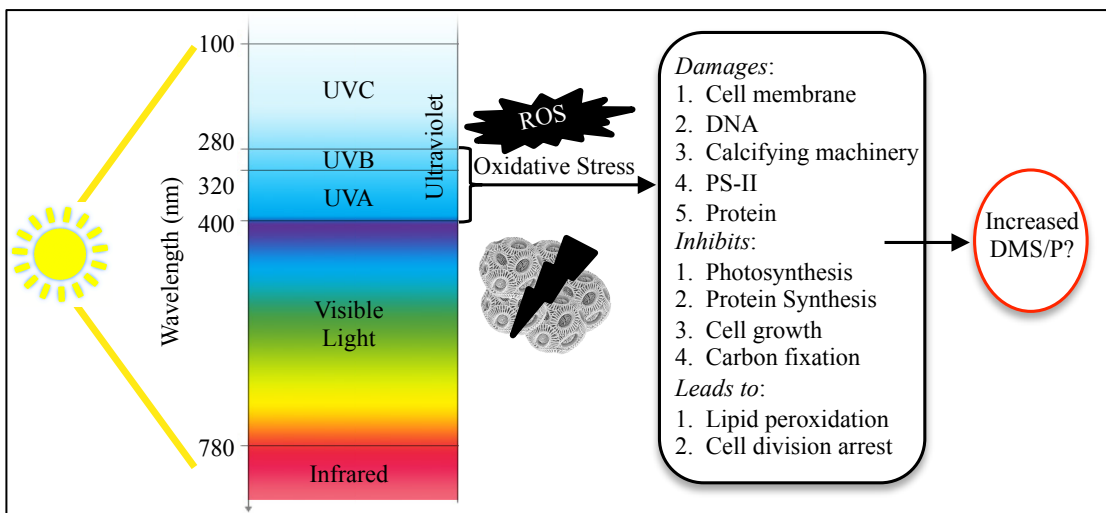
Figure 4.1 Of the solar radiation penetrating the marine euphotic zone, UVA (320-400) and UVB (280-320) can enhance the production of reactive oxygen species (ROS) in the chloroplasts of phytoplankton causing oxidative stress. Cells have developed a range of defence mechanisms or survival strategies but if the UV dose exceeds the cellular antioxidant systems it can prove fatal due to inhibition of protein synthesis and loss of membrane integrity. The experiments in this chapter consider whether an increase in the intracellular osmolyte DMSP or its breakdown products could be part of the UV-induced response to stress in *Emiliania huxleyi* (Photo of *E. huxleyi* taken from the Natural History Museum, London).

In addition to climate change, stratospheric ozone depletion and the associated increase in UVR have also attracted substantial research attention (Caldwell et al. 2007). Under clear skies, at temperate, subtropical and equatorial latitudes, total surface UVA is as high as 45-50 Wm^{-2} and UVB is as high as 7-8 Wm^{-2} (Holzinger and Lutz 2006). In the marine environment, these wavelengths of light penetrate into the euphotic zone (Obernosterer et al. 2001; Smith et al. 1992; Tedetti and Sempere 2006) and in clear waters, UVB penetrates to tens of meters (Boelen et al. 1999). In a study conducted in the central subtropical Atlantic ocean, Piazena et al. (2002) concluded that solar UVA penetrates to about 75-93% while UVB penetrates to about 25% of the depth of the photic zone. Recently, an attempt was made to determine the penetration of UVR through the water column based on a new global ocean-atmosphere model (Smyth 2011). The results from this model showed that the calculated UV doses varied in terms of the spectrum and season. The highest UV doses were calculated in the eastern Mediterranean Sea, the Sargasso Sea, the eastern Equatorial Pacific, the northern Patagonian Shelf, the northern Indian Ocean, and the latitude band of 20°S and 35°S in

the Southern hemisphere (Smyth 2011). When the mixed layer depth was shallow in July, the eastern Mediterranean Sea recorded the highest UV doses of ~ 0.5, 4, 7, and 10 kJ m^{-2} d^{-1} nm^{-1} at 305, 325, 340 and 380 nm, respectively (Smyth 2011).

Coccolithophores are widely distributed in the open oceans and are exposed to solar UVR especially when the mixed layer depth becomes shallower in the summertime (Nanninga and Tyrrell 1996). It is important to consider the effects of UVR on coccolithophores as these are one of the major living phytoplankton groups and they influence the global carbon cycle through calcification and photosynthetic carbon fixation and the sulphur cycle through the production of DMSP and its breakdown to DMS (Malin and Steinke 2004). The bloom-forming species *Emiliania huxleyi* is the most numerically abundant of the coccolithophore species and is found in all marine waters except the polar oceans. It appears to be able to adapt to varying light and temperature conditions inspite of sensitivity to UVR (Van Rijssel and Buma 2002). Studies suggest that *E. huxleyi* are tolerant to high light intensities (Nanninga and Tyrrell 1996). The function of the calicum carbonate coccoliths surrounding the cell is not certain, but it has been suggested that they might provide a protective cover to disperse light energy under high light irradiances (Paasche 2001). Conversely, other studies explain that the photoinhibition-tolerance of this organism is independent of coccoliths (Harris et al. 2005). It has been reported that UVA damages the calcifying machinery while UVB damages the photosynthetic apparatus in *E. huxleyi* cells (Guan and Gao 2010).

Long-term exposure to UVR, results in the acclimation of the *E. huxleyi* cells, forcing the cells to compromise on growth and invest energy into accumulating UV-absorbing compounds and calcification (Guan and Gao 2010). When *E. huxleyi* strain L was exposed to UVA, 10 to 25% increase in DMSP per cell (fmol) content was seen compared to the DMSP in cells exposed to only photosynthetically active radiation (PAR) (Slezak and Herndl 2003). Sunda et al. (2002) have shown that intracellular DMSP concentration increases in *E. huxleyi* 373 on exposure to solar UVR. These authors further hypothesised that because DMSP and its breakdown products are theoretically effective antioxidants they would therefore quench the harmful free

radicals produced in excess in the cell when exposed to UVR. However in contrast, there was no increase in intracellular DMSP when *E. huxleyi* strain L was subjected to UV light (Van Rijssel and Buma 2002). It could be that increased DMSP concentration due to oxidative stress differs between *E. huxleyi* strains, length of UV exposure or UV dosage dependent.

The aim of this study was to examine how *E. huxleyi* responds to artificial and natural UVR in terms of growth, efficiency of PSII (F_V:F_M), cell viability, intracellular DMSP concentration and DMS release. Investigating cell death or survival of three different *E. huxleyi* strains under UV induced stress gave the opportunity to examine the potential reach of the Sunda et al. (2002) hypothesis.

4.2 Methodology

4.2.1 Lighting conditions

In many published studies examining the effects of UV light, the light field is poorly characterised or simply assumed. Here the 240-700 nm spectrum of our in-house constructed UV cabinet with UVA lamps (Q-Panel lab UVA-340, 40W) and UVB lamps (Q-Panel lab UVB-313, 40W) was measured using a Macam SR9910 Spectroradiometer with version 7.07.1 software. PAR was recorded for 400-700 nm, UVA 320-400 nm, UVB 280-320 nm and UVC was 240-280 nm. The spectroradiometer could not detect wavelengths below 240 nm in the UVC region. PAR light was delivered by cool fluorescent light tubes (Philips Master TLD Reflex, 58W 840 Cool White). For the low, normal and high light conditions (hereafter referred to by the abbreviations: LL, NL and HL respectively), either 3, 6 and 17 light tubes were used. The light intensities achieved are shown in Table 4.1. The cultures were acclimatized for two generations under the experimental light intensity before exposing them to UVA+UVB light. For UVA exposure, one UVA lamp was used and for UVA+UVB exposure, one UVA lamp and one UVB lamp were switched on. In all cases a 14:10 light:dark cycle was applied. Control flasks were incubated under identical conditions but covered by a UVB cut-off filter (Mylar film-Secol Ltd) mounted on a wooden frame. The transmission of light

through the UVB cut-off filter was also tested using a scanning UV-Visible spectrophotometer.

Table 4.1 PAR light intensity conditions

Light intensity condition	abbreviation	µmol photons m^{-2} s^{-1}	W/m²
Low Light	LL	50	10
Normal Light	NL	100	20
High Light	HL	1000	250

Attempts were also made to expose *Emiliania huxleyi* 370, 373 and 1516 to solar UV radiation (see section 4.3.4). For this, batch cultures of the strains in mid-log phase were exposed to direct sunlight in quartz and borosilicate flasks placed on the roof. Due to the uncertainty of the weather conditions these experiments were done opportunistically so the cultures were not acclimated beforehand. The UVB cut-off filter described above was used for the control flasks.

4.2.2 Cell culture and growth measurements

Three strains of *Emiliania huxleyi* CCMP370, CCMP373 and CCMP1516 were grown; each in 1 L of f/2-Si medium in 2 L borosilicate conical flasks. Cultures were grown to mid-log phase in an incubator under a 14:10 light:dark cycle at 15°C. The acclimated cells were then dispensed into 500 ml quartz and borosilicate flasks. For each culture strain, the experiments were conducted with three control flasks (covered by a UVB cut-off filter) and three treated flasks. The various experimental treatments with different light conditions and different UV conditions are listed in Table 4.2.

Biomass was quantified as cell number and cell volume (Chapter 2, section 2.4); fluorescence and efficiency of PSII (F_V:F_M) were also measured (Chapter 2, section 2.5). DMS, DMSPd, DMSPp and DMSPt were measured by GC (Chapter 2, section 2.6) and

membrane permeability ('viability') was determined with SYTOX Green using the flow cytometer (Chapter 2, section 2.7).

Table 4.2 Experimental treatments with different light conditions and different UV conditions

UVR exposure in artificial light conditions			Label	UVA	UVB	Light intensity
UVA exposure				(Wm^{-2})	(Wm^{-2})	(Wm^{-2})
1	Quartz	NL + 100% UVA	a	1.17	0.073	18.8
	Quartz + filter	NL + 70% UVA	b	0.82	0.011	18.7
2	Borosilicate	NL + 100% UVA	a	1.17	0.058	19.2
	Borosilicate + filter	NL + 70% UVA	b	0.82	0.010	18.8
UVA+UVB exposure under a range of light intensities						
3	Quartz	NL + 100% UVA + 100% UVB	c	2	1	22
	Quartz + filter	NL + 70% UVA	b	1.4	0.068	18.8
4	Borosilicate	NL + 100% UVA + 80% UVB	d	2	0.8	19.5
	Borosilicate + filter	NL + 70% UVA	b	1.4	0.088	19.8
5	Quartz	LL + 100% UVA + 100% UVB	f	nd	nd	10
	Quartz + filter	LL + 70% UVA	e	nd	nd	10
6	Quartz	HL + 100% UVA + 100% UVB	h	nd	nd	250
	Quartz + filter	HL + 70% UVA	g	nd	nd	250
UVA+UVB exposure under natural light conditions			i			
7	Quartz	SR				
	Quartz + filter	SR - UVB				
8	Borosilicate	SR				
	Borosilicate + filter	SR - UVB				
Note: The filter used was a UVB cut-off filter. Borosilicate was transparent to 100% UVA and 80% UVB. Where readings were not recorded, nd (not determined) is mentioned in the table. For UVA and UVB under natural light conditions, refer to Figure 4.14. These values are not recorded in the above table due to the varying natural conditions.						

4.3 Results

4.3.1 UVB-cut off filter

Figure 4.2 shows a spectrum of the percentage transmittance for the UV cut-off filter. This clearly shows that the filter cuts off wavelengths in the UVB and UVC wavebands but transmits 70% light in the UVA waveband. Thus the control cultures were exposed to some portions of the UVA waveband. Without the use of the filter, 100%

transmittance of PAR, UVA and UVB was achieved. These observations were also confirmed by the spectroradiometer results in Fig. 4.3 (section 4.3.2).
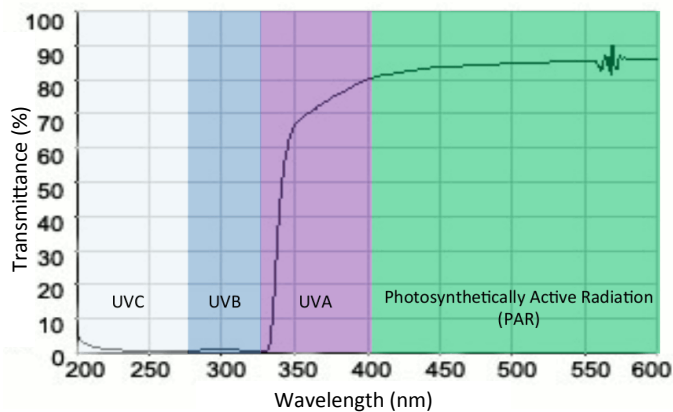
Figure 4.2 Transmittance Spectrum of the UV cut-off filter obtained using a scanning UV-Visible spectrophotometer.

4.3.2 PAR and UVR irradiance conditions

The spectroradiometer data (Fig. 4.3) revealed an interesting feature of the light sources used for this study. Under NL intensity conditions and without the UV light tubes in the cabinet, about 20 W/m^2 PAR was available but small quantities of UVA (0.22 W/m^2), UVB (0.02 W/m^2) and UVC (0.00024 W/m^2) were also recorded. With NL conditions and the UVA lamp, the spectroradiometer indicated UVA radiation of 1.17 W/m^2 and detected UVB and UVC region wavelengths giving intensities of 0.083 W/m^2 and 0.00052 W/m^2 respectively in the cabinet. With NL, UVA and UVB lamps switched on, the total UVA in the cabinet was 1.89 W/m^2 and UVB was 0.95 W/m^2. Extremely small quantities of UVC radiations of 0.0075 W/m^2 were detected in these artificial light sources, which may perhaps be ignored.

Another feature to note was that even though the total PAR in the cabinet was 20 W/m^2, the irradiance measured within the quartz flasks showed higher values. This was not the case with borosilicate flasks. This was probably due to light reflections within the walls of the quartz flask. Thus, under NL the total light intensity measured within quartz flasks was 22 W/m^2 and in borosilicate flasks was 20 W/m^2. The total UVA measured within

the quartz and borosilicate flasks was the same at 2 W/m^2, whilst UVB was 1 W/m^2 in the quartz flasks and 0.8 W/m^2 in the borosilicate flasks. This indicates that the borosilicate flasks were transparent to 100% UVA and 80% UVB.
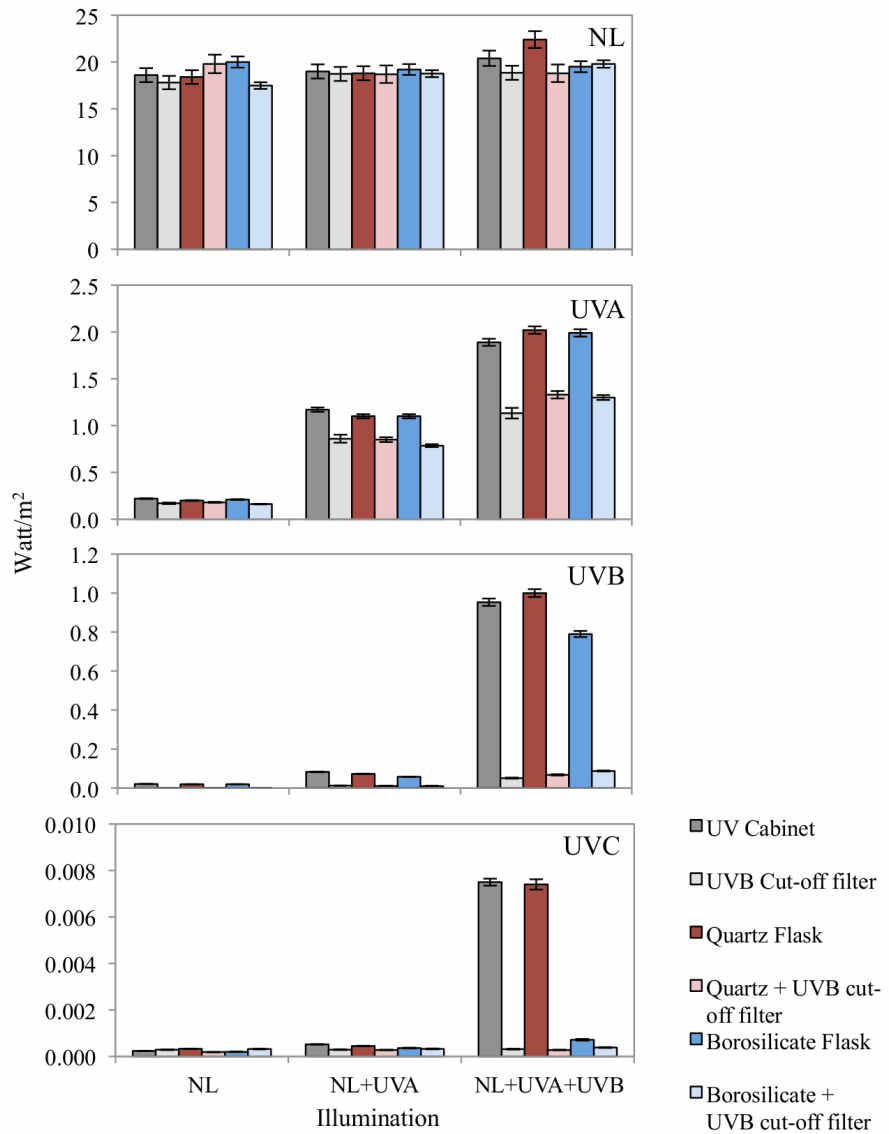
Figure 4.3 Irradiance (W/m²) from cool white fluorescent tubes (NL), alone or in combination with UVA and UVB lamps measured using a Macam SR990 Spectroradiometer. The bars represent the following: grey–the total available irradiance; light grey– the irradiance with a UVB cut-off filter; red–the irradiance within a quartz flask; pink–the irradiance in a quartz flask with a UVB cut-off filter; blue–irradiance in a borosilicate flask; and light blue–irradiance in a borosilicate flask with a UVB cut-off filter. The average value and range of data is shown (n=3). Where no range bars are visible, the data range was smaller than the symbol size.

The spectroradiometer data confirmed that the UVB cut-off filter efficiently transmitted 20 W/m^2 light in the PAR region of the spectrum and absorbed most of the UVB radiation. The quartz flask with a UVB cut-off filter is exposed to about 0.068 W/m^2 UVB whereas in a borosilicate flask with the UVB cut-off filter, UVB is about 0.088 W/m^2, which may perhaps be ignored. With the NL conditions and the UVA lamp, the UVB cut-off filter transmits 0.82 W/m^2 UVA which in effect is 70% of the 1.17 W/m^2 UVA received by a quartz or a borosilicate flask without the UV cut-off filter. Also, with the NL, UVA and UVB lamps switched on, the UVB cut-off filter transmits 1.4 W/m^2 UVA which in effect is 70% of the 2 W/m^2 UVA received by a quartz flask and a borosilicate flask without the UV cut-off filter.

4.3.3 UV light exposure in artificial light conditions

4.3.3.1 UVA exposure

E. huxleyi 1516 was exposed to UVA radiation with and without the UVB cut-off filter in NL in quartz and borosilicate flasks (both NL+70% UVA with filter control and NL+100% UVA without filter) for 7 days. All cultures illustrated essentially the same growth patterns in terms of cell density, cell volume and fluorescence (Fig. 4.4a-f). From day 3 to day 7, cell volume (Fig. 4.4 c, d) was slightly increased from 21 to 19 μm^3 in the NL+100% UVA exposed culture. Photosynthetic capacity (PC; F_V:F_M) (Fig. 4.4g, h) showed more variation between replicates and was slightly elevated on days 0 and 1 at 0.54 and 0.52 in the quartz NL+70% UVA with filter treatment. However, otherwise it remained quite similar in the 2 treatments. Intracellular DMSP concentration (Fig. 4.5a, b) also did not vary much despite the slightly elevated amount of DMSP per cell at 5.12 to 4.40 μM between days 2 to 7 in the quartz NL+100% UVA treatment (Fig. 4.5c). SYTOX Green staining also did not show any distinct differences between the control NL+70% UVA treatments and the NL+100% UVA exposed cultures.
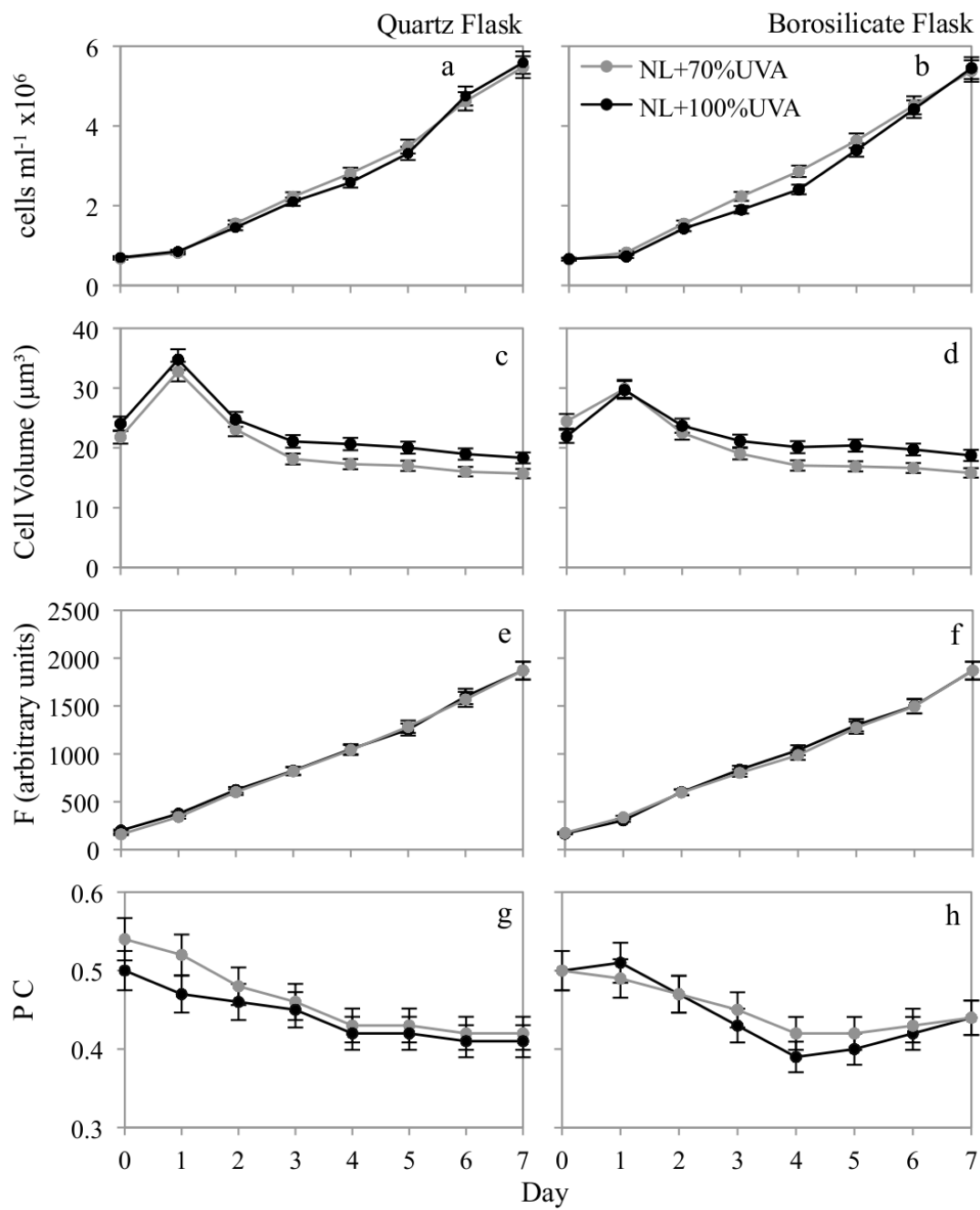
Figure 4.4 *E. huxleyi* 1516 exposed to UVA radiation in normal light (NL) conditions. (a, b) Cell density (cells ml^{-1} x 10^6), (c, d) cell volume (μm^3), (e, f) Fluorescence (F, arbitrary unit) (g, h) Photosynthetic capacity (PC). The grey line represents the control flasks covered with UVB cut-off filter NL+70% UVA, and the black line represents the NL+100% UVA exposed quartz flasks. The plots on the left are for quartz flasks and those on the right for borosilicate flasks. The average value and range of data is shown (n=3). Where no range bars are visible, the data range was smaller than the symbol size.
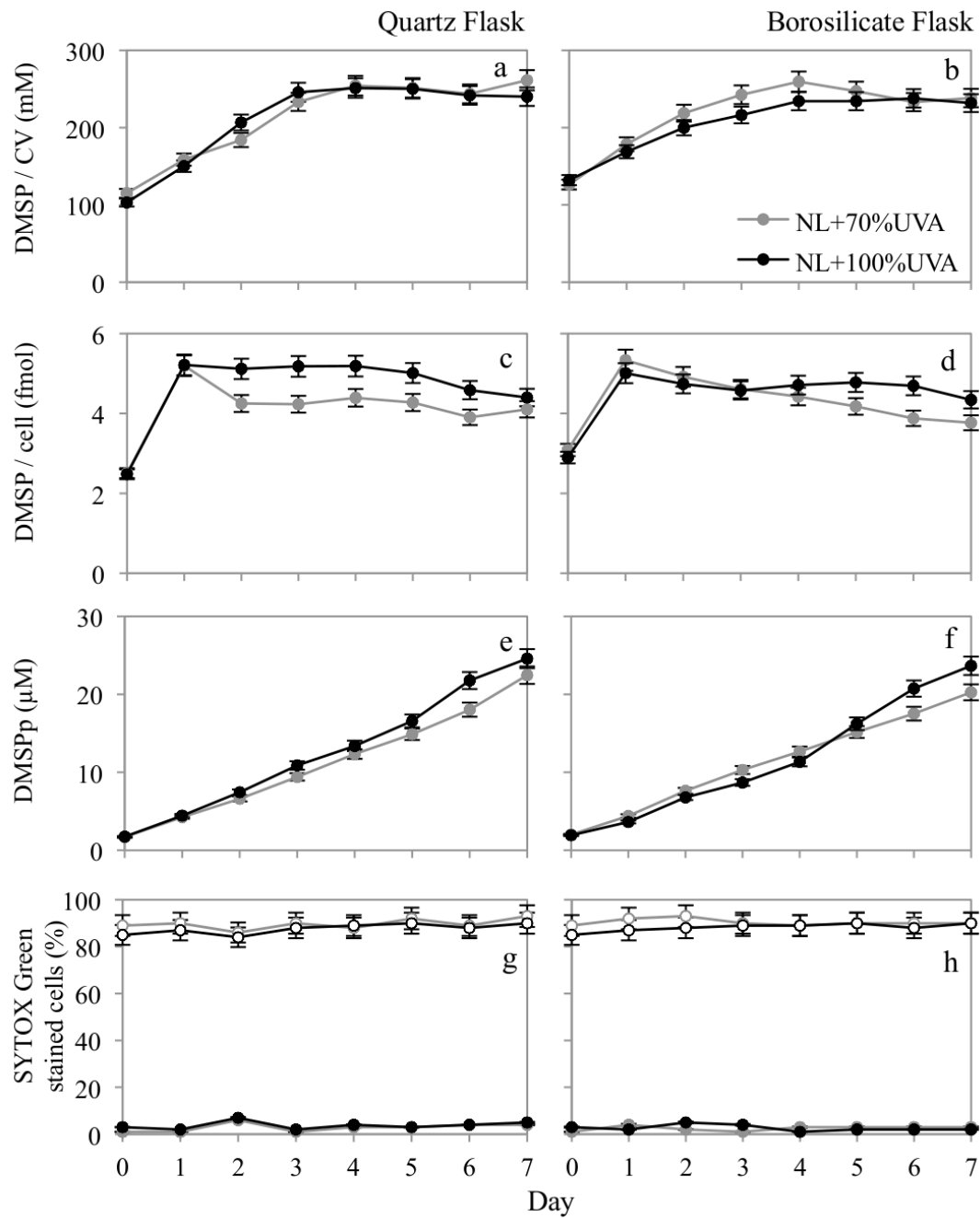
Figure 4.5 *E. huxleyi* 1516 exposed to UVA radiation in normal light (NL) conditions. (a, b) DMSP per cell volume (mM), (c, d) DMSP per cell (fmol), (e, f) DMSPp in the culture (µM) (g, h) SYTOX Green stained cells (%)–the open symbols show percentage of viable cell (cells unstained by SYTOX Green) and the closed symbols show percentage of cells with compromised cell membranes (SYTOX Green stained cells). The grey line represents the control flasks covered with UVB cut-off filter NL+70% UVA, and the black line represents the NL+100% UVA exposed quartz flasks. The plots on the left are for quartz flasks and those on the right for borosilicate flasks. The average value and range of data is shown (n=3). Where no range bars are visible, the data range was smaller than the symbol size.

4.3.3.2 UVA+UVB exposure under a range of light intensities

In this experiment three strains, *E. huxleyi* 370, 373 and 1516 were exposed to UVA+UVB radiation in quartz flask under LL, NL and HL conditions. Additionally, *E. huxleyi* 1516 was exposed to UVA+UVB radiation under NL conditions in borosilicate flasks. The spectroradiometer data (Fig. 4.3) revealed that borosilicate glass efficiently allowed the available PAR light and UVA to penetrate, but reduced the UVB-exposure to 80% UVB (0.8 Wm^{-2}) in contrast to the 100% UVB exposure of the cultures in quartz flasks. This reduced level of UVB exposure in *E. huxleyi* 1516 in borosilicate flask gave simultaneously one more condition to observe in the experiment.

4.3.3.2.1 Cell culture and growth measurements

The control UVB-filter cultures continued to grow throughout the experiment under NL, LL and HL conditions, but the three *E. huxleyi* strains varied in their specific growth rates (Table 4.3). Specific growth rates showed an increase from 0.45 to 0.70 in LL to HL conditions in *E. huxleyi* 370 and 373, while the specific growth rate in *E. huxleyi* 1516 increased from 0.45 to 0.62 in LL to NL conditions and remained unchanged at 0.61 in HL conditions. Table 4.3 also shows the specific growth rates for the three strains in NL, LL and HL conditions without UV radiation. These data were obtained after acclimation of the cells in the different light conditions at 15°C before exposing the cells to the UV treatments (growth curves not shown here) and are presented here only for comparison with specific growth rates of the UVB filter cultures.

Table 4.3 Specific Growth rates for acclimatized cells of *E. huxleyi* 370, 373 and 1516 under low light (LL, 50 µmol photons m^{-2} s^{-1}), normal light (NL, 100 µmol photons m^{-2} s^{-1}) and high light (HL, 1000 µmol photons m^{-2} s^{-1}) conditions at 15°C and specific growth rates for all the three strains with the UVB cut-off filter which would mean exposure to 70% UVA under the different light conditions.

Specific growth rate (µ, d^{-1})	*E. huxleyi* 370			*E. huxleyi* 373			*E. huxleyi* 1516		
	LL	NL	HL	LL	NL	HL	LL	NL	HL
With 70% UVA	0.46	0.57	0.70	0.45	0.53	0.70	0.45	0.62	0.61
Only PAR	0.50	0.62	0.80	0.50	0.62	0.80	0.52	0.65	0.80

Exposure of *E. huxleyi* 370, 373 and 1516 to UVA+UVB radiation for 72 hours under NL, LL and HL conditions in quartz flasks resulted in cell growth arrest with a steady decline in cell density (Fig. 4.6a-i). This suggests that the cells simply failed to tolerate the UV irradiance they were exposed to and it was clear to the naked eye that the cultures lost their pigmentation and turned colourless in 24 h. The cell growth in quartz flasks dropped between 24 to 72 hours from 370,000 to 70,000 in LL; 480,000 to 370,000 in NL and 270,000 to 90,000 cells ml^{-1} in HL conditions in UVB exposed *E. huxleyi* 370; from 100,000 to 44,000 in LL; 590,000 to 470,000 in NL and 200,000 to 145,000 cells ml^{-1} in HL in UVB exposed *E. huxleyi* 373 and from 150,000 to 74,000 in LL, 347,000 to 230,000 in NL and 360,000 to 184,000 cells ml^{-1} in HL conditions in UVB exposed *E. huxleyi* 1516. *E. huxleyi* 1516 exposed to UVA+UVB in borosilicate flask with reduced level of UVB exposure on the other hand showed growth inhibition and cell growth arrest (Fig. 4.6j). There was an increase in cell number at 0h from 500,000 to 983,000 cells ml^{-1} at 24 h in the borosilicate flasks after which the values remained consistent at ~ 980,000 cells ml^{-1} (Fig. 4.6 j). This contrasted with the gradual decline seen in cultures growing in quartz flasks.

Cell volume (Fig. 4.7) remained higher in the UVA+UVB exposed cultures than the control cultures. Cell volume in all the three UVA+UVB-exposed strains increased: to 40 and 60 μm^3 in *E. huxleyi* 370, 45 and 83 μm^3 in *E. huxleyi* 373 and 27 and 38 μm^3 in *E. huxleyi* 1516 at 72 h in LL and NL conditions respectively. But under HL conditions the cell volume remained similar to that of the control cultures at 27, 6 and 11 μm^3 for *E. huxleyi* 370, 373 and 1516. Cell volume of the UVB-exposed *E. huxleyi* 1516 cells in borosilicate flasks showed a higher increase of 52 μm^3 at 72 h than that seen in quartz flasks. This would indicate that reducing the UVB by only 20% allowed the cells to remain sufficiently active to increase in cell volume. Cell volume did not vary much in the control cultures of *E. huxleyi* 370 and 1516 under NL, LL and HL conditions, but *E. huxleyi* 373 increased in cell volume under NL and HL conditions.
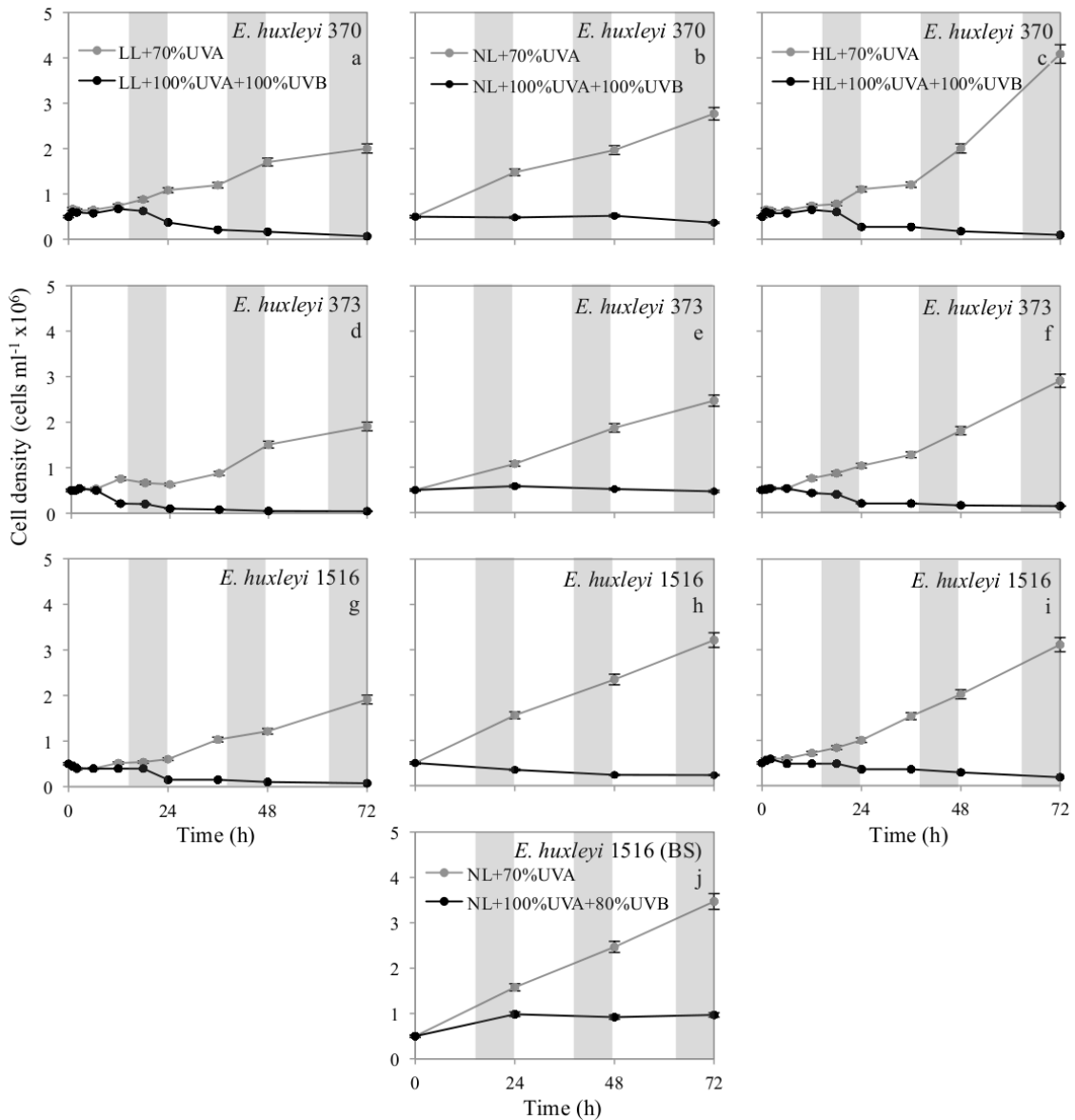
Figure 4.6 Comparison of cell density in *E. huxleyi* 370, 373 and 1516 exposed to UVA + UVB radiation with a 14L:10D cycle under low light (LL), normal light (NL) and high light (HL) conditions. The grey shading denotes the dark cycle. The grey line represents the control flasks with the UVB cut-off filter (+70% UVA) and the black line represents the UVA+UVB exposed flasks (100% UVA+100% UVB). BS stands for borosilicate flask (j; 80% UVB exposure) and all other plots show results for quartz flasks. The average value and range of data is shown (n=3). Where no range bars are visible, the data range was smaller than the symbol size.
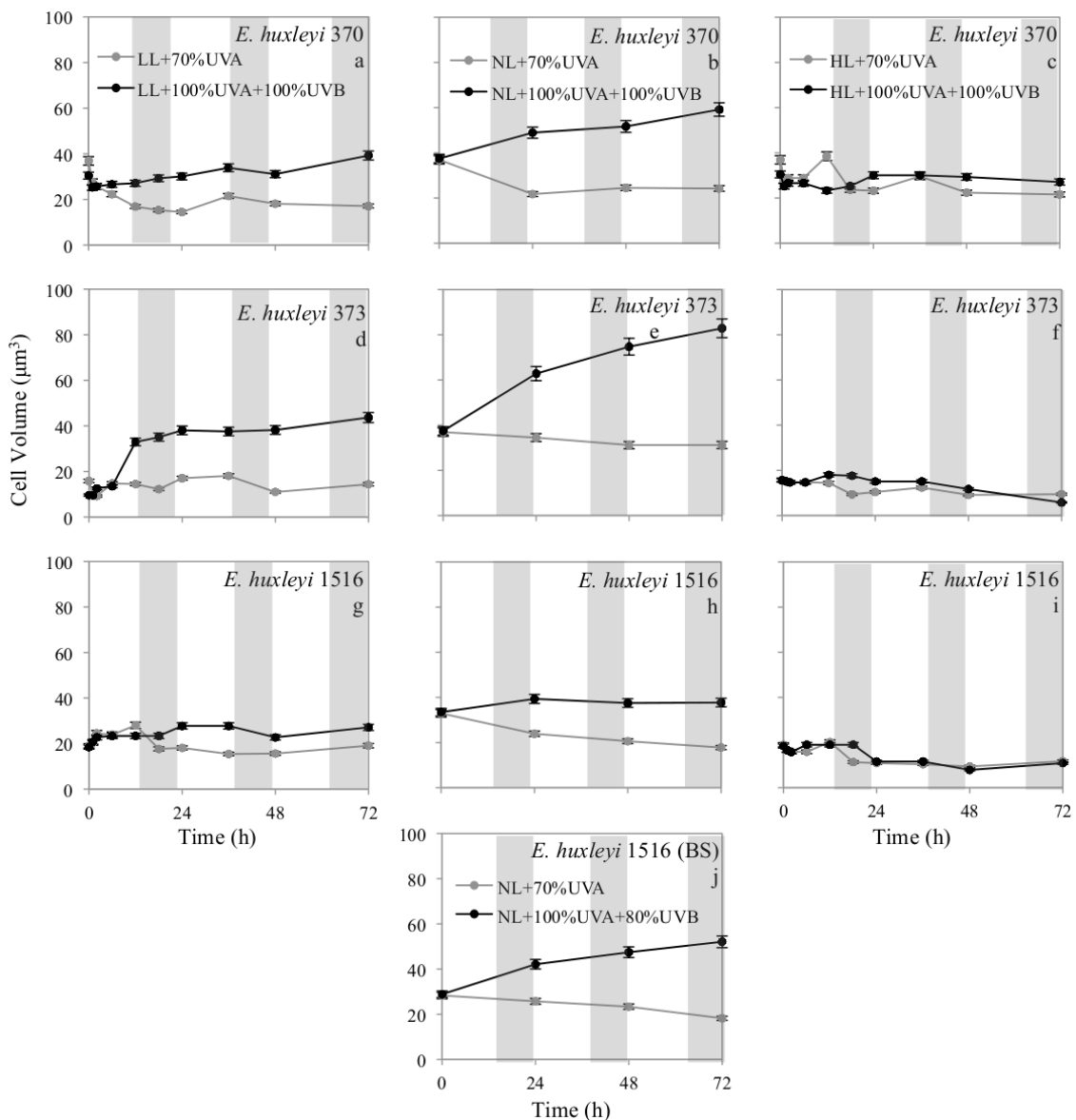
Figure 4.7 Comparison of cell volume in *E. huxleyi* 370, 373 and 1516 exposed to artificial UVR in the 14L:10D cycle under low light (LL), normal light (NL) and high light (HL) conditions. The grey shade is the dark cycle. The grey line represents the control flasks with the UVB cut-off filter (+70% UVA) and the black line represents the UVA+UVB exposed flasks (100% UVA+100% UVB). BS stands for borosilicate flask (j; 80% UVB exposure) and all other plots show results for quartz flasks. The average value and range of data is shown (n=3). Where no range bars are visible, the data range was smaller than the symbol size.

Alongside the lack of growth (Fig. 4.6) fluorescence also declined in the UVA+UVB exposed cultures (Fig. 4.8a-i). Maximum fluorescence value of 422 was observed in *E. huxleyi* 373 and 146 for *E. huxleyi* 370 under NL conditions while it mostly ranged between 20 and 2 under LL, NL and HL conditions for all the three strains. *E. huxleyi* 1516 in borosilicate flask remained unaltered at 520 since 24 hours of exposure till the last reading at 72 h (Fig. 4.8j). Fluorescence values in the control cultures under NL conditions appeared much higher than under the LL and HL conditions.

Photosynthetic capacity (Fig. 4.9a-i) dropped considerably to ~ 0.1 after 24 h in the UVA+UVB exposed quartz flask cultures for all the three strains under LL, NL and HL conditions. However, at 48 h the cell photosynthetic capacity had improved, it was noted at ~ 0.2 for *E. huxleyi* 370, 373 and 1516 under LL, *E. huxleyi* 373 under NL and *E. huxleyi* 370 and 373 under HL conditions. Although increasing it still remained lower than the photosynthetic capacity for cells in the control culture flask. Photosynthetic capacity did not appear to differ much in the control cultures under the different light conditions.

E. huxleyi 1516 exposed to UVA+UVB in borosilicate dropped only to 0.39 at 24 h and increased to match control culture at 0.42 at 48 h. This would indicate reducing the UVB by only 20% allowed the cells to remain sufficiently active to even increase in cell volume (Fig. 4.7j). This retention of activity is evident when comparing the substantial drop in photosynthetic capacity in the 100% UVB cultures (Fig 4.9 h) with the similar values for the 80% UVB and UVB-screened borosilicate glass cultures (Fig 4.9j). With 80% UVB fluorescence was retained at the initial value (Fig. 4.8 j).
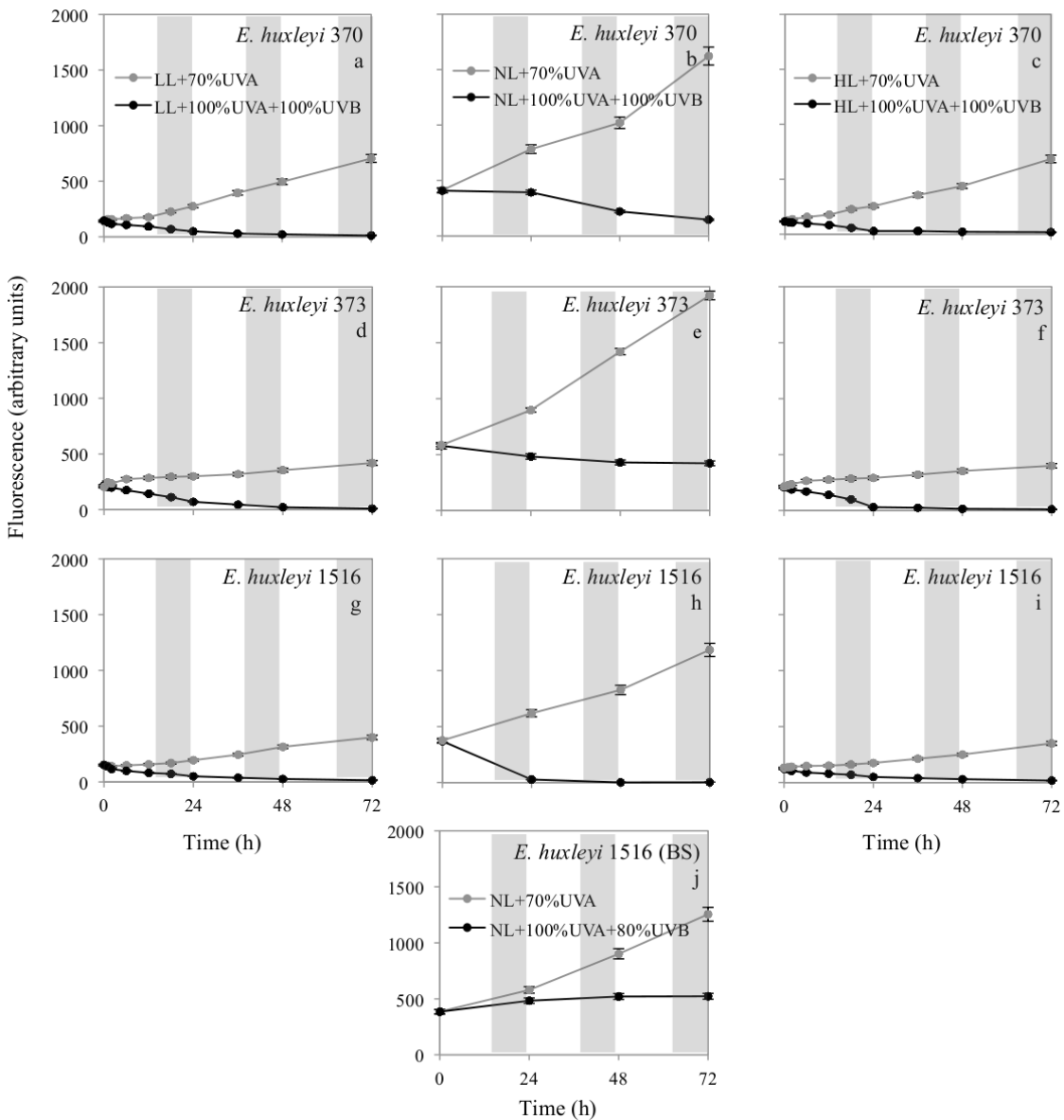
Figure 4.8 Comparison of fluorescence in *E. huxleyi* 370, 373 and 1516 exposed to artificial UVR in the 14L:10D cycle under low light (LL), normal light (NL) and high light (HL) conditions. The grey shade is the dark cycle. The grey line represents the control flasks with the UVB cut-off filter (+70% UVA) and the black line represents the UVA+UVB exposed flasks (100% UVA+100% UVB). BS stands for borosilicate flask (j; 80% UVB exposure) and all other plots show results for quartz flasks. The average value and range of data is shown (n=3). Where no range bars are visible, the data range was smaller than the symbol size.
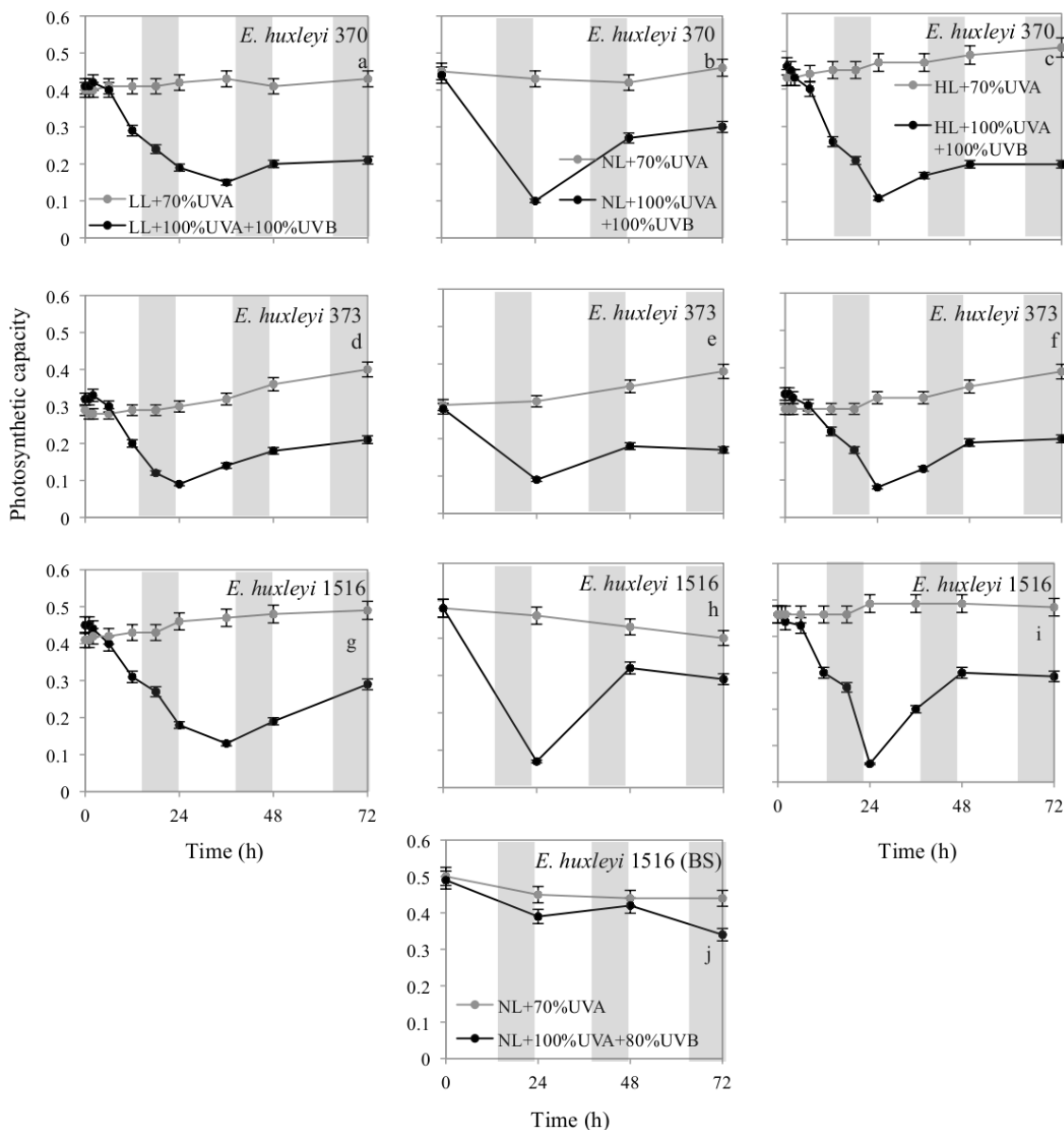
Figure 4.9 Comparison of cell photosynthetic capacity in *E. huxleyi* 370, 373 and 1516 exposed to artificial UVR in the 14L:10D cycle under low light (LL), normal light (NL) and high light (HL) conditions. The grey shade is the dark cycle. The grey line represents the control flasks with the UVB cut-off filter (+70% UVA) and the black line represents the UVA+UVB exposed flasks (100% UVA+100% UVB). BS stands for borosilicate flask (j; 80% UVB exposure) and all other plots show results for quartz flasks. The average value and range of data is shown (n=3). Where no range bars are visible, the data range was smaller than the symbol size.

4.3.3.2.2 Intracellular DMSP concentrations and cellular DMSP

Intracellular DMSP concentration (per cell volume mM; Fig. 4.10), DMSP per cell (fmol; Fig. 4.11) and the culture DMSP (μM; Fig. 4.12) in the UVA+UVB-exposed cultures decreased by 24 h. DMSP per cell volume was noted at 80, 34 and 188 mM in *E. huxleyi* 370; 93, 19 and 219 mM in *E. huxleyi* 373 and 105, 83 and 268 mM in *E. huxleyi* 1516 at 72 h under LL, NL and HL conditions respectively. DMSP per cell was 3.1, 2 and 5.1 fmol in *E. huxleyi* 370; 4, 1.6 and 1.3 fmol in *E. huxleyi* 373 and 2.9, 3.2 and 2.9 fmol in *E. huxleyi* 1516 at 72 h under LL, NL and HL conditions respectively. While DMSP value in the culture was noted at 0.2, 0.7 and 0.5 μM in *E. huxleyi* 370; 0.2, 0.7 and 0.2 μM in *E. huxleyi* 373 and 0.2, 0.7 and 0.5 μM in *E. huxleyi* 1516 at 72 h under LL, NL and HL conditions respectively.

Although there was no increase in DMSP concentrations when the cells were exposed to UVA+UVB, the acclimatized control cultures in LL and HL conditions showed higher intracellular DMSP (300-400 mM), in contrast with the lower intracellular DMSP (150-200 mM) in the NL condition.

In borosilicate flasks, DMSP per cell in *E. huxleyi* 1516 was higher after 24 h at 5.9 fmol and remained consistent till 72 h compared to the control culture (Fig 4.11j). Intracellular DMSP concentrations decreased on exposure to 80% UVB for 48 hours where values at ~ 140 mM were close to those of the control cultures, but then dropped to 98 mM at 72 h (Fig. 4.10j). Overall higher DMSP concentrations, DMSP per cell and DMSP per cell volume values were noted with 80% UVB when compared to the 100% UVB exposed cultures (Fig 4.10 h, j; Fig 4.11 h, j and Fig. 4.12h, j). The total DMSP concentration in the screened control cultures showed similar concentrations in the quartz and borosilicate flasks (Fig. 4.12 h, j), but the 100% UVB-exposed cultures in the quartz flasks showed low 1-3 μM DMSP compared to 3-6 μM DMSP in the 80% UVB-exposed cultures in the borosilicate flasks. This suggests that UVB irradiation decreases DMSP production.
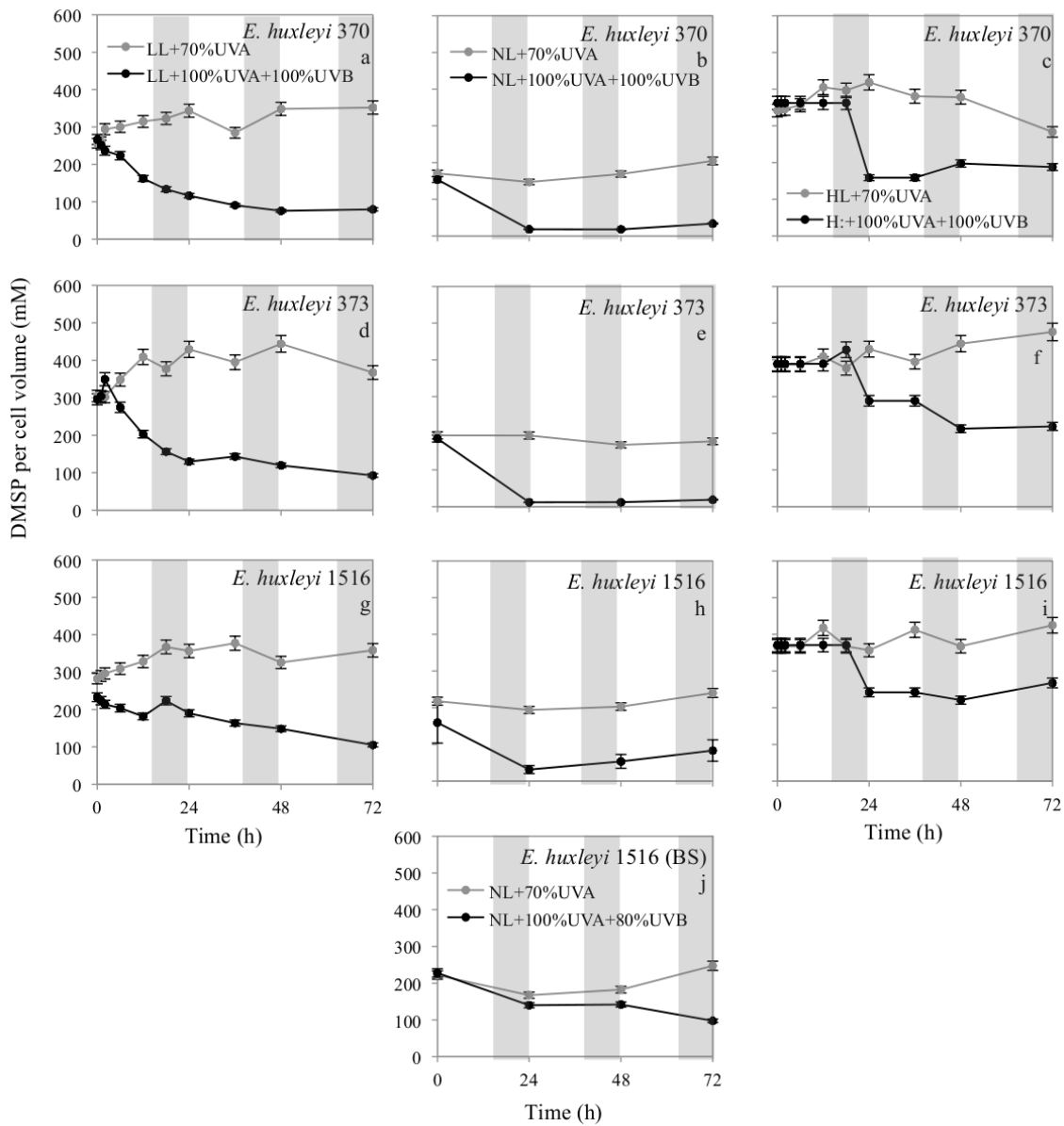
Figure 4.10 Comparison of DMSP per cell volume (mM) in *E. huxleyi* 370, 373 and 1516 exposed to artificial UVR in the 14L:10D cycle under low light (LL), normal light (NL) and high light (HL) conditions. The grey shade is the dark cycle. The grey line represents the control flasks with the UVB cut-off filter (+70% UVA) and the black line represents the UVA+UVB exposed flasks (100% UVA+100% UVB). BS stands for borosilicate flask (j; 80% UVB exposure) and all other plots show results for quartz flasks. The average value and range of data is shown (n=3). Where no range bars are visible, the data range was smaller than the symbol size.
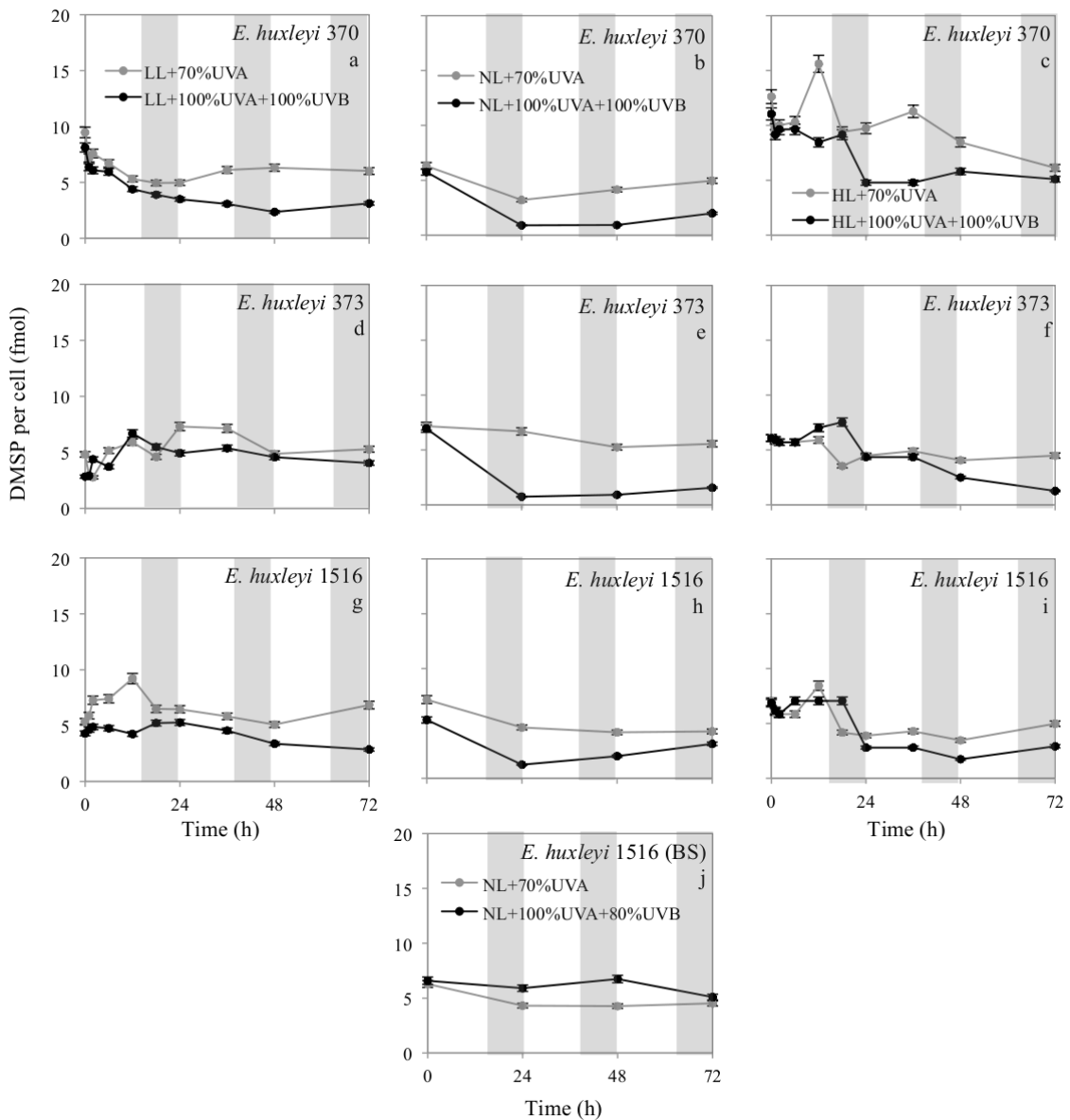
Figure 4.11 Comparison of DMSP per cell (fmol) in *E. huxleyi* 370, 373 and 1516 exposed to artificial UVR in the 14L:10D cycle under low light (LL), normal light (NL) and high light (HL) conditions. The grey shade is the dark cycle. The grey line represents the control flasks with the UVB cut-off filter (+70% UVA) and the black line represents the UVA+UVB exposed flasks (100% UVA+100% UVB). BS stands for borosilicate flask (j; 80% UVB exposure) and all other plots show results for quartz flasks. The average value and range of data is shown (n=3). Where no range bars are visible, the data range was smaller than the symbol size.
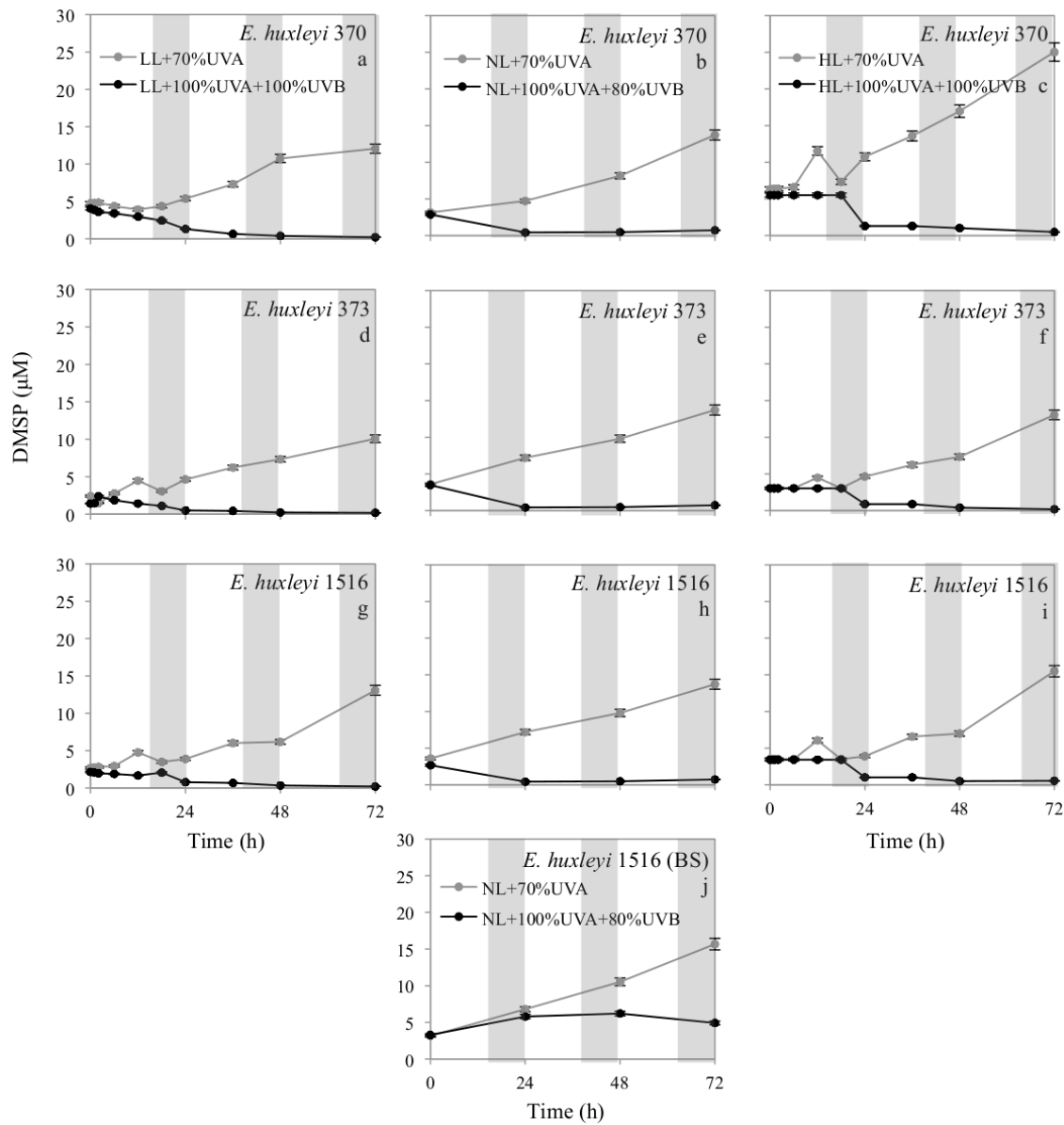
Figure 4.12 Comparison of DMSP (μM) in *E. huxleyi* 370, 373 and 1516 exposed to artificial UVR in the 14L:10D cycle under low light (LL), normal light (NL) and high light (HL) conditions. The grey shade is the dark cycle. The grey line represents the control flasks with the UVB cut-off filter (+70% UVA) and the black line represents the UVA+UVB exposed flasks (100% UVA+100% UVB). BS stands for borosilicate flask (j; 80% UVB exposure) and all other plots show results for quartz flasks. The average value and range of data is shown (n=3). Where no range bars are visible, the data range was smaller than the symbol size.

4.3.3.2.3 SYTOX Green Staining

The SYTOX Green staining data revealed that of the cells exposed to UVR under LL conditions *E. huxleyi* 370 showed 24%, *E. huxleyi* 373 showed 26% and *E. huxleyi* 1516 showed 23%; while under NL conditions *E. huxleyi* 370 showed 14%, *E. huxleyi* 373 showed 13% and *E. huxleyi* 1516 showed 17%; and under HL conditions *E. huxleyi* 370 showed 20%, *E. huxleyi* 373 showed 22% and *E. huxleyi* 1516 showed 12% of cells with compromised cell membranes at 72 h (Fig. 4.13). These values show a lower percentage of cells with compromised membranes under NL conditions when compared to the percentage of compromised cells under LL and HL conditions at 72 h. This effect is also mirrored in the percentages of viable cells which is 82, 86 and 81% in *E. huxleyi* 370, 373 and 1516 under NL conditions when compared to the 70, 71 and 72% in *E. huxleyi* 370, 373 and 1516 under LL conditions and 73, 73, and 79% in *E. huxleyi* 370, 373 and 1516 under HL conditions, respectively. SYTOX Green staining did not show any noticeable variation in the percentage of compromised cells in the control cultures under different light conditions in all the three strains. In comparison to the *E. huxleyi* 1516 cultures in the UVB-exposed quartz flasks, the cultures in the borosilicate flasks (Fig. 4.13j) showed lower percentage of compromised cells 14% at 72 h and a slightly higher number of viable cells of 83% at 72 h in *E. huxleyi* 1516. This was probably due to the reduced 20% UVB in the borosilicate flask.
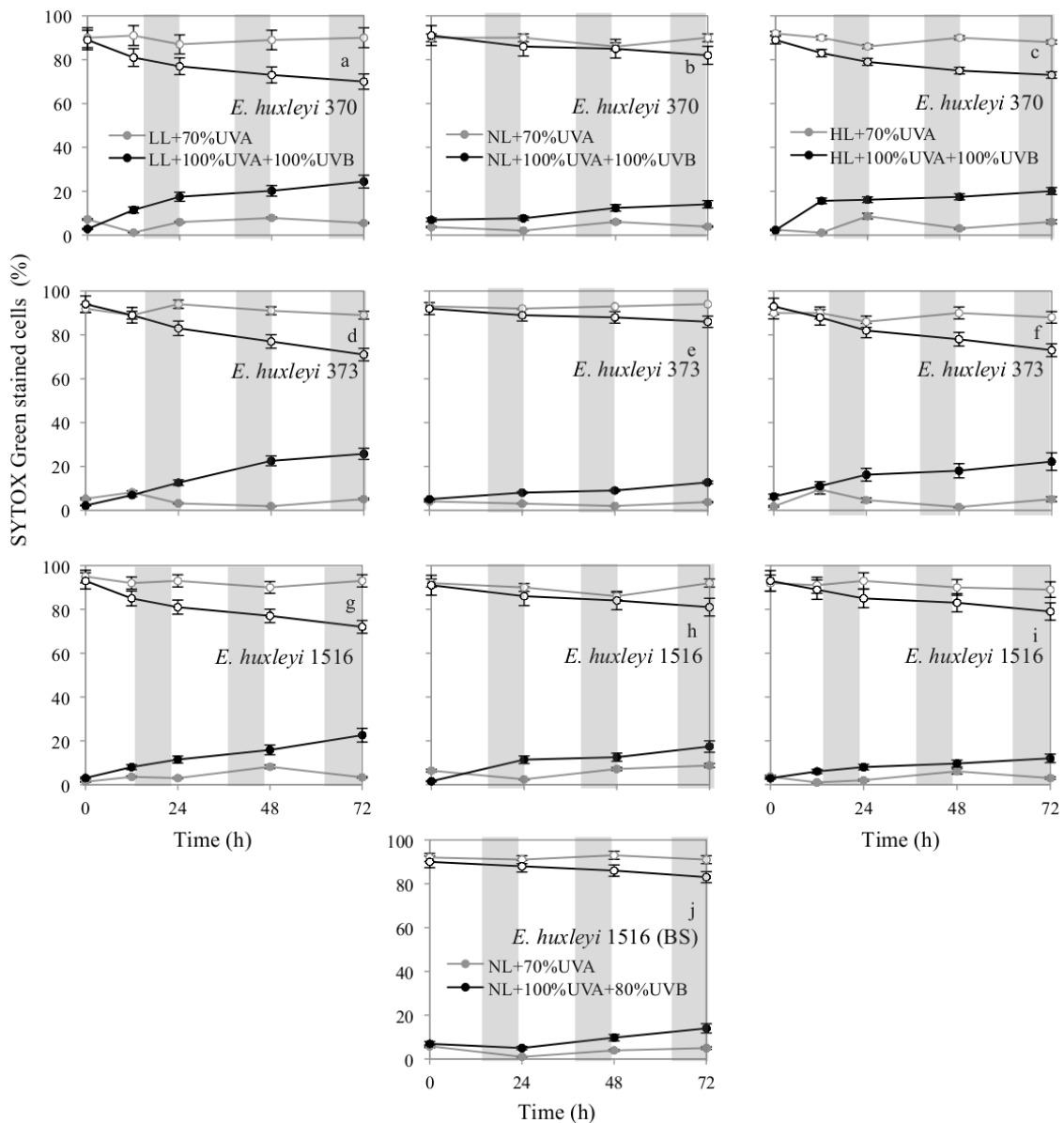
Figure 4.13 Comparison of percentage SYTOX Green stained cells- compromised and viable cells in *E. huxleyi* 370, 373 and 1516 exposed to artificial UVR in the 14L:10D cycle under low light (LL), normal light (NL) and high light (HL) conditions. The grey shade is the dark cycle. The grey line represents the control flasks with the UVB cut-off filter (+70% UVA) and the black line represents the UVA+UVB exposed flasks (100% UVA+100% UVB). The open symbols show percentage of viable cell (cells unstained by SYTOX Green) and the closed symbols show percentage of cells with compromised cell membranes (SYTOX Green stained cells). BS stands for borosilicate flask (j; 80% UVB exposure) and all other plots show results for quartz flasks. The average value and range of data is shown (n=3). Where no range bars are visible, the data range was smaller than the symbol size.

4.3.4 UVA+UVB exposure under natural light conditions

An experiment was carried out in May 2010 where cultures were exposed to direct sunlight for 72 hours. A rapid decline in cell numbers was seen within the first few hours of exposure. Fluorescence and photosynthetic capacity decreased dramatically and SYTOX Green staining revealed almost 90% cells with compromised cell membranes indicating mass cell death. Cell volume could not be measured as the remains of cells in the flasks clumped together as white fluffy masses. On analyzing DMSP in the culture, a decrease from 3 to 0.3 μM was found over a 72 h period.

The experiment was repeated from 23-26 August 2010. During this period *E. huxleyi* 370, 373 and 1516 cultures were exposed to short sunny intervals with most of the day being moderately cloudy with a few rain spells. As it was not possible to deploy the spectroradiometer during this experiment, Figure 4.14a, b shows solar radiation and air temperature data from (WeatherQuest, UEA) for 23-26 August 2010 from Morley station (near Wymondham, ~ 7 miles SW of UEA). Alongside this data UVA and UVReff (Fig. 4.14c, d) was obtained from the Health Protection Agency's Chilton Station (near Oxford, ~ 157 miles SW of UEA). UVReff is effective UVR, or erythemally effective UVR, and it is measured using a detector that has its spectral sensitivity biased towards those wavelengths that cause erythema (skin reddening). Hence, the detector gives most weight to the UVB and less to the UVA although it detects both. The spectral weighting is inherent in the detector, and so cannot be 'unpicked' to give a UVB value, but erythemal efficacy has been used as a surrogate measure for other biological effects where the appropriate spectral weighting is unknown. There were no exclusive measurements for UVB, but UVReff can be considered to include the risky UVB radiations.

Throughout the day, the air temperature varied between 10 to 20°C with an average of about 15°C (Fig. 4.14a). On the roof, the cultures were also exposed to an average of 250 Wm^{-2} solar radiation with varying intensity up to a maximum of 850 Wm^{-2} (Fig. 4.14b). The mean UVA < 10 Wm^{-2} with a maximum of 40 Wm^{-2} (Fig. 4.14c) and mean UVReff (includes UVB) was < 0.02 Wm^{-2} with a maximum of 0.1 Wm^{-2} (Fig. 4.14d).
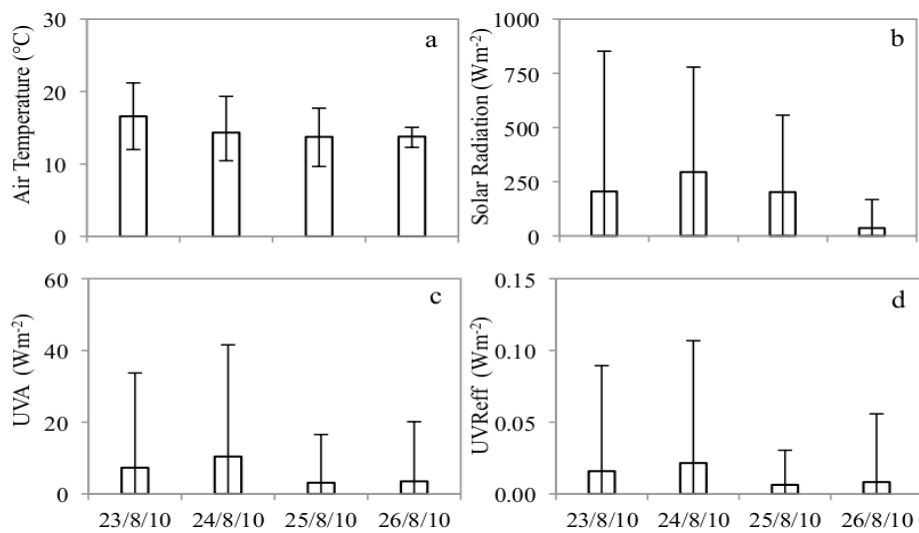
Figure 4.14 Data from 23rd to 26th August 2010 for (a) air temperature (°C), (b) solar radiation (Wm^{-2}) from Morley station and (c) UVA (Wm^{-2}) and (d) UVReff (Wm^{-2}) obtained from Chilton station. Average data for the day is shown and the bars represent the range of the parameter through out the day.

Batch cultures of *E. huxleyi* 370, 373 and 1516 in quartz flasks and *E. huxleyi* 1516 in borosilicate flasks were grown to mid-log phase in controlled laboratory conditions with a 14:10 L:D cycle and 20 Wm^{-2} PAR at 17 °C, and then exposed to natural solar radiation without acclimatising the cells. Control cultures with the UVB cut-off filter (SR–UVB) showed increasing cell density (0.6, 0.4 and 0.42 x 10^6 cells ml^{-1} in *E. huxleyi* 370, 373 and 1516 respectively) in contrast with the distinct decline (0.36, 0.3 and 0.27 x 10^6 cells ml^{-1} in *E. huxleyi* 370, 373 and 1516 respectively) in cell number in the SR-exposed cultures at 24 h (Fig. 4.15 a, c, e, g). On prolonged exposure, control cultures showed further growth to 1.2, 0.9 and 1 x 10^6 cells ml^{-1} in *E. huxleyi* 370, 373 and 1516 respectively while SR exposed cells showed further decrease to 0.16 and 0.13 x 10^6 cells ml^{-1} in *E .huxleyi* 370 and 373 while it remained almost consistent at 0.25 x 10^6 cells ml^{-1} in *E. huxleyi* 1516 from 24 to 72 h. The SR exposed *E. huxleyi* 1516 in the borosilicate flasks followed the same trend when compared to SR exposed *E. huxleyi* 1516 in quartz flasks but declined to a low of 0.16 x 10^6 cells ml^{-1} at 24 h and then stabilized at 0.12 x 10^6 cells ml^{-1} from 48 to 72 h.
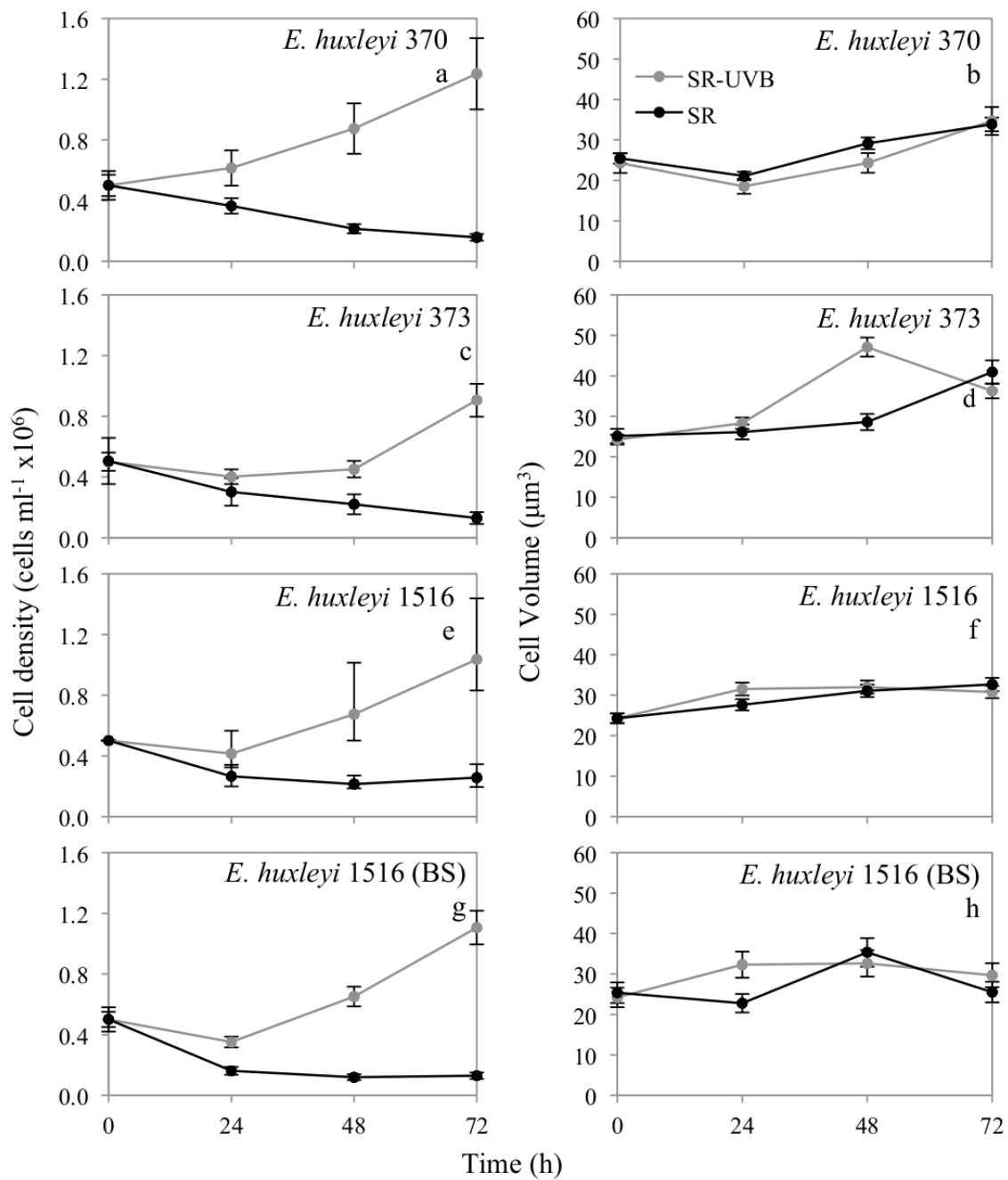
Figure 4.15 Comparison of cell density and cell volume in *E. huxleyi* 370, 373 and 1516 exposed to solar radiation (SR). The grey line represents the control flasks covered with the UVB cut-off filter and the black line represents the unscreened flasks exposed to solar radiation (SR-UVB). BS stands for borosilicate flask and all other plots show results in quartz flasks. The average value and range of data is shown (n=3). Where no range bars are visible, the data range was smaller than the symbol size.
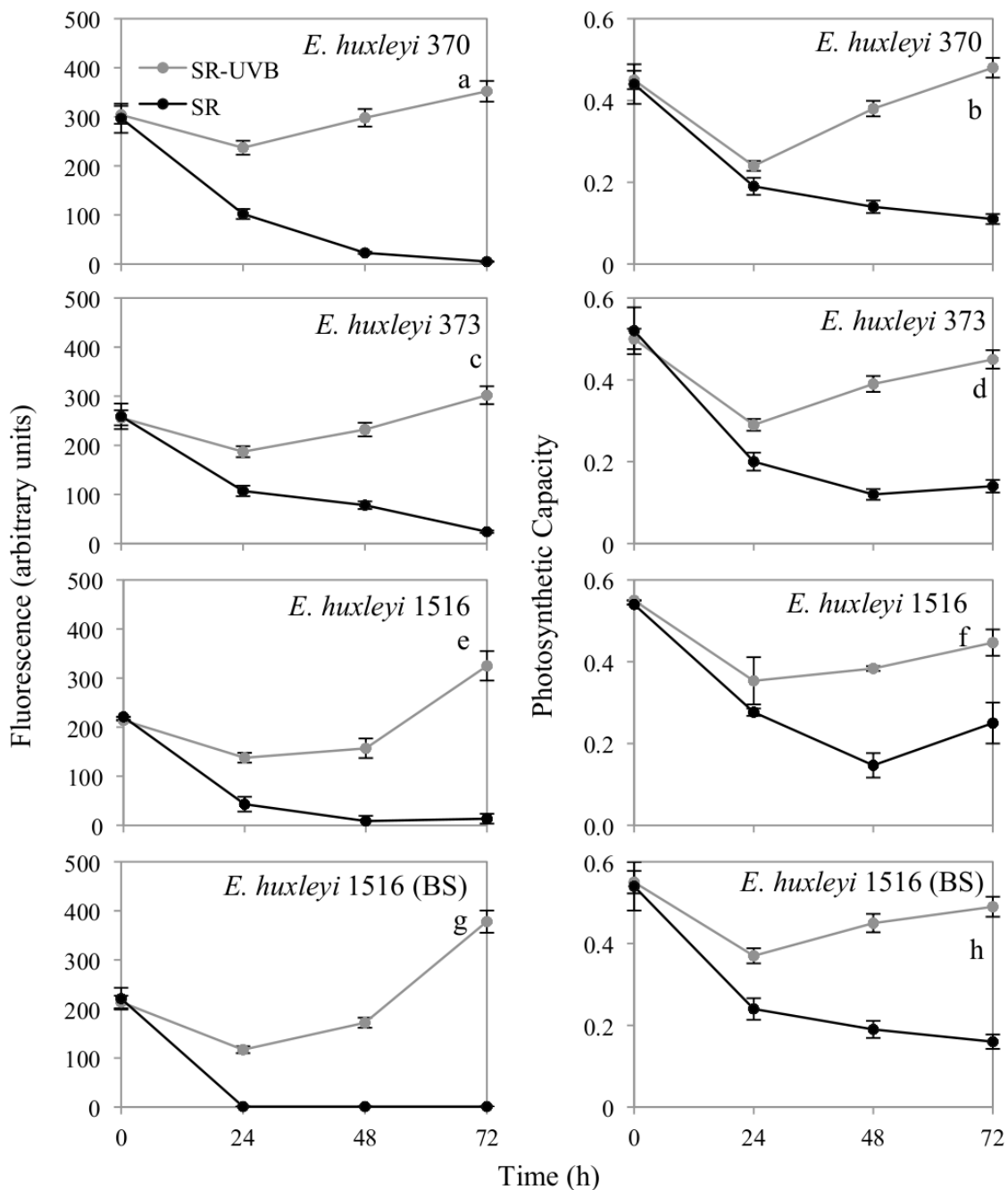
Figure 4.16 Comparison of cell fluorescence and cell photosynthetic capacity in *E. huxleyi* 370, 373 and 1516 exposed to solar radiation (SR). The grey line represents the control flasks covered with the UVB cut-off filter and the black line represents the unscreened flasks exposed to solar radiation (SR-UVB). BS stands for borosilicate flask and all other plots show results in quartz flasks. The average value and range of data is shown (n=3). Where no range bars are visible, the data range was smaller than the symbol size.

The cell volume of the SR-exposed cells did not show a clear pattern (Fig. 4.15b, d, f, h), remaining broadly similar to the control cultures with the exception of the *E. huxleyi* 373 control value of 47 μm^3 at 48 hours and the *E. huxleyi* 1516 control value of 32 μm^3 at 24 hours in borosilicate flask. Fluorescence (Fig. 4.16a, c, e, g) decreased dramatically in all the SR-exposed cultures and was noted at 5, 24 and 13 in *E. huxleyi* 370, 373 and 1516 in quartz flasks at 72 h while *E. huxleyi* 1516 in borosilicate flask dropped to 1 in 24 h and remained 1 till 72 h. It also declined in the UVB-screened cultures after 24 hours to 237, 187, 138 and 117 in *E. huxleyi* 370, 373, 1516 in quartz and *E. huxleyi* 1516 in borosilicate flasks but subsequently increased to values of 352, 302, 325 and 378 at 72 h in all the four cultures respectively.

Photosynthetic capacity (Fig. 4.16b, d, f, h) declined in the screened cultures at 24 hours to 0.24, 0.29, 0.35 and 0.37 in *E. huxleyi* 370, 373 and 1516 in quartz flask and *E. huxleyi* 1516 in borosilicate flask before increasing at the subsequent time points to reach higher than 0.45 at 72 h in all the cultures. In the SR-exposed *E. huxleyi* 370 and borosilicate flask 1516 cultures it dropped to 0.19 and 0.24 at 24 h and further kept decreasing to 0.11 and 0.16 at 72 h. On the other hand, in *E. huxleyi* 373 and quartz flask 1516 cultures it dropped to 0.12 and 0.15 at 48 h and then slightly increased to 0.14 and 0.25 at 72 h.

These results showed that *E. huxleyi* 1516 in borosilicate flask though screening 20% UVB showed more pronounced results for cell growth, cell volume, fluorescence and photosynthetic capacity when compared to the *E. huxleyi* 1516 in quartz flask.

Interestingly, DMSP per cell volume and DMSP per cell for all the three strains of the SR-exposed cultures in quartz flasks showed higher values compared to the screened cultures (Fig. 4.17a, c, e) and compared to the lower values in borosilicate flasks (Fig. 4.17g). DMSP per cell volume was higher in exposed quartz flasks at 562, 482 and 434 mM compared to screened quartz flasks at 200, 190 and 222 mM in *E. huxleyi* 370, 373 and 1516 while it was lower in exposed borosilicate flasks at 230 mM compared to the screened borosilicate flasks at 519 mM at 72 h. DMSP per cell was higher in exposed quartz flasks at 19, 20 and 13 fmol compared to screened quartz flasks at 7 fmol in *E. huxleyi* 370, 373 and 1516 while it was lower in the exposed borosilicate flasks at 6 fmol
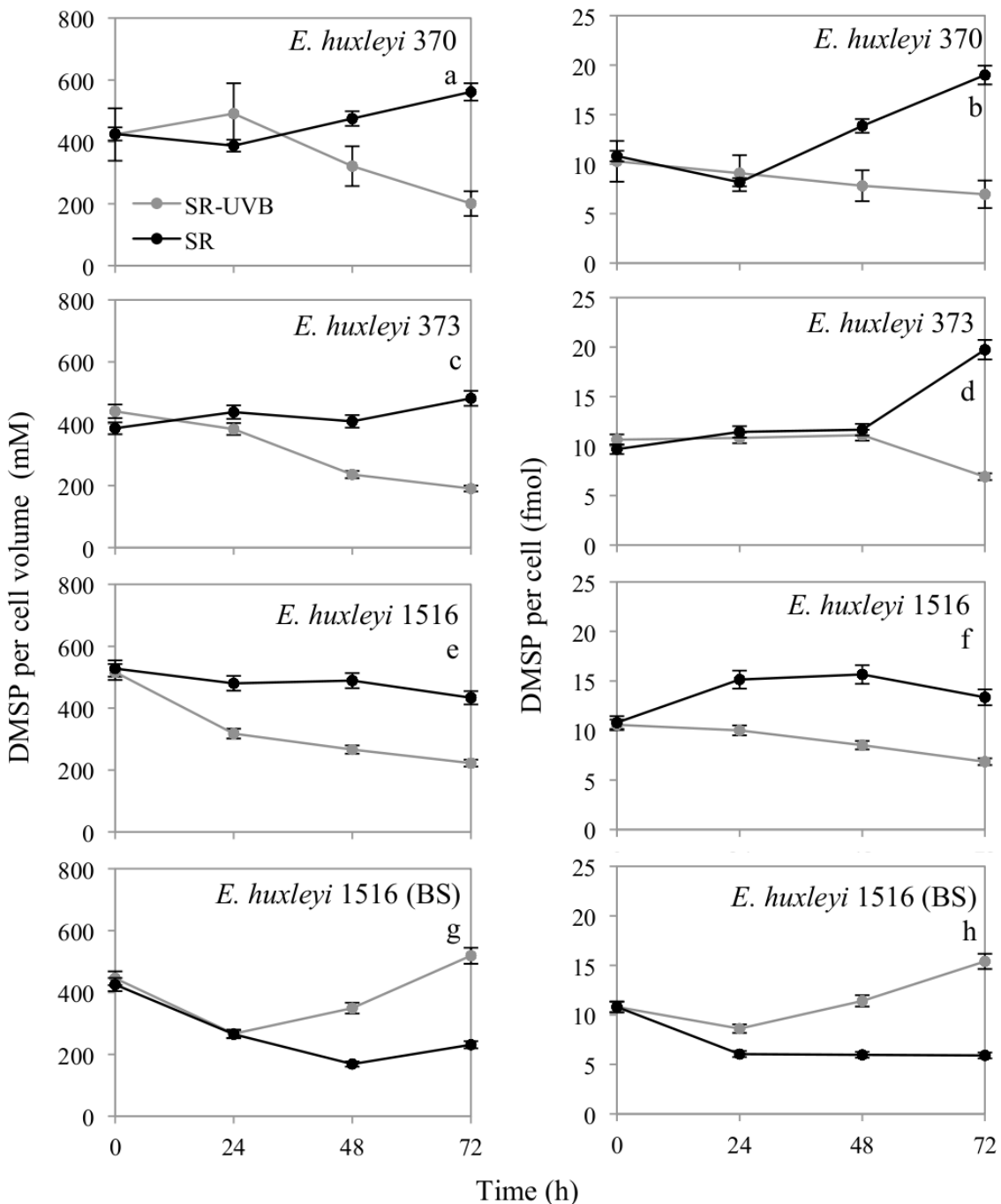
Figure 4.17 Comparison of DMSP per cell volume (mM) and DMSP per cell (fmol) in *E. huxleyi* 370, 373 and 1516 exposed to solar radiation (SR). The grey line represents the control flasks covered with the UVB cut-off filter and the black line represents the unscreened flasks exposed to solar radiation (SR-UVB). BS stands for borosilicate flask and all other plots show results in quartz flasks. The average value and range of data is shown (n=3). Where no range bars are visible, the data range was smaller than the symbol size.
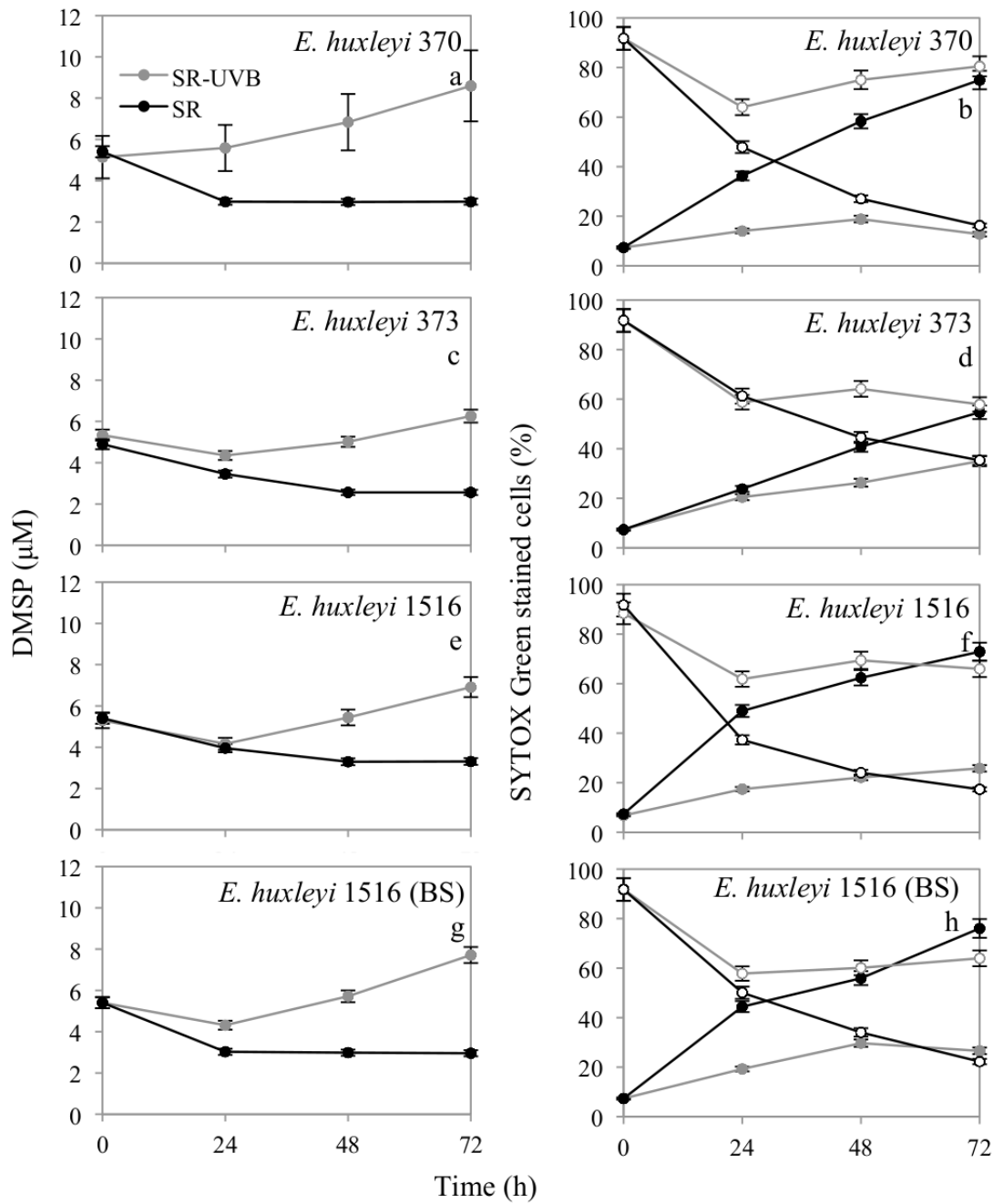
Figure 4.18 Comparison of DMSP in the culture (µM) and SYTOX Green stained cells (%) in *E. huxleyi* 370, 373 and 1516 exposed to solar radiation (SR). In plots b, d, f and h-the open symbols show percentage of viable cell (cells unstained by SYTOX Green) and the closed symbols show percentage of cells with compromised cell membranes (SYTOX Green stained cells). The grey line represents the control flasks covered with the UVB cut-off filter and the black line represents the unscreened flasks exposed to solar radiation (SR-UVB). BS stands for borosilicate flask and all other plots show results in quartz flasks. The average value and range of data is shown (n=3). Where no range bars are visible, the data range was smaller than the symbol size.

compared to screened borosilicate flasks at 15 fmol at 72 h. Such an increase was not observed in the artificial UVA+UVB radiation experiment described earlier (section 4.3.3.2). An overall decrease was seen in the culture concentration of DMSP in the SR-exposed cultures in both quartz and borosilicate flasks (Fig. 4.18a, c, e, g). These values were seen to drop in the initial 48 h in the SR-exposed quartz flasks of *E. huxleyi* 373 and 1516 from 4.9 to 2.6 and 5.4 to 3.3 μM and stabilized for the next 24 hours while it dropped in the initial 24 hours in the SR-exposed quartz flasks of *E. huxleyi* 370 and SR-exposed borosilicate flasks of *E. huxleyi* 1516 from 5.4 to 3 μM in both and then stabilized for the next 48 hours.

SYTOX-staining exhibited higher percentages of compromised cells in the SR-exposed cultures with 80% in *E. huxleyi* 370; 55% in *E. huxleyi* 373; 73% in *E. huxleyi* 1516 in quartz and 76% in *E. huxleyi* 1516 in borosilicate flask at 72 h (Fig. 4.18 b, d, f, h). This was also reflected in the lower percentages of viable cells at 16% in *E. huxleyi* 370; 35% in *E. huxleyi* 373; 17% in *E. huxleyi* 1516 in quartz and 22% in *E. huxleyi* 1516 in borosilicate flasks at 72 h (Fig. 4.18 b, d, f, h).

4.3.5 Recovery in normal light (NL) conditions following UVA+UVB exposure

At the end of the 72 h exposure to artificial UVA+UVB and NL and the solar radiation experiment, the incubations were continued under NL and the cultures were monitored for re-growth. Figures 4.20 and 4.21 show that after a long lag phase cells began to grow normally in terms of cell numbers and cell volume reached a normal range. DMSP concentrations also seem to increase to its normal concentrations. This was a small test intended only to establish cell survival following exposure to UV radiation. Whilst the results were positive it is impossible to know whether this signifies that UVR damage can be reversed in the absence of UV and the presence of PAR.
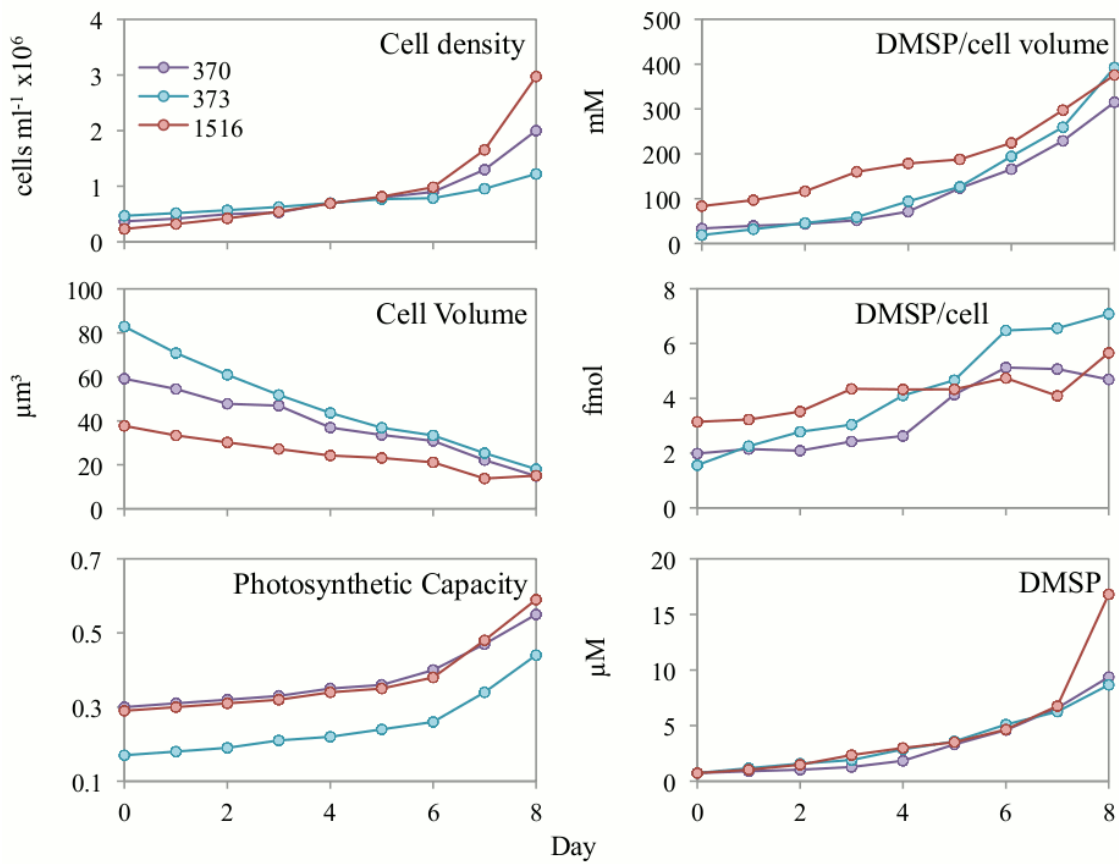
Figure 4.19 The re-growth of UVA+UVB-exposed cells of *E. huxleyi* 370, 373 and 1516 switched to normal light conditions. Data for cell density, cell volume, photosynthetic capacity and DMSP concentration are shown for single cultures. The purple, blue and red lines are for *E. huxleyi* 370, 373 and 1516 respectively.
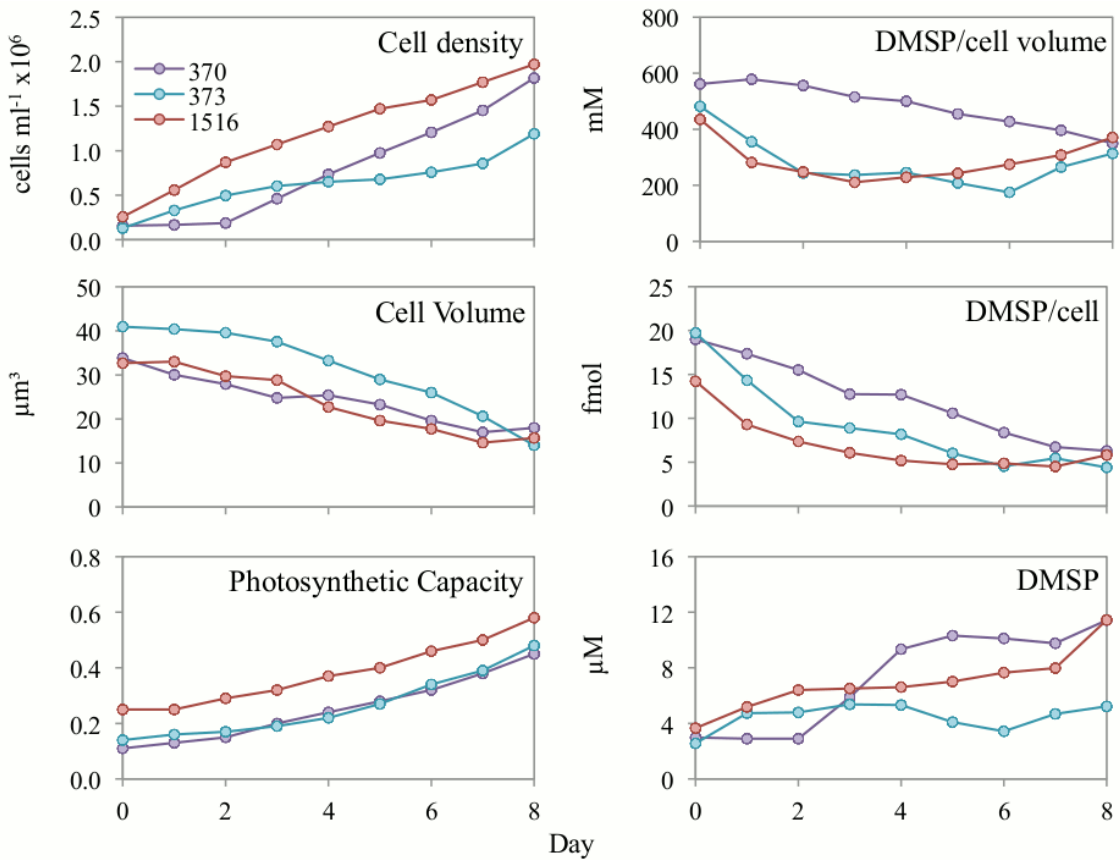
Figure 4.20 The re-growth of solar radiation-exposed cells of *E. huxleyi* 370, 373 and 1516 switched to normal light conditions. Data for cell density, cell volume, photosynthetic capacity and DMSP concentrations are shown for single cultures. The purple, blue and red lines are for *E. huxleyi* 370, 373 and 1516 respectively.

4.4 Discussion

In this investigation, nine scenarios described in Table 4.2 (see section 4.2.2) were considered: (a) exposure to NL+100% UVA; (b) exposure to NL+70% UVA; (c) exposure to NL+100% UVA+100% UVB; (d) exposure to NL+100% UVA+80% UVB (borosilicate v/s quartz); (e) exposure to LL+70% UVA; (f) exposure to LL+100% UVA+100% UVB; (g) exposure to HL+70% UVA; (h) exposure to HL+100% UVA+100% UVB; and (i) exposure to UVA+UVB in natural light conditions.

4.4.1 UVA exposure

Under scenarios (a) and (b), the 30% difference in the percentage of UVA exposure between the 2 treatments did not make a difference to cell division, fluorescence, photosynthetic capacity and DMSP content in the *E. huxleyi* cultures, even though the higher exposure to UVA radiation resulted in lower specific growth rates (Table 4.3). In addition SYTOX Green staining revealed < 10% cells with compromised membranes, suggesting the lack of cell death with UVA exposure enhanced by 30%.

Studies assert that phytoplankton photosynthesis is considerably hindered by solar UVA radiation (320-400 nm) in the upper euphotic zone in the marine and freshwater environment (Kim and Watanabe 1993), with the decrease in photosynthetic rate hindering the growth of phytoplankton populations and primary productivity in aquatic environments. In lakes and marine environments a thermocline sometimes forms in the upper euphotic zone. Vincent et al. (1984) suggested through measurement of chlorophyll *a* fluorescence, that photoinhibition in surface phytoplankton commonly occurs in lakes when the wind is weak and the water stratifies at a shallow depth, because surface phytoplankton are exposed to high levels of UVA radiation.

When assessing the effect of UVA on primary productivity in aquatic environments it is important to understand whether UVA inhibition of phytoplankton photosynthesis is a short-term and reversible response or an irreversible one leading to significant retardation of cellular growth and ultimately cell death. Kim and Watanabe (1994) highlighted the importance of the light history of the cells, which is decided by their position within the water column, and concluded that the process of inhibition of photosynthesis by UVA and subsequent recovery are not managed by a simple mechanism. These authors studied the inhibitory effects of UVA on a diatom and other cultured algae and found that the photosynthetic rate recovered, with prolonged exposure to UVA. In addition, they found that the short-term response to UVA, indicated by rapid inhibition of the photosynthetic rate and DCMU-induced fluorescence, was species specific. Further, they observed that the long-term response to UVA, suggested by the increase in the lag growth phase of the algae *Chlorella ellipsoidea,* was

161

caused by inhibition of photosynthesis. Growth recovered by means of enhancement of chlorophyll *a* content under prolonged exposure to UVA, implying that continuous exposure to UVA encouraged recovery and acclimation mechanisms to develop in algal cells. Acclimation is sufficiently protective against UVA damage and primary productivity is not depressed. In this context, persistence of the phytoplankton in the upper photic zone, where UVA is sufficient to induce acclimation, is not necessarily disadvantageous for primary production. This suggests that adaptive mechanisms occur among natural phytoplankton in the water column. Such information is important for assessing the effect of UVA on phytoplankton ecology and primary productivity in natural environments. However, in the aquatic system, if phytoplankton cells move through the mixing water column and are exposed occasionally to UVA, acclimation may not occur.

In this study, it can be concluded that the UVA light levels were not sufficient to cause any damage and that the 30% reduced UVA light levels did not make any difference on cell growth and intracellular DMSP.

4.4.2 UVA+UVB exposure under a range of light intensities

Phytoplankton cells exist in a fluctuating physical environment and are exposed to different light regimes depending on their position in the water column. The UVB dose to which the organisms are exposed within the water column depends on the distribution of the phytoplankton cells and this is controlled by vertical mixing. The decisive factors in terms of UV exposure are the time phytoplankton cells spend in the surface waters where the UVB intensity is highest, compared to time at depth where UVB is attenuated and PAR levels may or may not be sufficient to sustain growth. Phytoplankton cells react differently to varying PAR intensities. Under light-saturated conditions, growth rates are high, and the cellular concentration of light-capturing pigments (e.g. chlorophyll *a* and fucoxanthin) are low, while the opposite is found under low light conditions (Falkowski and Owens 1980; Goericke and Welschmeyer 1992). Excessive irradiance can inhibit growth rates and induce production of photoprotective pigments (Demers et al. 1991).

The aim of the present study was to assess the responses of algal cells to UVA+UVB radiation and different PAR intensities. The impact of the different light regimes and light intensities on growth, cell morphology, fluorescence, membrane integrity and DMSP content was studied. *E. huxleyi* was chosen as a test organism because this algae is widely distributed in oceanic waters (Brown and Yoder 1994) including tropical and sub-tropical waters where UVA+UVB radiation is high. It is possible that this species might also serve as a model for species found at high latitudes, where the influence of increased UVB radiation due to ozone depletion is believed to be most evident (Björn et al. 1998; Vernet and Smith 1997).

Here UVB radiation supplied at an intensity of 0.8 Wm^{-2} and 1 Wm^{-2} and PAR intensities of 50, 100 and 1000 μmol photons m^{-2} s^{-1} resulted in cell growth inhibition and increased cell volume in *E. huxleyi*. Garde and Cailliau (2000) exposed *E. huxleyi* to a UVB dose of 0.52 Wm^{-2} in different PAR intensities (53, 106 and 176 μmol photons m^{-2} s^{-1}) and observed reduced growth rates and changes in the incorporation and excretion rate of ^{14}C and indications of DNA damage in the form of cell division arrest and enlarged cell volume.

Specific growth rate of non-UV exposed *E. huxleyi* cells increased with increasing PAR intensity (Table 4.3; i.e. at 50, 100 and 1000 μmol photons m^{-2} s^{-1}; μ ~ 0.5, 0.6 and 0.8 d^{-1} respectively). However, whilst exposure to 70% UVA decreased the specific growth rate, SYTOX Green did not indicate any cell damage. Similarly, Harris et al. (2005) examined the growth rate, pigment composition, and noninvasive chlorophyll *a* fluorescence parameters for a non-calcifying strain of *E. huxleyi* grown at different light intensities. They observed that the specific growth rate increased with increase in photon flux density: at 50, 100, 200, and 800 μmol photons m^{-2} s^{-1}; the growth rate μ was 0.38, 0.62, 0.70 and 0.82 d^{-1} respectively.

Moving on to consider scenarios (b) to (g) listed in section 4.4, it can be concluded that UVB radiation had a greater affect on *E. huxleyi* than UVA radiation. With UVA+UVB exposure, photosynthetic capacity decreased dramatically, cell division ceased, cell numbers declined on prolonged exposure and ~ 20% cells had compromised cell membranes. Another interesting feature noted in this study was that reducing the

exposure to 80% UVB (0.8 Wm^{-2}) made a difference to the cells. In this case cell growth arrest was observed, but cell numbers did not decline and cell volume showed a higher increase than in cultures exposed to 1 Wm^{-2} UVB. This would imply that an increase in cell volume indicates metabolic activity but no cellular division. This feature was also observed when *E. huxleyi* was exposed to high UVB in natural light (section 4.3.4). Also, fluorescence of the 80% UVB exposed cells did not increase and remained rather consistent (Fig. 4.8j), while photosynthetic capacity (Fig. 4.9j) of the 80% UVB exposed cells remained slightly low in the range of 0.35-0.45, unlike the non-UVB exposed cells consistent at 0.45. Intracellular DMSP of the cells exposed to 80% UVB decreased after exposure for 24 hours whereas at 72 hours the DMSP concentration levelled off in the treated and control cultures. Such an increase was not seen in cells exposed to 100% UVB (1 Wm^{-2}): DMSP concentrations (1-3 µM) were lower in cultures exposed to 100% UVB compared to the 80% UVB-exposed cultures (3-6 µM). This suggests that the higher intensity UVB irradiation decreased DMSP production. The cells exposed to 100% UVB also had reduced cell membrane integrity (value% with compromised membranes). Thus, the 20% difference in UVB intensity had a much greater impact on *E. huxleyi* cells than the 30% difference in UVA exposure (section 4.4.1).

The UVB doses used in this study were representative of the UVB doses found in the top layer of clear oceanic waters and were also used previously in culture studies (Braga et al. 2002). Also, *E. huxleyi* is a common bloom-forming algae with a wide geographic distribution, it may be therefore suggested that current UVB intensities have an impact on primary production and phytoplankton biomass.

4.4.3 UVA+UVB exposure under natural light conditions

Gao et al. (2007a) studied the dinoflagellate, *Heterosigma akashiwo* exposed to solar radiation. They observed a significant decrease in the effective quantum yield was observed during high irradiance periods (i.e., local noon), but the cells partially recovered during the evening hours. They further suggested that although *H. akashiwo* is a sensitive species, it was able acclimate relatively within 3-5 days by synthesizing UV-absorbing compounds and thus reducing the impact on photosystem II or growth. Also,

studies conducted on natural phytoplankton assemblages exposed to natural UVR in Lake Erie showed that UV radiation inhibited electron transport and decreased the efficiency of photosystem II (F_V/F_M) (Marwood et al. 2000). In eutrophic waters with high concentrations of phytoplankton, the UVB radiation is attenuated within the first meter of the water column (Häder 1997; Kirk 1994), while UVB in more oligotrophic regions can penetrate several meters into the water column (Smith et al. 1992).

When exposing cultures to solar radiation, an increase in the range of 500-600 mM in DMSP per cell volume concentrations and DMSP per cell to 20 fmol was observed in the three strains whereas with artificial UV-light conditions DMSP concentration was reduced. There may be some other factor involved in the synthesis of DMSP, which needs to be isolated in future experiments. Perhaps the uncontrolled temperature, induced DMSP synthesis in the cultures exposed to solar radiation. This may be more apparent by the overall increased DMSPp concentrations observed in the control cultures exposed to solar radiation when compared with the cultures exposed to artificial light and UV conditions.

4.4.4 Recovery in normal light (NL)

Several researchers have demonstrated that UV exposure primarily affects photosystem II (Grzymski et al. 2001) and that the damage may be reversible (Vass et al. 2000). Recovery from UV damage has been observed for cyanobacterial cells incubated under visible light (Kumar et al. 2003), in dim light for natural phytoplankton, cyanobacteria and green algae (Vincent and Roy 1993) and in the dark (Braga et al. 2002). It has been shown that cells may also overcome damage by protection or acclimation mechanisms that relieve the lethal impact of UV (Vincent and Roy 1993). The mechanisms for preventing harmful effects of UV include enhanced cellular carotenoid synthesis in the cyanobacteria *Microcystis aeruginosa* (Paerl et al. 1983), production of UV-absorbing pigments or mycosporine-like compounds in dinoflagellates (Carreto et al. 1990; Garcia-Pichel and Castenholz 1993; Negri et al. 1992) and increased cell volume in diatoms (Behrenfeld et al. 1992). In the experiments presented here, recovery and repair of the cellular mechanisms in the presence of PAR led to cell regrowth and normal DMSP

synthesis. This suggests that *E. huxleyi* has the ability to repair the damage caused by UVB.

4.4.5 Overall effects on DMSP content

The quantity and quality of light received by phytoplankton may partially control DMS concentrations in the oceans through their impact on DMSP synthesis and transformation. The influence of irradiance on DMS concentrations is derived from the hypothesized function of DMSP and its breakdown products as scavengers of reactive oxygen species in phytoplankton (Sunda et al. 2002), or alternatively from a proposed role as a secondary metabolite, channeling photosynthetic overcapacity (Stefels 2000). However, clear understanding and direct evidence for either the presumed antioxidant role or for the proposed metabolic overflow mechanism are lacking.

Various studies document changes in intracellular DMSP concentration under UV-stress conditions for several phytoplankton species and strains, but results are not always consistent (Table 4.4). Hefu and Kirst (1997) showed that DMSP production in laboratory cultures of *Phaeocystis antarctica* was inhibited by UV radiation. They observed a decrease in the production of DMSP under PAR+UVA+UVB and a marked depression in total DMSP concentration with UVA+UVB after 3 h, however, the conversion rate of DMSP dissolved to DMS was significantly increased with UV radiation. On the other hand, a recent study on the response in terms of intracellular DMSP, dissolved DMSP and DMS concentrations involved *E. huxleyi* exposed to acute (1 h) increases in photon flux densities of PAR and UVR was examined in cells acclimated to low light (LL, 30 μmol m^{-2} s^{-1}) and high light (HL, 300 μmol m^{-2} s^{-1}) (Archer et al. 2010). They observed greater photoinhibition in LL-acclimated cells which corresponded with increased accumulation of DMSP to a level 21% higher than the initial concentration, contrasting with a 5% decrease in HL-acclimated cells. Archer et al. (2010) further showed that the exposure to UV decreased the rates of intracellular accumulation of DMSP and conversely, PAR + UV exposure stimulated the net production of dissolved DMSP and DMS in both HL-acclimated and LL-acclimated cultures, compared with high PAR alone. These results indicate a direct link between

acute photo-oxidative stress and DMSP synthesis in *E. huxleyi*, however the physiological basis for increased release of DMSP and DMS from cells due to high PAR+UV exposure is uncertain. Another such study investigating the influence of PAR intensities similar to those at 15 m (700 µmol m^{-2} s^{-1}) and 25 m depth (400 µmol m^{-2} s^{-1}) in the subtropical Atlantic Ocean and the effect of short-term exposure to UVR showed a 10 to 25% increase in the per-cell amount and intracellular DMSP as compared to *E. huxleyi* (strain L) exposed to only PAR (Slezak and Herndl 2003). Furthermore they observed that the intracellular DMSP concentration was always higher in PAR+UV-exposed *E. huxleyi* than in PAR-exposed *E. huxleyi*, despite the small but significant increase in cell volume of *E. huxleyi* after exposure to PAR+UV as compared to PAR exposure only. Van Rijssel and Buma (2002) have reported that UVR-induced stress does not affect DMSP synthesis in *E. huxleyi*. They observed that with increasing UVR dose, cellular DMSP content increased but the intracellular DMSP concentrations remained constant at the level typical for the applied temperature and salinity conditions, due to accompanying increase in cell size. They further explained that the increased cellular DMSP content did not compensate, for the decreased growth rates, resulting in an overall decrease in the total amount of DMSP produced in the cultures.

In this study, the different PAR intensities and exposure to UVA+UVB did not show an increase in DMSP concentration and per cell amount, perhaps due to the instantaneous breakdown to DMS, however, there is no evidence to show this. Yet the presented results imply that when UV causes growth rate reduction of *E. huxleyi* in situ, DMSP fluxes are likely to be reduced too.

Table 4.4 Table summarising previous studies documenting effects of UVA+UVB+PAR or solar radiation on DMSP concentrations and DMS release.

Authors	UV-A	UV-B	PAR		Remarks	Species	DMSP and DMS observations
	Wm^{-2}		µmol photons/m²/s	Wm^{-2}			
Archer et al. 2010	70 µmol photons/m²/s	1 µmol photons/m²/s	30	7	Acute light stress and recovery laboratory experiments	E. huxleyi (B92/11)	Intracellular DMSP, DMSPd and DMS increased.
			300	65	E. huxleyi from Plymouth culture collection		
			500	110			
Slezak and Herndl 2003	0.035-0.124	0.005	400	90	PAR intensity similar to that at 15 m (700 µmol PAR/m²/s) and 25 m depth (400 µmol PAR/m²/s) in subtropical atlantic ocean.	E. huxleyi strain L	10 to 25 % increase in per cell DMSP
	0.079-0.285	0.01	700	150			
Sunda et al. 2002	Solar radiation				Culture experiment	E. huxleyi CCMP 374	Intracellular DMSP and DMS per cell volume increased
Harada et al. 2009	8.65	1.55	450	100	50 % higher UV:PAR than natural radiation based on measurements taken at Dauphin island.	A. carterae (dinoflagellate)	No change in DMS/Chl nor DMSOp/Chl
	3.4	0.6	600	130	approx 15 % higher UV:PAR		
Van Rijsell and Buma, 2002	0.075	0.01	200	40	UVA and UVB spectrum shown in paper	E. huxleyi strain L	Intracellular DMSP remained constant. DMSP per cell increased. DMSPt decreased.
Hefu and Kirst, 1997	21	3.1	80	20	Laboratory studies	P. antarctica	DMSPt decreased, conversion rate of DMSPd to DMS increased.
	11.47	2.53					
	9.06	0.51					
	7.6	0.1					
	3.31	0.02					

4.5 Conclusions

UV-induced stress did not result in an increase in intracellular DMSP concentration in the artificial light set-up but an increase occurred on exposure to solar radiation just like in Sunda et al. 2002. There is a substantial difference in the intracellular DMSP concentrations seen in these 2 experiments. It is possible that any additional DMSP in the artificial UV condition might have undergone lysis to form DMS and acrylate, both more effective antioxidants than DMSP according to Sunda et al 2002. Alternatively, enhanced DMSP production might be strain-dependant. Under the artificial UVA radiation used here, cells grew normally and there was no measureable variations observed in intracellular DMSP concentrations. This may have occurred due to pre-acclimation of cells to UVA light. How the recovery and acclimation mechanisms occur in natural situations provides an interesting target for future study. The inhibition and recovery processes should also be studied in relation to DMSP synthesis and diurnal changes in UVR dose and vertical mixing of phytoplankton cells.

Chapter 5

Light Deprivation and Re-illumination: Effects on DMSP and DMS in *Emiliania huxleyi*

Chapter 5: Light Deprivation and Re-illumination: Effects on DMSP and DMS in *Emiliania huxleyi*

5.1 Background and significance

Photosynthesis and other processes leading to cellular growth are essentially light-dependent processes. Marine phytoplankton generally have to cope with a fluctuating light environment due to diel variations in irradiance that drive daily rhythms in various physiological parameters. Light also varies on longer temporal scales, for instance, it is not uncommon for phytoplankton to face up to 6 months of long nights or long days in the natural environment at the higher latitudes (Barnes and Hughes 1999). Additionally, sea ice can significantly reduce light penetration into the upper ocean affecting the phytoplankton communities below the ice (Hollibaugh et al. 2007). There are growing implications for *Emiliania huxleyi* expanding its regime into the higher latitudes (Balch et al. 2011; Winter et al. 2008) causing them to face light limitation or total light deprivation at certain times of year. When deep water mixing occurs a surface water mass can be subducted along a convergent front causing a sudden transfer of phytoplankton to darkness or the case of a storm event where the phytoplankton are mixed into the aphotic zone. In some species coccoliths might alter buoyancy, helping cells maintain access to sunlight or nutrients; for example, heavy coccoliths could increase a cell's density allowing the coccolithophere to sink to deeper waters where nutrients are plentiful, thus reaching light deprived ocean areas (Klaveness and Paasche 1979; Young 1987; Young 1994). *E. huxleyi* is a bloom-forming coccolithophore and aggregates of these blooms may sink into the aphotic zone. The ability to survive in the dark is also a parameter that changes in different phytoplankton groups for example, silicifiers can survive for weeks in darkness (Peters 1996; Peters and Thomas 1996) unlike calcifiers. This difference should be considered especially during winter, when the mixing depth is deeper than the euphotic zone.

Here I investigated whether darkness could be used as a tool to cause cell lysis and ultimately induce cell death with or without the release of DMS or whether the cells

would initiate the release of DMSP as a response to the light-deprivation stress. The observations would highlight a link between DMSP metabolism and cell death. DMSP is produced and released in stress conditions and there are various reports that suggest that light fluctuations cause increase in intracellular DMSP in response to oxidative stress (see Chapter 1). The effect of re-exposure to a light:dark cycle after prolonged darkness and the differences between three different *E. huxleyi* strains was also considered.

5.2 Methodology

Three strains of *Emiliania huxleyi* - 370, 373 and 1516 (CCMP) were investigated. In each case an inoculum of 100,000 cells ml^{-1} was dispensed into 1 L Erlenmeyer flasks (Fig. 5.1) containing 750 ml of the medium. The flasks were fitted with a glass tube sealed within a cotton bung with one end dipped into the culture and the other end fitted with a 0.22 μm sterile Acrodisc filter (manufacturer) and a 2-way luer lock to enable subsampling under dark conditions. Sub-sampling was done using 10 ml gas-tight syringes at the same time each day i.e. one hour after the light cycle commenced. Before collecting the first subsample for analyses, a small amount of culture was removed from the flask to avoid using any liquid previously trapped in the tubing. Great care was taken to keep the cultures axenic throughout the experiment and a DAPI stain (Chapter 2, section 2.3) was done at the start and end of each experiment.
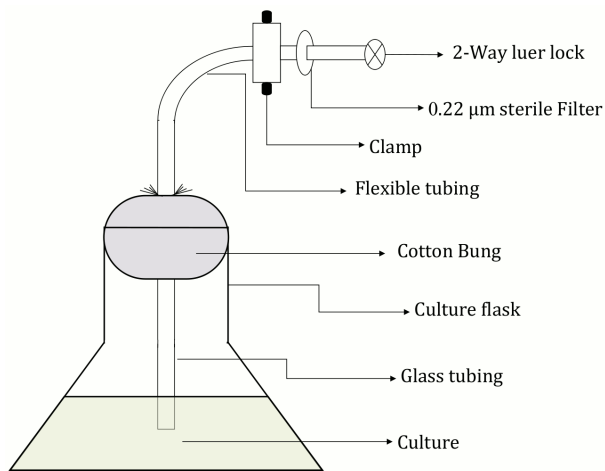
Figure 5.1 Schematic of Erlenmeyer flask set-up to allow routine sub-sampling whilst minimising exposure to light while subsampling culture aliquots for experimental measurements.

The growth experiments were conducted for different lengths of time according to the growth of each strain: 10 days for *E. huxleyi* 370 and 373, and 18 days for *E. huxleyi* 1516 which had a longer log phase. All strains were grown to mid-log phase at 17°C with a 14:10 light:dark cycle and photosynthetically active radiation supplied at 100 µmol m^{-2} s^{-1}. For each strain 3 replicates were grown under the light:dark cycle (control) and 3 under continuous darkness. The dark flasks were wrapped in several layers of aluminium foil and switched to total darkness on day 3 in *E. huxleyi* 370 and 373 and day 5 in *E. huxleyi* 1516) and remained in the dark for 7 days for *E. huxleyi* 370 and 373 and 13 days for *E. huxleyi* 1516.

Alongside the growth experiment, 9 standard 1 L cultures with identical inoculum were incubated to mid-log phase, switched to total darkness and then re-exposed to the control light-dark conditions after various days to monitor for any re-growth. After being in prolonged darkness for 2, 3 and 4 days in the *E. huxleyi* 370 and 373 cultures and 3, 6 and 9 days in *E. huxleyi* 1516, a set of three flasks on days 5, 6 and 7 in *E. huxleyi* 370 and 373 and on days 8, 11 and 14 in *E. huxleyi* 1516 were re-exposed to the light-dark cycle and cell density was further monitored for another few more days (Results in section 5.3.6). So also, at the end of the experiment on day 10 with *E. huxleyi* 370 and 373 and on day 18 with *E. huxleyi* 1516 cultures, the darkened flasks were re-exposed to the light-dark cycle and cell density was further monitored for a few more days.

Biomass was quantified as cell number (cells ml^{-1}) and cell volume and fluorescence, and the efficiency of photosystem II was measured (Chapter 2, sections 2.4 and 2.5). DMS, DMSPd, DMSPp and DMSPt were measured by GC (Chapter 2, section 2.6). Membrane permeability ('viability') was determined with SYTOX Green using the flow cytometer (Chapter 2, section 2.7).

5.3 Results

5.3.1 Cell culture and growth measurements

The growth rates of the three strains were: *E. huxleyi* 370, 0.82 d^{-1}, *E. huxleyi* 373, 0.65 d^{-1} and *E. huxleyi* 1516 0.57 d^{-1}. At mid-log phase, day 3 in *E. huxleyi* 370 and 373 and day 5 for *E. huxleyi* 1516 cell density was ~ 0.5 x 10^6 cells ml^{-1} in *E. huxleyi* 370 and *E. huxleyi* 1516 and ~ 0.3 x 10^6 cells ml^{-1} in *E. huxleyi* 373 (Fig. 5.2 a, c, e). Cell numbers continued to increase daily in the control flasks under light-dark conditions and reached 6.7 and 5.1 x 10^6 cells ml^{-1} on day 10 for *E. huxleyi* 370 and 373 and 4.5 x 10^6 cells ml^{-1} on day 18 for *E. huxleyi* 1516. After day 3 in *E. huxleyi* 370 (Fig. 5.2 a) and 373 (Fig. 5.2 c) and after day 5 in *E. huxleyi* 1516 (Fig. 5.2 e) the cultures were switched to dark conditions. The cell density followed the controls for a day, but subsequently growth ceased and cell numbers stabilised at ~ 1.2 x 10^6 cells ml^{-1} in *E. huxleyi* 370 and 1516 while cell numbers in *E. huxleyi* 373 decreased to 0.3 x 10^6 cells ml^{-1} on day 10. These observations are reflected distinctly in Ln cell density plots (Fig. 5.2 b, d, e).

Fluorescence in the control cultures continued to increase to 1656, 1656 and 1869 whereas it declined to 98, 243 and 13 in all the three light-deprived *E. huxleyi* 370, 373 and 1516 cultures (Fig. 5.3a, c, e). Also, as seen in Figure 5.3 b, d, f, there was a notable decrease in the photosynthetic capacity of the three light-deprived cultures. The control cultures usually maintained their photosynthetic capacity in the range of 0.5 to 0.6 but the light-deprived cultures decreased to 0.1 under prolonged darkness. However, it is worth noting that *E. huxleyi* 1516 followed control for 6 days after being in the dark when compared to only 1 and 2 days in *E. huxleyi* 373 and 370 before all started to decrease.

These being naked cells, calcification was not an issue here. Cell volume decreased to 12 and 8 μm^3 in light-deprived cultures of *E. huxleyi* 373 and 1516, but this was not so distinct in *E. huxleyi* 370 following culture at 16 μm^3 (Fig. 5.4 a, b, c). Cell volume in the light-exposed cultures ranged between 18 to 25 μm^3 in *E. huxleyi* 370, 33 to 47 μm^3 in *E. huxleyi* 373 and 18 to 30 μm^3 in *E. huxleyi* 1516.
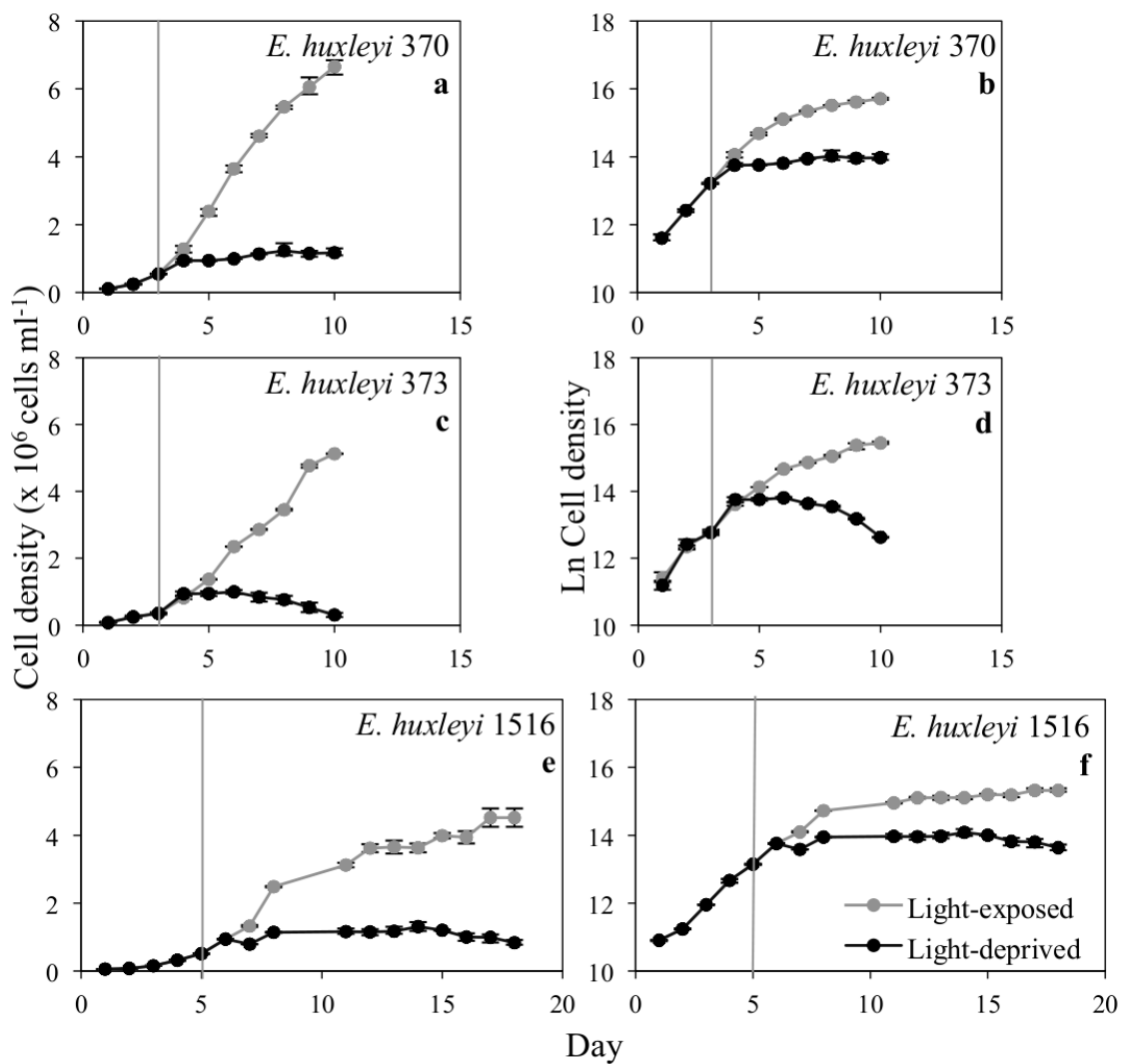
Figure 5.2 A comparison of light exposure and light deprivation effects on cell density (cells ml^{-1}) (a, c, e) and Ln Cell density (b, d, f) in batch cultures of *Emiliania huxleyi* 370, 373 and 1516. The grey line represents the control culture grown under a 14:10 light:dark cycle and the dark lines are the light-deprived cultures. The vertical line at day 3 in *E. huxleyi* 370 and 373 and at day 5 in *E. huxleyi* 1516 depicts when the experimental flasks were put in the dark. In this and all subsequent figures in this chapter, the average value and range of data is shown (n=3). Where no range bars are visible, the data range was smaller than the symbol size.
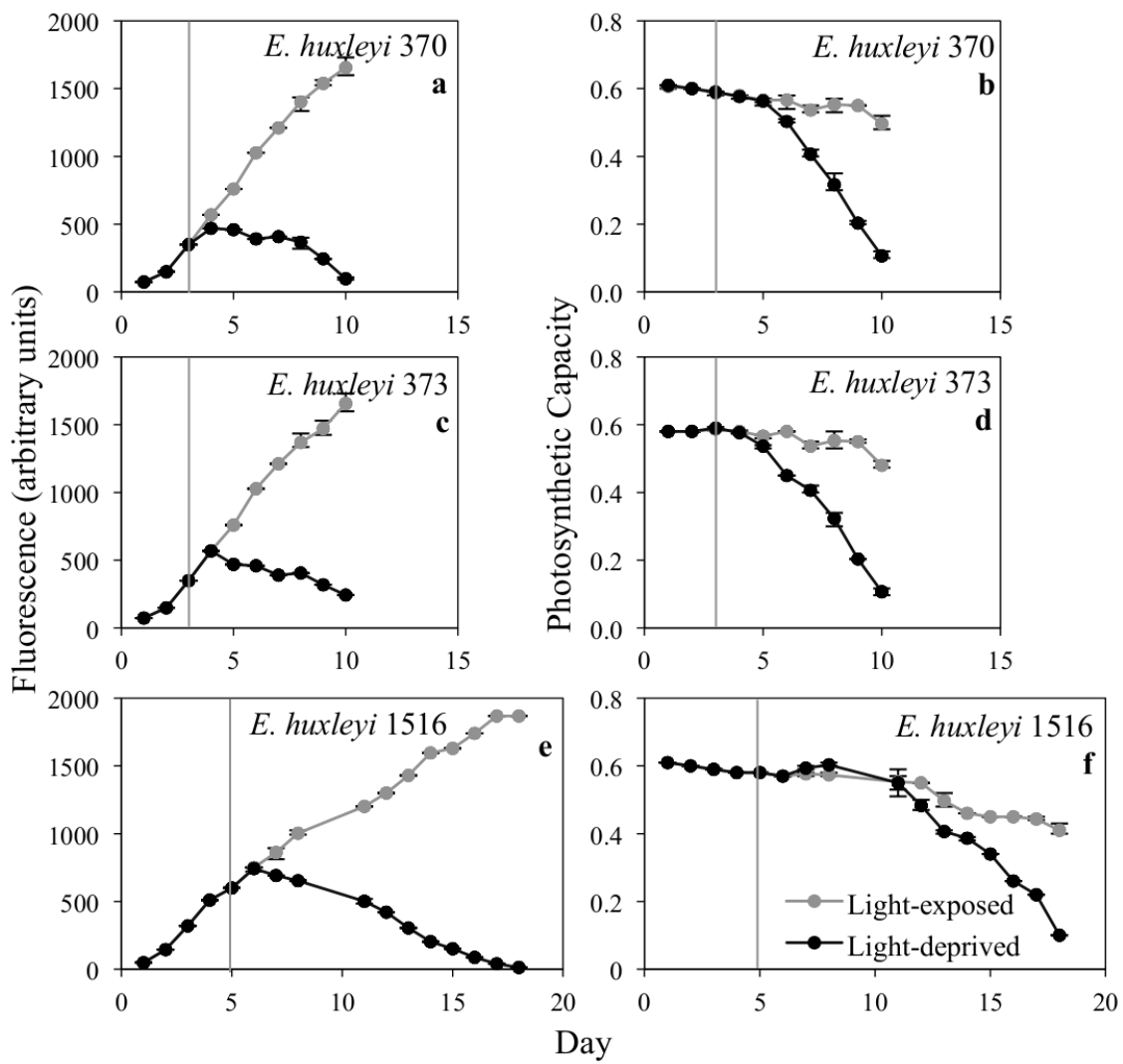
Figure 5.3 A comparison of light exposure and light deprivation effects on the fluorescence (arbitrary units) (a, c, e) and Photosynthetic capacity (b, d, f) in batch cultures of *Emiliania huxleyi* 370, 373 and 1516. The grey line represents the control culture grown under a 14:10 light:dark cycle and the dark lines are the light-deprived cultures. The vertical line at day 3 in *E. huxleyi* 370 and 373 and at day 5 in *E. huxleyi* 1516 depicts when the experimental flasks were put in the dark
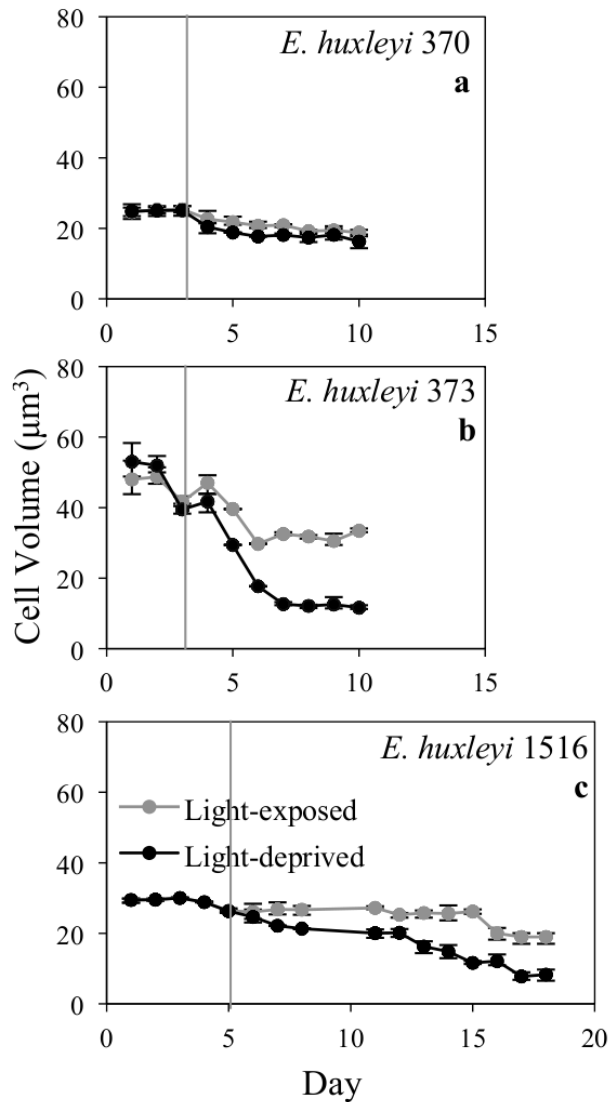
Figure 5.4: A comparison of light exposure and light deprivation effects on the cell volume (μm^3) in batch cultures of *Emiliania huxleyi* strains (a) 370, (b) 373 and (c) 1516. The grey line represents the control culture grown under a 14:10 light:dark cycle and the dark lines are the light-deprived cultures. The vertical line at day 3 in *E. huxleyi* 370 and 373 and at day 5 in *E. huxleyi* 1516 depicts when the experimental flasks were put in the dark.

5.3.2 Intracellular DMSP and DMS concentration

In this section, we discuss per cell volume data for DMS, dissolved DMSP (DMSPd) and total DMSP (DMSPt) in comparison to intracellular DMSP (DMSPp per cell volume) data (Fig. 5.5 and 5.6).
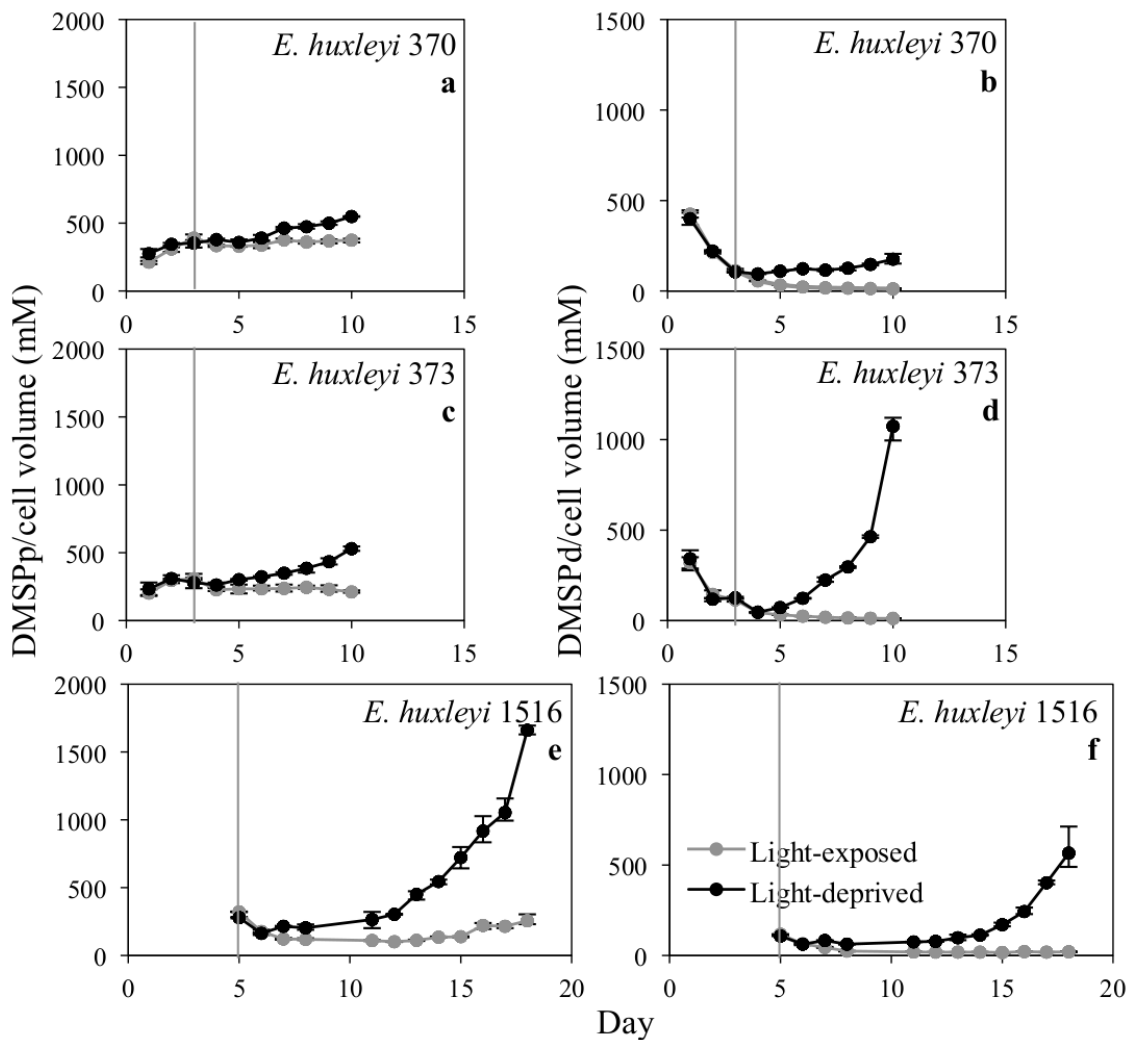
Figure 5.5 A comparison of the light exposure versus light deprivation effects on DMSP parameters (referenced to biovolume; mM) particulate DMSP (a, c, e) and dissolved DMSP (b, d, f) in batch cultures of *Emiliania huxleyi* CCMP370, CCMP373 and CCMP1516. The grey line represents the control culture grown under a 14:10 light:dark cycle and the dark lines are the light-deprived cultures. The vertical line at day 3 in *E. huxleyi* 370 and 373 and at day 5 in *E. huxleyi* 1516 depicts when the experimental flasks were put in the dark.
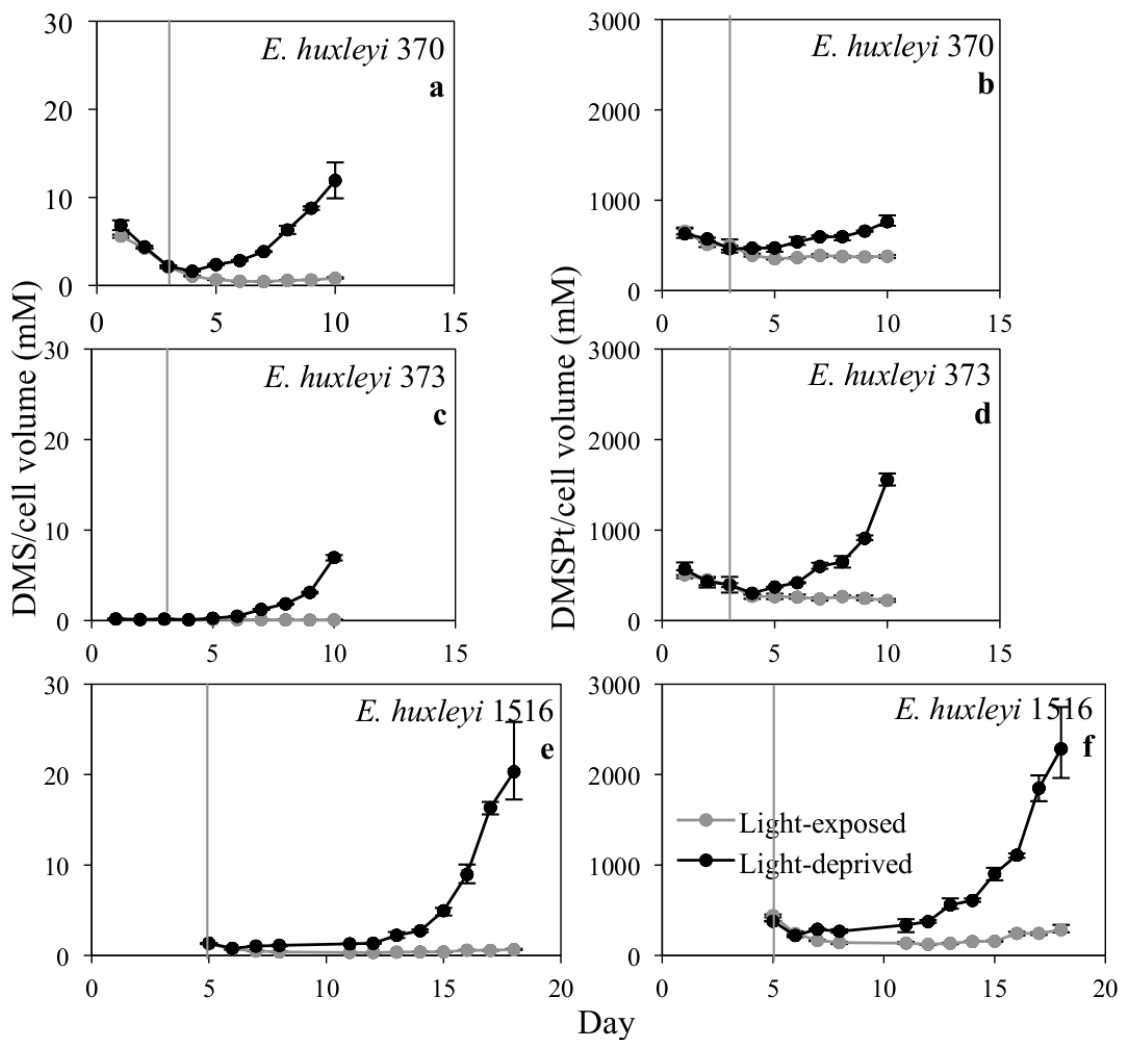
Figure 5.6 A comparison of light exposure and light deprivation effects on the intracellular DMS and DMSP parameters (mM) - DMS per cell volume (a, c, e) and total DMSP per cell volume (b, d, f) in batch cultures of *Emiliania huxleyi* 370, 373 and 1516. The grey line represents the control culture grown under a 14:10 light:dark cycle and the dark lines are the light-deprived cultures. The vertical line at day 3 in *E. huxleyi* 370 and 373 and at day 5 in *E. huxleyi* 1516 depicts when the experimental flasks were put in the dark.

DMSPp per cell volume ranged from 212 to 375, 212 to 230 and 256 to 321 mM concentrations in the light-exposed *E. huxleyi* 370, 373 and 1516 cultures compared to 353 to 550, 280 to 530 and 280 to 1660 mM concentrations in light deprived *E. huxleyi* 370, 373 and 1516 (Fig. 5.5a, c, e). From day 3 when the cultures were placed in total darkness, DMSPp per cell volume showed an increase in all the three strains but *E. huxleyi* 1516 strain showed a dramatic increase to 1660 mM.

179

DMSPd per cell volume (mM units) ranged widely from 12 to 400, 12 to 341 and 20 to 108 mM in *E. huxleyi* 370, 373 and 1516 under normal light-dark conditions (Fig. 5.5b, d, f). In *E. huxleyi* 370 and 373 DMSPd decreased from 400 and 341 mM on day 1 to about 106 and 125 mM on day 3 respectively and from day 3 onwards, DMSPd continued to decrease from 106 and 125 mM to 12 mM at day 10 under normal light-dark cycle. On the other hand on switching to total darkness, DMSPd showed the opposite trend and increased from 106 to 176, 125 to 1073 and 108 to 566 mM in *E. huxleyi* 370, 373 and 1516.

In the light-dark cycle, DMS per cell volume (mM units) was extremely low compared to DMSPp and DMSPd per cell volume (Fig. 5.6a, c, e). The light-deprived cultures showed an increase in DMS per cell volume with highest increase recorded at 20 mM for *E. huxleyi* 1516. In the light-exposed condition only *E. huxleyi* 370 showed a decrease in DMS per cell volume from 6 mM on day 1, to about 2 mM on day 3 and down to 0.8 mM by day 10. In *E. huxleyi* 373 and1516 the DMS per cell volume concentration remained low at < 0.1 and 1 mM, respectively for the duration of the experiment. Culture flasks switched to total darkness showed the opposite trend with an increase in DMS per cell volume ranging from 2 to 12, 0.1 to 7 and 1.4 to 20 mM in *E. huxleyi* 370, 373 and 1516.

DMSPt per cell volume (mM units) varied between 380 to 680 mM in *E. huxleyi* 370, 222 to 568 mM in *E. huxleyi* 373 and 284 to 378 mM in *E. huxleyi* 1516 under normal light-dark conditions (Fig. 5.6b, d, f). A gradual decrease in DMSPt per cell volume concentration was seen in the first three days of the experiment in all three strains. On switching to total darkness, DMSPt per cell volume then showed the opposite trend increasing from 463 to 761, 395 to 1556 and 379 to 2284 mM in *E. huxleyi* 370, 373 and1516. Thus all three strains varied substantially in their intracellular DMSPt concentrations in the dark treatment.

5.3.3 Cellular DMSP and DMS concentration

In the previous section, I presented DMSPp, DMSPd, DMS and DMSPt data referenced to the biovolume of cells and expressed as a mM value. Here I discuss the results in

terms of quantity of DMSPp, DMSPd, DMS and DMSPt on a per cell basis expressed as a fmol value.

In Figure 5.7 and 5.8, DMSPp, DMSPd, DMS and DMSPt are calculated per cell number to determine cellular DMSP and DMS amounts. An overall increase in per cell DMSP and DMS was seen in the light-deprived cultures with a few exceptions observed in DMSPp per cell in *E. huxleyi* 370 and 373.

DMSPp per cell in light-deprived *E. huxleyi* 370 and 373 did not vary much in the light-exposed cultures (Fig. 5.7a, c, e). DMSPp per cell was noted to range from 6 to 10 and 4 to 10 fmol in *E. huxleyi* 370 and 373 in both light-exposed and light deprived cultures after day 3. On the other hand, an increase was seen from 4 to 14 fmol in the DMSPp per cell amounts in the light-deprived *E. huxleyi* 1516. The light-exposed culture was consistent at about 5 fmol after day 7 of the experiment.

From Figure 5.7 (b, d, f) DMSPd per cell values show an overall increase in the light-deprived cultures. Under normal light conditions cellular DMSPd per cell ranged widely from 0.2 to 10 fmol in *E. huxleyi* 370, 0.4 to 18 fmol in *E. huxleyi* 373 and 0.3 to 3 fmol in *E. huxleyi* 1516. A drop in DMSPd per cell from 10 to 2.7 and 18 to 5 fmol was seen in the first three days of the experiment in *E. huxleyi* 370 and 373. From day 3 onwards, cellular DMSPd has continued to decrease from 2.7 fmol to 0.2 fmol in *E. huxleyi* 370 and from 5 to 0.4 in *E. huxleyi* 373. On switching to total darkness, DMSPd per cell was consistent in the range of about 2 to 3 fmol in *E. huxleyi* 370. While DMSPd per cell value in *E. huxleyi* 373 when darkened decreased from 5 to 2 fmol in 1 day and then increased to 12.5 fmol on day 10 which is almost 30 times the value seen in the light-exposed cultures (0.4 fmol) for the same day. Light-deprived *E. huxleyi* 1516 culture also first decreased from 2.8 to 1.5 fmol in 1 day, then stabilised at ~ 1.5 fmol till day 14 and then increased to 4.5 fmol on day 18.
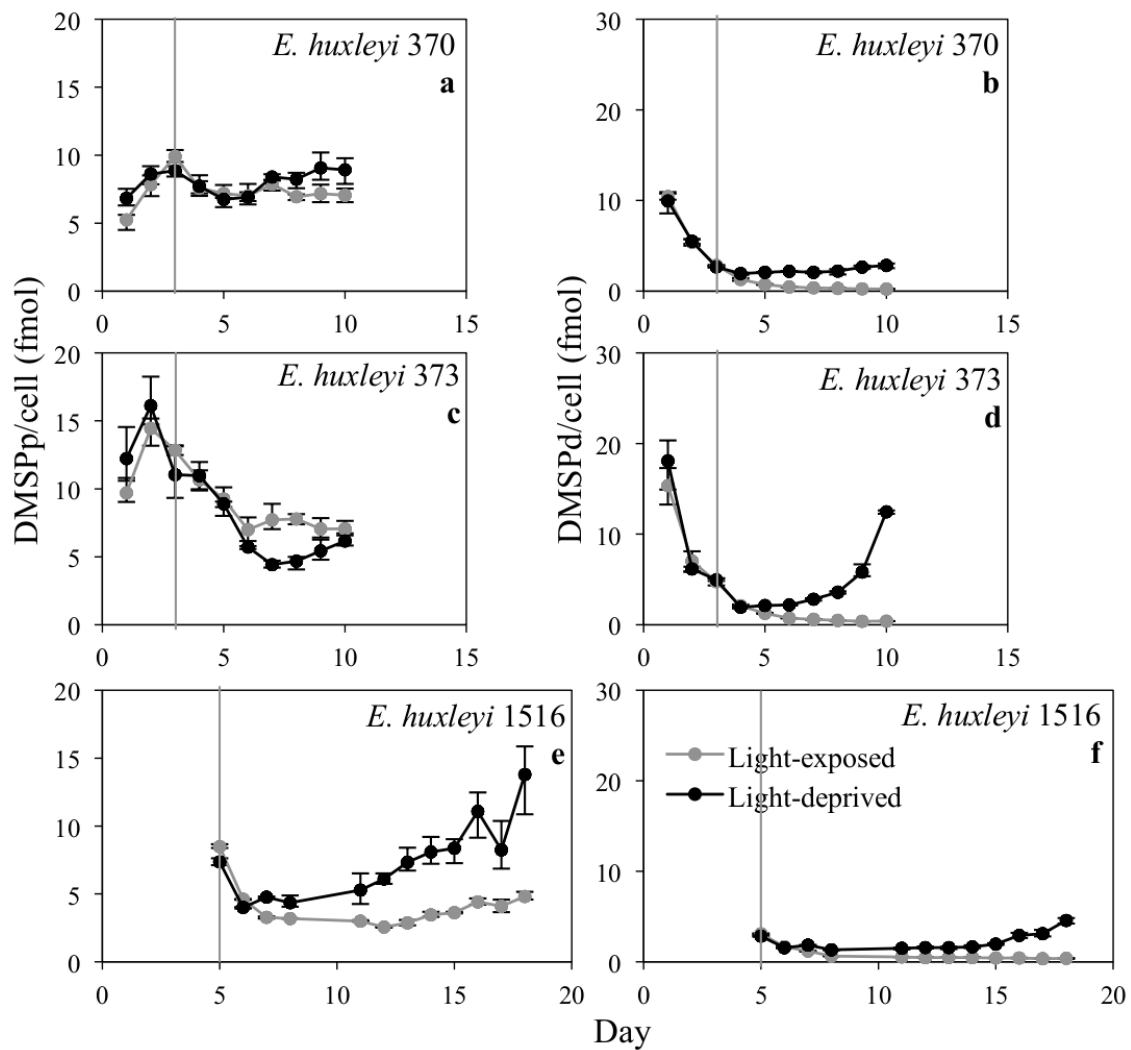
Figure 5.7 A comparison of light exposure and light deprivation effects on the cellular DMSP content (fmol) –particulate DMSP per cell (a, c, e) and dissolved DMSP per cell (b, d, f) in batch cultures of *Emiliania huxleyi* 370, 373 and 1516. The grey line represents the control culture grown under a 14:10 light:dark cycle and the dark lines are the light-deprived cultures. The vertical line at day 3 in *E. huxleyi* 370 and 373 and at day 5 in *E. huxleyi* 1516 depicts when the experimental flasks were put in the dark.
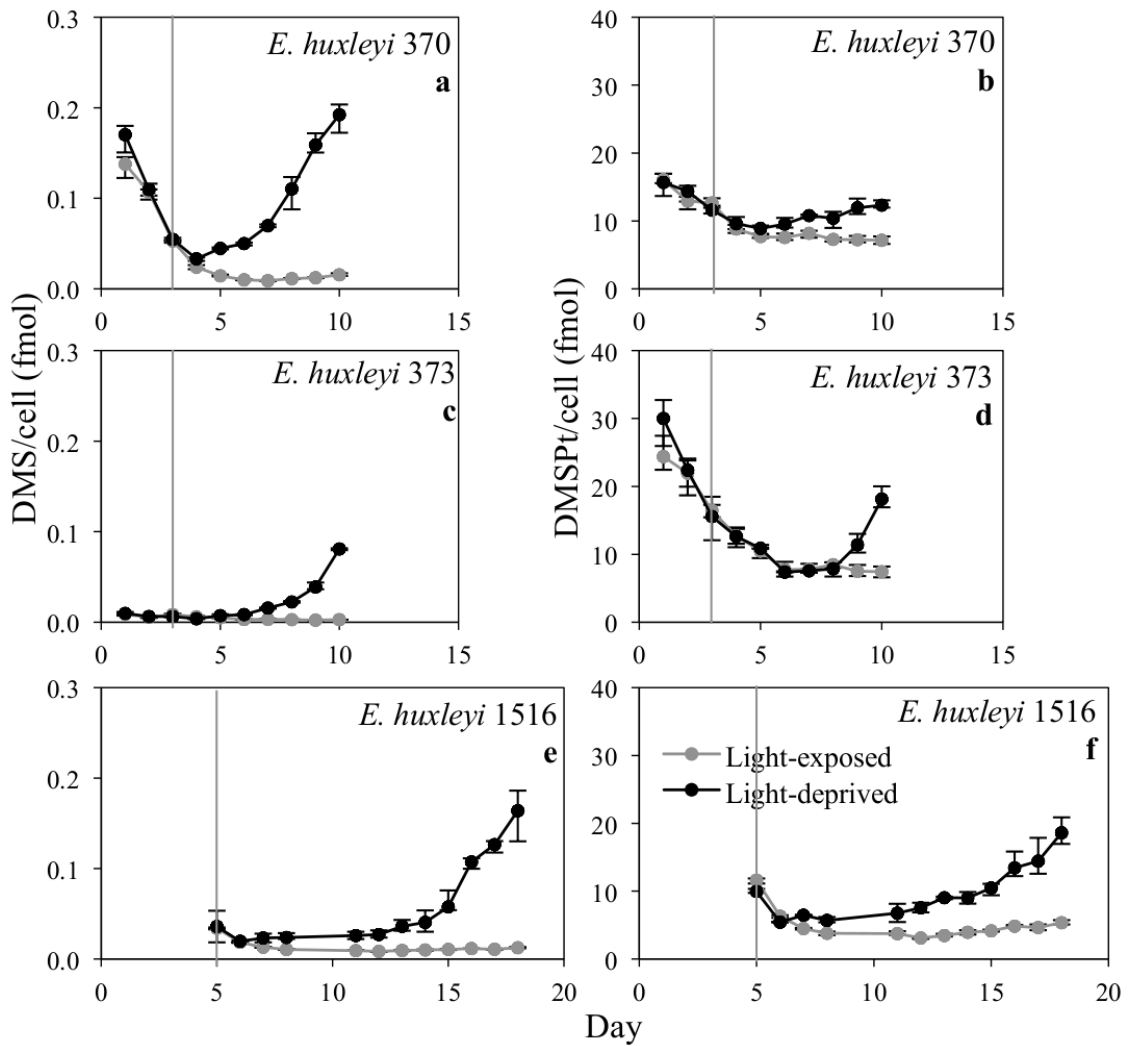
Figure 5.8 A comparison of light exposure and light deprivation effects on the cellular DMS and DMSP content (fmol) –DMS per cell (a, c, e) and total DMSP per cell (b, d, f) in batch cultures of *Emiliania huxleyi* 370, 373 and 1516. The grey line represents the control culture grown under a 14:10 light:dark cycle and the dark lines are the light-deprived cultures. The vertical line at day 3 in *E. huxleyi* 370 and 373 and at day 5 in *E. huxleyi* 1516 depicts when the experimental flasks were put in the dark.

A strain-specific increase in DMS per cell amounts was recorded in the light-deprived cultures. Under the light-dark conditions, DMS per cell (Fig. 5.8a, c, e) ranged from 0.01 to 0.14, 0.002 to 0.009 and 0.01 to 0.03 fmol in *E. huxleyi* 370, 373 and 1516. In *E. huxleyi* 370 a sharp decrease from 0.14 to 0.05 fmol was seen in the first 3 days of the experiment. On switching to total darkness, DMS per cell showed an increasing trend from 0.05 to 0.2, 0.006 to 0.1 and 0.03 to 0.16 fmol in *E. huxleyi* 370, 373 and 1516.

In prolonged darkness, DMSPt per cell was known to increase very slightly in all the three strains (Fig. 5.8b, d, f). In the light-dark cycle, DMSPt per cell ranged from 7 to 16, 7 to 25 and 3 to 12 fmol in *E. huxleyi* 370, 373 and 1516 respectively. A decrease from 16 to 12 and 25 to 16 fmol DMSPt per cell was seen in the first three days. In total darkness, DMSPt per cell showed a gradual increase to 13, 18 and 18 fmol in *E. huxleyi* 370, 373 and 1516. While *E. huxleyi* 370 followed control for only a day, *E. huxleyi* 373 followed control from days 3 to 8.

5.3.4 DMSP and DMS in the culture

In Figures 5.9 and 5.10 the DMSPp, DMSPd, DMS and DMSPt data are shown as straightforward concentrations per litre of culture expressed as µM. Overall, for the light-deprived cultures increase in the DMSPd and DMS and on the other hand, decrease in DMSPp and DMSPt concentrations were observed.

In the light-exposed cultures, DMSPp (Fig. 5.9a, c, e) ranged from 1 to 50, 2 to 40 and 5 to 22 µM in *E. huxleyi* 370, 373 and 1516. After the switchover to darkness, DMSPp showed a much lower but gradually increasing concentration from about 6 to 10 µM in *E. huxleyi* 370 compared to 5 to 50 µM increase in the light-exposed *E. huxleyi* 370. In light-deprived *E. huxleyi* 373, DMSPp decreased from 12 to 5 µM while the light-exposed culture increased from 12 to 40 µM. The light-deprived *E. huxleyi* 1516 culture increased from 5 to 15 µM lower than the increase of 5 to 23 µM in the light-exposed *E. huxleyi* 1516.

In all three strains, cultures exposed to the light-dark cycle showed a consistent DMSPd concentrations varying between 1 to 2 µM (Fig. 5.9b, d, f). A steady increase in DMSPd was seen in the light-deprived cultures where DMSPd approximately doubled in *E. huxleyi* 370 and 373 from 1.4 to 3.3 and 1.7 to 3.8 µM by day 10 and from 1.4 to 3.8 µM by day 18 in *E. huxleyi* 1516.

DMS concentrations varied among the three strains with *E. huxleyi* 373 having the lowest DMS concentrations of ~ 0.001 to 0.01µM, and *E. huxleyi* 370 and 1516 ranging between 0.01 to 0.1 and 0.01 to 0.05 µM respectively under the light-dark cycle (Figure
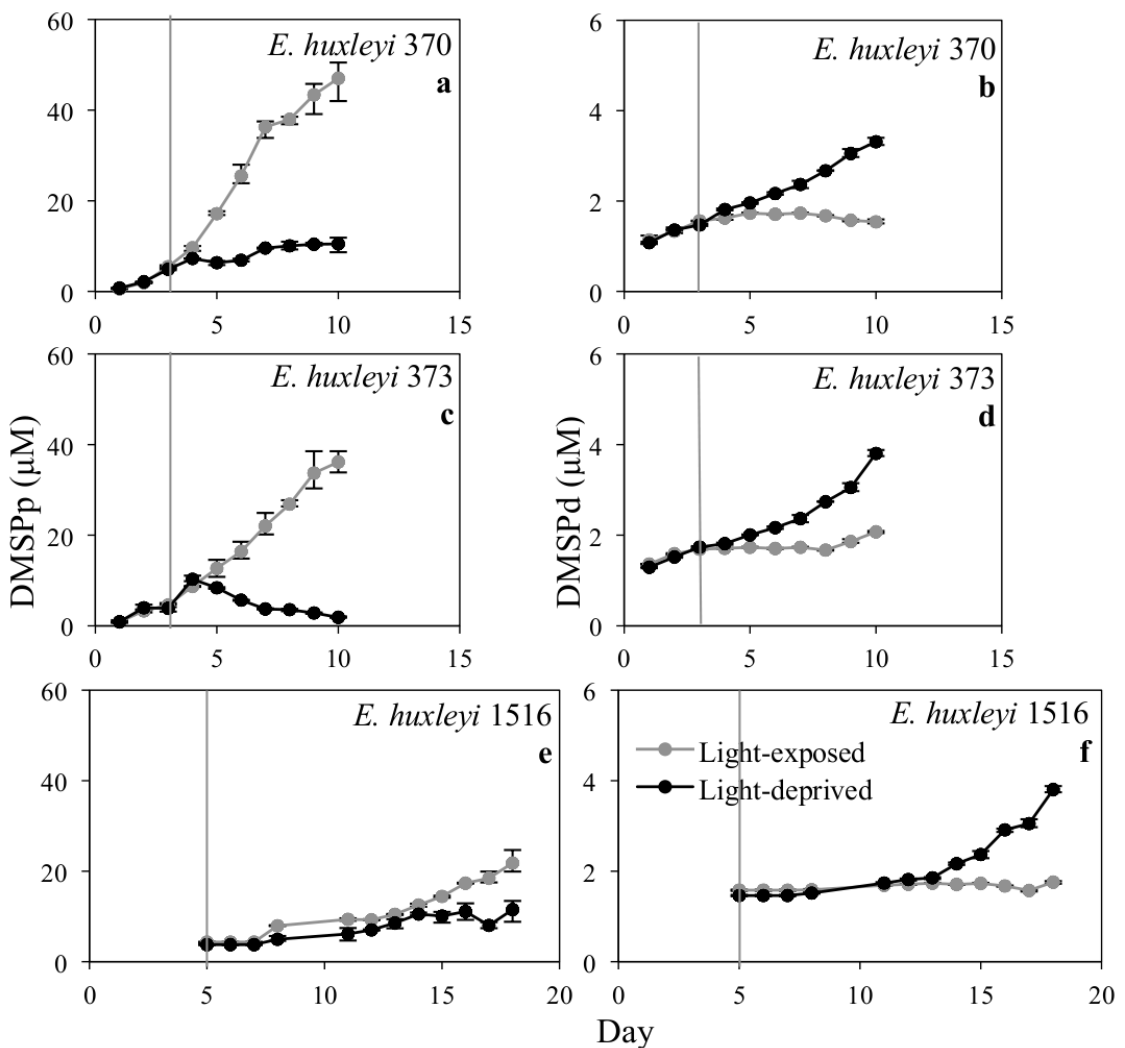
Figure 5.9 A comparison of light exposure and light deprivation effects on the DMSP concentration in the culture media (μM) – particulate DMSP (a, c, e) and dissolved DMSP (b, d, f) in batch cultures of *Emiliania huxleyi* 370, 373 and 1516. The grey line represents the control culture grown under a 14:10 light:dark cycle and the dark lines are the light-deprived cultures. The vertical line at day 3 in *E. huxleyi* 370 and 373 and at day 5 in *E. huxleyi* 1516 depicts when the experimental flasks were put in the dark. Data for days 0 to 5 in *E. huxleyi* 1516 was not collected.

5.10a, c, e). In contrast with the other two strains, the light-deprived *E. huxleyi* 373 cultures did not show much increase in DMS. DMS increased from 0.03 to 0.24 μM in the light-deprived *E. huxleyi* 370 while in *E. huxleyi* 1516, little increase in DMS was seen up to the day 12 after which, DMS increased to a high of 0.13 μM.
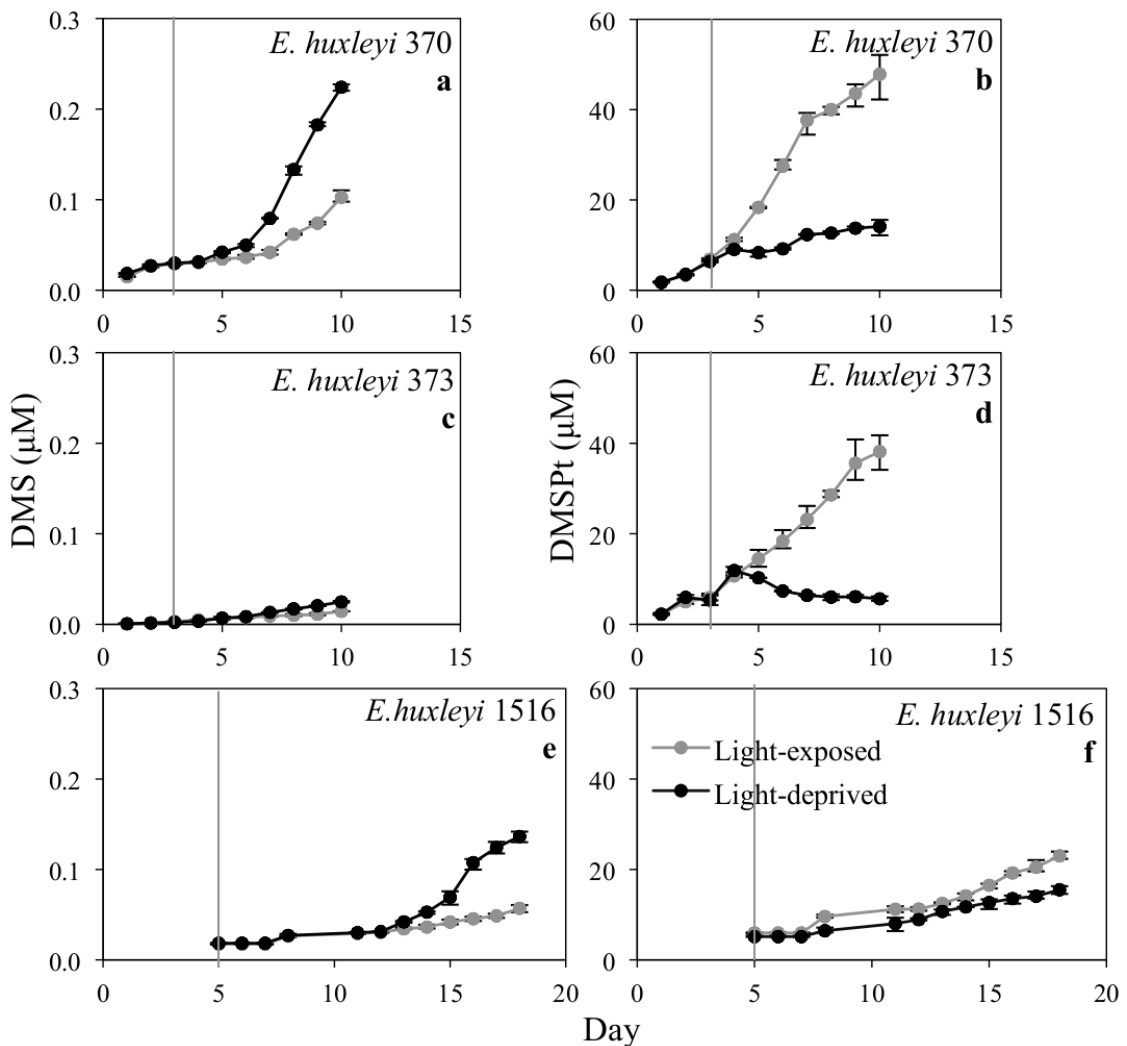
Figure 5.10 A comparison of light exposure and light deprivation effects on the DMS and total DMSP concentration in the culture media (μM) –DMS (a, c, e) and total DMSP (b, d, f) in batch cultures of *Emiliania huxleyi* 370, 373 and 1516. The grey line represents the control culture grown under a 14:10 light:dark cycle and the dark lines are the light-deprived cultures. The vertical line at day 3 in *E. huxleyi* 370 and 373 and at day 5 in *E. huxleyi* 1516 depicts when the experimental flasks were put in the dark. Data for days 0 to 5 in *E. huxleyi* 1516 was not collected.

DMSPt concentrations also varied amongst the three strains (Fig. 5.10b, d, f). Under the light-dark cycle, the data for *E. huxleyi* 370 displayed the maximum range of 1 to 50 μM, whereas for *E. huxleyi* 373 it increased up to 40 μM. For *E. huxleyi* 1516 the range was 5 to 25 μM. DMSPt values in the light-deprived cultures were lower than the concentrations seen in the light-exposed cultures. After the switch to darkness, *E.*

huxleyi 370 followed the control for a day and then lagged, on day 10 the DMSPt was low at 14 μM; *E. huxleyi* 373 followed the control for 2 days and then decreased and lagged behind at 5.6 μM on day 10 and *E. huxleyi* 1516 also followed the control for 2 days but then increased very slightly and lagged behind to read 15.5 μM on day 18.

5.3.5 Membrane permeability using SYTOX Green stain

Before the cultures were switched to total darkness (i.e. from days 1 to 3 in *E. huxleyi* 370 and 373 and days 1 to 5 in *E. huxleyi* 1516), cell densities were almost equal in all the cultures and the percentage of compromised cells was low at around 1%, indicating high percentage of cell membrane integrity (Fig. 5.11). When the cultures were placed in total darkness cell numbers remained constant for *E. huxleyi* 370 and 1516, but reduced in *E. huxleyi* 373 (section 5.3.1). From this point, the percentage of compromised cells also began to increase suggesting that membrane integrity diminished with light limitation. As already seen, photosynthetic capacity (F_V:F_M) decreased rapidly in the light-deprived cultures (Fig. 5.3b, d, f). On the final day of sampling for each strain, the *E. huxleyi* 370 and 373 cultures had 40% and 50% and *E. huxleyi* 1516 had 60% of compromised cells. Once the light-dark cycle cultures reached the stationary growth phase (Fig. 5.2b, d, f) the cultures began to exhibit decreases in cell photosynthetic capacity indicating that the photosynthetic efficiency of photosystem II had decreased (Fig. 5.3b, d, f), however, there was significant change in the fraction of compromised cells detected at this time. At the last sampling point less than 10% of the cells were stained in the *E. huxleyi* 370 and 373 cultures, and less than 6% in *E. huxleyi* 1516 (Fig. 5.11).

5.3.6 Light re-exposure on the growth of *Emiliania huxleyi*

Cultures in prolonged darkness were re-exposed to light-dark conditions to monitor for any re-growth. After being in darkness for 2, 3, 4 and 7 days, cell density failed to increase in *E. huxleyi* 370 and 373 cultures, rather the data show a steady decrease indicating no capacity for recovery when exposed to normal light-dark cycle conditions (Fig 5.12 a, b). On the other hand, when *E. huxleyi* 1516 cultures were placed in

complete darkness and re-exposed to light-dark conditions after 3, 6, 9 and 13 days, a normal increase in cell number was noted suggesting cell regrowth.
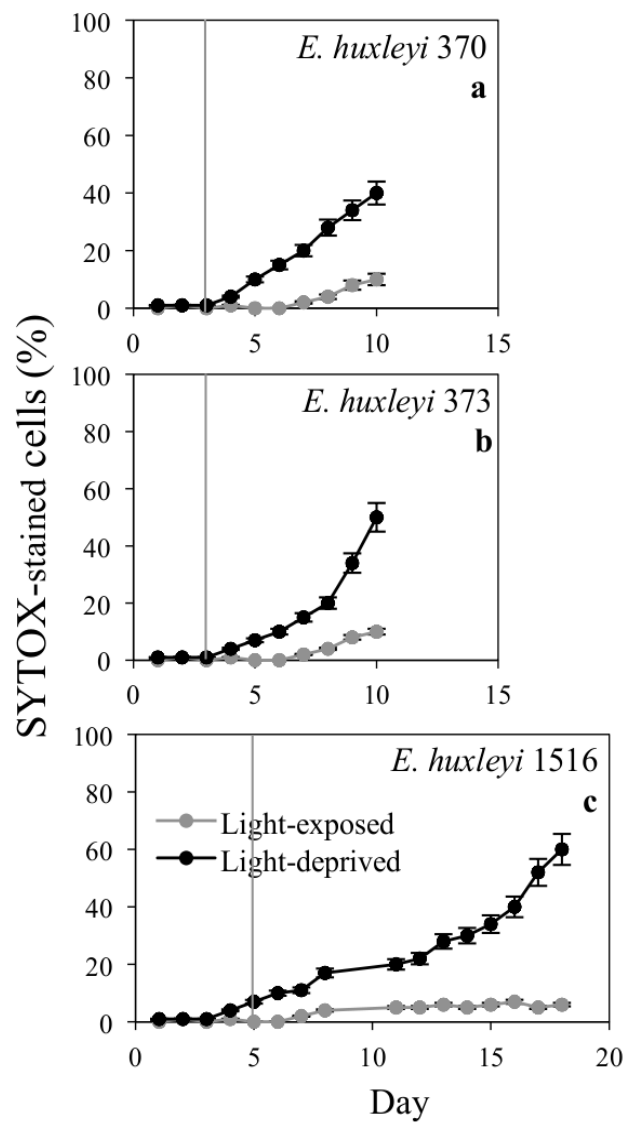
Figure 5.11 A comparison of the light exposure and light deprivation effects on membrane permeability in batch cultures of *Emiliania huxleyi* (a) 370, (b) 373 and (c) 1516. The plots show percentage SYTOX-Green stained cells. The grey line represents the control culture grown under a 14:10 light:dark cycle and the dark lines are the light-deprived cultures. The vertical line at day 3 in *E. huxleyi* 370 and 373 and at day 5 in *E. huxleyi* 1516 depicts when the experimental flasks were put in the dark.
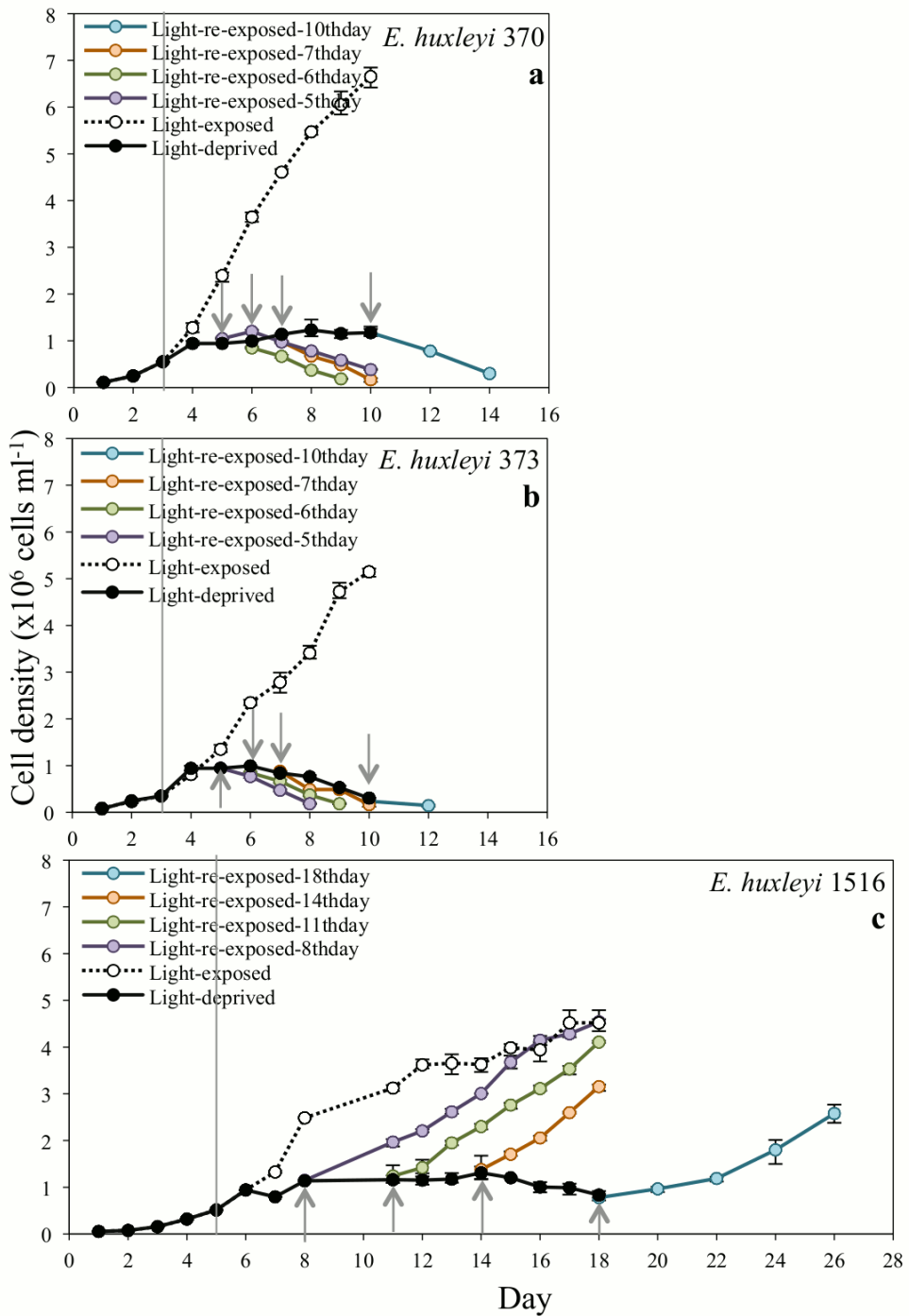
Figure 5.12 Effect of light-dark re-exposure on the growth of *Emiliania huxleyi* (a) 370, (b) 373 and (c) 1516. Plots show cell density (cells ml^{-1}). The open circles represent the control culture grown under a 14:10 light:dark cycle and the closed circles are the light-deprived cultures. The line at day 3 in *E. huxleyi* 370 and 373 and at day 5 in *E. huxleyi* 1516 depicts when the experimental flasks were darkened. The coloured circles are the light re-exposed culture flasks and the arrows indicate the day on which the flasks were re-exposed to the light-dark conditions.

5.4 Discussion

Effect of light deprivation and re-illumination *on the cultures:* The three *E. huxleyi* strains exhibited variable responses when deprived of light. The three strains differed greatly in their specific growth rate, cell volume and quantitative responses to dark stress in terms of DMSP and DMS (Table 5.1). Not surprisingly, fluorescence and photosynthetic efficiency of the cells of all the three strains were adversely affected by darkness (Fig. 5.3), with *E. huxleyi* 373 affected the most in terms of growth in cell number (Fig. 5.2).

Re-exposing the light-deprived cultures to light-dark conditions revealed that only *E. huxleyi* 1516 was able to re-grow (Fig. 5.12) and although the photosynthetic capacity gradually declined after 6 days (Fig. 5.3) the cell numbers were maintained in the dark. Similar survival and re-growth has also been reported for the pelagophyte *Aureococcus anophagefferens* and in this case there was no significant damage to its photosynthetic apparatus after 2 weeks in continuous darkness (Popels et al. 2007). Findings on growth parameters described in this chapter match well with Wolfe et al. (2002) where cell division arrest and a 30% reduction in cell volume was seen in *E. huxleyi* CCMP 373 after 24 h of dark stress. They further observed that cell growth recommenced and cell volumes increased within a day of re-exposure to light.

In another study on the freshwater chlorophyte *Scenedesmus* placed at low temperature in continuous darkness for 30 days, cell density and photosynthetic activity were affected but regrowth occurred when re-exposed to the light:dark cycle at 25°C though at a slightly lower growth rate. (Wu et al. 2007) Here, it is possible that the sudden exposure to light could not be tolerated by the light-deprived *E. huxleyi* 370 and 373 despite there being more than 50% viable cells (results from SYTOX Green staining-not shown).

It was previously shown that non-spore forming diatom species *Thalassiosira gravida* is insensitive to light deprivation and can survive several weeks in a good physiological condition (Smayda and Mitchell-Innes 1974). *Thalassiosira weissflogii* is also known to be tolerant to light-deprivation (Berges and Falkowski 1998).

Table 5.1 Comparison of growth and DMSP parameters in *Emiliania huxleyi* in the light-dark cycle and prolonged darkness.

Parameter	Light-Dark cycle			Prolonged darkness		
	Emiliania huxleyi					
	370	**373**	**1516**	**370**	**373**	**1516**
Specific Growth Rate μ (d^{-1})	0.82	0.65	0.57	-	-	-
Final Cell Density (x10^6 cells ml^{-1})	5.1	6.7	4.5	1.2	0.31	0.83
Cell diameter (μm)	3.3-3.6	3.9-4.6	3.3-3.9	3.1-3.4	2.7-4.3	2.5-3.5
Cell volume (μm^3)	18-25	30-50	18-30	16-20	10-42	8-22
DMSPp/Cell volume (mM)	212-390	210-310	100-321	350-550	260-530	160-1660
DMSPd/Cell volume (mM)	12-400	12-341	15-120	95-176	45-1073	60-566
DMS/Cell volume (mM)	0.4-6	0.08-0.2	0.33-1.30	1.6-12	0.09-7	0.8-20
DMSPt/Cell volume (mM)	350-680	220-568	120-450	460-761	300-1600	220-2300
DMSPp/Cell (fmol)	6-10	4-13	2-5	6-10	4-11	4-14
DMSPd/Cell (fmol)	0.2-10	0.4-18	0.3-3	2-3	2-12.5	1.3-4.6
DMS/Cell (fmol)	0.01-0.14	0.002-0.01	0.01-0.03	0.03-0.2	0.006-0.1	0.02-0.16
DMSPt/Cell (fmol)	7-16	7-25	3-12	8-12	7-18	5-19
DMSPp (μM)	1-50	2-40	4-22	5-11	2-12	3-15
DMSPd (μM)	1.54-1.75	1.5-2	1.6-1.7	1.4-3.3	1.7-3.8	1.4-3.8
DMS (μM)	0.02-0.1	0.002-0.01	0.01-0.06	0.03-0.24	0-0.02	0.02-0.14
DMSPt (μM)	1-50	1-40	5-25	5-15	5-12	5-15.5

Note: Approximate values for *E. huxleyi* 370 and 373 are over a growth period of 10 days and from day 3 onwards while, values for *E. huxleyi* 1516 are over a growth period of 18 days and from day 5 onwards in order to compare the light-exposed and light-deprived cultures.

Light deprivation weakens the ability of cells to metabolise and carry out new cell synthesis (Berges and Falkowski 1998). In this study, all three strains faced cell division arrest thus cell growth was inhibited under light-deprived conditions. This indicates that

Emiliania huxleyi 370, 373 and 1516 have a low tolerance to light deprivation due to limited ability to divide using the cell resources acquired previously. A few studies associating darkness with cell death have been reported e.g. for the chlorophyte *Dunaliella tertiolecta* (Berges and Falkowski 1998) and the dinoflagellate *Amphidinium carterae* (Franklin and Berges 2004). On another note, Peters (1996) conducted a detailed study on three species of temperate diatoms in continuous darkness and observed cell survival in *Ditylum brightwellii* and *Thalassiosira punctigera* for up to 35 days and *Rhizosolenia setigeru* survived 21 days. Later after 49 days in prolonged darkness, mass cell mortality occurred in all species.

Survival in prolonged darkness seems to be mainly related to the period the photosynthetic apparatus is maintained intact. Viability has been previously associated with the preservation of the photosynthetic apparatus (Dehning and Tilzer 1989; Peters and Thomas 1996) and a decline in F_V/F_M ratio is usually inferred as an indication of stress to the photosynthetic apparatus (Allakhverdiev et al. 2008). In the present study, the three *Emiliania huxleyi* strains were able to continue photosynthesis as soon as light was deprived but after being in prolonged darkness, photosynthetic ability decreased (Fig. 5.3). This indicates that the photosynthetic apparatus was impaired and in prolonged darkness, the photosynthetic apparatus did not recover. A study on *Dunaliella euchlora* revealed complete loss of photosynthetic ability after a 5 day dark period (Yentsch and Reichert 1963). Similar observations were also reported by Dehning and Tilzer (1989) for the green alga *Scenedesmus acuminatus,* where a decrease of cellular chlorophyll *a* fluorescence caused a reduction in photosynthetic capacity.

Effect of light deprivation on membrane permeability: SYTOX Green staining and flow cytometry established that by day 10, only about 40% in *E. huxleyi* 370, 50% in *E. huxleyi* 373 and 20% in *E. huxleyi* 1516 of the cells in light-deprived cultures lost cell membrane integrity. The increase in compromised membranes is probably an important preliminary stage to complete cell lysis and may need to be an important consideration when examining the impact of stress on marine biogeochemistry. For instance loss of membrane integrity could initiate the release of biogeochemically relevant compounds like DMSP and DMS to the environment. Such a mechanism has been suggested as the

cause of DMS generation during microzooplankton grazing on phytoplankton (Wolfe and Steinke 1996). Fredrickson and Strom (2008) have shown that DMSP deters grazing rates and proposed DMSP to work as a microzooplankton grazing deterrent. Previous studies have suggested that loss of membrane integrity may facilitate the release of cellular contents and be responsible for phytoplankton exudates and some proportion of the soluble DNA found in the ocean (Bjornsen 1988). Furthermore, as leaky cell membranes will affect the exchange of ions and metabolites across the cell wall (Veldhuis et al. 2001), cellular enzymes with specific physiochemical requirements for optimum activity may be influenced by the change in cellular conditions. Therefore when attempting to budget the distribution of compounds between the particulate and dissolved phase, an estimate of cell integrity is important so as not to underestimate particulate content of the intact cells.

Effect of light deprivation on DMSP and DMS: This study revealed an increase in intracellular DMSP, DMSPd and DMS, though a decrease in DMSPt (μM) in the culture was seen in light-deprived *E. huxleyi* 370, 373 and 1516.

The pie charts in Figure 5.13 are provided to better visualise the data presented in figures 5.5 to 5.10. In a culture, total DMSP (DMSPt) is calculated by adding DMSP particulate (DMSPp), dissolved DMSP (DMSPd) and DMS. This calculated DMSPt ideally will be equal to observed DMSPt but technical and practical limitations do create a marginal difference (error) between these two values. Thus we can arrive at the following equation:

DMSPt (calculated) = DMSPp + DMSPd + DMS +/– error

In the pie charts we have represented this equation in the form of 4 wedges: DMSPp, DMSPd, DMS and the error.

Figure 5.13 Comparison of the various DMS and DMSP fractions in *E. huxleyi* 370, 373 and 1516 incubated under a L:D cycle or prolonged darkness. Each pie chart represents average total DMSP from day 3 onwards in *E. huxleyi* 370 and 373 and day 5 onwards in *E. huxleyi* 1516: the timepoints when the cultures were darkened. Row A represents per cell volume concentrations. Row B represents per cell amounts and Row C gives concentrations in the culture media. The blue fraction is DMSPp, the red fraction is DMSPd, yellow fraction is DMS and the purple fraction is the analytical error (minus error is when the addition of the fractions > total DMSP and plus error is when the addition of the fractions < total DMSP).
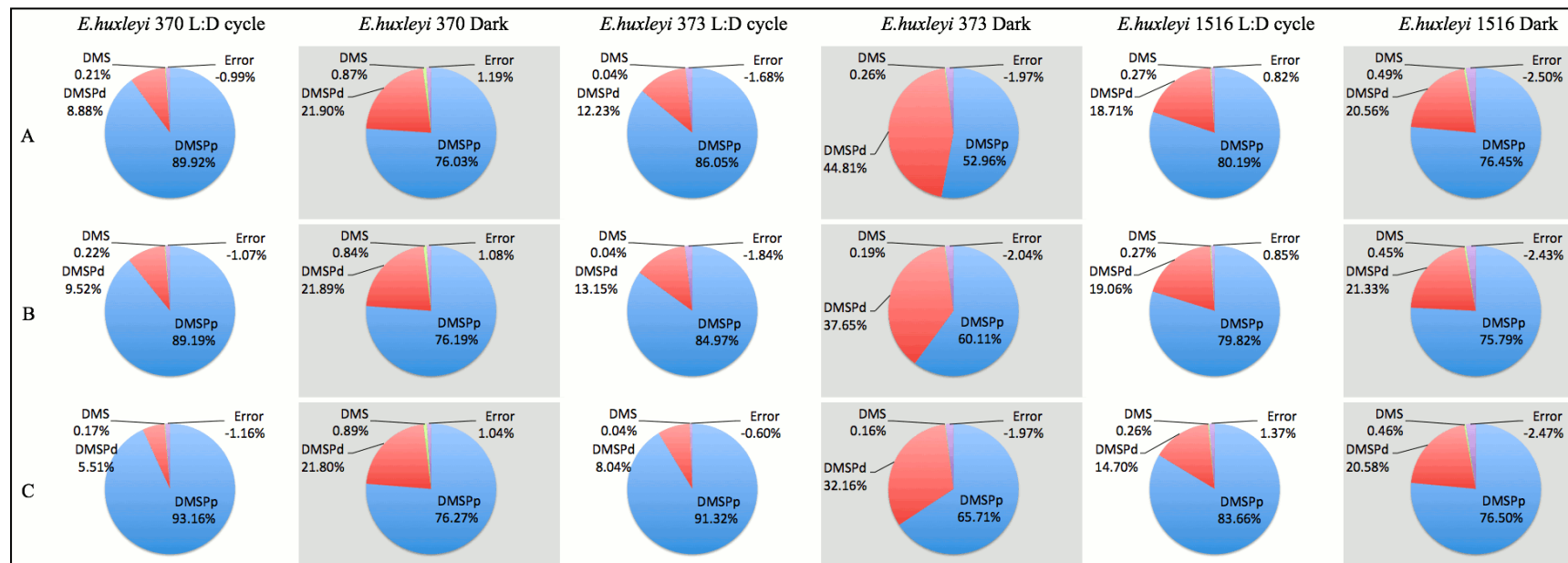
These pie charts exhibit the difference in composition of DMSP and DMS in a culture with and without darkness. It can be seen that in prolonged darkness, the average DMSPd fraction doubles in *E. huxleyi* 370 and quadruples in *E. huxleyi* 373, but remains similar to the light-exposed culture in the case of *E. huxleyi* 1516. The DMS fraction is 4 times greater in *E. huxleyi* 370, 50 times more in *E. huxleyi* 373 and doubles in *E. huxleyi* 1516. This suggests that in prolonged darkness there is an overall increase in the production of DMSP, but a portion of this goes to the dissolved DMSP and DMS fractions.

A study was conducted with exponential-phase *E. huxleyi* transferred to continuous darkness (Wolfe et al. 2002), cells decreased in cell volume and DMSP content within 24 h but DMSP content per unit cell volume remained relatively steady. DMS accumulated as long as cells remained in the dark, but on re-exposing to a light:dark cycle DMS accumulation ceased within 24 h (Wolfe et al. 2002). However, *E. huxleyi* CCMP 373, which contains a highly active *in vitro* DMSP lyase (refer to Steinke et al 1998), produced only transient accumulations of DMS in the dark. Wolfe et al. (2002) concluded that this was due to production and associated oxidation or uptake of DMS, because cells of this strain rapidly removed DMS added to cultures. Wolfe et al. (2002) also tested three strains of the dinoflagellate *Alexandrium tamarense* with high *in vitro* DMSP lyase activity but this showed no DMS production in the dark, and all strains appeared to remove additions of DMS. *Alexandrium tamarense* CCMP 1771 also removed dimethyl disulfide, an inhibitor of bacterial DMS consumption. The results discussed in this study do not completely correlate to the data presented in the above-mentioned study by Wolfe et al. (2002).

In this study, darkness was examined as a trigger of cell death and DMSP cleavage in *E. huxleyi*, which certainly impaired the photosynthetic capacity and increased the number of cells with compromised membranes. It also induced increased intracellular DMSP and DMS levels in the cultures. But this light deprivation experiment raises an important argument as to why exactly DMSP would be produced by the cell when faced with light deprivation. Ultimately all discussion simply leads to a very important question as to where exactly would DMSP be produced in the cell. Is it being produced in the

chloroplast or in the mitochondria or in the endoplasmic reticulum at optimum light conditions? The evidence in higher plants points to production in the chloroplasts, but it may not necessarily remain in the chloroplast as it is an osmolyte and needs to be in the cytoplasm. The cleavage of DMSP by marine phytoplankton is not clearly elucidated. Although DMSP and DMSP lyase occurs in marine algae, the net DMS production during active growth is low (Wolfe and Steinke 1996). It has been hypothesized that DMSP and DMSP lyase enzyme are physically separated within a cell (Wolfe and Steinke 1996) and stress perhaps triggers DMSP cleavage by compromising intracellular membranes and bringing previously compartmentalised spaces together.

When cells are in darkness or in the night cycle, they respire and use the sugars that are a by-product of photosynthesis giving out carbon dioxide, water and energy. In this study, cells that were previously under a 14:10 light:dark cycle before going into darkness, produced intracellular DMSP, some of which may have been cleaved by DMSP lyase to produce DMS. Reallocation of carbon to DMSP may be a strategy to help keep cells alive or a mechanism that is triggered in order to relax the cells from the overburden of respiration. Thus when photosynthesis has been disabled in the cells and the sugars are not being produced for respiration to occur, biosynthesis of methionine would lead to DMSP production, which would be an excellent antioxidant. But the process in which the cell has no light to perform photosynthesis, directs the cells to continue respiration finally using up all the stored sugars and other bigger molecules like lipids, with the remaining oxygen left for the cell to carry out respiration. This would put the cells under intense stress and cause cell lysis.

Wolfe et al. (2002) suggest algal DMS accumulation according to a light-dark pattern. They further explain that DMS accumulates in the dark and is removed in the light by the reactive oxygen by-products of photosynthesis. They proposed two ways in which DMS accumulation occurs; up-regulation of DMSP cleavage (DMS production) and down-regulation of DMS removal by radicals produced from photosynthesis. From their experimental data involving *E. huxleyi* 370 and 373, Wolfe et al. (2002) concluded that up-regulation of DMSP cleavage in dark-stressed cells was responsible for the accumulated DMS seen only after the cells remained in prolonged darkness.

Hydroxyl radicals produced during photosynthesis (Niyogi 1999) is proposed to be dissipated by interaction with DMSP (Sunda et al. 2002). They further propose that the products of DMSP enzymatic cleavage react at a faster rate with the hydroxyl radical than DMSP and that this could combat oxidative stress. Stefels (2000) suggested that biosynthesis of DMSP could represent an overflow mechanism. In this study, darkness induced an increase in DMSP biosynthesis and cleavage resulting in higher intracellular DMSP concentration in all three strains but lower cellular DMSP content in *E. huxleyi* 370 and 373, however, DMS increased. Perhaps DMSP biosynthesis and its cleavage help cells survive in darkness experienced due to being mixed into the aphotic zone or at higher latitudes where prolonged seasonal darkness occurs.

5.5 Conclusions

There are very few reports concerning how haptophytes respond to darkness. The aim of this study was to consider the possible role of DMSP in *E. huxleyi* in cells under light deprivation. The results highlight DMSP biosynthesis and DMSP cleavage as adaptive responses to light-deprivation as evidenced by the production and accumulation of DMS in light-deprived cultures. There is a distinct difference between strains in terms of growth and DMSP characteristics. The *E. huxleyi* 1516 strain has the lowest range of DMSP per cell volume concentrations among the 3 strains and the highest concentrations in the dark and this may indicate the involvement in general cellular metabolism during dark stress.

Chapter 6

Herbicide-induced Oxidative Stress: Effects on DMSP and DMS in *Emiliania huxleyi*

Chapter 6: Herbicide-induced Oxidative Stress: Effects on DMSP and DMS in *Emiliania huxleyi*

6.1 Background and significance

All biological systems produce reactive oxygen species (ROS) such as the superoxide radical (O_2^-), singlet oxygen ($^1O_2$), hydrogen peroxide (H_2O_2) and the hydroxyl radical (HO·) (Gadjev et al. 2008). However, the production and accumulation of ROS beyond the capacity of an organism to quench these reactive species can be damaging or even fatal (Lesser 2006). In photosynthetic organisms both photosynthesis and respiration can result in oxidative stress (Apel and Hirt 2004; Foyer and Noctor 2003). Oxidative stress can be combated by the various enzymatic and non-enzymatic antioxidant defence mechanisms (refer Chapter 1, section 1.2.2) (Apel and Hirt 2004; Mallick and Mohn 2000) in biological systems by quenching the $^1O_2$ at the site of production and quenching or reducing the flux of reduced oxygen intermediates like O_2^- and H_2O_2 to prevent the production of HO·, the most damaging of the ROS. This project investigates one such potential antioxidant system: The DMSP antioxidant system.

It has been proposed that DMSP could be the key compound in an antioxidant cascade in marine phytoplankton (Sunda et al 2002). Theoretical data suggests that the osmolyte DMSP, and especially its breakdown products DMS, acrylic acid dimethylsulphoxide (DMSO) and methane sulphanic acid (MSA), could be highly effective antioxidants (Sunda et al. 2002). The function of these compounds would be to scavenge harmful cytotoxic oxygen free radicals such as the superoxide anion and hydroxyl radicals under conditions that cause oxidative stress. Sunda et al. (2002) suggested the antioxidant function for DMSP in marine algae and showed that solar ultraviolet radiation, CO_2 limitation, Fe limitation, Cu^{+2} elevation and H_2O_2 elevation led to the upregulation in activity of the well known antioxidant enzyme ascorbate peroxidase (APX) alongside substantial increases in intracellular DMSP concentration, and in some cases DMS production.

In this study, paraquat (also known as methyl viologen) a well-known non-selective herbicide was used to artificially and directly catalyze the formation of reactive oxygen species in the bloom-forming coccolithophore *E. huxleyi* in the presence of light and oxygen.

***Action of paraquat (methyl viologen)*:**
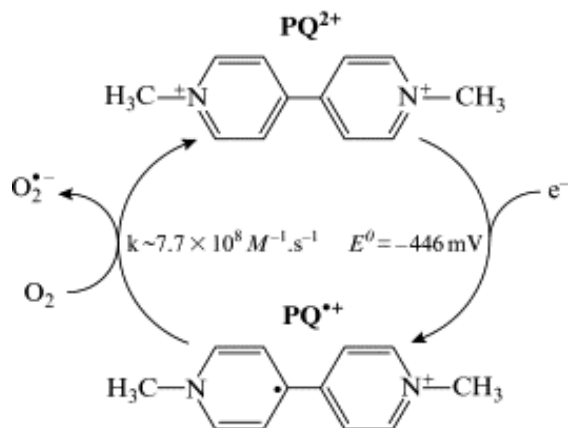
Figure 6.1 Paraquat also known as methyl viologen (IUPAC name- 1,1'-Dimethyl-4,4'-bipyridinium dichloride), is a dication (PQ^{2+}) that undergoes univalent reduction to produce a paraquat radical ($PQ\cdot^{+}$), which then reacts rapidly with oxygen to produce superoxide (O_2^-), a harmful reactive oxygen species. (Diagram from Cochemé and Murphy (2009)).

Paraquat (Fig. 6.1) is widely used in higher plant research (Bonilla et al. 1998; Broadbent et al. 1995; Bus and Gibson 1984; Donahue et al. 1997; Franqueira et al. 1999; Franqueira et al. 2000; Qiao et al. 2002). Paraquat interacts with the electron transfer components associated with photosystem I (PSI) (Devine et al. 1993) (Fig. 6.2). Under normal circumstances, when light hits the chlorophyll reaction centre in the chloroplast, the electron is excited and transferred to ferredoxin (Fd), which in turn is then sent to the primary electron acceptor NADP+, forming NADPH. These high-energy electrons are the source of energy for cellular biosynthesis. Paraquat is very electronegative and binds to the protein ferredoxin near PSI and competes with NADP+ as an electron acceptor. Thus, rather than the electron entering the electron transport pathway, it is acquired by paraquat and as a result no NADPH is produced. When the

herbicide is reduced by an electron, it rapidly transfers the electron to oxygen, forming highly ROS including the superoxide anions and hydroxyl ions (Bus and Gibson 1984). This initiates a cascade of free radical reactions that causes extensive cellular damage. Thus the herbicide uncouples the energy of photosynthesis from the cellular biosynthetic machinery and if the concentration of paraquat is high enough and the cell cannot combat the ROS with its antioxidant systems, the energy can prove lethal.
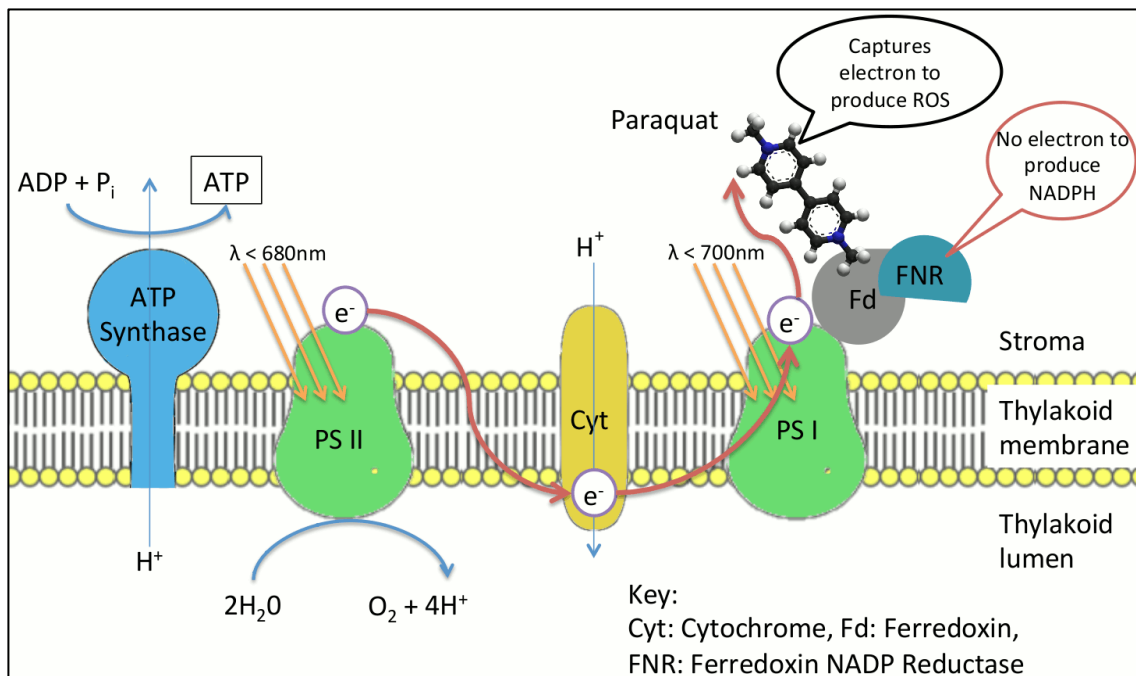
Figure 6.2 Mode of action of paraquat in chloroplast.

It is important to note that Fytizas (1980) has reported that in marine ecosystems there can be 50 to 70% loss of paraquat from seawater within 24 h, perhaps due to paraquat-resistant bacterial breakdown. Nonetheless paraquat continues to find use in studies of oxidative stress in marine ecology. Mayer (1987) reported in the acute toxicity handbook of chemicals to estuarine organisms, that marine algae are relatively resistant to paraquat and require higher dosages to produce significant growth inhibition compared to fresh water algae.

Given that DMSP is proposed to act as an antioxidant, I used paraquat to cause oxidative stress and then monitored the aspects of the stress response in *E. huxleyi* and looked for

changes in the DMSP system to see if further support could be found for the antioxidant function hypothesis. The expectation was that under stress intracellular DMSP production and DMS release would increase as part of an upregulation of the cellular antioxidant systems.

6.2 Methodology

Most of the work presented in this chapter was conducted on *E. huxleyi* 1516, though strains 370 and 373 were examined to establish whether paraquat-induced oxidative stress was strain dependent.

6.2.1 Culture conditions

Batch cultures of *E. huxleyi* (CCMP 370 and 373; naked cells and CCMP 1516; originally calcifying but lost its liths with culture in f/2 medium) were in grown seawater enriched with f/2 nutrients with the omission of Si, at 17°C under a 14:10 light:dark cycle at 100 µmol m^{-2} s^{-1}. More details are given in Chapter 2.

6.2.2 Parameters measured

Cell counts and cell volume were monitored on the Coulter counter and *in vivo* fluorescence and the efficiency of Photosystem II were measured with a phytoPAM (see details in Chapter 2). Given that the cells were naked, there was no need for an acidification step to remove coccoliths before estimating cell volume. DMS, DMSPd, DMSPp and DMSPt were all measured on the GC (Chapter 2, section 2.6), membrane permeability ('viability') was determined with SYTOX-green using the flow cytometer (Chapter 2, section 2.7). Hydrogen peroxide was also measured (Chapter 2, section 2.9). Utmost care was taken to keep the cultures axenic throughout the experiment and this was checked with a DAPI stain (Chapter 2, section 2.3) at the start and end of each experiment.

6.2.3 Establishing the effective paraquat concentration

In this study, various concentrations of paraquat (0.05 to 5 mM) were tested to decide an effective working concentration of paraquat. The strains were exposed to paraquat for 24 h and cell numbers, cell volume, fluorescence, photosynthetic capacity and intracellular DMSP were measured. On the basis of these results (Results 6.3.1), a final working concentration of 1 mM paraquat was selected, as at this concentration cell death was not induced.

6.2.4 Electronic trigger setting on the flow cytometer

A test was conducted to determine the electronic trigger parameter. This is essential to limit the signals to those derived from the particles of interest (for example, a cell) and ignore debris and 'spikes' from electronic noise. In studies on phytoplankton, data acquisition is triggered on red fluorescence (FL3) to reduce interference from non-fluorescent particles (Brussaard et al. 2001), but there could be higher chances of losing key information like dead cells while studying cell death processes. Since oxidative stress can result in the death of some cells, the use of light scatter as the trigger was tested. A series of various triggers was applied (Side scatter - SSC, Forward scatter - FSC, Red - FL3, Green - FL1 and orange – FL2 fluorescence) at values ranging from 0 to 750 (0, 52, 100, 250, 500 and 750). Based on the potential detection of all events collected, SSC was found to be more sensitive at a threshold of 0. Thus cell sorting was triggered at SSC.

6.2.5 Cell sorting: protocol and optimization

Since paraquat inhibits cell growth, it may be proposed that a subpopulation of oxidatively stressed cells are upregulating DMSP than the population as a whole, such that the elevation is masked. This idea was tested by flow cytometric cell sorting. Cells of *E. huxleyi* 1516 were sorted using a Cytopeia influx (Chapter 2, section 2.8) after 72 h exposure to paraquat. The control sample and the paraquat-exposed *E. huxleyi* 1516 samples were first passed through a 30 μm Partec filter to avoid clogging in the cell sorting system. The sorted cell populations were collected into 15 ml Falcon tubes

containing 3 ml filtered seawater (FSW) at room temperature. The experimental plan was to use 0.1 μm FSW of 33 psu as the sheath fluid in the BD influx cell sorter, but this led to high background being detected, so sorting was done with a low saline sheath fluid (10 mM NaCl). Cell sorting analysis was triggered on side scatter = 20; 488 nm 20 mW and 635 nm 30 mW.

The sorting process involved a long time, like even up to 60 minutes to collect 3 x 10^6 cells, so it was crucial to know the minimum number of cells required for the detection of intracellular DMSP and DMSP per cell. A test was therefore conducted to determine the minimum number of cells that were needed for a DMS signal on the GC. For this, various volumes of the control and the 72 h paraquat-treated cultures were gently filtered through 25 mm GF/F filters using a hand pump. The total volume filtered was kept a constant 3 ml, adjusting the volume of FSW for each of the culture volumes. The results from this test suggested that although a decent DMS signal could be acquired from 100,000 cells, sorting more than 1,000,000 cells was more advisable (see section 6.3.3). Cell volume measurements of the sorted cells were done on the Coulter counter to allow calculation of intracellular DMSP values.

6.2.5.1 The pre-concentration step

A constant number of 1.5 x 10^6 cells were sorted and each sample was sorted in biological triplicate. Cell sorting was based on the emission of red fluorescence (670 nm), as the number of cells emitting red fluorescence was high and so the sorting time was reduced and triplicate sorts were possible.

The time involved in sorting 1.5 x 10^6 cells for the paraquat-treated samples was 40 mins compared to 20 mins for the control culture samples. Thus a pre-concentration step was adopted to again reduce sorting time and achieve triplicate sorts. For this, two cell pre-concentration techniques were tried: a centrifugation method and a plate-concentration method. Out of the two, based on the flow cytometric data profiles, the plate-concentration method achieved the best results in terms of the least loss of cells due to pre-concentration and there being no significant difference in the cell emissions. The centrifugation method caused greater losses in cell number, especially in the

paraquat exposed cells. Finally, the time involved in sorting 1.5 x 10^6 cells for the paraquat-treated samples was 10 mins compared to 5 mins for the control culture samples.

A.   Centrifugation Method: Initial tests with different timings involved and rotation speeds were carried out to establish the best settings for the centrifugation method. Loss of cells using flow cytometric analyses was noted above 15 mins and at speeds above 5310 g (5000 rpm) for the paraquat treated samples. Based on the results of these tests, 2 ml of the control and treated cultures were centrifuged for 10 mins at a speed of 3398 g (4000 rpm) at 21°C. After centrifugation, the sample was divided into three portions: Supernatant 1 (top 0.2 ml), Supernatant 2 (1.4 ml below the supernatant 1) and the re-suspended pellet (bottom 0.4 ml). A non-centrifuged control sample and a vortex re-suspended centrifuged sample were also examined on the flow cytometer. Cell numbers did not match up indicating loss of cells during centrifugation. Losses were greater (30%) for the paraquat treated culture than the control culture suggesting that the paraquat-exposed cells could not withstand centrifugation stress.

B.   Plate-concentration Method: In the plate concentration method, 3 sequential 200 μl aliquots of the culture sample were placed in the well of a multi-well plate. Each well containing the sample was concentrated by gently sucking through the filter at the base of the well with a syringe. The filter was not allowed to go dry such that the cells were concentrated in a 200 μl volume. This volume was then re-suspended in 3 ml FSW and ready for sorting.
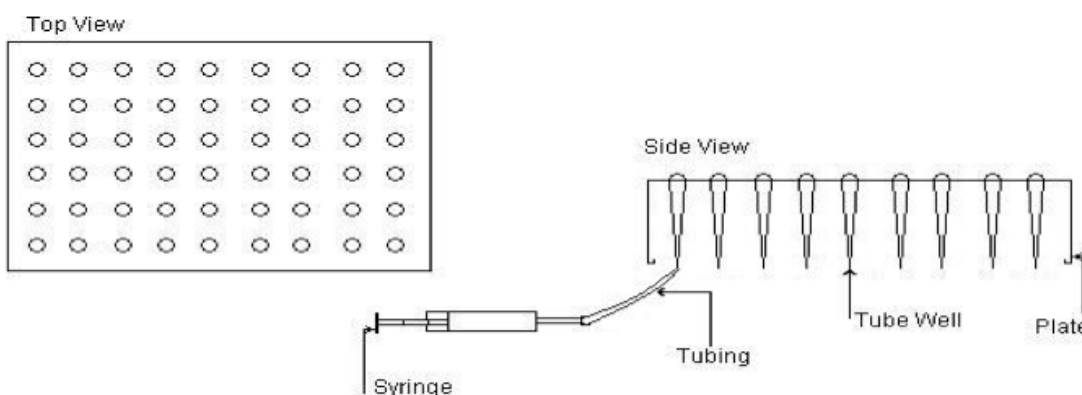
Figure 6.3 Plate-Concentration Method with top view and side view of the plate.

Prior to sorting, the pre-concentrated cells were run through the FACS calibur to examine any changes in fluorescence of the cells, which may have occurred as a negative effect of the plate-concentration method (Results 6.3.3). Overall the plate-concentration method proved suitable for cell pre-concentration and was adopted to reduce sorting time.

6.2.6 Reaction between DMSP and paraquat

Two conical flasks capped with cotton bungs and two borosilicate tubes with screw-capped lids were set up under sterile conditions to test the reaction between DMSP and paraquat. A known concentration of DMSP (60 µM) was prepared from a DMSP standard diluted in f/2-Si media and dispensed into the flasks and tubes. To one of the flask and tube, a known concentration of paraquat was added to a final concentration of 1 mM. The main difference in the flask and tube set-up was that, sterility was maintained in the tube set-up by the use of sterile glassware and DMSP and paraquat solutions were prepared in sterile conditions ensuring no inclusion of bacteria, while in the flask set-up, the sterile technique was not followed. This was done to see the effect of bacterial action on DMSP and DMSP + paraquat. The flasks and tubes were all placed in an incubator for about 5 days under the same light and temperature conditions used for the paraquat-induced oxidative stress experiments. The results of this experiment are shown in Results 6.3.8.

6.3 Results

6.3.1 Effective concentration of paraquat

Batch cultures of initial cell density of ~ 500,000 cells ml^{-1} of *E. huxleyi* 370, 373 and 1516, were exposed to various concentrations of paraquat ranging from 0.05, 0.1, 0.5, 1, 2, 3, 4 and 5 mM for 24 h (Fig. 6.4 and 6.5). Measurements were made at 0 h and then at 24 h. With increasing concentration of paraquat the cell densities reduced relative to those of the controls after the 24 h exposure and with 1 mM paraquat there was essentially no growth suggesting cell growth arrest (Table 6.1). The initial cell volume at

0 h, was 30 μm^3 for *E. huxleyi* 370, and 25 μm^3 for 373 and 1516 (Table 6.1), but after 24 h exposure to various concentrations of paraquat, a clear and well-replicated increase in cell volume at 39, 37 and 36 μm^3 for *E. huxleyi* 370, 373 and 1516 (Table 6.1) was observed in all three strains exposed to 1 mM paraquat, while no increase in cell volume was seen at < 1 mM. At concentrations above 1 mM the replication of the data was poor even when a repeat testing was carried out. SYTOX Green staining of cells exposed to > 1 mM paraquat revealed 50% or more compromised cells after 24 h exposure (Fig. 6.5). With 1 mM SYTOX Green indicated 18% of the *E. huxleyi* 370 and 1516 and 29% of the *E. huxleyi* 373 cells with compromised membranes. The main aim with paraquat exposure was not to induce cell death but enhance oxidative stress and to test its effect on intracellular DMSP. In this context, figure 6.4 shows a clear decrease in photosynthetic capacity, indicating stress, at 1 mM paraquat for all three strains. Samples exposed to paraquat concentrations > 1 mM showed lower F_V/F_M ratio and very low fluorescence suggesting low photosynthetic capacity and a high level of stress (Fig. 6.4). There was no matching pattern in the intracellular DMSP concentration data, rather a decrease in DMSPp was observed. From the above results, 1 mM was selected as the effective concentration of paraquat.

Table 6.1 Comparison of the effect of 1 mM paraquat on *E. huxleyi* 370, 373 and 1516 versus a control. Data are shown for time 0 and 24 h.

Parameter	*E. huxleyi* 370			*E. huxleyi* 373			*E. huxleyi* 1516		
	0 h	24 h		0 h	24 h		0 h	24 h	
		0 mM	1 mM		0 mM	1 mM		0 mM	1 mM
Cell density (cells ml^{-1}x 10^3)	500	1,078	512	500	944	519	500	1,071	502
Cell Volume (μm^3)	30	31	39	25	25	37	25	26	36
Fluorescence (arbitrary unit)	200	376	191	150	280	148	150	279	147
Photosynthetic Capacity	0.6	0.60	0.41	0.58	0.57	0.41	0.59	0.59	0.48
Intracellular DMSP (mM)	200	214	180	400	417	251	200	254	189
DMSP/Cell (fmol)	6	2.76	3.52	6.00	6.36	5.11	4.08	4.58	3.78
SYTOX Green stained cells (%)	< 1	1	18	< 1	1	29	< 1	1	18
Viable cells (%)	95	89	75	95	89	67	95	89	75
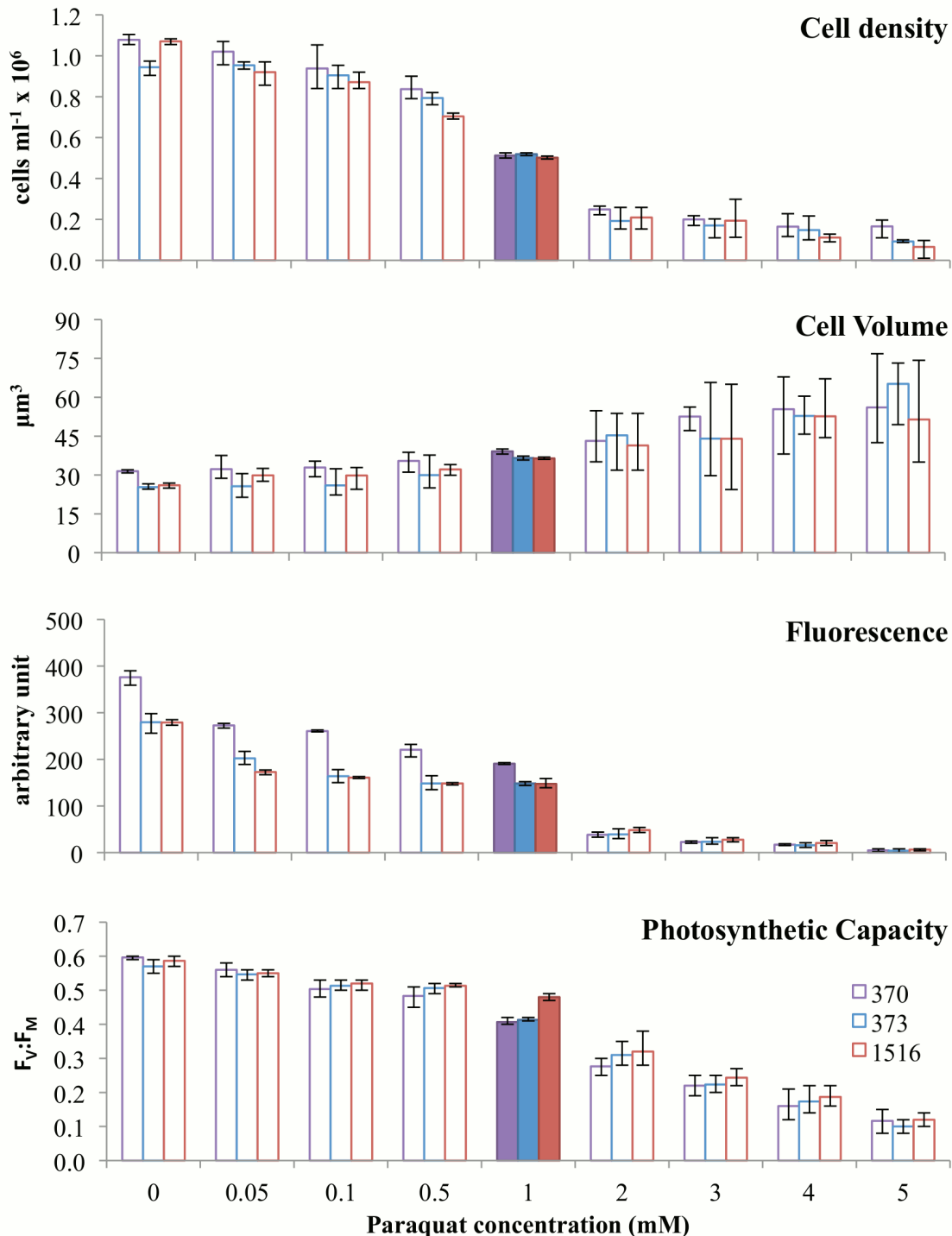
Figure 6.4 Three strains of *E. huxleyi* were exposed to various concentrations of paraquat and the effect on cell density, cell volume, fluorescence and photosynthetic capacity was measured after exposure for 24 h. Purple, blue and red bars denote *E. huxleyi* 370, 373 and 1516 respectively. The solid bars indicate effective paraquat concentration selected as a working concentration. The error bars represent range of data (n=3).
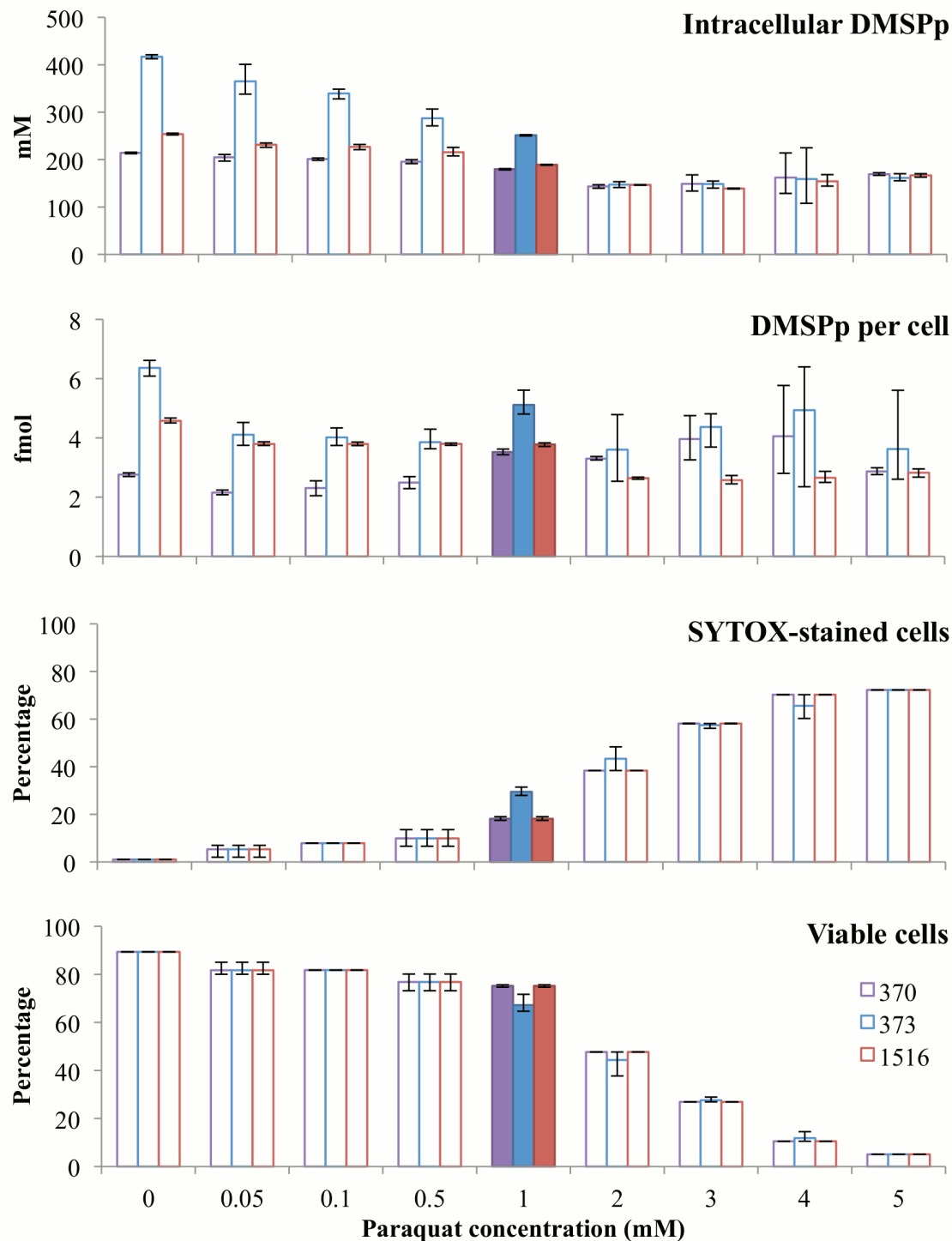
Figure 6.5 Three strains of *E. huxleyi* were exposed to various concentrations of paraquat and the effect on intracellular DMSPp, DMSPp per cell, sytox-stained cells and viable cells after exposure for 24 h. Purple, blue and red bars denote *E. huxleyi* 370, 373 and 1516 respectively. The solid bars indicate effective paraquat concentration selected as a working concentration. The error bars represent range of data (n=3).

6.3.2 Paraquat exposure time-series experiments

A 72 h time-series exposure to 1 mM paraquat with intermittent measurements was carried out on *E. huxleyi* 370 and 373 (Fig. 6.6 and 6.7) and 48, 72 and 120 h time-series exposures were carried out using *E. huxleyi* 1516 (Fig. 6.8 to 6.14).

In the 48 h time-series exposure experiment, the various parameters were measured at 0, 1 and 2 h followed by 2 h time intervals for the first 24 hours and at 6 h intervals for the next 24 hours. In the 72 h time-series experiment, the various parameters were recorded on a daily basis while the measurements for the 120 h time-series exposure were done at 0, 2 and 12 h followed by 12 h time intervals. The 120 h time-series was conducted with the culture in its exponential growth phase for the first three days, but then it reached the stationary phase after 72 h.

6.3.2.1 Cell culture and growth measurements

Within all time-series exposures, cell growth inhibition was noted with paraquat after 24 h. Cell density did not decrease over time but it was clear that after 48 h the cell density in the control cultures was almost double at 1.5 and 2.2 x 10^6 cells ml^{-1} in *E. huxleyi* 370 and 373 and at 1.5, 1.8 and 1.9 x 10^6 cells ml^{-1} in 120, 72 and 48 h exposed *E. huxleyi* 1516 than compared to the paraquat-exposed cultures at 0.6 x 10^6 cells ml^{-1} in *E. huxleyi* 370 and 373 and at 0.6, 1.2 and 1.1 x 10^6 cells ml^{-1} in 120, 72 and 48 h exposed *E. huxleyi* 1516 respectively (Fig. 6.6, 6.7 and 6.8).

In the 120 h time-series, cell aggregation was visual after 72 hours in the control culture while, since paraquat arrests cell cycle, growth in the paraquat-exposed culture was inhibited. Cell volume was generally higher in the paraquat-exposed cultures at 37 and 39 μm^3 in *E. huxleyi* 370 and 373 at 72 h and at 37, 21 and 44 μm^3 in 120, 72 and 48 h paraquat-exposed *E. huxleyi* 1516 (Fig. 6.6, 6.7 and 6.8).
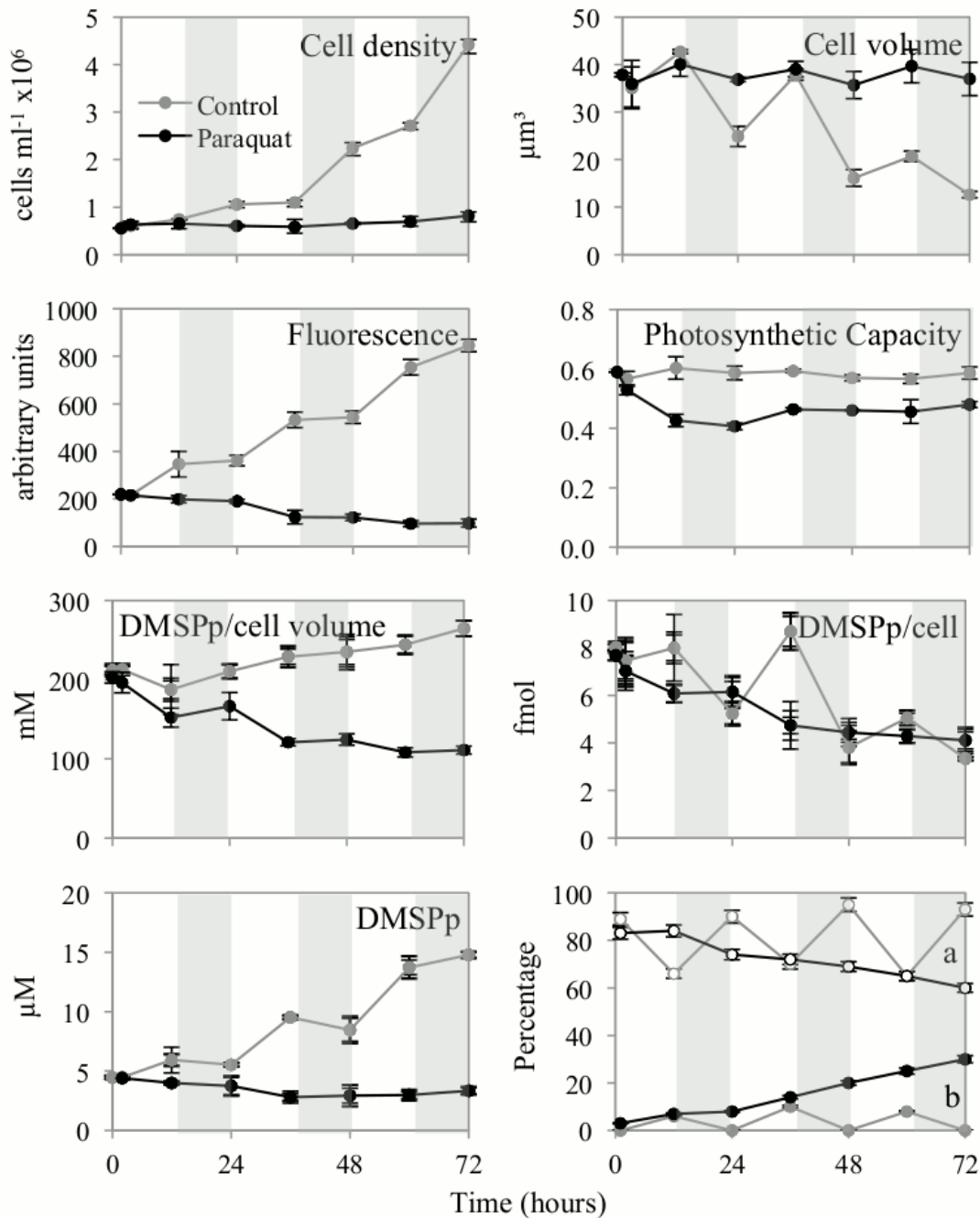
Figure 6.6 A 72 h time series exposure on *E. huxleyi* 370 to 1 mM paraquat in the L:D cycle. The above plots display cell density, cell volume, fluorescence, photosynthetic capacity, DMSPp per cell volume (mM), DMSPp per cell (fmol) and DMSPp in the culture (μM). The bottom plot on the right shows percentage of (a) viable cells (open symbols) and (b) cells with compromised membranes (closed symbols) after SYTOX Green stain addition The grey line denotes the control (not exposed to paraquat) and the black line denotes the paraquat-exposed cultures. The average value and range of data is shown (n=3). Where no range bars are visible, the data range was smaller than the symbol size.
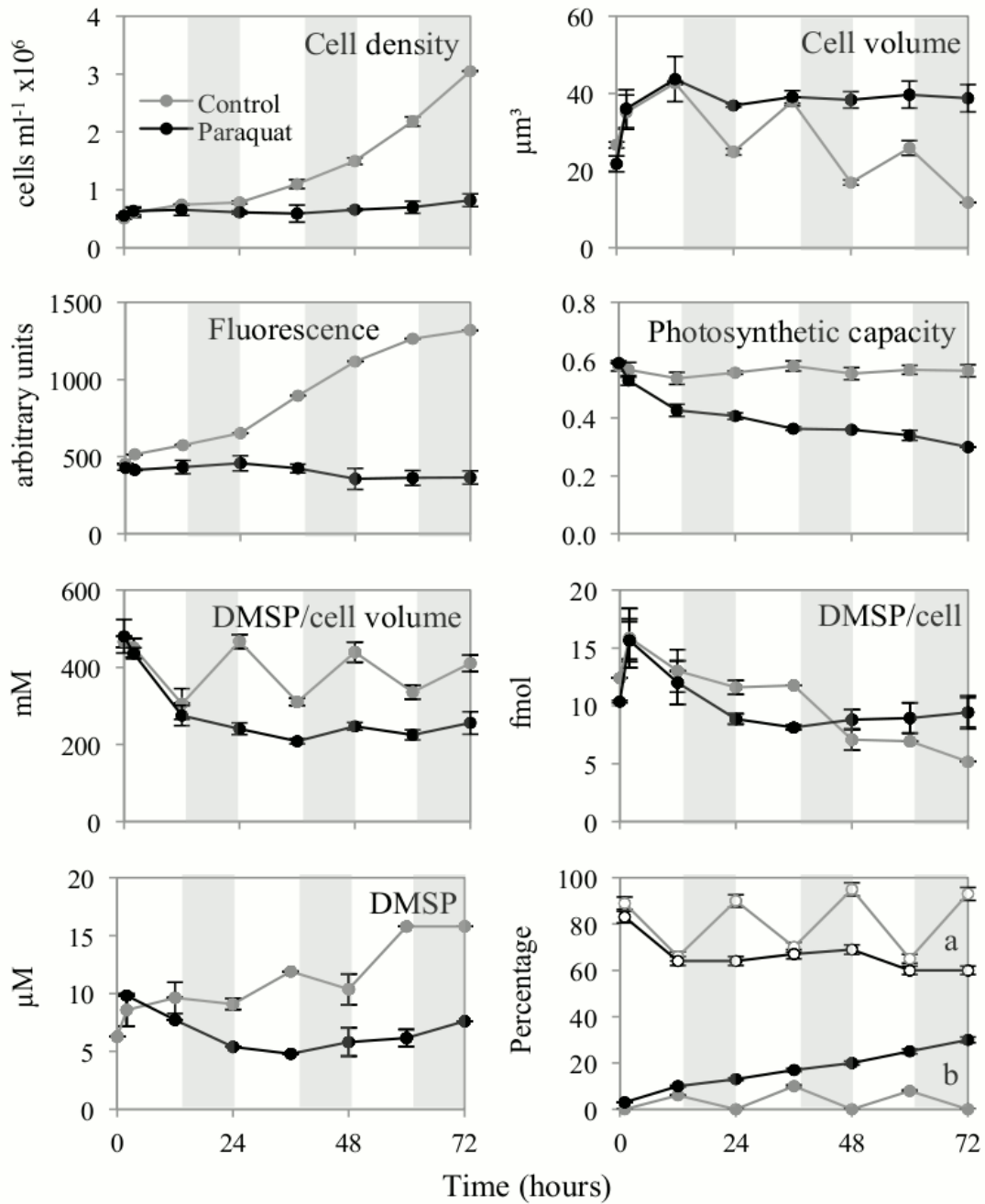
Figure 6.7 A 72 h time series exposure on *E. huxleyi* 373 to 1 mM paraquat in the L:D cycle. The above plots display cell density, cell volume, fluorescence, photosynthetic capacity, DMSPp per cell volume (mM), DMSPp per cell (fmol) and DMSPp in the culture (µM). The bottom plot on the right shows percentage of (a) viable cells (open symbols) and (b) cells with compromised membranes (closed symbols) after SYTOX Green stain addition The grey line denotes the control (not exposed to paraquat) and the black line denotes the paraquat-exposed culture. The average value and range of data is shown (n=3). Where no range bars are visible, the data range was smaller than the symbol size.
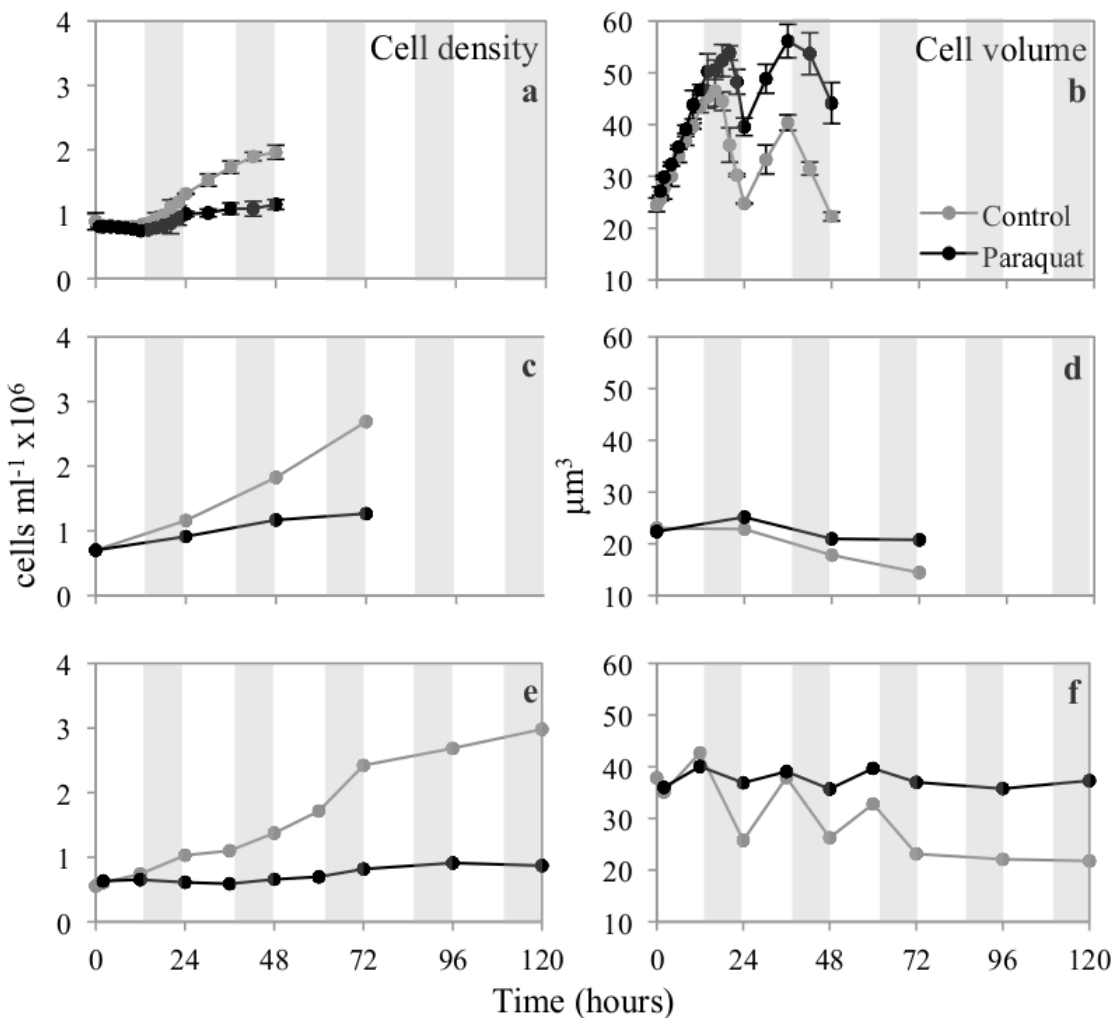
Figure 6.8 Time series exposure of *E. huxleyi* 1516 to 1 mM paraquat over 48, 72 and 120 h with a L:D cycle. Plots a, c and e show cell density and plots b, d and f show cell volume. The grey line denotes the control (not exposed to paraquat) and the black line denotes the paraquat-exposed culture. The average value and range of data is shown (n=3). Where no range bars are visible, the data range was smaller than the symbol size.

Fluorescence in the paraquat exposed culture remained fairly constant in the range of 100 to 200 and 360 to 430 for *E. huxleyi* 370 and 373 over the 72 h time series and in the range of 60 to 220, 150 to 290 and 250 to 300 for *E. huxleyi* 1516 over the 120, 72 and 48 h time series respectively when compared to increasing control cultures reaching a maximum of 1320 value in *E. huxleyi* 373 at 72 h (Fig. 6.6, 6.7 and 6.9).

A sharp decrease was seen in the photosynthetic capacity within 24 h at 0.41 in *E. huxleyi* 370 and 373 and at 0.41, 0.48 and 0.53 in *E. huxleyi* 1516 over the 120, 72 and 48 h time series respectively (Fig. 6.6, 6.7 and 6.9). All the cultures were seen with some recovery after 24 h except *E. huxleyi* 373 which decreased further and reached 0.3 by 72 h. The fairly stabilized fluorescence and photosynthetic capacity does suggest chances of regrowth and recovery in absence of stressor.
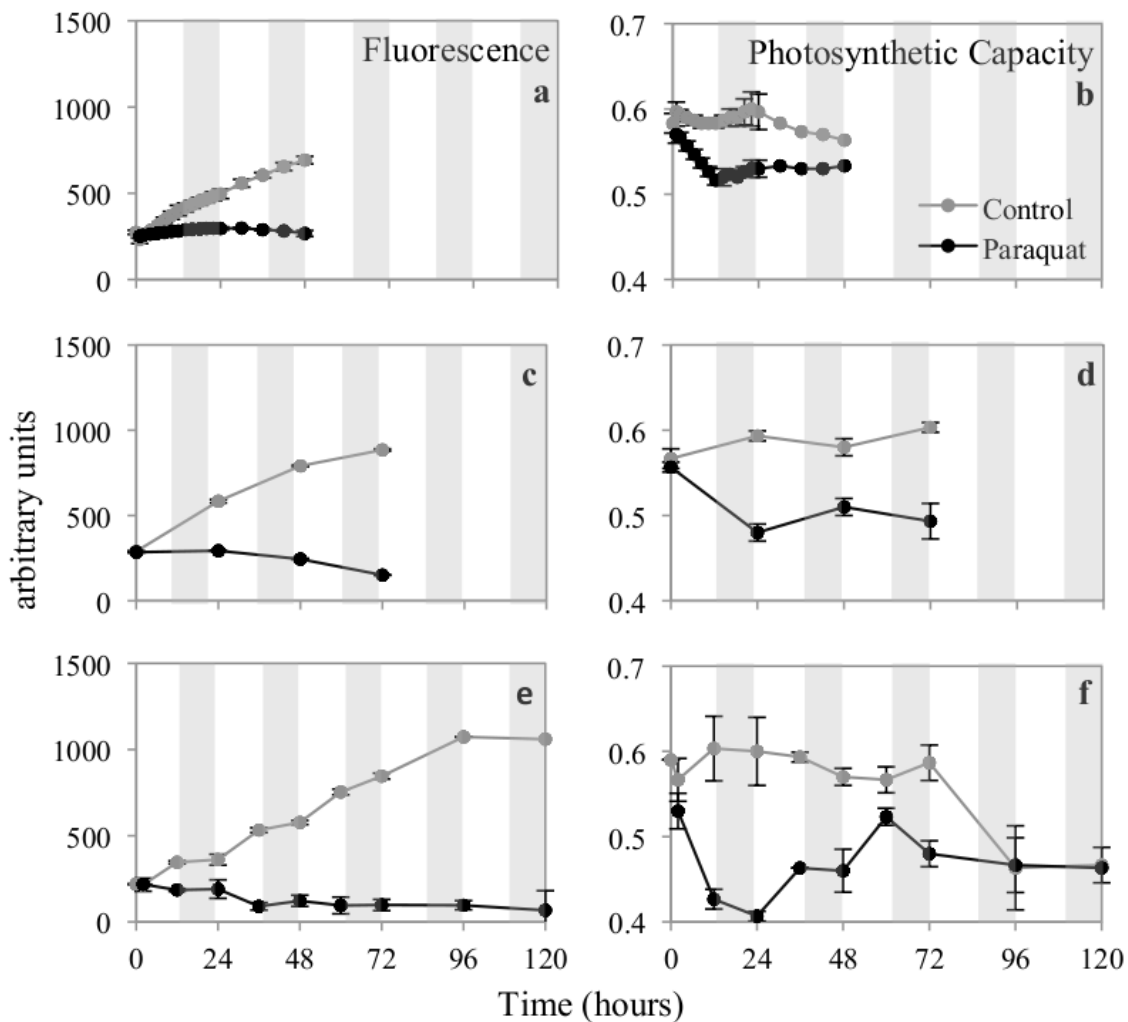
Figure 6.9 Time series exposure of *E. huxleyi* 1516 to 1 mM paraquat over 48, 72 and 120 h with a L:D cycle. Plots a, c and e show fluorescence and plots b, d and f show photosynthetic capacity. The grey line denotes the control (not exposed to paraquat) and the black line denotes the paraquat-exposed culture. The average value and range of data is shown (n=3). Where no range bars are visible, the data range was smaller than the symbol size.

6.3.2.2 SYTOX Green staining

Increase in membrane permeability in *E. huxleyi* 370, 373 and 1516 during oxidative stress on exposure to paraquat was revealed with SYTOX Green staining and flow cytometry (Fig. 6.6, 6.7, 6.10 and 6.11). The percentage of compromised cells were noted to be 30% in *E. huxleyi* 370 and 373 at 72 h and at 55, 32 and 20% in 120, 72 and 48 h exposed *E. huxleyi* 1516, compared to 3% in *E. huxleyi* 370 and 373 at 72 h and at 4, 3 and 0.1% in 120, 72 and 48 h exposed *E. huxleyi* 1516, last reading in the control culture.

Cultures exposed to paraquat showed a decrease in the percentage of viable cells. The percentage of viable cells were noted to be 60% in *E. huxleyi* 370 and 373 at 72 h and at 40, 65 and 70% in 120, 72 and 48 h exposed *E. huxleyi* 1516, compared to 93% in *E. huxleyi* 370 and 373 at 72 h and at 85, 95 and 95% in 120, 72 and 48 h exposed *E. huxleyi* 1516, in the control culture.

The cell viability of the control cultures i.e. without paraquat, remained constant, in the range of almost 80 to 100% over the time period. In the 48 h time series, it is interesting to note that a higher percentage of control cells are SYTOX Green stained (Fig. 6.6, 6.7, 6.10 and 6.11) over the course of the light period and the cell volume is at its peak (Fig. 6.6, 6.7 and 6.8).
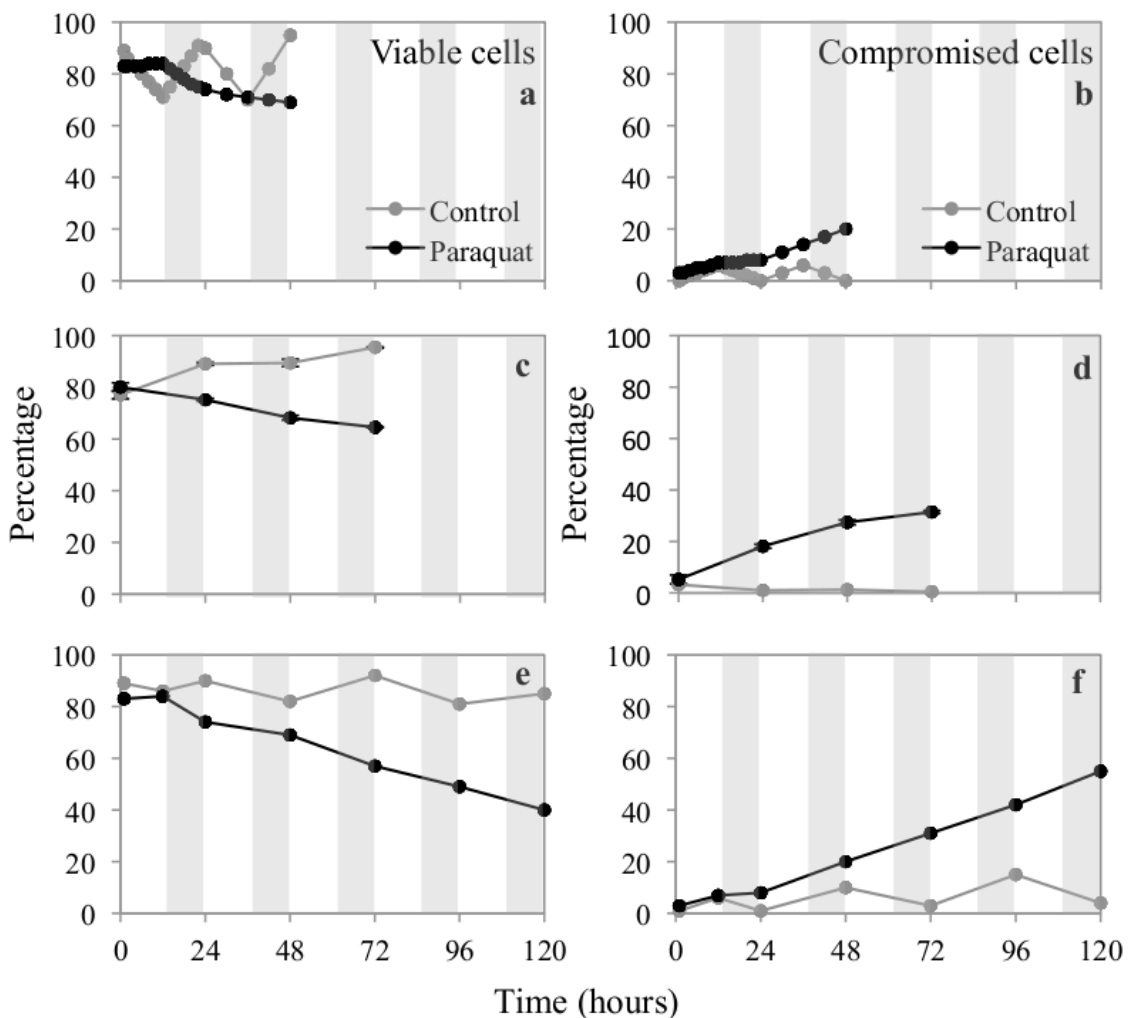
Figure 6.10 Time series exposure of *E. huxleyi* 1516 to 1 mM paraquat over 48, 72 and 120 h with a L:D cycle. Plots a, c and e show percentage viable cells and plots b, d and f show percentage of cells with compromised membranes after SYTOX Green stain addition. The grey line denotes the control (not exposed to paraquat) and the black line denotes the paraquat-exposed culture. The average value and range of data is shown (n=3). Where no range bars are visible, the data range was smaller than the symbol size.
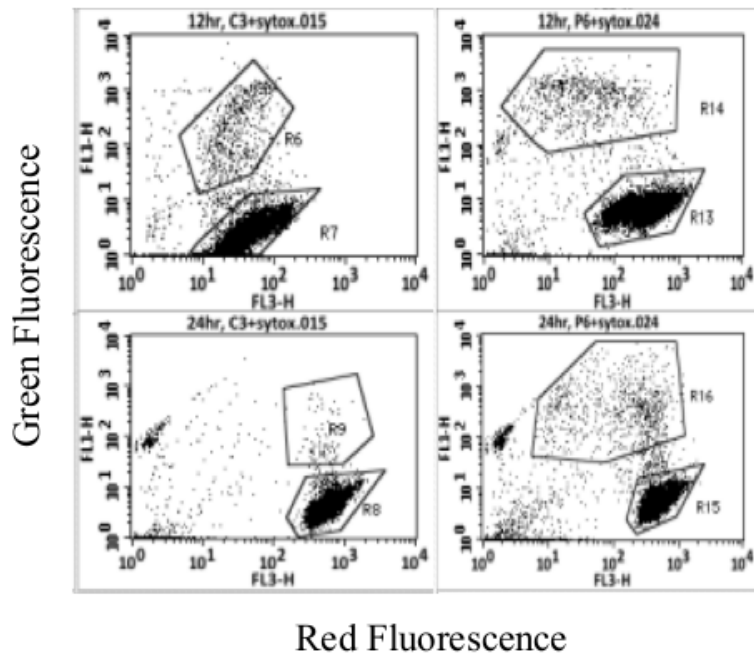
Figure 6.11 Snapshot of cytograms after SYTOX Green additions at 12 h and 24 h. On the top left, Control + SYTOX at 12 h (R7-viable cells and R6-compromised cells). On the bottom left, Control + SYTOX at 24 h (R8-viable cells and R9-compromised cells). On the top right, Paraquat + SYTOX at 12 h (R13-viable cells and R14-compromised cells). On the bottom right, Paraquat +SYTOX at 24 h (R15-viable cells and R16-compromised cells). At 12 h an increase in SYTOX-Green stained cells was observed and this has been noted at every interval of 12 h in a time series. The above snapshot is only an example.

6.3.2.3 Particulate DMSP analyses

In all the time-series for paraquat exposed *E. huxleyi* 370, 373 and 1516 the DMSP particulate (DMSPp) has been calculated and represented as DMSPp per cell volume (mM) (Fig. 6.6, 6.7 and 6.12), DMSPp per cell (fmol) (Fig. 6.6, 6.7 and 6.12) and DMSPp (μM) (Fig. 6.6, 6.7 and 6.13).

DMSPp per cell volume showed a decreasing trend for all the time exposures and strains with concentrations at 111 and 256 mM in *E. huxleyi* 370 and 373 at 72 h and at 77, 257 and 60 mM in 120, 72 and 48 h exposed *E. huxleyi* 1516, compared to control at 265 and 410 mM in *E. huxleyi* 370 and 373 at 72 h and at 197, 445 and 342 mM in 120, 72 and 48 h exposed *E. huxleyi* 1516, at same time points (Fig. 6.6, 6.7 and 6.12).
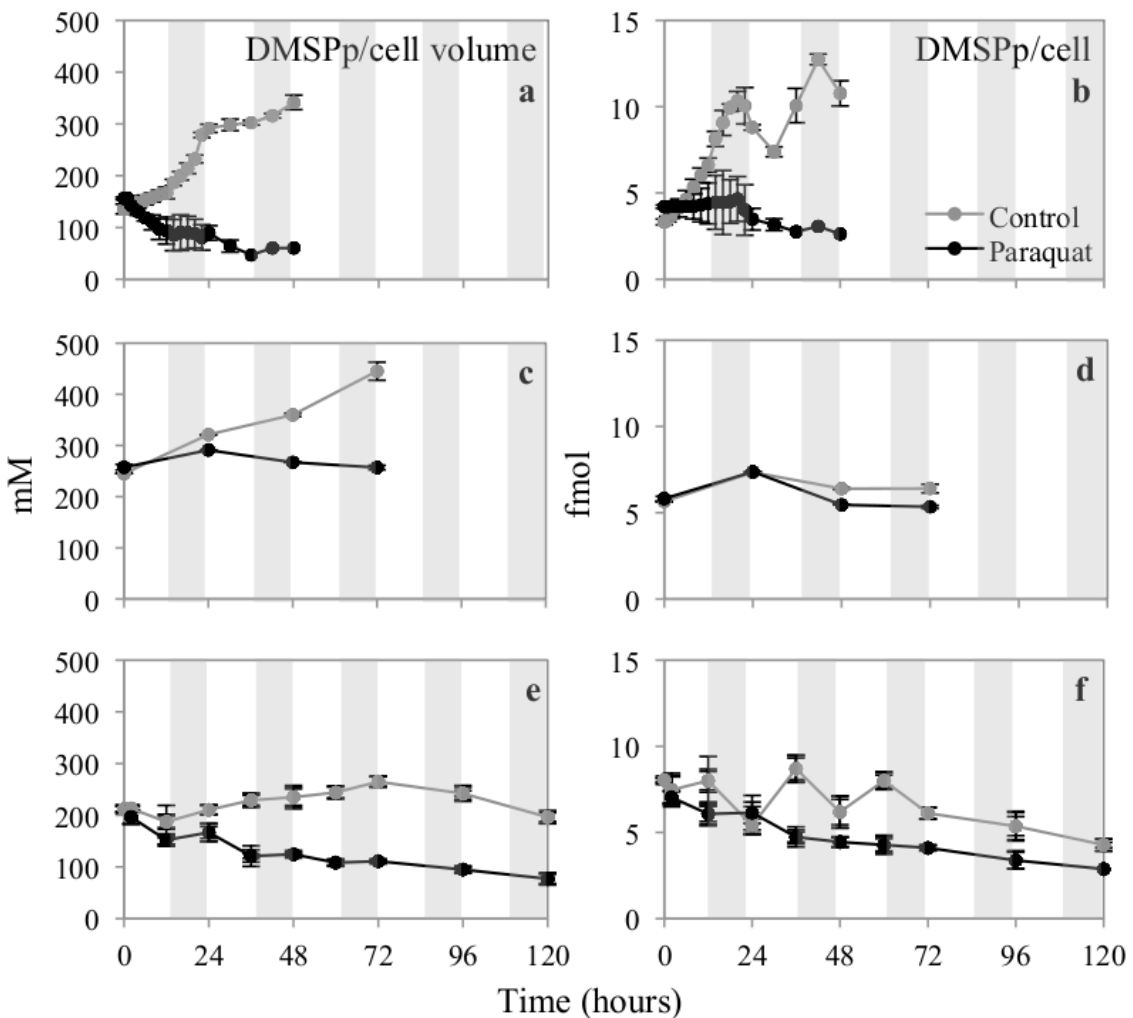
Figure 6.12 Time series exposure of *E. huxleyi* 1516 to 1 mM paraquat over 48, 72 and 120 h with a L:D cycle. Plots a, c and e show DMSPp per cell volume (mM) and plots b, d and f show DMSPp per cell (fmol). The grey line denotes the control (not exposed to paraquat) and the black line denotes the paraquat-exposed culture. The average value and range of data is shown (n=3). Where no range bars are visible, the data range was smaller than the symbol size.
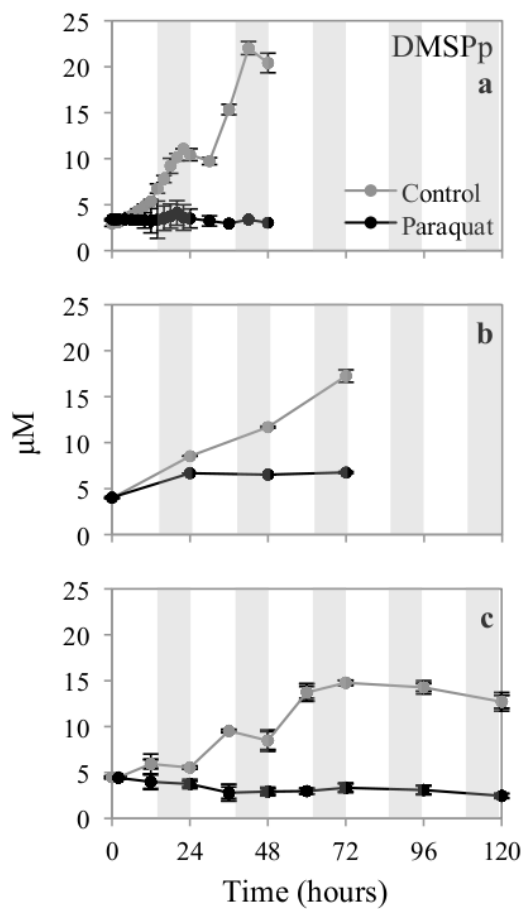
Figure 6.13 Time series exposure of *E. huxleyi* 1516 to 1 mM paraquat over 48, 72 and 120 h with a L:D cycle. Plots a, b and c show DMSPp (µM) in the culture. The grey line denotes the control (not exposed to paraquat) and the black line denotes the paraquat-exposed culture. The average value and range of data is shown (n=3). Where no range bars are visible, the data range was smaller than the symbol size.

DMSPp per cell also followed the decreasing trend for all the 120, 72 and 48 h time exposures in *E. huxleyi* 1516 with values at 2.9, 5.3 and 2.6 fmol respectively when compared to the control values at 4.3, 6.4 and 10.8 fmol. While 72 h exposed *E. huxleyi* 370 and 373 after decreasing initially increased at 4.11 and 9.4 fmol compared to the control at 3.4 and 5.2 fmol at 72 h (Fig. 6.6, 6.7 and 6.12).

DMSPp in the culture too followed the decreasing trend for all the time exposures and strains with low concentrations at 3.4 and 7.6 µM in *E. huxleyi* 370 and 373 at 72 h and at 2.5, 6.8 and 3 µM in 120, 72 and 48 h exposed *E. huxleyi* 1516, when compared to

14.8 and 15.8 µM in *E. huxleyi* 370 and 373 at 72 h and at 12.7, 17.2 and 20.4 µM in 120, 72 and 48 h exposed *E. huxleyi* 1516, at same points (Fig. 6.6, 6.7 and 6.13).

6.3.2.4 Total DMSP, dissolved DMSP and DMS analyses

DMS, DMSPd and DMSPt analyses were conducted only with *E. huxleyi* 1516 in the 72 h time-series exposure experiment (Fig. 6.14 and 6.15). This analysis was conducted mainly to test any increased levels of DMS or DMSPd observed in the paraquat-exposed condition (Fig. 6.14). There was no increase in DMS in the culture, but dissolved DMSP was higher in concentration compared to the control culture. DMS for paraquat-exposed cultures was noted to be low at 0.1 mM per cell volume concentration, 0.002 fmol per cell and 0.01 µM in the culture compared to control at 0.8 mM per cell volume concentration, 0.01 fmol per cell and 0.06 µM in the culture whereas DMSPd was noted to be high at 79 mM per cell volume concentration, 1.5 fmol per cell or 3.2 µM in the culture compared to control at 30 mM per cell volume concentration, 0.4 fmol per cell and 2.3 µM in the culture.

The overall total production of DMSP as seen from the DMSPt (Fig. 6.15) measurements was still found to be lower at 230 mM per cell volume concentration, 4.4 fmol per cell and 9.3 µM in the paraquat-exposed culture than in the control at 316.4 mM per cell volume concentration, 4.6 fmol per cell and 23.9 µM in the culture.

Thus there was no increase in intracellular DMSP concentrations with paraquat-induced oxidative stress and DMS production was also lower in the paraquat-exposed culture.
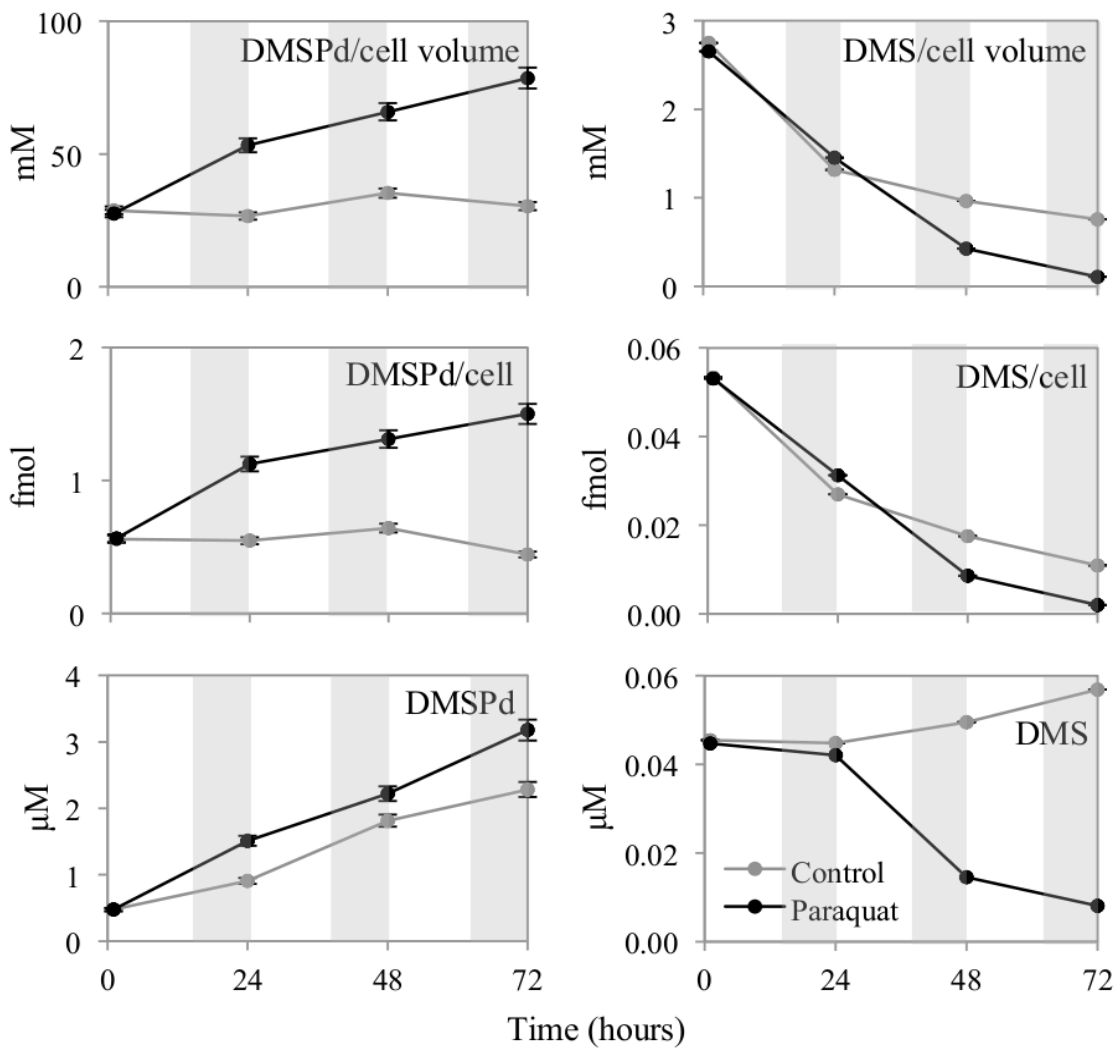
Figure 6.14 A 72 h time series exposure on *E. huxleyi* 1516 to 1 mM paraquat in the L:D cycle. The plots on the left display DMSPd per cell volume (mM), DMSPd per cell (fmol) and DMSPd in the culture (μM) and on the right, DMS per cell volume (mM), DMS per cell (fmol) and DMS in the culture (μM). The grey line denotes the control (not exposed to paraquat) and the black line denotes the paraquat-exposed culture. The average value and range of data is shown (n=3). Where no range bars are visible, the data range was smaller than the symbol size.
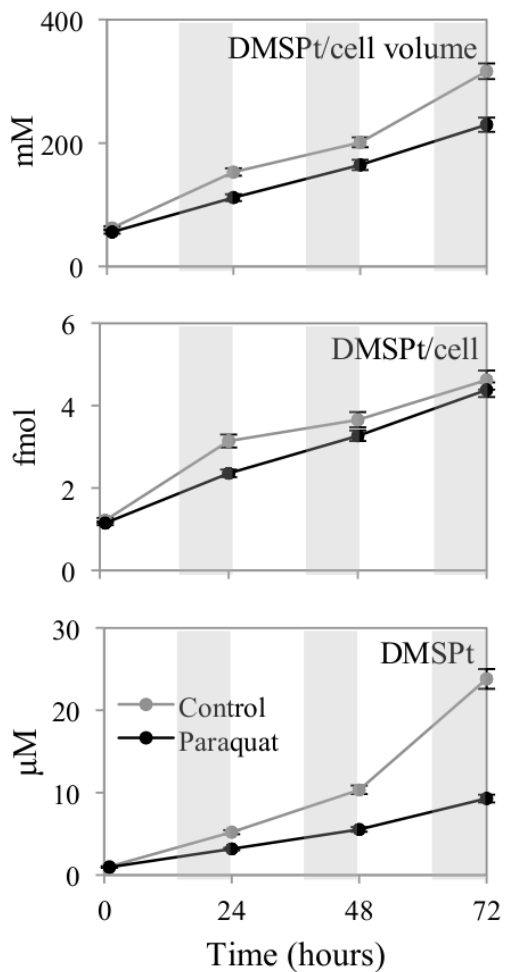
Figure 6.15 A 72 h time series exposure on *E. huxleyi* 1516 to 1 mM paraquat in the L:D cycle. The above plots display DMSPt per cell volume (mM), DMSPt per cell (fmol) and DMSPt in the culture (μM). The grey line denotes the control (not exposed to paraquat) and the black line denotes the paraquat-exposed culture. The average value and range of data is shown (n=3). Where no range bars are visible, the data range was smaller than the symbol size.

6.3.3 Cell sorting optimization

As mentioned before in section 6.2.5, it was crucial to know the minimum number of cells required for the detection of DMSP per cell to minimise the long sorting times required for the paraquat-treated cells (Fig. 6.16). Experiments revealed that when the cell numbers were 100,000 per 3 ml sample or less, DMSP per cell levels tended towards a very high value, which may not have been the actual DMSP levels in the sample but an artifact of the instrumental analyses. Thus it was not advisable to sort cells as low as a 100,000 in number.
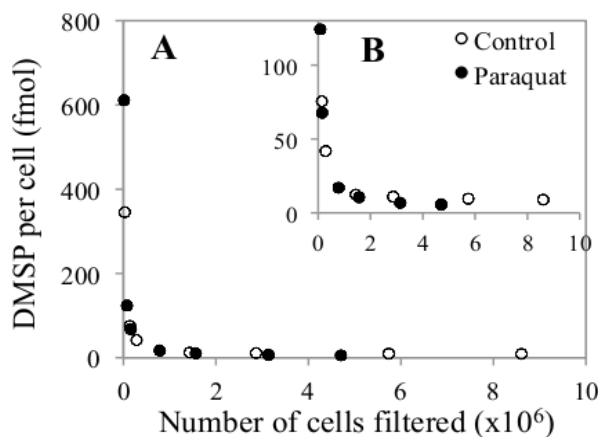
Figure 6.16 DMSP per cell for non-sorted control and paraquat-exposed *E. huxleyi* cells v/s Number of cells filtered per 3 ml sample. Plot B is the magnified view of Plot A. In plot B, the highest values are omitted. The open circles denote control and the closed circles denote paraquat exposed culture. Only average data values have been shown.

Figure 6.17 shows the volume range (0.01 – 3 ml) of the culture used in filtration, with the total volume kept constant at 3 ml. This plot clearly shows that culture volumes lower than 0.5 ml filtered, result in very high DMSP/cell content. It could be the inaccuracies in counting a very low number of cells in culture volumes less than 0.5 ml introduced in 3 ml FSW.
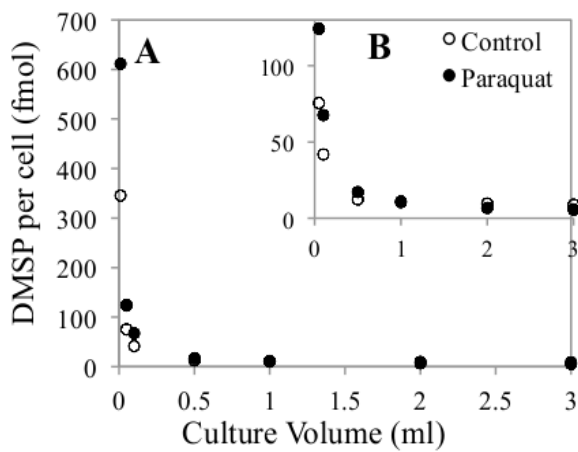
Figure 6.17 DMSP per cell for non-sorted control and treated *E. huxleyi* cells v/s Volume of culture filtered. Plot B is the magnified view of Plot A. In plot B, the highest values have been omitted. The open circles denote control and the closed circles denote paraquat exposed culture. Only average data values have been shown.

Sorting 1.5×10^6 cells from paraquat-treated cultures took 20 mins to sort as opposed to 10 mins for the control culture samples. Thus a pre-concentration step was necessary to reduce sorting time and achieve triplicate sorts. For this, two pre-concentration techniques were tried: the centrifugation method and the plate-concentration method. Out of the two, based on the flow cytometric data profiles, the plate-concentration method achieved the best results in terms of the least loss of cells (< 3%) due to pre-concentration and there was also no change in the cell fluorescence emissions. The centrifugation method resulted in substantial losses in cell number (30%), especially in the paraquat-exposed cells. The pre-concentration method reduced the sorting times to half the time i.e. 10 mins for the paraquat-treated cultures and 5 mins for the control culture samples.

At 72 h, cell sorting of the control culture sample resulted in one major cell population emitting red fluorescence (670 nm) whereas the paraquat-exposed culture had two distinct populations: one with high red fluorescence (Red +ve) and the other with low red fluorescence (Red -ve).

As seen below in Figure 6.18, there was no significant effect on the sorted cells in terms of DMSP per cell concentrations due to the pre-concentration step using the plate-

concentration method. Thus the plate-concentration method was suitable for pre-concentration of cells and this reduced sorting time.
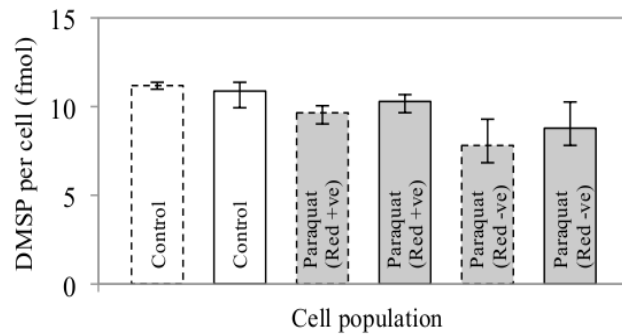
Figure 6.18 Comparison of DMSP per cell (fmol) from the sorted cells without the pre-concentration step (bars with dashed outline) and sorting done with the pre-concentration step using the plate-concentration method (bars with solid outline). The error bars denote the range of the biological triplicates.

6.3.4 Effects of sorting

It was also necessary to determine whether sorting would have any effect on the volume of a cell, as deriving intracellular DMSP values is essentially dependent on cell volume. For this, cell volume was measured on the Coulter counter before and after sorting the cells of the control and paraquat-exposed cultures (Fig. 6.19). It can be concluded that cell volume apparently undergoes a change during sorting. After sorting the cells, the cell volume increased by 15% with the control cells and decreased by 5% with the paraquat-exposed cells.
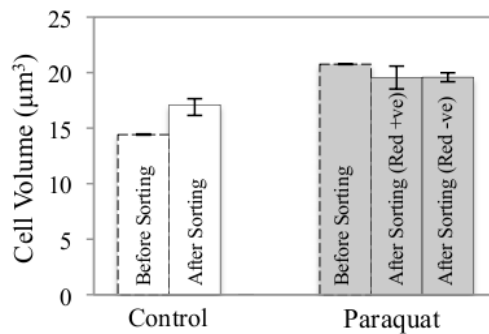
Figure 6.19 Changes in cell volume in control and paraquat exposed cell populations of *E. huxleyi* 1516. The white and the grey bars denote the average value for the control and paraquat-exposed cell populations respectively. The error bars show the range of data (n=3).

Another interesting feature was observed in the control cell population after the cells were being sorted. On observing the cells with side scatter, two populations were distinguishable from each other although their emissions remained the same (Fig. 6.20). This was not noted in the paraquat-exposed cells. This may be attributed to the fact that the cells in the control culture were in their late exponential phase and cell sorting may have forced the cells on the verge of cell division to divide. This observation could have been verified further with microscope pictures but was not feasible at that time.
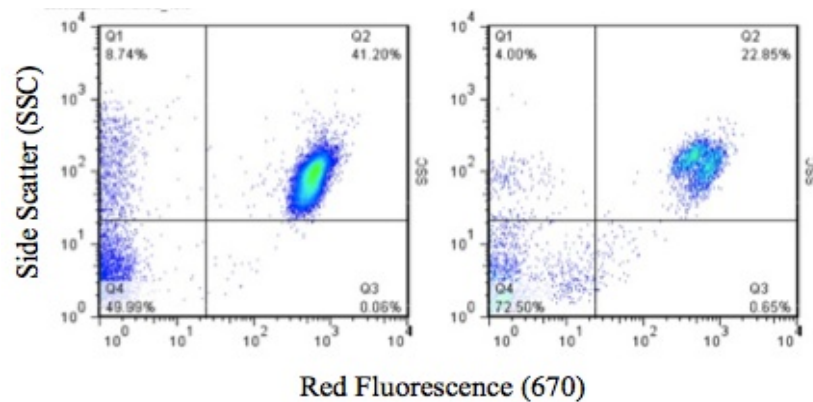
Figure 6.20 The cytogram on the left shows the control cell population at 72 h before cell sorting and on the right, the cytogram represents the control cell population after cell sorting as seen from side scatter (SSC) v/s red fluorescence (670).

6.3.5 DMSP content in sorted cells

After sorting cells based on fluorescence emissions, decreases in intracellular DMSP concentrations and per cell DMSP amounts were observed in the paraquat sorted cell populations (Fig. 6.21 and 6.22). The paraquat-exposed cells seem to have lower DMSP levels exactly as seen in the DMSP bulk measurements (Fig. 6.11 and 6.12). The major difference between figures 6.21 and 6.22 is the number of cells sorted and the 'type' of cell volume values used in deriving the intracellular DMSP concentration and DMSP per cell amount. The 'type' of cell volume values essentially means cell volume before cell sorting or cell volume after cell sorting.

In figure 6.21, 1.5×10^6 cells were sorted and the cell volume was measured on the Coulter counter after sorting. This may account for the higher intracellular DMSP values

seen in figure 6.21(a). In figure 6.22, 1.0 x 10^6 cells were sorted and the cell volume used in deriving intracellular DMSP was taken before the cells were sorted. The difference in cell volume after sorting (see section 6.3.4) resulted in magnified values of intracellular DMSP, whereas DMSP per cell and DMSP (µM) values were not hugely affected.
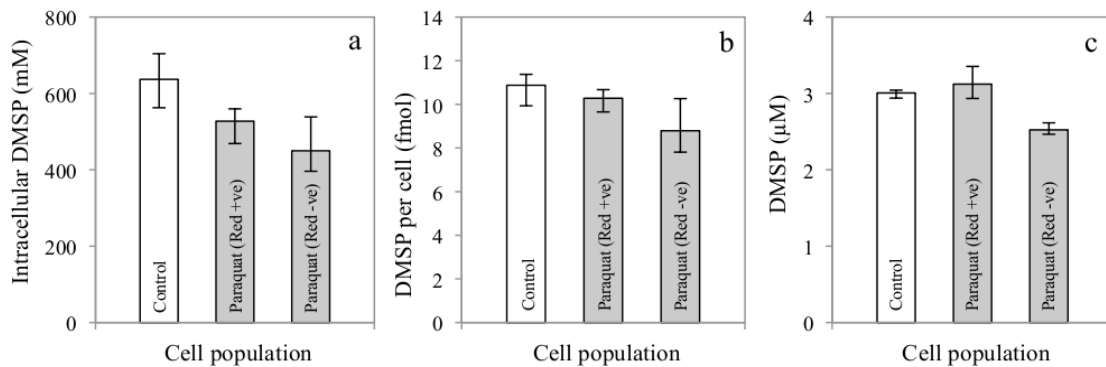
Figure 6.21 DMSP content in sorted *E. huxleyi* 1516 cells. (a) Intracellular DMSP (mM) is derived from cell volume values after sorting (b) DMSP per cell (fmol) and (c) DMSP (µM). Here 1.5 x 10^6 cells were sorted. The white and the grey bars denote the average value for the control and paraquat-exposed cell populations respectively. The error bars show the range of data (n=3).
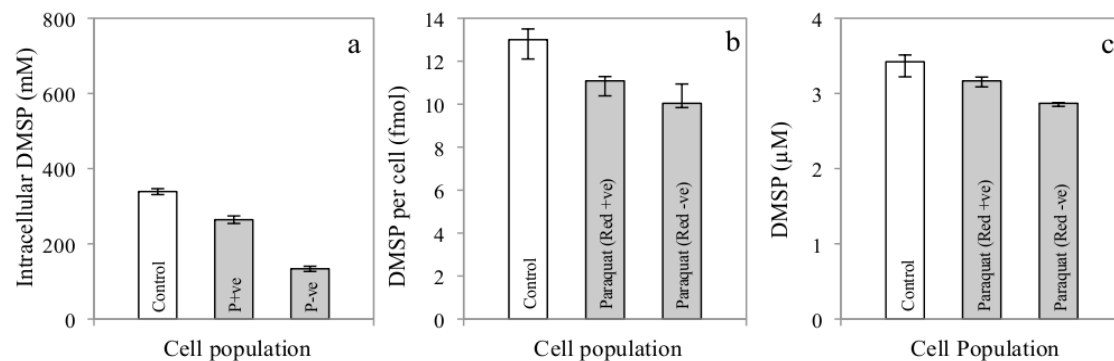
Figure 6.22 DMSP content in sorted *E. huxleyi* 1516 cells. (a) Intracellular DMSP (mM) is derived from cell volume values before sorting (b) DMSP per cell (fmol) and (c) DMSP (µM). Here 1.0 x 10^6 cells were sorted. The white and the grey bars denote the average value for the control and paraquat-exposed cell populations respectively. The error bars show the range of data (n=3).

6.3.6 Re-growth experiment

An aliquot of paraquat-exposed cells from *E. huxleyi* 370, 373 and 1516 was dispensed in fresh f/2-Si media after 72 h. Figure 6.23 shows that cells began to grow normally in terms of cell numbers and cell volume quickly dropped to a normal range. DMSP concentrations seem to increase to its normal concentrations. This was a small test to establish that paraquat was not killing the cells and that some cells were in a state to re-grow when normal conditions returned.
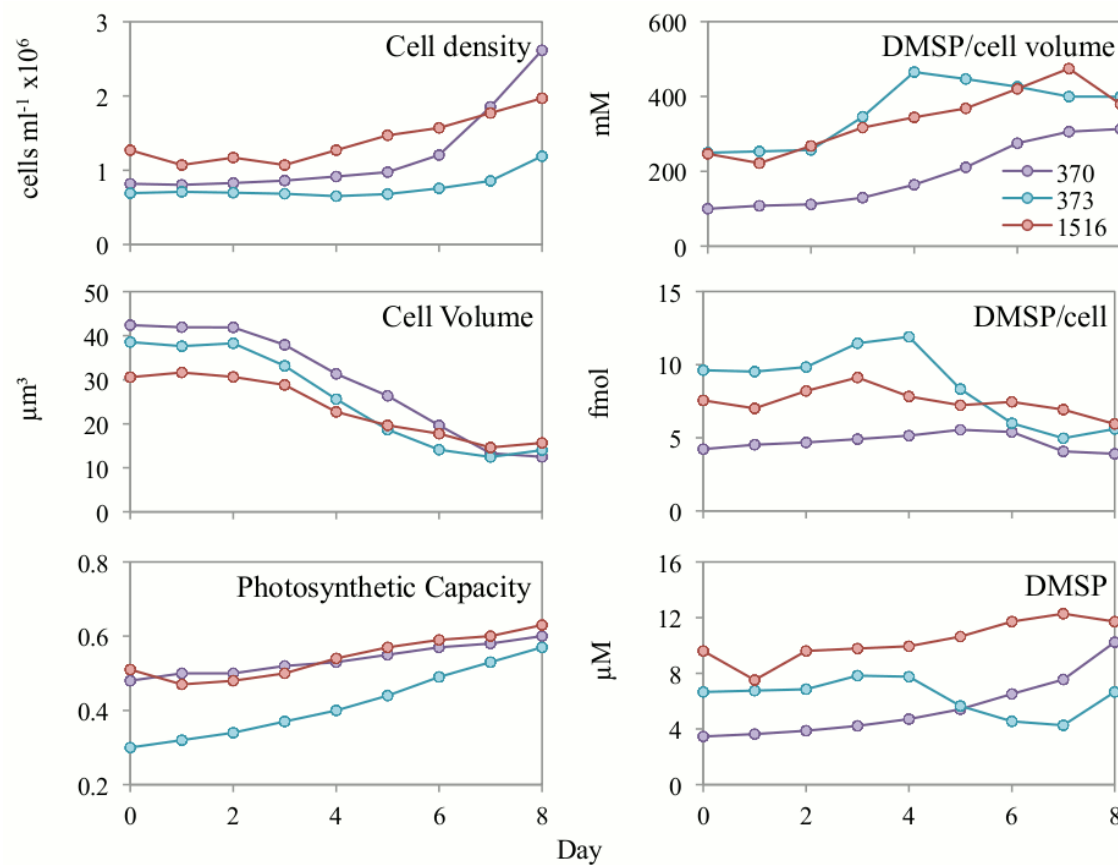
Figure 6.23 Influence of paraquat-exposed cells of *E. huxleyi* 370, 373 and 1516 dispensed in fresh media after 72 h on cell density, cell volume, photosynthetic capacity and DMSP concentrations. The purple, blue and red lines show average values and represents *E. huxleyi* 370, 373 and 1516 respectively.

6.3.7 Hydrogen peroxide measurements

Hydrogen peroxide (H_2O_2) analyses were done to give a measure of oxidative stress in paraquat-exposed cultures. A clear increase was seen in H_2O_2 in the medium of the

paraquat-exposed culture over the 72 h time series. The first 3 hours did not show any distinct variation in H_2O_2 between the control and paraquat-exposed cultures (Fig. 6.24). It may be noted that with the increasing cell numbers in the control culture, the H_2O_2 excretions actually decreased suggesting that either production slowed or there was an increased chemical loss of H_2O_2.
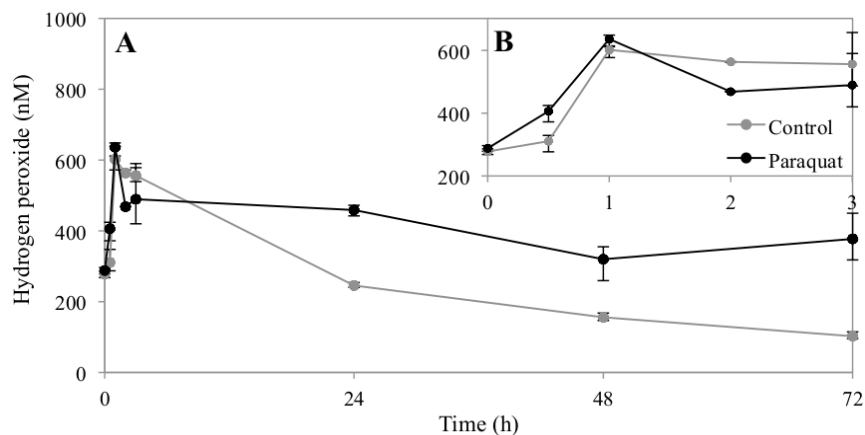
Figure 6.24 Hydrogen peroxide (H_2O_2) excretion in *E. huxleyi* 1516 exposed to 1 mM paraquat. Plot B is the magnified view of the first 3 hours of the time course. The grey line denotes the control (not exposed to paraquat) and the black line denotes the paraquat-exposed culture. The average value and range of data is shown (n=3). Where no range bars are visible, the data range was smaller than the symbol size.

6.3.8 Reaction between DMSP and paraquat

The flask containing 60 µM DMSP showed a decrease in DMSP concentrations over a period of 5 days (Fig. 6.25). This must be due to bacterial breakdown of DMSP to DMS or DMSP uptake occurring over the 5-day period. However, the flask containing 1 mM paraquat + DMSP did not show the same decrease in DMSP, suggesting that paraquat is not responsible for breaking down a DMSP molecule and that probably paraquat has anti-bacterial properties. In the sterile tubes there was no decrease in the DMSP concentration over 5 days. It can be concluded that the decrease in DMSP concentrations observed and reported in this study are not due to any reaction with paraquat.
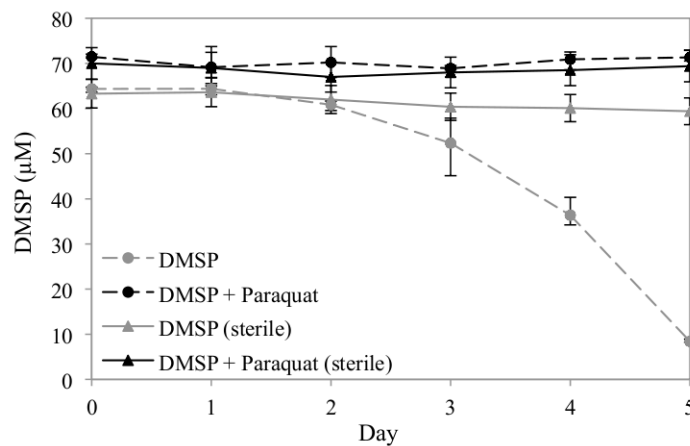
Figure 6.25 Testing for potential reaction of DMSP with paraquat. The grey solid and dotted lines are the control DMSP solution without paraquat and the black solid and dotted line represents the DMSP + paraquat. The circle symbols denote the reaction in the presence of bacteria and the triangle symbols denotes sterile conditions. The average values are shown and error bars represent the range of data (n=3). Where no error bars are seen, the data range was smaller than the symbol size.

6.4 Discussion

In this study, paraquat was used to catalyze the formation of reactive oxygen species (ROS) in the presence of light and oxygen thus causing oxidative stress on the photosynthetic nanoeukaryote *Emiliania huxleyi* strains CCMP 370, 373 and 1516. The objective was to artificially induce oxidative stress in order to test the proposed link between oxidative stress and DMSP metabolism. One mM Paraquat was chosen as the effective concentration (effective concentration being the concentration of a substance that causes a defined magnitude of response in a given system). Here *E. huxleyi* was exposed to various concentrations of paraquat ranging from 0.05 to 5 mM for 24 hours and a reduction in cell number and increase in cell volume was seen. Such growth inhibition is also seen in the freshwater microalga *Chlamydomonas eugametos* when it is exposed to paraquat (Franqueira et al. 2000). The authors also further proposed that DMSP is oxidized during times of stress, such as that caused by natural tissue necrosis or by administration of an oxidative stressor such as paraquat. It has been widely reported that cell volume increases on exposure to paraquat. For example, Bray et al. (1993) studied the ultrastructure of *Chlamydomonas reinhardtii* after paraquat exposure

and explained that cells may appear swollen due to the incapacity to complete cell division and due to failures in regulation of cellular volume as a consequence of the high levels of oxidative radicals formed. They also explained that damage to the membranes of the contractile vacuole apparatus in these cells can result in water retention by the cell and hence cells appear swollen under the electron microscope.

In this study, up to ~ 30% of cells had compromised cell membranes after 72 h as indicated by SYTOX Green staining. Loss of membrane integrity during exposure to 1 mM paraquat has also been shown to occur in *E. huxleyi* CCMP 1516 (Evans 2004). On a 12-hourly basis in the time-series experiments, it was interesting to note that a high number of control cells were SYTOX Green stained and the cell volume was at its peak. This may be because larger cells are at their point of dividing the cell wall and membranes may stretch in such a way that the nucleic acid stain SYTOX Green, is able to penetrate the membrane. SYTOX Green stain is recommended as an indicator of dead cells (Brussaard et al. 2001; Lebaron et al. 1998; Roth et al. 1997) and is not supposed to cross the membranes of live cells (Roth et al. 1997; Veldhuis et al. 1997, 2001). However, the data presented here strongly suggests that viable cells in the state of division have permeable membranes (Fig. 6.10 and 6.11). At 24 h and 48 h within the assay, the number of live cells in the control culture increased and with most cells having already completed their division cycle, cells with compromised membranes are almost negligible. On the other hand, cells exposed to paraquat allow the SYTOX Green stain to access the cells because oxidative stress induces the production of reactive oxygen species (ROS), and with the production of superoxide radicals, hydrogen peroxide and hydroxyl radical (the most damaging of the ROS) they lose their membrane integrity. Chlorophyll *a* fluorescence (red fluorescence) also decreases with prolonged exposure to paraquat and this might be a deliberate adaptation to limit further ROS production.

In this study, there was no increase in intracellular DMSP (DMSPp) concentration or DMSPp per cell nor any increase in DMS levels. However, DMSPd was higher compared to the control. Overall, the total DMSP measurements were lower in the treated sample than in the control. Such an observation was also reported by Van Rijssel

and Buma (2002) when *E. huxleyi* strain L was subjected to UV light. Recently, an experiment using paraquat on the leaves of *Spartina alterniflora* (Smooth cordgrass) also did not result in DMSP synthesis nor accumulation but DMSO increased suggesting increased oxidation of DMSP to DMSO (Husband et al. 2012). Based on increased DMSPd levels observed in this study, it could be the case that DMSP may be immediately lysed to DMS, which is then quickly oxidized to DMSO, methane sulphinic acid and other products due to the over-production of free radicals under oxidative stress conditions. Perhaps, the rate at which DMSP lyases operate under oxidative stress may be strain-specific. Environmental stress is thought to increase the intracellular concentration of DMSP in several marine algae. Sunda et al. (2002) have shown increased intracellular DMSP in *E. huxleyi* 373 subjected to UV radiation, increased Cu ions, carbon dioxide limitation and iron deficiency. Intracellular DMSP and DMSO concentrations were also significantly higher in leaves of *Spartina alterniflora* when treated with paraquat than untreated control leaves suggesting that they may be able to rapidly increase synthesis of DMSP in response to oxidative stress (Kiene and Husband 2003).

Since paraquat inhibits cell growth it may be proposed that a few oxidatively stressed cells are upregulating DMSP and most cells are not, such that the elevation is masked. This idea was tested by flow cytometric cell sorting. At 72 h, the cells were sorted using a Cytopeia inFlux and a single cell population was identified for the control population, whereas the paraquat exposed cells had developed two distinct sub-populations distinguished by their relative amounts of red fluorescence. A pre-concentration step was necessary to reduce sorting time and achieve triplicate sorts. For this, two pre-concentration techniques were tested involving centrifugation and a filter well plate-concentration method. Out of the two, based on the flow cytometric data profiles, the plate-concentration method achieved the best results with the least loss of cells and no changes in cell fluorescence emissions. The centrifugation method caused cell losses, especially in the paraquat-exposed cells. Sorted cells based on fluorescence emissions showed no significant increase in intracellular DMSP concentrations and per cell DMSP amounts.

High concentrations of hydrogen peroxide indicated that oxidative stress was successfully induced. When paraquat exposed cells were transferred to fresh media, re-growth occurred and DMSP levels were in the normal range thus establishing the fact that paraquat was not causing total mortality and that some cells were in a suitable physiological state for re-growth when normal conditions were returned.

6.5 Conclusions

The data suggest that, contrary to the hypothesis of Sunda et al 2002, oxidative stress does not always result in increased DMSPp concentration in *E. huxleyi*. Alternatively there is a balance between enhanced DMSP production and its use as an antioxidant in cells under oxidative stress.

Chapter 7

General Discussion and Conclusions

Chapter 7: General Discussion and Conclusions

7.1 Summary

This thesis describes the influence of stress conditions on intracellular dimethylsulphoniopropionate (DMSP) and dimethylsulphide (DMS) release in *Emiliania huxleyi*. With the opportunity to work on a diatom species and three different strains of *E. huxleyi*, the data also highlights the observation that the response to stress conditions varied between diatoms and coccolithophores (Chapter 3) and within the *E. huxleyi* strains (Chapters 3 to 6).

Cells were examined in batch cultures during nutrient limitation, exposure to artificial UV radiation, natural solar radiation, under light deprivation and with the application of the herbicide paraquat (also known as methyl viologen). In response to these stress conditions, *E. huxleyi* cells demonstrated cell growth arrest (no increase in cell number) and on return to normal conditions, regrowth and recovery of the cells occurred. This has been a key outcome of the physiological mechanisms that *E. huxleyi* uses to cope with environmental stress.

The major findings of this project include the transformation of particulate DMSP (DMSPp) to dissolved DMSP (DMSPd), with the release of DMS and loss of total DMSP (DMSPt) under stress conditions. This would suggest how rapidly DMSP or DMS is 'exuded' when cell lysis occurs. However within this study, although various severe, but ecologically important physiological stresses were applied, mass cell membrane lysis leading to mass cell death did not occur. This outcome strongly suggests DMSP metabolism as part of the stress response of *E. huxleyi* from cells that had intact cell membranes and were therefore viable, perhaps indicating active exudation under light deprivation and on exposure to solar radiation.

7.2 Discussion

Very little is known about cell survival mechanisms in unicellular organisms. *E. huxleyi* are particularly important DMSP producers among pelagic unicellular algae, as they form large blooms during spring and summer (Malin et al. 1993; Marandino et al. 2008; Oguz and Merico 2006). There are several field studies reporting high DMS levels associated with blooms (Holligan et al. 1993a; Malin et al. 1993; Matrai and Keller 1993), but what controls the conversion of DMSP to DMS in *E. huxleyi* is not fully understood. DMS and acrylic acid are formed in *E. huxleyi* by a group of isozymes known as DMSP lyases, which are naturally present in DMSP-producing phytoplankton (Steinke et al. 1998) but what triggers the DMSP lyase activity has not been adequately investigated. Various studies document changes in intracellular DMSP (DMSPp per cell volume) concentration under stress conditions for several phytoplankton species and strains, but results are not always consistent.

Here in all of the stress conditions, cells of *E. huxleyi* 370, 373 and 1516 underwent cell growth arrest but varied in other physiological responses (Table 7.1). Cell volume increased in N- and P-limitation, on exposure to UV and in herbicide-induced oxidative stress in all three strains. This increased cell volume and cell growth arrest may indicate metabolic activity but no cellular division. Exposure to solar radiation did not show a change in cell volume in all three strains and light deprivation resulted in no change in *E. huxleyi* 370, while a decrease in *E. huxleyi* 370 and 1516. In addition, under stress conditions, a decrease in photosynthetic capacity ($F_V:F_M$; photosynthetic efficiency of the PSII) was observed (Table 7.1), which is known to be a sensitive parameter indicating physiological stress (Suggett et al. 2009). However, under nutrient limiting conditions no change in photosynthetic capacity was seen in the three *E. huxleyi* strains, also reported in *E. huxleyi* 1516 in Franklin et al. (2012).

A decrease in intracellular DMSP concentration (DMSPp per cell volume) was seen with exposure to UV radiation in all three strains and under N- and P-limitation in *E. huxleyi* 370 and 373 with no change in *E. huxleyi* 1516, whereas it increased on exposure to solar radiation in all three strains (Table 7.2). Light-deprived cultures also

showed a substantial increase in intracellular DMSP and DMS after ~ 5 days in all three strains. Paraquat addition (1 mM), which promotes the formation of reactive oxygen species, resulted in up to ~ 30% of cells with compromised membranes after 72 h (SYTOX Green staining) in all three strains. Flow cytometry revealed two cell sub-populations in paraquat-treated cells on the basis of red fluorescence and these were sorted in the case of *E. huxleyi* 1516 and analysed but no increase in intracellular DMSP concentration was seen. The data suggest that stress does not always result in increased intracellular DMSPp concentration in *E. huxleyi*. In all of the above stress treatments, it was interesting to observe a decrease in DMSPp culture concentrations emphasising the decrease observed in the DMSPt culture concentrations (excluding UVR exposure-DMSPt data not collected) with increasing DMSPd and DMS concentrations (Table 7.2).

Table 7.1 Comparing the physiological growth responses in *E. huxleyi* 370, 373 and 1516 to various stress conditions. The dark grey shade denotes 'an increase', the medium grey shade denotes 'no change' and the light grey shade denotes 'a decrease'. Numbers inserted in every box represents the number of times the experiments were conducted.

	E. huxleyi 370						*E. huxleyi* 373						*E. huxleyi* 1516					
	N-limitation	P-limitation	UV exposure	Solar Radiation	Light deprivation	Paraquat exposure	N-limitation	P-limitation	UV exposure	Solar Radiation	Light deprivation	Paraquat Exposure	N-limitation	P-limitation	UV exposure	Solar Radiation	Light deprivation	Paraquat exposure
Cell density (cells ml⁻¹)	3	3	3	1	3	3	3	3	3	1	3	3	3	3	3	1	5	14
Cell volume (µm³)	3	3	3	1	3	3	3	3	3	1	3	3	3	3	3	1	5	14
Fluorescence (a.u.)	3	3	3	1	3	3	3	3	3	1	3	3	3	3	3	1	5	14
Photosynthetic capacity	3	3	3	1	3	3	3	3	3	1	3	3	3	3	3	1	5	14
Compromised cells (%)	3	3	3	1	3	3	3	3	3	1	3	3	3	3	3	1	5	14

Table 7.2 Comparing the effect of various stresses on DMSP and DMS concentrations in *E. huxleyi* 370, 373 and 1516. The dark grey shade denotes 'an increase', the medium grey shade denotes 'an almost equal to' and the light grey shade denotes 'a decrease' in values compared to the control cultures. Numbers inserted in every box represents the number of times the experiments were conducted. Boxes without numbers show expected data based on findings within this work or results from published literature.

		E. huxleyi 370						*E. huxleyi* 373						*E. huxleyi* 1516					
		N-limitation	P-limitation	UV exposure	Solar Radiation	Light deprivation	Paraquat exposure	N-limitation	P-limitation	UV exposure	Solar Radiation	Light deprivation	Paraquat Exposure	N-limitation	P-limitation	UV exposure	Solar Radiation	Light deprivation	Paraquat exposure
DMSPp	Intracellular (mM)	3	3	3	1	3	3	3	3	3	1	3	3	3	3	3	1	5	14
	Cellular (fmol)	3	3	3	1	3	3	3	3	3	1	3	3	3	3	3	1	5	14
	Culture (µM)	3	3	3	1	3	3	3	3	3	1	3	3	3	3	3	1	5	14
DMSPd	Intracellular (mM)	2	2			2		2	2			2		3	3			3	5
	Cellular (fmol)	2	2			2		2	2			2		3	3			3	5
	Culture (µM)	2	2			2		2	2			2		3	3			3	5
DMS	Intracellular (mM)	2	2			2		2	2			2		3	3			3	5
	Cellular (fmol)	2	2			2		2	2			2		3	3			3	5
	Culture (µM)	2	2			2		2	2			2		3	3			3	5
DMSPt	Intracellular (mM)	2	2			2		2	2			2		3	3			3	5
	Cellular (fmol)	2	2			2		2	2			2		3	3			3	5
	Culture (µM)	2	2			2		2	2			2		3	3			3	5

Various theories have been proposed for the physiological roles of DMSP and DMS and the environmental factors that regulate their production in marine algae, though most remain unverified. In this project, I have reconsidered the recently proposed antioxidant role for DMSP and its cleavage product DMS. Sunda et al. (2002) suggested the antioxidant function of the DMSP system, based on elevated concentrations of intracellular DMSP under stress conditions. Intracellular DMSP increased under N, P, Si and CO_2 limitations, in the coastal diatom *Thallassiosira pseudonana* (Bucciarelli and Sunda 2003)*,* under Fe limitation in *Phaeocystis* species (Stefels and Van Leeuwe 1998) and in *E. huxleyi* on exposure to solar UV radiation (Sunda et al. 2002), artificial UV radiation (Archer et al. 2010), high Cu^{+2} and H_2O_2 (Sunda et al. 2002). But, no change in

intracellular DMSP concentrations and little or no dissolved DMSP was reported for *E. huxleyi* CCMP 374 under nitrogen limitation although DMSP lyase activity increased, resulting in elevated DMS concentrations, thus upholding the antioxidant function for the DMSP system (Sunda et al. 2007). Stefels et al. (2007) argues that DMSP would be expected to decline while mopping up the reactive oxygen species. She further adds that if the stress reaction results in increased de novo synthesis (up-regulation) of DMSP then, a subsequent overshoot production of DMSP would lead to increased intracellular concentrations of DMSP and/or one of the breakdown products. Such an overshoot production in intracellular DMSP and DMSP per cell was observed in *E. huxleyi* under light deprivation and on exposure to solar radiation. But total DMSP in the culture remained low in comparison to the control culture. It may be highlighted that among all stress treatments, higher number of cells with compromised cell membranes was noted with exposure to solar radiation and under light-deprived conditions (up to 50% compromised cells in *E. huxleyi* 373 and up to 70% in *E. huxleyi* 370 and 1516 after 72 h exposure to solar radiations, while 40%, 50% and 20% compromised cells in *E. huxleyi* 370, 373 and 1516 respectively after 10 days of light deprivation).

The data displays elevated concentrations of the cleavage product DMS with a decline in intracellular concentrations of DMSP in *E. huxleyi* under N-limitation and P-limitation, suggesting support for the antioxidant function of the DMSP system but the decrease in total DMSP raises doubt, although the only explanation here for a loss in total DMSP would be the involvement of the DMSP system in effectively scavenging the harmful radicals resulting in its loss or breakdown.

Also in another attempt to enhance oxidative stress (demonstrated by elevated concentrations of H_2O_2 – Chapter 6, section 6.3.7) in *E. huxleyi* cells, with the use of the herbicide paraquat, a decrease in intracellular DMSP and DMS was repeatedly observed. So also, the work of sorting based on fluorescence clearly showed a decrease in intracellular DMSP concentrations in the sub-populations of paraquat-induced oxidative stressed cells. This may have occurred due to the possible rapid oxidation of DMS to dimethylsulphoxide (DMSO) or other oxidised sulphur species. DMSO is a more effective antioxidant (Lee and De Mora 1999) than the proposed DMSP (Sunda et al.

2002) and is found in the chloroplast (Jakob and Heber 1996). The DMSP data here shows a consistent increase in dissolved DMSP also reported by Archer et al. (2010) and a consistent decrease in total DMSP in the culture under stress conditions, which might suggest an alternative role or additional explanation to the antioxidant function of the DMSP system.

7.3 Alternative explanations

Advanced research in this field with cutting-edge technologies have broadened our insight into the various processes taking place in a cell but hypothesis put forward on the phytoplankton cell survival pathways and cell death processes remain as non-established facts. In these experiments, re-growth or recovery of the cells occurred after prolonged periods of stress and a higher percentage of *E. huxleyi* cells had intact cell membranes although challenged with oxidative stress. This would reveal DMSP as a cellular response to stress implying that DMSP acts as a signalling molecule exuded by cells afflicted by stress to the nearby viable or cells with intact membrane.

Under stress conditions, not all cells would react at the same time and in the same way but would have different responses and response times based on the extent of the stress. In all of the stress treatments here, DMSPd per cell volume, DMSPd per cell and DMSPd in the culture increased as a function of time, which may have occurred from the lysed cells and the small percentage of cells with compromised cell membranes revealed by SYTOX Green staining. This transformation of the DMSP content to DMSPd within these cells with compromised cell membranes is due to the antioxidant mechanism to scavenge the enhanced ROS. The DMSPd released out of the cells accompanied by DMS from these cells with compromised membranes extends out to the neighbouring cells warning them of stress. This response of elevated DMSPd and DMS by the stressed cells triggers defence mechanisms in other non-stressed cells to stay on guard to protect the photosynthetic apparatus in the chloroplast. This is reflected in the photosynthetic capacity of the cells. The cells increase in cell volume but refrain from cell division in order to conserve cellular energy. In this way, DMSPd and DMS

function as a signalling molecule to other cells not directly affected by the stress and subsequently survive and re-grow or recover when normal conditions return.

7.4 Limitations and suggestions for further research

Cell sorting based on fluorescence has been a new technique used in this study and more research and development would be necessary to optimise the technique. Cell sorting can have effects on the cell volume as shown in Chapter 6, section 6.3.4, therefore it would be necessary to devise a method by which sorting would have minimum effects on cell volume. So also, a thorough study would be advisable to list other physiological changes related to the sorting technique.

Another observation noted after the cells were being sorted, was the development of two populations distinguishable from each other in the control cell population, although their emissions remained the same in side scatter (Chapter 6, section 6.3.4, Fig. 6.20). This may be attributed to the fact that the cells in the control culture were in their late exponential phase and cell sorting may have forced the cells on the verge of cell division to divide. This observation could not be verified further with microscope pictures as it was not feasible at that time, but it would be necessary to know if the sorting technique also results in forcibly splitting cells on the verge of cell division or simply to learn that cell sorting technique can also be used to sort cells at the point of division.

Measuring DMSP lyase activity in sorted and non-sorted cells would be an interesting observation for future research. On sorting the physiologically stressed cells based on fluorescence, if an increase in DMSP lyase activity is measured, then it can proposed that DMSP lyases are involved in cellular protection against oxidative stress. This will also provide explanation of the decrease in intracellular DMSP and the viability of the cells of *E. huxleyi*.

Filtration of cells under gentle vacuum pressure for particulate DMSP may result in loss of intracellular DMSP caused by cell lysis, which also explains the increased DMSPd. But this was not the case here, as the total DMSP in the culture was found to be low in comparison with the control cultures. It would be generally very important to devise a

new method for filtration of the cells to avoid filtration artefacts when quantifying intracellular DMSP or per cell DMSP as discussing processes within a cell would require accurate measurements. Sunda et al. (2002) have reported elevated intracellular DMSP concentrations in *E. huxleyi* under CO_2 limitation using gravity filtration with a small filtration volume of $1 - 2$ ml.

During the herbicide-induced stress, on *E. huxleyi* 1516, DMS was not observed unlike under N- and P-limitations and light-deprivation. It is hypothesised that DMS may have been oxidised to DMSO. If this were the case, it would be relatively important to measure and quantify the concentrations of DMSO. If conversion of DMS to DMSO actually took place, it would raise questions if the other strains also showed a decrease in DMS or an increase.

ROS quantification is another very important measurement when discussing oxidative stress. Flow cytometry combined with fluorescent stains and other intracellular ROS stains could be applied to determine the other oxidative species besides hydrogen peroxide.

In the 48 h time-series paraquat exposure experiments (Chapter 6, section 6.3.2.2), SYTOX Green measurements on a 12-hourly basis, showed a high number of control cells being labeled and the cell volume was also high. This may explain that when viable cells are at the point of division, the membranes may stretch in such a way that the nucleic acid stain SYTOX Green, is able to penetrate the membrane. SYTOX Green stain is recommended as an indicator of dead cells (Brussaard et al. 2001; Lebaron et al. 1998; Roth et al. 1997) and is not supposed to cross the membranes of live cells (Roth et al. 1997; Veldhuis et al. 1997, 2001). However, the data presented here strongly suggests that viable cells in the state of division have permeable membranes (Fig. 6.10 and 6.11). This needs further testing with live stain indicators like the CMFDA stain used in Franklin et al. 2012.

7.5 Conclusions

It can be concluded that environmental stress does not always increase intracellular DMSP and DMS concentration in *Emiliania huxleyi* and that responses to stress can be species-specific and strain-specific. This may indicate that DMSP and its breakdown product DMS may not always act as an antioxidant system. Alternatively, there is a balance between enhanced DMSP production and its use as an antioxidant in cells under oxidative stress. Thus the work presented in this thesis refutes the hypothesis presented in Chapter 1 (section 1.7).

References

Ackman RG, Dale J, Hingley J (1966) Deposition of dimethyl-β-propiothetin in Atlantic cod during feeding experiments. Journal of the Fisheries Research Board of Canada 23: 487-497

Affenzeller MJ, Darehshouri A, Andosch A, Lutz C, Lutz-Meindl U (2009) Salt stress-induced cell death in the unicellular green alga *Micrasterias denticulata*. Journal of Experimental Botany 60: 939-954

Agusti S, Satta MP, Mura MP, Benavent E (1998) Dissolved esterase activity as a tracer of phytoplankton lysis: Evidence of high phytoplankton lysis rates in the northwestern Mediterranean. Limnology and Oceanography 43: 1836-1849

Al-Hasan RH, Hantash FM, Radwan SS (1991) Enriching marine macroalgae with eicosatetraenoic (arachidonic) and eicosapentaenoic acids by chilling. Applied Microbiology and Biotechnology 35: 530-535

Allakhverdiev SI, Kreslavski VD, Klimov VV, Los DA, Carpentier R, Mohanty P (2008) Heat stress: an overview of molecular responses in photosynthesis. Photosynthesis Research 98: 541-550

Allakhverdiev SI, Murata N (2004) Environmental stress inhibits the synthesis de novo of proteins involved in the photodamage-repair cycle of photosystem II in *Synechocystis* sp. PCC 6803. Biochimica et Biophysica Acta 1657: 23-32

Andreae MO (1985) Dimethylsulfide in the water column and the sediment porewaters of the Peru upwelling area. Limnology and Oceanography 30: 1208-1218

Andreae MO (1986) The ocean as a source of atmospheric sulfur compounds. In: P. B-M (ed) The role of air-sea exchange in geochemical cycling. Rcidel, Dordrecht pp 331-362

Andreae MO (1990) Ocean-atmosphere interactions in the global biogeochemical sulfur cycle. Marine Chemistry 30: 1-29

Andreae MO, Barnard WR (1984) The marine chemistry of dimethylsulfide. Marine Chemistry 14: 267-279

Andreae MO, Raemdonck H (1983) Dimethyl sulfide in the surface ocean and the marine atmosphere: a global view. Science 221: 744-747

Anning T, MacIntyre HL, Pratt SM, Sammes PJ, Gibb S, Geider RJ (2000) Photoacclimation in the marine diatom *Skeletonema costatum*. Limnology and Oceanography 45: 1807-1817

Antia NJ, Harrison PJ, Oliveira L (1991) The role of dissolved organic nitrogen in phytoplankton nutrition, cell biology and ecology. Phycologia 30: 1-89

Apel K, Hirt H (2004) Reactive oxygen species: Metabolism, oxidative stress, and signal transduction. Annual Review of Plant Biology 55: 373-399

Aravind L, Dixit VM, Koonin EV (2001) Apoptotic Molecular Machinery: Vastly increased complexity in vertebrates revealed by genome comparisons. Science 291: 1279-1284

Archer SD, Ragni M, Webster R, Airs RL, Geider RJ (2010) Dimethyl sulfoniopropionate and dimethyl sulfide production in response to photoinhibition in *Emiliania huxleyi*. Limnology and Oceanography 55: 1579-1589

Archer SD, Widdicombe CE, Tarran GA, Rees AP, Burkill PH (2001) Production and turnover of particulate dimethylsulponiopropionate during a coccolithophore bloom in the northern North Sea. Aquatic Microbial Ecology 24: 225-241

Aro E-M, Virgin I, Andersson B (1993) Photoinhibition of photosystem II. Inactivation, protein damage and turnover. Biochimica et Biophysica Acta (BBA) - Bioenergetics 1143: 113-134

Arsalane W, Rousseau B, Duval J-C (1994) Influence of the pool size of the xanthophyll cycle on the effects of light stress in a diatom: competition between photoprotection and photoinhibition. Photochemistry and Photobiology 60: 237-243

Asada K (1999) The water-water cycle in chloroplasts: Scavenging of active oxygens and dissipation of excess photons. Annual Review of Plant Physiology and Plant Molecular Biology 50: 601-639

Asada K, Takahashi M (1987) Production and scavenging of active oxygen in photosynthesis. In: Kyle DJ, Osmond CB, Arntzen CJ (eds) Photoinhibition. Elsevier, Amsterdam, pp 228-287

Ayers GP, Cainey JM (2007) The CLAW hypothesis: A review of the major developments. Environmental Chemistry 4: 366-374

Ayers GP, Gillett RW (2000) DMS and its oxidation products in the remote marine atmosphere: implications for climate and atmospheric chemistry. Journal of Sea Research 43: 275-286

Balch WM, Drapeau DT, Bowler BC, Lyczskowski E, Booth ES, Alley D (2011) The contribution of coccolithophores to the optical and inorganic carbon budgets during the Southern Ocean gas exchange experiment: New evidence in support of the "Great Calcite Belt" hypothesis. Journal of Geophysical Research 116: C00F06

Balseiro E, Sol Souza M, Modenutti B, Reissig M (2008) Living in transparent lakes: Low food P : C ratio decreases antioxidant response to ultraviolet radiation in *Daphnia*. Limnology and Oceanography 53: 2383-2390

Barnard WR, Andreae MO, Iverson RL (1984) Dimethylsulfide and *Phaeocystis poucheti* in the southeastern Bering Sea. Continental Shelf Research 3: 103-113

Barnes R, Hughes R (1999) An Introduction to Marine Ecology

Bates TS, Cline JD, Gammon RH, Kelly-Hansen SR (1987) Regional and seasonal variations in the flux of oceanic dimethylsulfide to the atmosphere. Journal of Geophysical Research 92: 2930-2938

Bates TS, Quinn PK (1997) Dimethylsulfide (DMS) in the equatorial Pacific Ocean (1982 to 1996): Evidence of a climate feedback? Geophysical Research Letters 24: 861-864

Baumann K-H (2004) Importance of size measurements for coccolith carbonate flux estimates. Micropaleontology 50: 35-43

Baumann MEM, Brandini FP, Staubes R (1994) The influence of light and temperature on carbon-specific DMS release by cultures of *Phaeocystis antarctica* and three Antarctic diatoms. Marine Chemistry 45: 129-136

Bayne BL 1975 Proceedings of the Ninth European Marine Biology Symposium 213-238

Beardall J, Roberts S, Raven JA (2005) Regulation of inorganic carbon acquisition by phosphorus limitation in the green alga *Chlorella emersonii*. Canadian Journal of Botany 83: 859-864

Beardall J, Sobrino C, Stojkovic S (2009) Interactions between the impacts of ultraviolet radiation, elevated CO2, and nutrient limitation on marine primary producers. Photochemical and Photobiological Sciences 8: 1257-1265

Behrenfeld MJ, Hardy JT, Lee HI (1992) Chronic effects of ultraviolet-B radiation on growth and cell volume of *Phaeodactylum* (Bacillariophyceae). Journal of Phycology 28: 757-760

Behrenfeld MJ, O'Malley RT, Siegel DA, McClain CR, Sarmiento JL, Feldman GC, Milligan AJ, Falkowski PG, Letelier RM, Boss ES (2006) Climate-driven trends in contemporary ocean productivity. Nature 444: 752-755

Belviso S, Kim S-K, Rassoulzadegan F, Krajka B, Nguyen BC, Mihalopoulos N, Buat-Ménard P (1990) Production of dimethylsulfonium propionate (DMSP) and dimethylsulfide (DMS) by a microbial food web. Limnology and Oceanography 35: 1810-1821

Berg G, Thoms S, LaRoche J (2005) Identification of genes encoding components of the autophagic machinery in the unicellular marine eukaryotic phytoplankton *Aureococcus anophagefferens*

Berges JA, Falkowski PG (1998) Physiological stress and cell death in marine phytoplankton: induction of proteases in response to nitrogen or light limitation. Limnology and Oceanography 43: 129-135

Berges JA, Franklin DJ, Harrison PJ (2001) Evolution of an artificial seawater medium: Improvements in enriched seawater, artificial water over the last two decades. Journal of Phycology 37: 1138-1145

Berges JA, Franklin DJ, Harrison PJ (2004) Corrigendum: Evolution of an artificial seawater medium: Improvements in enriched seawater, artificial water over the last two decades. Journal of Phycology 40: 619-619

Berman-Frank I, Bidle KD, Haramaty L, Falkowski P (2004) The demise of the marine cyanobacterium, *Trichodesmium* spp., via an autocatalyzed cell death pathway. Limnology and Oceanography 49: 997-1005

Berman-Frank I, Rosenberg G, Levitan O, Haramaty L, Mari X (2007) Coupling between autocatalytic cell death and transparent exopolymeric particle production in the marine cyanobacterium *Trichodesmium*. Environmental Microbiology 9: 1415-1422

Bertrand EM, Saito MA, Lee PA, Dunbar RB, Sedwick PN, DiTullio GR (2011) Iron limitation of a springtime bacterial and phytoplankton community in the Ross Sea: implications for vitamin B12 nutrition. Frontiers in Microbiology 2

Bidle KD, Bender SJ (2008) Iron starvation and culture age activate metacaspases and programmed cell death in the marine diatom *Thalassiosira pseudonana*. Eukaryotic Cell 7: 223-236

Bidle KD, Falkowski PG (2004) Cell death in planktonic, photosynthetic microorganisms. Nature Reviews in Microbiology 2: 643-655

Bidle KD, Haramaty L, Barcelos ERJ, Falkowski P (2007) Viral activation and recruitment of metacaspases in the unicellular coccolithophore, *Emiliania huxleyi*. Proceedings of the National Academy of Sciences of the United States of America 104: 6049-6054

Björn LO, Callaghan TV, Gehrke C, Johanson U, Sonesson M, Gwynn-Jones D (1998) The problem of ozone depletion in northern Europe. Ambio 27: 275-279

Bjornsen PK (1988) Phytoplankton exudation of organic matter: Why do healthy cells do it? Limnology and Oceanography 33: 151-154

Boelen P, Obernostere I, Vink AA, Buma AGJ (1999) Attenuation of biologically effective UV radiation in tropical Atlantic waters measured with a biochemical DNA dosimeter. Photochemistry and Photobiology 69: 34-40

Bonadonna F, Caro S, Jouventin P, Nevitt GA (2006) Evidence that blue petrel, *Halobaena caerulea*, fledglings can detect and orient to dimethyl sulfide. Journal of Experimental Biology 209: 2165-2169

Bonilla S, Conde D, Blanck H (1998) The photosynthetic responses of marine phytoplankton, periphyton and epipsammon to the herbicides paraquat and simazine. Ecotoxicology 7: 99-105

Bouchard JN, Campbell DA, Roy S (2005) Effects of UV-B radiation on the D1 protein repair cycle of natural phytoplankton communities from three latitudes (Canada, Brazil, and Argentina). Journal of Phycology 41: 273-286

Boyce DG, Lewis MR, Worm B (2010) Global phytoplankton decline over the past century. Nature 466: 591-596

Boyd P, LaRoche J, Gall M, Frew R, McKay RML (1999) Role of iron, light, and silicate in controlling algal biomass in subantarctic waters SE of New Zealand. Journal of Geophysical Research 104: 13395-13408

Bozhkov PV, Smertenko AP, Zhivotovsky B (2010) Aspasing out metacaspases and caspases: proteases of many trades. Science signaling 3: pe48

Braga GUL, Rangel DEN, Flint SD, Miller CD, Anderson AJ, Roberts DW (2002) Damage and recovery from UV-B exposure in conidia of the entomopathogens *Verticillium lecanii* and *Aphanocladium album*. Mycologia 94: 912-920

Bratbak G, Egge JK, Heldal M (1993) Viral mortality of the marine alga *Emiliania huxleyi* (Haptophyceae) and the termination of the algal bloom. Marine Ecology Progress Series 93: 39-48

Bratbak G, Levasseur M, Michaud S, Cantin G, Fernández E, Heimdal BR, Heldal M (1995) Viral activity in relation to *Emiliania huxleyi* blooms: a mechanism of DMSP release? Marine Ecology Progress Series 128: 133-142

Braven J, Evens R, Butler EI (1984) Amino acids in sea water. Chemistry and Ecology 2: 11-21

Bray DF, Bagu JR, Nakamura K (1993) Ultrastructure of *Chlamydomonas reinhardtii* following exposure to paraquat: comparison of wild type and a paraquat-resistant mutant. Canadian Journal of Botany 71: 174-182

Brimblecombe P, Shooter D (1986) Photo-oxidation of dimethylsulphide in aqueous solution. Marine Chemistry 19: 343-353

Broadbent P, Creissen GP, Kular B, Wellburn AR, Mullineaux PM (1995) Oxidative stress responses in transgenic tobacco containing altered levels of glutathione reductase activity. Plant Journal 8: 247-255

Brown CW, Yoder JA (1994) Coccolithophorid blooms in the global ocean. Journal of Geophysical Research 99: 7467-7482

Brown M, Miller K (1992) The ascorbic acid content of eleven species of microalgae used in mariculture. Journal of Applied Phycology 4: 205-215

Brugger A, Slezak D, Obernosterer I, Herndl GJ (1998) Photolysis of dimethylsulfide in the northern Adriatic Sea: Dependence on substrate concentration, irradiance and DOC concentration. Marine Chemistry 59: 321-331

Bruland KW (1989) Complexation of zinc by natural organic ligands in the central North Pacific. Limnology and Oceanography 34: 269-285

Brussaard CP (2004) Viral control of phytoplankton populations--a review. Journal of Eukaryotic Microbiology 51: 125-138

Brussaard CPD, Marie D, Thyrhaug R, Bratbak G (2001) Flow cytometric analysis of phytoplankton viability following viral infection. Aquatic Microbial Ecology 26: 157-166

Brussaard CPD, Noordeloos AAM, Riegman R (1997) Autolysis kinetics of the marine diatom *Ditylum brightwellii* (bacillariophyceae) under nitrogen and phosphorus limitation and starvation. Journal of Phycology 33: 980-987

Brussaard CPD, Riegman R, Noordeloos AAM, Cadée GC, Witte H, Kop AJ, Nieuwland G, van Duyl FC, Bak RPM (1995) Effects of grazing, sedimentation and phytoplankton cell lysis on the structure of a coastal pelagic food web. Marine Ecology Progress Series 123: 259-271

Bucciarelli E, Sunda WG (2003) Influence of CO_2, nitrate, phosphate, and silicate limitation on intracellular dimethylsulfoniopropionate in batch cultures of the coastal diatom *Thalassiosira pseudonana*. Limnology and Oceanography 48: 2256-2265

Buitenhuis E, Pangerc T, Franklin D, Le Quere C, Malin G (2008) Growth rates of six coccolithophorid strains as a function of temperature. Limnology and Oceanography: 1181-1185

Buma AGJ, Boelen P, Jeffrey WH (2003) UVR-induced DNA damage in aquatic organisms In: Helbling EW, Zagarese HE (eds) UV effects in aquatic organisms and ecosystems. Royal Society of Chemistry, Cambridge, England., pp 291-327

Bus JS, Gibson JE (1984) Paraquat: model for oxidant-initiated toxicity. Environmental Health Perspectives 55: 37-46

Butow B, Wynne D, Sukenik A, Hadas O, Tel-Or E (1998) The synergistic effect of carbon concentration and high temperature on lipid peroxidation in *Peridinium gatunense*. Journal of Plankton Research 20: 355-369

Butow BJ, Wynne D, Tel-Or E (1997) Antioxidative protection of *Peridinium gatunense* in lake Kinneret: seasonal and daily variation. Journal of Phycology 33: 780-786

Cade-Menun BJ, Paytan A (2010) Nutrient temperature and light stress alter phosphorus and carbon forms in culture-grown algae. Marine Chemistry 121: 27-36

Cadenas E (1989) Biochemistry of Oxygen Toxicity. Annual Review of Biochemistry 58: 79-110

Caldwell MM, Bornman JF, Ballare CL, Flint SD, Kulandaivelu G (2007) Terrestrial ecosystems, increased solar ultraviolet radiation and interactions with other climate change factors. Photochemical and Photobiological Sciences 6: 252-266

Cannon WB (1926) Physiological regulation of normal states: some tentative postulates concerning biological homeostatics. In: Pettit A (ed) A Charles Richet: ses amis, ses collègues, ses élèves, Paris: Éditions Médicales, pp 91

Cantoni GL, Anderson DG (1956) Enzymatic cleavage of dimethylpropiothetin by *Polysiphonia lanosa.* Journal of Biological Chemistry 222: 171-177

Carmona-Gutierrez D, Frohlich KU, Kroemer G, Madeo F (2010) Metacaspases are caspases. Doubt no more. Cell Death Differentiation 17: 377-378

Carreto JI, Carignan MO, Daleo G, Marco SGD (1990) Occurrence of mycosporine-like amino acids in the red-tide dinoflagellate *Alexandrium excavatum*: UV-photoprotective compounds? Journal of Plankton Research 12: 909-921

Caruana A (2010) DMS and DMSP production by marine dinoflagetllates. PhD Thesis. School of Emvironmental Sciences, University of East Anglia, UK

Cembella AD, Antia NJ, Harrison PJ, Rhee G-Y (1984) The utilization of inorganic and organic phosphorous compounds as nutrients by eukaryotic microalgae: A multidisciplinary perspective: Part 2. Critical Reviews in Microbiology 11: 13-81

Challenger F (1951) Biological methylation. Advanced Enzymology 12: 429-491

Challenger F, Simpson MI (1948) Studies on biological methylation. XII. A precursor of the dimethyl sulfide evolved by *Polysiphonia fastigiata*, dimethyl-2-carboxyethyl sulfonium hydroxide and its salts. Journal of Chemical Society 3: 1591-1597

Charlson RJ, Lovelock JE, Andreae MO, Warren SG (1987) Oceanic phytoplankton, atmospheric sulfur, cloud albedo and climate. Nature 326: 655-661

Charlson RJ, Rodhe H (1982) Factors controlling the acidity of natural rainwater. Nature 295: 683-685

Christaki U, Belviso S, Dolan JR, Corn M (1996) Assessment of the role of copepods and ciliates in the release to solution of particulate DMSP. Marine Ecology Progress Series 141: 119-127

Cline JD, Bates TS (1983) Dimethyl sulfide in the equatorial Pacific Ocean: A natural source of sulfur to the atmosphere. Geophysical Research Letters 10: 949-952

Cochemé HM, Murphy MP (2009) Chapter 22 The uptake and interactions of the redox cycler paraquat with mitochondria. In: William SA, Immo ES (eds) Methods in Enzymology. Academic Press, pp 395-417

Collén J, Davison IR (1997) *In vivo* measurement of active oxygen production in the brown alga *Fucus evanescens* using $2'$,$7'$-dichlorohydrofluorescein diacetate. Journal of Phycology 33: 643-648

Collén J, Pedersén M (1996) Production, scavenging and toxicity of hydrogen peroxide in the green seaweed *Ulva rigida*. European Journal of Phycology 31: 265-271

Collén J, Rio MJ, García-Reina G, Pedersén M (1995) Photosynthetic production of hydrogen peroxide by *Ulva rigida* (Chlorophyta). Planta 196: 225-230

Colmer TD, Teresa W-M. F, Läuchli A, Higashi RM (1996) Interactive effects of salinity, nitrogen and sulphur on the organic solutes in *Spartina alterniflora* leaf blades. Journal of Experimental Botany 47: 369-375

Cooper WJ, Matrai PA (1989) Distribution of dimethyl sulfide in the oceans Biogenic Sulfur in the Environment. American Chemical Society, pp 140-151

Cotner JB, Ammerman JW, Peele ER, Bentzen E (1997) Phosphorus-limited bacterioplankton growth in the Sargasso Sea. Aquatic Microbial Ecology 13: 141-149

D'Autreaux B, Toledano MB (2007) ROS as signalling molecules: mechanisms that generate specificity in ROS homeostasis. Nature Reviews in Molecular Cell Biology 8: 813-824

Dacey JWH, Blough NV (1987) Hydroxide decomposition of dimethysulfoniopropionate to form dimethylsulfide. Geophysical Research Letters 14: 1246-1249

Dacey JWH, Wakeham SG (1986) Oceanic dimethylsulfide: Production during zooplankton grazing on phytoplankton. Science 233: 1314-1316

Darroch L (2003) The production of dimethylsulphoxide (DMSO) in seawater. PhD Thesis. School of Environmental Sciences, University of East Anglia, UK

Davidson AT (1998) The impact of UVB radiation on marine plankton. Mutation Research 422: 119-129

Davidson AT, Bramich D, Marchant HJ, McMinn A (1994) Effects of UV-B irradiation on growth and survival of Antarctic marine diatoms. Marine Biology 119: 507-515

Dawes CJ, Kovach C, Friedlander M (1993) Exposure of *Gracilaria* to various environmental conditions. II: The effect on fatty acid composition. De Gruyter, Berlin, Allemagne

De Pinto MC, Paradiso A, Leonetti P, De Gara L (2006) Hydrogen peroxide, nitric oxide and cytosolic ascorbate peroxidase at the crossroad between defence and cell death. Plant Journal 48: 784-795

Dean AP, Estrada B, Nicholson JM, Sigee DC (2008) Molecular response of Anabaena flos-aquae to differing concentrations of phosphorus: A combined Fourier transform infrared and X-ray microanalytical study. Phycological Research 56: 193-201

Dehning I, Tilzer MM (1989) Survival of *Scenedesmus acuminatus* (Chlorophyceae) in Darkness. Journal of Phycology 25: 509-515

Demers S, Roy S, Gagnon R, Vignault C (1991) Rapid light-induced changes in cell fluorescence and in xanthophyll-cycle pigments of *Alexandrium excavatum* (Dinophyceae) and *Thalassiosira pseudonana* (Bacillariophyceae): a photo-protection mechanism. Marine Ecology Progress Series 76: 185-193

Demmig-Adams B, Adams WW (1996) The role of xanthophyll cycle carotenoids in the protection of photosynthesis. Trends in Plant Science 1: 21-26

Denman KL, Brasseur G, Chidthaisong A, Ciais P, Cox PM, Dickinson RE, Hauglustaine D, Heinze C, Holland E, Jacob D, Lohmann U, Ramachandran S, da Silva Dias PL, Wofsy SC, Zhang X (2007) Couplings between changes in the climate system and biogeochemistry. In: Solomon S, D. Qin, M. Manning, Z. Chen, M. Marquis, K.B. Averyt, M.Tignor and H.L. Miller (ed) Climate Change 2007: The physical science basis. Contribution of working group I to the fourth assessment report of the intergovernmental panel on climate change. Cambridge University Press., Cambridge, United Kingdom and New York, NY, USA.

Devine M, Duke SO, Fedtke C (1993) Physiology of herbicide action P T R Prentice Hall, Englewood Cliffs, N.J.

Dickson DMJ, Kirst GO (1987) Osmotic adjustment in marine eukaryotic algae: The role of inorganic ions, quaternary ammonium, tertiary sulphonium and carbohydrate solutes. I. Diatoms and a Rhodophyte. New Phytologist 106: 645-655

Diffey BL (1991) Solar ultraviolet radiation effects on biological systems. Physics in Medicine and Biology 36: 299-328

Donahue JL, Okpodu CM, Cramer CL, Grabau EA, Alscher RG (1997) Responses of antioxidants to paraquat in pea leaves (Relationships to Resistance). Plant Physiology 113: 249-257

Doney SC (2006) Oceanography - Plankton in a warmer world. Nature 444: 695-696

Downing JA, Osenberg CW, Sarnelle O (1999) Meta-analysis of marine nutrient-enrichment experiments: variation in the magnitude of nutrient limitation. Ecology 80: 1157-1167

Dufernez F, Derelle E, Noël C, Sanciu G, Mantini C, Dive D, Soyer-Gobillard M-O, Capron M, Pierce RJ, Wintjens R, Guillebault D, Viscogliosi E (2008) Molecular characterization of iron-containing superoxide dismutases in the heterotrophic dinoflagellate *Crypthecodinium cohnii*. Protist 159: 223-238

Dupont CL, Goepfert TJ, Lo P, Wei LP, Ahnerz BA (2004) Diurnal cycling of glutathione in marine phytoplankton: Field and culture studies. Limnology and Oceanography 49: 991-996

Durmaz Y (2007) Vitamin E (α-tocopherol) production by the marine microalgae *Nannochloropsis oculata* (Eustigmatophyceae) in nitrogen limitation. Aquaculture 272: 717-722

Durnford DG, Falkowski PG (1997) Chloroplast redox regulation of nuclear gene transcription during photoacclimation. Photosynthesis Research 53: 229-241

Ehling-Schulz M, Scherer S (1999) UV protection in cyanobacteria. European Journal of Phycology 34: 329-338

Elser JJ, Bracken ME, Cleland EE, Gruner DS, Harpole WS, Hillebrand H, Ngai JT, Seabloom EW, Shurin JB, Smith JE (2007) Global analysis of nitrogen and phosphorus limitation of primary producers in freshwater, marine and terrestrial ecosystems. Ecology Letters 10: 1135-1142

Emillani C (1993) Viral extinctions in deep-sea species. Nature 366: 217-218

Enoksson M, Salvesen GS (2010) Metacaspases are not caspases-always doubt. Cell Death Differentiation 17: 1221

Estep KW, Nejstgaard JC, Skjoldal HR, Rey F (1990) Predation by copepods upon natural populations of *Phaeocystis pouchetii* as a function of the physiological state of the prey. Marine Ecology Progress Series 67: 235-249

Evans C (2004) The influence of marine viruses on the production of dimethyl sulphide (DMS) and related compounds from *Emiliania huxleyi.* PhD Thesis. School of Environmental Sciences, University of East Anglia, UK

Evans C, Kadner SV, Darroch LJ, Wilson WH, Liss PS, Malin G (2007) The relative significance of viral lysis and microzooplankton grazing as pathways of dimethylsulfoniopropionate (DMSP) cleavage: An *Emiliania huxleyi* culture study. Limnology and Oceanography 52: 1036-1045

Evans C, Malin G, Mills GP, Wilson WH (2006) Viral infection of *Emiliania huxleyi* (Prymnesiophyceae) leads to elevated production of reactive oxygen species. Journal of Phycology 42: 1040-1047

Fábregas J, Maseda A, Domínguez A, Otero A (2004) The cell composition of *Nannochloropsis* sp. changes under different irradiances in semicontinuous culture. World Journal of Microbiology and Biotechnology 20: 31-35

Falkowski PG, LaRoche J (1991) Acclimation to spectral irradiance in algae. Journal of Phycology 27: 8-14

Falkowski PG, Owens TG (1980) Light-shade adaptation: Two strategies in marine phytoplankton. Plant Physiology 66: 592-595

Falkowski PG, Raven JA (1997) Aquatic Photosynthesis. Blackwell Science, Maldane, Massachusetts

Ferek RJ, Andreae MO (1984) Photochemical production of carbonyl sulfide in marine surface waters. Nature 307: 148-150

Fisher TR, Gustafson AB, Sellner K, Lacouture R, Haas LW, Wetzel RL, Magnien R, Everitt D, Michaels B, Karrh R (1999) Spatial and temporal variation of resource limitation in Chesapeake Bay. Marine Biology 133: 763-778

Flores J-A, Colmenero-Hidalgo E, Mejía-Molina AE, Baumann K-H, Henderiks J, Larsson K, Prabhu CN, Sierro FJ, Rodrigues T (2010) Distribution of large *Emiliania huxleyi* in the Central and Northeast Atlantic as a tracer of surface ocean dynamics during the last 25,000 years. Marine Micropaleontology 76: 53-66

Flynn KJ, Butler I (1986) Nitrogen sources for the growth of marine microalgae: role of dissolved free amino acids. Marine Ecology Progress Series 34: 281-304

Foyer CH, Noctor G (2003) Redox sensing and signalling associated with reactive oxygen in chloroplasts, peroxisomes and mitochondria. Physiologia Plantarum 119: 355-364

Foyer CH, Noctor G (2005) Oxidant and antioxidant signalling in plants: a re-evaluation of the concept of oxidative stress in a physiological context. Plant, Cell & Environment 28: 1056-1071

Franklin DJ, Airs RL, Fernandes M, Bell TG, Bongaerts RJ, Berges JA, Malin G (2012) Identification of senescence and death in *Emiliania huxleyi* and *Thalassiosira pseudonana*: Cell staining, chlorophyll alterations, and dimethylsulfoniopropionate (DMSP) metabolism. Limnology and Oceanography 57: 305-317

Franklin DJ, Berges JA (2004) Mortality in cultures of the dinoflagellate *Amphidinium carterae* during culture senescence and darkness. Proceedings of the Royal Society B: Biological Sciences 271: 2099-2107

Franklin DJ, Brussaard CPD, Berges JA (2006) What is the role and nature of programmed cell death in phytoplankton ecology? European Journal of Phycology 41: 1-14

Franklin LA, Forster RM (1997) The changing irradiance environment: consequences for marine macrophyte physiology, productivity and ecology. European Journal of Phycology 32: 207-232

Franqueira D, Cid A, Torres E, Orosa M, Herrero C (1999) A comparison of the relative sensitivity of structural and functional cellular responses in the alga Chlamydomonas eugametos exposed to the herbicide paraquat. Archives of Environmental Contamination and Toxicology 36: 264-269

Franqueira D, Orosa M, Torres E, Herrero C, Cid A (2000) Potential use of flow cytometry in toxicity studies with microalgae. The Science of The Total Environment 247: 119-126

Fredrickson KA, Strom SL (2008) The algal osmolyte DMSP as a microzooplankton grazing deterrent in laboratory and field studies. Journal of Plankton Research 31: 135-152

Fridovich I (1986) Biological effects of the superoxide radical. Archives of Biochemistry and Biophysics 247: 1-11

Fridovich I (1998) Oxygen toxicity: a radical explanation. Journal of Experimental Biology 201: 1203-1209

Fulda S, Gorman AM, Hori O, Samali A (2010) Cellular stress responses: cell survival and cell death. International Journal of Cell Biology 2010: 214074

Fytizas R (1980) Toxicity of paraquat to three marine organisms. Bulletin of Environmental Contamination and Toxicology 25: 283-288

Gadjev I, Stone JM, Gechev TS (2008) Programmed cell death in plants: new insights into redox regulation and the role of hydrogen peroxide. International Review of Cell and Molecular Biology 270: 87-144

Gage DA, Rhodes D, Nolte KD, Hicks WA, Leustek T, Cooper AJ, Hanson AD (1997) A new route for synthesis of dimethylsulphoniopropionate in marine algae. Nature 387: 891-894

Gao K, Guan W, Helbling EW (2007a) Effects of solar ultraviolet radiation on photosynthesis of the marine red tide alga Heterosigma akashiwo (Raphidophyceae). Journal of photochemistry and photobiology. B, Biology 86: 140-148

Gao K, Ma Z (2008) Photosynthesis and growth of Arthrospira (Spirulina) platensis (Cyanophyta) in response to solar UV radiation, with special reference to its minor variant. Environmental and Experimental Botany 63: 123-129

Gao K, Wu Y, Li G, Wu H, Villafane VE, Helbling EW (2007b) Solar UV radiation drives CO2 fixation in marine phytoplankton: a double-edged sword. Plant Physiology 144: 54-59

Garbayo I, Cuaresma M, Vílchez C, Vega JM (2008) Effect of abiotic stress on the production of lutein and β-carotene by Chlamydomonas acidophila. Process Biochemistry 43: 1158-1161

Garcia-Pichel F, Castenholz R (1993) Occurrence of UV-absorbing, mycosporine-like compounds among cyanobacterial isolates and an estimate of their screening capacity. Applied and Environmental Microbiology 59: 163-169

Garde K, Cailliau C (2000) The impact of UV-B radiation and different PAR intensities on growth, uptake of 14 C, excretion of DOC, cell volume, and pigmentation in the marine prymnesiophyte, *Emiliania huxleyi*. Journal of Experimental Marine Biology and Ecology 247: 99-112

Garvey M, Moriceau B, Passow U (2007) Applicability of the FDA assay to determine the viability of marine phytoplankton under different environmental conditions. Marine Ecology Progress Series 352: 17-26

Gauthier DA, Turpin DH (1997) Interactions between inorganic phosphate (Pi) assimilation, photosynthesis and respiration in the Pi-limited green alga *Selenastrum minutum*. Plant, Cell & Environment 20: 12-24

Geider RJ, MacIntyre HL, Kana TM (1997) Dynamic model of phytoplankton growth and acclimation: responses of the balanced growth rate and the chlorophyll a:carbon ratio to light, nutrient-limitation and temperature. Marine Ecology Progress Series 148: 187-200

Georgiou T, Yu YN, Ekunwe S, Buttner MJ, Zuurmond A, Kraal B, Kleanthous C, Snyder L (1998) Specific peptide-activated proteolytic cleavage of *Escherichia*

coli elongation factor Tu. Proceedings of the National Academy of Sciences of the United States of America 95: 2891-2895

Gerbersdorf S, Schubert H (2011) Vertical migration of phytoplankton in coastal waters with different UVR transparency. Environmental Sciences Europe 23: 36

Gerringa LJA, Rijkenberg MJA, Timmermans R, Buma AGJ (2004) The influence of solar ultraviolet radiation on the photochemical production of H2O2 in the equatorial Atlantic Ocean. Journal of Sea Research 51: 3-10

Gerschman R, Gilbert DL, Nye SW, Dwyer P, Fenn WO (2005) Oxygen poisoning and X-irradiation: A mechanism in common. Science of Aging Knowledge Environment 2005: cp1- (2005)

Gibson JAE, Garrick RC, Burton HR, McTaggart AR (1990) Dimethylsulfide and the algae *Phaeocystis pouchetii* in antarctic coastal waters. Marine Biology 104: 339-346

Glibert PM (1988) Primary productivity and pelagic nitrogen cycling. In: Blackburn TH, Sorensen J (eds) Nitrogen cycling in coastal marine environments. John Wiley & Sons Ltd, New York, pp 3-31

Goericke R, Welschmeyer NA (1992) Pigment turnover in the marine diatom *Thalassiosira weissflogii*. II. The 14CO2-labeling kinetics of carotenoids. Journal of Phycology 28: 507-517

Goes JI, Handa N, Taguchi S, Hama T, Saito H (1995) Impact of UV radiation on the production patterns and composition of dissolved free and combined amino acids in marine phytoplankton. Journal of Plankton Research 17: 1337-1362

Gorbunov MY, Kolber ZS, Lesser MP, Falkowski PG (2001) Photosynthesis and photoprotection in symbiotic corals. Limnology and Oceanography 46: 75-85

Graf H-F, Feichter J, Langmann Br (1997) Volcanic sulfur emissions: Estimates of source strength and its contribution to the global sulfate distribution. Journal of Geophysical Research 102: 10727-10738

Grasshoff K, Ehrhardt M, Kremling K, Almgren T (1976) Methods of seawater analysis. Verlag Chemie Weinheim

Green JC, Course PA, Tarran GA (1996) The life-cycle of *Emiliania huxleyi*: A brief review and a study of relative ploidy levels analysed by flow cytometry. Journal of Marine Systems 9: 33-44

Greene RC (1962) Biosynthesis of dimethyl-β-propiothetin. The Journal of Biological Chemistry 237: 2251-2254

Grime JP (1979) Plant strategies and vegetation processes., John Wiley, Chichester

Gröne T, Kirst GO (1992) The effect of nitrogen deficiency, methionine and inhibitors of methionine metabolism on the DMSP contents of *Tetraselmis subcordiformis* (Stein). Marine Biology 112: 497-503

Gruber N (2004) The dynamics of the marine nitrogen cycle and its influence on atmospheric CO2 variations. In: Oguz T, Follows M (eds) Carbon Climate Interactions. Kluwer Academic, Rotterdam, pp 97-148

Grzymski J, Orrico C, Schofield O (2001) Monochromatic ultraviolet light induced damage to photosystem II efficiency and carbon fixation in the marine diatom *Thalassiosira pseudonana* (3H). Photosynthesis Research 68: 181-192

Guan WC, Gao KS (2010) Impacts of UV radiation on photosynthesis and growth of the coccolithophore *Emiliania huxleyi* (Haptophyceae). Environmental and Experimental Botany 67: 502-508

Guilbault GG, Kramer DN, Hackley EB (1967) New substrate for fluorometric determination of oxidative enzymes. Analytical Chemistry 39: 271-271

Guillard RR, Ryther JH (1962) Studies of marine planktonic diatoms. I. *Cyclotella nana* Hustedt, and *Detonula confervacea* (Cleve) Gran. Canadian Journal of Microbiology 8: 229-239

Haas P (1935) The liberation of methyl sulphide by seaweed. Biochemistry Journal 29: 1297-1299

Häder D-P (2011) Does enhanced solar UV-B radiation affect marine primary producers in their natural habitats? Photochemistry and Photobiology 87: 263-266

Häder D-P, Sinha RP (2005) Solar ultraviolet radiation-induced DNA damage in aquatic organisms: potential environmental impact. Mutation Research 571: 221-233

Häder DP (1997) Penetration and effects of solar UV-B on phytoplankton and macroalgae. Plant Ecology 128: 5-13

Häder DP, Kumar HD, Smith RC, Worrest RC (2007) Effects of solar UV radiation on aquatic ecosystems and interactions with climate change. Photochemical and Photobiological Sciences 6: 267-285

Haldrup A, Jensen PE, Lunde C, Scheller HV (2001) Balance of power: a view of the mechanism of photosynthetic state transitions. Trends in Plant Science 6: 301-305

Halliwell B, Gutteridge JMC (1999) Free Radicals in Biology and Medicine. Oxford University Press, New York

Halmann M, Steinberg M (1999) Greenhouse Gas Carbon Dioxide Mitigation. Lewis Publ., Boca Raton, FL

Hannen EJ, Gons HJ (1997) UVC-induced lysis and detritus production of Oscillatoria limnetica in a two-stage continuous-flow system. Journal of Plankton Research 19: 723-733

Harada H, Vilacosta M, Cebrian J, Kiene R (2009) Effects of UV radiation and nitrate limitation on the production of biogenic sulfur compounds by marine phytoplankton. Aquatic Botany 90: 37-42

Harris GN, Scanlan DJ, Geider RJ (2005) Acclimation of *Emiliania huxleyi* (prymnesiophyceae) to photon flux density. Journal of Phycology 41: 851-862

Harrison PJ, Waters RE, Taylor FJR (1980) A broad spectrum artificial sea water medium for coastal and open ocean phytoplankton. Journal of Phycology 16: 28-35

He Y-Y, Häder D-P (2002a) Involvement of reactive oxygen species in the UV-B damage to the cyanobacterium *Anabaena* sp. Journal of Photochemistry and Photobiology B: Biology 66: 73-80

He Y-Y, Häder D-P (2002b) Reactive oxygen species and UV-B: effect on cyanobacteria. Photochemical and Photobiological Sciences 1: 729-736

Hefu Y, Kirst GO (1997) Effect of UV-radiation on DMSP content and DMS formation of *Phaeocystis antarctica*. Polar Biology 18: 402-409

Heraud P, Wood BR, Tobin MJ, Beardall J, McNaughton D (2005) Mapping of nutrient-induced biochemical changes in living algal cells using synchrotron infrared microspectroscopy. FEMS Microbiology Letters 249: 219-225

Hinz DJ, Nielsdóttir MC, Korb RE, Whitehouse MJ, Poulton AJ, Moore CM, Achterberg EP, Bibby TS (2012) Responses of microplankton community

structure to iron addition in the Scotia Sea. Deep Sea Research Part II: Topical Studies in Oceanography 59–60: 36-46

Hockin NL, Mock T, Mulholland F, Kopriva S, Malin G (2012) The response of diatom central carbon metabolism to nitrogen starvation is different from that of green algae and higher plants. Plant Physiology 158: 299-312

Hollibaugh JT, C. L, E. MA (2007) Microbiology in polar oceans. Oceanography 20(2): 140-145

Holligan PM, Fernandez E, Aiken J, Balch WM, Boyd P, Burkill PH, Finch M, Groom SB, Malin G, Muller K, Purdie DA, Robinson C, Trees CC, Turner SM, van der Wal P (1993a) A biogeochemical study of the coccolithophore, *Emiliania huxleyi*, in the North Atlantic. Global Biogeochemical Cycles 7: 879-900

Holligan PM, Groom SB, Harbour DS (1993b) What controls the distribution of the coccolithophore, *Emiliania huxleyi*, in the North Sea? Fisheries Oceanography 2: 175-183

Holligan PM, Turner SM, Liss PS (1987) Measurements of dimethyl sulphide in frontal regions. Continental Shelf Research 7: 213-224

Holzinger A, Lutz C (2006) Algae and UV irradiation: effects on ultrastructure and related metabolic functions. Micron 37: 190-207

Hu H, Zhou Q (2010) Regulation of inorganic carbon acquisition by nitrogen and phosphorus levels in the *Nannochloropsis* sp. World Journal of Microbiology and Biotechnology 26: 957-961

Humby PL, Durnford DG (2006) Photoacclimation: physiological and molecular responses to changes in light environments In: Huang B (ed) Plant-Environment Interactions, CRC Press

Husband JD, Kiene RP, Sherman TD (2012) Oxidation of dimethylsulfoniopropionate (DMSP) in response to oxidative stress in *Spartina alterniflora* and protection of a non-DMSP producing grass by exogenous DMSP + acrylate. Environmental and Experimental Botany 79: 44-48

Iglesias-Rodríguez MD, Brown CW, Doney SC, Kleypas J, Kolber D, Kolber Z, Hayes P, Falkowski PG (2002) Representing key phytoplankton functional groups in ocean carbon cycle models: Coccolithophorids. Global Biogeochemical Cycles 16: 1-20

Imai I, Ishida Y, Hata Y (1993) Killing of marine phytoplankton by a gliding bacterium *Cytophaga* sp., isolated from the coastal sea of Japan. Marine Biology 116: 527-532

Iverson RL, Nearhoof FL, Andreae MO (1989) Production of dimethylsulfonium propionate and dimethylsulfide by phytoplankton in estuarine and coastal waters. Limnology and Oceanography 34: 53-67

Jakob B, Heber U (1996) Photoproduction and detoxification of hydroxyl radicals in chloroplasts and leaves and relation to photoinactivation of photosystems I and II. Plant Cell Physiology 37: 629-635

Ji Y, Sherrell RM (2008) Differential effects of phosphorus limitation on cellular metals in *Chlorella* and *Microcystis*. Limnology and Oceanography 53: 1790-1804

Jiménez C, Capasso JM, Edelstein CL, Rivard CJ, Lucia S, Breusegem S, Berl T, Segovia M (2009) Different ways to die: cell death modes of the unicellular chlorophyte *Dunaliella viridis* exposed to various environmental stresses are

mediated by the caspase-like activity DEVDase. Journal of Experimental Botany 60: 815-828

Kaiser E, Herndl GJ (1997) Rapid recovery of marine bacterioplankton activity after Inhibition by UV radiation in coastal waters. Applied and Environmental Microbiology 63: 4026-4031

Kakinuma M, Coury D, Kuno Y, Itoh S, Kozawa Y, Inagaki E, Yoshiura Y, Amano H (2006) Physiological and biochemical responses to thermal and salinity stresses in a sterile mutant of *Ulva pertusa* (Ulvales, Chlorophyta). Marine Biology 149: 97-106

Kapuscinski J (1995) DAPI: a DNA-specific fluorescent probe. Biotechnic and Histochemistry 70: 220-233

Karentz D, Cleaver JE, Mitchell DL (1991) Cell survival characteristics and molecular responses of Antarctic phytoplankton to Ultraviolet-B radiation. Journal of Phycology 27: 326-341

Karl DM, Bjorkman KM, Dore JE, Fujieki L, Hebel DV, Houlihan T, Letelier RM, Tupas LM (2001) Ecological nitrogen-to-phosphorus stoichiometry at station ALOHA. Deep Sea Research Part II: Topical Studies in Oceanography 48: 1529-1566

Karsten U, Kirst G, Wiencke C (1992) Dimethylsulphoniopropionate (DMSP) accumulation in green macioalgae from polar to temperate regions: interactive effects of light versus salinity and light versus temperature. Polar Biology 12: 603-607

Kawakami SK, Gledhill M, Achterberg EP (2006) Production of phytochelatins and glutathione by marine phytoplankton in response to metal stress. Journal of Phycology 42: 975-989

Kayano K, Shiraiwa Y (2009) Physiological regulation of coccolith polysaccharide production by phosphate availability in the coccolithophorid *Emiliania huxleyi*. Plant Cell Physiology 50: 1522-1531

Keller MD (1988) Dimethyl sulfide production and marine phytoplankton: the importance of species composition and cell size. Biological Oceanography 6: 375-382

Keller MD, Bellows WK (1996) Physiological aspects of the production of dimethylsulfoniopropionate (DMSP) by marine phytoplankton. Biological and environmental chemistry of DMSP and related sulfonium compounds. Plenum Press, New York: 131–142

Keller MD, Bellows WK, Guillard RR (1989) Dimethyl sulphide production in marine phytoplankton Biogenic Sulphur in the environment, pp 167-182

Keller MD, Kiene RP, Matrai PA, Bellows WK (1999a) Production of glycine betaine and dimethylsulfoniopropionate in marine phytoplankton. I. Batch cultures. Marine Biology 135: 237-248

Keller MD, Kiene RP, Matrai PA, Bellows WK (1999b) Production of glycine betaine and dimethylsulfoniopropionate in marine phytoplankton. II. N-limited chemostat cultures. Marine Biology 135: 249-257

Kettle AJ, Andreae MO, Amouroux D, Andreae TW, Bates TS, Berresheim H, Bingemer H, Boniforti R, Curran MAJ, DiTullio GR, Helas G, Jones GB, Keller MD, Kiene RP, Leck C, Levasseur M, Malin G, Maspero M, Matrai P, McTaggart AR, Mihalopoulos N, Nguyen BC, Novo A, Putaud JP,

Rapsomanikis S, Roberts G, Schebeske G, Sharma S, SimÛ R, Staubes R, Turner S, Uher G (1999) A global database of sea surface dimethylsulfide (DMS) measurements and a procedure to predict sea surface DMS as a function of latitude, longitude, and month. Global Biogeochemical Cycles 13: 399-444

Khotimchenko SV, Yakovleva IM (2005) Lipid composition of the red alga *Tichocarpus crinitus* exposed to different levels of photon irradiance. Phytochemistry 66: 73-79

Kieber DJ, Jiao J, Kiene RP, Bates TS (1996) Impact of dimethylsulfide photochemistry on methyl sulfur cycling in the equatorial Pacific Ocean. Journal of Geophysical Research 101: 3715-3722

Kiene RP (1992) Dynamics of dimethyl sulfide and dimethylsulfoniopropionate in oceanic water samples. Marine Chemistry 37: 29-52

Kiene RP (1996) Production of methanethiol from dimethylsulfoniopropionate in marine surface waters. Marine Chemistry 54: 69-83

Kiene RP, Bates TS (1990) Biological removal of dimethyl sulphide from sea water. Nature 345: 702-705

Kiene RP, Husband JD (2003) Annual Report Summary: DMSP and its role as an antioxidant in the salt marsh macrophyte *Spartina alterniflora.*

Kiene RP, Linn LJ (2000) Distribution and turnover of dissolved DMSP and its relationship with bacterial production and dimethylsulfide in the gulf of Mexico. Limnology and Oceanography 45: 849-861

Kiene RP, Linn LJ, Gonzalez J, Moran MA, Bruton JA (1999) Dimethylsulfoniopropionate and methanethiol are important precursors of methionine and protein-sulfur in marine bacterioplankton. Applied and Environmental Microbiology 65: 4549-4558

Kiene RP, Slezak D (2006) Low dissolved DMSP concentrations in seawater revealed by small-volume gravity filtration and dialysis sampling. Limnology and Oceanography: Methods 4: 80-95

Kim D-S, Watanabe Y (1993) The effect of long wave ultraviolet radiation (UV-A) on the photosynthetic activity of natural population of freshwater phytoplankton. Ecological Research 8: 225-234

Kim D-S, Watanabe Y (1994) Inhibition of growth and photosynthesis of freshwater phytoplankton by ultraviolet A (UVA) radiation and subsequent recovery from stress. Journal of Plankton Research 16: 1645-1654

Kirk JTO (1994) Optics of UV-B radiation in natural waters. Archives of Hydrobiology 43: 1-16

Kirst GO (1990) Salinity tolerance of eukaryotic marine algae. Annual Review of Plant Physiology and Plant Molecular Biology 41: 21-53

Kirst GO, Thiel C, Wolff H, Nothnagel J, Wanzek M, Ulmke R (1991) Dimethylsulfoniopropionate (DMSP) in icealgae and its possible biological role. Marine Chemistry 35: 381-388

Klaveness D, Paasche E (1979) Physiology of coccoilithophorids. In: M. L, H. HS (eds) Biochemistry and physiology of protozoa. Academic Press, New York, pp 191-213

Kloster S (2006) DMS cycle in the marine ocean-atmosphere system - a global model study. Biogeosciences 3: 29-51

Klotz LO (2002) Oxidant-induced signaling: effects of peroxynitrite and singlet oxygen. Biological chemistry 383: 443-456

Krom MD, Herut B, Mantoura RFC (2004) Nutrient budget for the eastern Mediterranean: Implications for phosphorus limitation. Limnology and Oceanography 49: 1582-1592

Kumar A, Tyagi MB, Singh N, Tyagi R, Jha PN, Sinha RP, Häder D-P (2003) Role of white light in reversing UV-B-mediated effects in the N2-fixing cyanobacterium *Anabaena* BT2. Journal of Photochemistry and Photobiology B: Biology 71: 35-42

Lana A, Bell TG, Simó R, Vallina SM, Ballabrera-Poy J, Kettle AJ, Dachs J, Bopp L, Saltzman ES, Stefels J, Johnson JE, Liss PS (2011a) An updated climatology of surface dimethlysulfide concentrations and emission fluxes in the global ocean. Global Biogeochemical Cycles 25: 1-17

Lana A, Simó R, Vallina S, Dachs J (2011b) Re-examination of global emerging patterns of ocean DMS concentration. Biogeochemistry: 1-10

Lane N (2008) Origins of death. Nature 453: 583-585

Latifi A, Ruiz M, Zhang CC (2009) Oxidative stress in cyanobacteria. FEMS Microbiology Reviews 33: 258-278

Lebaron P, Catala P, Parthuisot N (1998) Effectiveness of SYTOX Green stain for bacterial viability assessment. Applied and Environmental Microbiology 64: 2697-2700

Leck C, Larsson U, BÂgander LE, Johansson S, Hajdu S (1990) Dimethyl sulfide in the Baltic Sea: Annual variability in relation to biological activity. Journal of Geophysical Research 95: 3353-3363

Ledyard KM, Dacey JWH (1994) Dimethylsulfide production from dimethylsulfoniopropionate by a marine bacterium. Marine Ecology Progress Series 110: 95-103

Ledyard KM, DeLong EF, Dacey JWH (1993) Characterization of a DMSP-degrading bacterial isolate from the Sargasso Sea. Archives of Microbiology 160: 312-318

Lee PA, De Mora SJ (1999) Intracellular dimethylsulfoxide (DMSO) in unicellular marine algae: speculations on its origin and possible biological role. Journal of Phycology 35: 8-18

Leonardos N, Harris GN (2006) Comparative effects of light on pigments of two strains of *Emiliania huxleyi* (haptophyta). Journal of Phycology 42: 1217-1224

Lessard EJ, Merico A, Toby T (2005) Nitrate: Phosphate ratios and *Emiliania huxleyi* blooms. Limnology and Oceanography 50: 1020-1024

Lesser MP (2006) Oxidative stress in marine environments: Biochemistry and Physiological Ecology. Annual Review of Physiology 68: 253-278

Lesser MP, Shick JM (1989) Effects of irradiance and ultraviolet radiation on photoadaptation in the zooxanthellae of *Aiptasia pallida*: primary production, photoinhibition, and enzymic defenses against oxygen toxicity. Marine Biology 102: 243-255

Liss P, Malin G, Turner SM, Holligan PM (1994) Dimethyl sulphide and *Phaeocystis*: A review. Journal of Marine Systems 5: 41-53

Liss PS, Malin G, Turner SM (1993) Production of DMS by marine phytoplankton. Dimethylsulphide: oceans, atmosphere and climate. Proc. international symposium, Belgirate, 1992: 1-14

Litchman E, Neale PJ, Banaszak AT (2002) Increased sensitivity to ultraviolet radiation in nitrogen-limited dinoflagellates: photoprotection and repair. Limnology and Oceanography 47: 86-94

Liu C-H, Shih M-C, Lee T-M (2000) Free proline levels in *ulva* (chlorophyta) in response to hypersalinity: elevated NaCl in seawater versus concentrated seawater (Note). Journal of Phycology 36: 118-119

Llabres M, Agusti S (2006) Picophytoplankton cell death induced by UV radiation: Evidence for oceanic Atlantic communities. Limnology and Oceanography 51: 21-29

Loebl M, Cockshutt AM, Campbell DA, Finkel ZV (2010) Physiological basis for high resistance to photoinhibition under nitrogen depletion in *Emiliania huxleyi*. Limnology and Oceanography 55: 2150-2160

Logan BA, Demmig-Adams B, Rosenstiel TN, Adams Iii WW (1999) Effect of nitrogen limitation on foliar antioxidants in relationship to other metabolic characteristics. Planta 209: 213-220

Lovelock J (1979) Gaia: a new look at life on earth. Oxford University Press: Oxford, UK

Lovelock JE (1972) Gaia as seen through atmosphere. Atmospheric Environment 6: 579

Lovelock JE, Margulis L (1974) Atmospheric homeostasis by and for biosphere - Gaia Hypothesis. Tellus 26: 2-10

Lynn SG, Kilham SS, Kreeger DA, Interlandi SJ (2000) Effect of nutrient availability on the biochemical and elemental stoichiometry in the freshwater diatom *Stephanodiscus minutulus* (bacillariophyceae). Journal of Phycology 36: 510-522

MacIntyre HL, Kana TM, Anning T, Geider RJ (2002) Photoacclimation of photosynthesis irradiance response curves and photosynthetic pigments in microalgae and cyanobacteria. Journal of Phycology 38: 17-38

Mackas DL (2011) Does blending of chlorophyll data bias temporal trend? Nature 472: E4-E5

Malin G, Liss PS, Turner SM (1994) Dimethyl sulphide: Production and atmospheric consequnces. In: Green JC, Leadbeater BSC (eds) The haptophyte algae. , Clarendon, pp 303-320

Malin G, Steinke M (2004) Dimethyl sulfide production: what is the contribution of the coccolithophores? In: Thierstein HR, Young J (eds) Coccolithophores: From Molecular Processes to Global Impact. Springer, pp 127-164

Malin G, Turner S, Liss P, Holligan P, Harbour D (1993) Dimethylsulphide and dimethylsulphoniopropionate in the Northeast atlantic during the summer coccolithophore bloom. Deep Sea Research Part I: Oceanographic Research Papers 40: 1487-1508

Malin G, Turner SM, Liss PS (1992) Sulfur: the plankton/climate connection. Journal of Phycology 28: 590-597

Mallick N, Mohn FH (2000) Reactive oxygen species : response of algal cells. Journal of Plant Physiology 157

Marandino CA, De Bruyn WJ, Miller SD, Saltzman ES (2008) DMS air/sea flux and gas transfer coefficients from the North Atlantic summertime coccolithophore bloom. Geophysical Research Letters 35

Marandino CA, De Bruyn WJ, Miller SD, Saltzman ES (2009) Open ocean DMS air/sea fluxes over the eastern South Pacific Ocean. Atmospheric Chemistry and Physics 9: 345-356

Marie D, Simon N, Vaulot D (2005) Phytoplankton cell counting by flow cytometry Algal culturing techniques. , Elsevier Press, pp 253–269

Martinez JM, Schroeder DC, Larsen A, Bratbak G, Wilson WH (2007) Molecular dynamics of *Emiliania huxleyi* and cooccurring viruses during two separate mesocosm studies. Applied and Environmental Microbiology 73: 554-562

Martínez LF, Mahamud MM, Lavín AG, Bueno JL (2012) Evolution of phytoplankton cultures after ultraviolet light treatment. Marine Pollution Bulletin 64: 556-562

Marwood CA, Smith REH, Furgal JA, Charlton MN, Solomon KR, Greenberg BM (2000) Photoinhibition of natural phytoplankton assemblages in Lake Erie exposed to solar ultraviolet radiation. Canadian Journal of Fisheries and Aquatic Sciences 57: 371-379

Matrai PA, Keller MD (1993) Dimethylsulfide in a large-scale coccolithophore bloom in the Gulf of Maine. Continental Shelf Research 13: 831-843

Matrai PA, Keller MD (1994) Total organic sulfur and dimethylsulfoniopropionate in marine phytoplankton: intracellular variations. Marine Biology 119: 61-68

Maxwell K, Johnson GN (2000) Chlorophyll fluorescence - A practical guide. Journal of Experimental Botany 51: 659-668

Mayer KF (1987) Acute toxicity handbook of chemicals to estuarine organisms

Mc Lachlan J (1973) Growth media-marine. In: Stein JR (ed) Handbook of phycological methods: Culture methods and growth measurements. . Cambridge University Press, Cambridge, pp 25-51

McKenzie RL, Björn LO, Bais AF, Ilyas M (2003) Changes in biologically-active ultraviolet radiation reaching the Earth's surface. Photochemical and Photobiological Sciences 2: 5 - 15

McQuatters-Gollop A, Reid PC, Edwards M, Burkill PH, Castellani C, Batten S, Gieskes W, Beare D, Bidigare RR, Head E, Johnson R, Kahru M, Koslow JA, Pena A (2011) Is there a decline in marine phytoplankton? Nature 472: E6-E7

McTaggart A, Burton H (1993) Aspects of the biogeochemistry of dimethylsultide (DMS) and dimethylsulfoniumpropionate (DMSP) at an Antarctic coastal site. In: Restelli G, Angeletti G (eds) Dimethylsulphide: oceans, atmosphere, and climate. Kluwer Academic, Dordrecht, The Netherlands, pp 43-52

Mehler AH (1951) Studies on reactions of illuminated chloroplasts: I. Mechanism of the reduction of oxygen and other hill reagents. Archives of Biochemistry and Biophysics 33: 65-77

Millero FMM (2006) Chemical oceanography. CRC Press, Taylor & Francis.

Mock T, Gradinger R (2000) Changes in photosynthetic carbon allocation in algal assemblages of Arctic sea ice with decreasing nutrient concentrations and irradiance. Marine Ecology Progress Series 202: 1-11

Mock T, Kroon BMA (2002) Photosynthetic energy conversion under extreme conditions—II: the significance of lipids under light limited growth in Antarctic sea ice diatoms. Phytochemistry 61: 53-60

Moffett JW, Zafiriou OC (1990) An investigation of Hydrogen peroxide chemistry in surface waters of vineyard sound with $H_2^{18}O_2$ and $^{18}O_2$. Limnology and Oceanography 35: 1221-1229

Moharikar S, D'Souza JS, Kulkarni AB, Rao BJ (2006) Apoptotic-like cell death pathway is induced in unicellular chlorophyte *Chlamydomonas reinhardtii* (chlorophyceae) cells following UV irradiation: detection and functional analyses. Journal of Phycology 42: 423-433

Moller IM, Jensen PE, Hansson A (2007) Oxidative modifications to cellular components in plants. Annual Review of Plant Biology 58: 459-481

Montagnes DJS, Berges JA, Harrison PJ, Taylor FJR (1994) Estimating carbon, nitrogen, protein, and chlorophyll a from volume in marine phytoplankton. Limnology and Oceanography 39: 1044-1060

Moore CM, Mills MM, Achterberg EP, Geider RJ, La Roche J, Lucas MI, McDonagh EL, Pan X, Poulton AJ, Rijkenberg MJA, Suggett DJ, Ussher SJ, Woodward EMS (2009) Large-scale distribution of Atlantic nitrogen fixation controlled by iron availability. Nature Geoscience 2: 867-871

Moore CM, Mills MM, Langlois R, Milne A, Achterberg EP, La Roche J, Geider RJ (2008) Relative influence of nitrogen and phosphorus availability on phytoplankton physiology and productivity in the oligotrophic sub-tropical North Atlantic Ocean. Limnology and Oceanography 53: 291-305

Moore CM, Suggett DJ, Hickman A, Kim YN, Tweddle JF, Sharples J, Geider RJ, Holligan P (2006) Phytoplankton photoacclimation and photoadaptation in response to environmental gradients in a shelf sea. Limnology and Oceanography 51: 936-949

Mopper K, Kieber DJ (2000) Marine photochemistry and its impact on carbon cycling. In: De Mora S, Demers S, Vernet M (eds) The effects of UV radiation in the marine environment. Cambridge University Press, Cambridge, UK, pp 101-130

Mopper K, Kieber DJ (2002) Photochemistry and the cycling of carbon, sulphur, nitrogen and phosphorus In: Hansell DA, Carlson CA (eds) Biogeochemistry of Marine Dissolved Organic Matter. Academic Press, San Diego, CA., pp 455-507

Morales CE, Bedo A, Harris RP, Tranter PRG (1991) Grazing of copepod assemblages in the north-east Atlantic: the importance of the small size fraction. Journal of Plankton Research 13: 455-472

Morel FMM, Reinfelder JR, Roberts SB, Chamberlain CP, Lee JG, Yee D (1994) Zinc and carbon co-limitation of marine phytoplankton. Nature 369: 740-742

Morris I, Glover HE, Yentsch CS (1974) Products of photosynthesis by marine phytoplankton: the effect of environmental factors on the relative rates of protein synthesis. Marine Biology 27: 1-9

Murik O, Kaplan A (2009) Paradoxically, prior acquisition of antioxidant activity enhances oxidative stress-induced cell death. Environmental Microbiology 11: 2301-2309

Murrell MC, Stanley RS, Lores EM, DiDonato GT, Smith LM, Flemer DA (2002) Evidence that phosphorus limits phytoplankton growth in a Gulf of Mexico estuary: Pensacola Bay, Florida, USA. Bulletin of Marine Science 70: 155-167

Mutlu YB, Isik O, Uslu L, Koc K, Durmaz Y (2011) The effects of nitrogen and phosphorus deficiencies and nitrite addition on the lipid content of *Chlorella vulgaris* (Chlorophyceae). African Journal of Biotechnology 10: 453-456

Nanninga HJ, Tyrrell T (1996) Importance of light for the formation of algal blooms by *Emiliania huxleyi*. Marine Ecology Progress Series 136: 195-203

Negri RM, Carreto JI, Benavides HR, Akselman R, Lutz VA (1992) An unusual bloom of *Gyrodinium* cf. *aureolum* in the Argentine sea: community structure and conditioning factors. Journal of Plankton Research 14: 261-269

Nevitt GA (2008) Sensory ecology on the high seas: the odor world of the *Procellariiform* seabirds. Journal of experimental biology 211: 1706-1713

Nevitt GA, Bonadonna F (2005) Sensitivity to dimethyl sulphide suggests a mechanism for olfactory navigation by seabirds. Biology Letters 1: 303-305

Nevitt GA, Haberman K (2003) Behavioral attraction of Leach's storm-petrels (*Oceanodroma leucorhoa*) to dimethyl sulfide. Journal of experimental biology 206: 1497-1501

Nevitt GA, Veit RR, Kareiva P (1995) Dimethyl sulfide as a foraging cue for Antarctic *Procellariiform* Seabirds. Nature 376: 680-682

Nguyen BC, Belviso S, Mihalopoulos N, Gostan J, Nival P (1988) Dimethyl sulfide production during natural phytoplanktonic blooms. Marine Chemistry 24: 133-141

Niki T, Shimizu M, Fujishiro A, Kinoshita J (2007) Effects of salinity downshock on dimethylsulfide production. Journal of Oceanography 63: 873-877

Nishiguchi MK, Somero GN (1992) Temperature- and concentration-dependence of compatibility of the organic osmolyte β-dimethylsulfoniopropionate. Cryobiology 29: 118-124

Nishiyama Y, Allakhverdiev SI, Murata N (2006) A new paradigm for the action of reactive oxygen species in the photoinhibition of photosystem II. Biochimica et Biophysica Acta 1757: 742-749

Niyogi KK (1999) Photoprotection revisited: Genetic and molecular approaches. Annual Review of Plant Physiology and Plant Molecular Biology 50: 333-359

Niyogi KK (2009) Photoprotection and high light responses In: Harris E, Stein D (eds) The Chlamydomonas sourcebook, Academic press, MA, USA

Noctor G, Foyer CH (1998) Ascorbate and glutathione: Keeping active oxygen under control. Annual Review of Plant Physiology and Plant Molecular Biology 49: 249-279

Obernosterer I, Ruardij P, Herndl GJ (2001) Spatial and diurnal dynamics of dissolved organic matter (DOM) fluorescence and H2O2 and the photochemical oxygen demand of surface water DOM across the subtropical Atlantic Ocean. Limnology and Oceanography 46: 632-643

Oguz T, Merico A (2006) Factors controlling the summer *Emiliania huxleyi* bloom in the Black Sea: A modeling study. Journal of Marine Systems 59: 173-188

Ohki K (1999) A possible role of temperate phage in the regulation of *Trichodesmium* biomass, Monaco

Okada H, Honjo S (1975) Distribution of coccolithophores in marginal seas along the western Pacific Ocean and in the Red Sea. Marine Biology 31: 271-285

Okada H, McIntyre A (1979) Seasonal distribution of modern coccolithophores in the western North Atlantic Ocean. Marine Biology 54: 319-328

Okamoto OK, Hastings JW (2003) Genome-wide analysis of redox-regulated genes in a dinoflagellate. Gene 321: 73-81

Okamoto OK, Robertson DL, Fagan TF, Hastings JW, Colepicolo P (2001) Different regulatory mechanisms modulate the expression of a dinoflagellate iron-superoxide dismutase. Journal of Biological Chemistry 276: 19989-19993

Olaizola M, Roche J, Kolber Z, Falkowski PG (1994) Non-photochemical fluorescence quenching and the diadinoxanthin cycle in a marine diatom. Photosynthesis Research 41: 357-370

Osmond CB (1994) What is photoinhibition? Some insights from comparison of shade and sun plants. In: Baker NR, Boyer JR (eds) Photoinhibition: molecular mechanisms to the field. Bios Scientific Publications, Oxford pp 1-24

Otte ML, Morris JT (1994) Dimethylsulphoniopropionate (DMSP) in *Spartina alterniflora* Loisel. Aquatic Botany 48: 239-259

Paasche E (1998) Roles of nitrogen and phosphorus in coccolith formation in *Emiliania huxleyi* (Prymnesiophyceae). European Journal of Phycology 33: 33-42

Paasche E (2001) A review of the coccolithophorid *Emiliania huxleyi* (Prymnesiophyceae), with particular reference to growth, coccolith formation, and calcification-photosynthesis interactions. Phycologia 40: 503-529

Paasche E, Brubak S (1994) Enhanced calcification in the coccolithophorid *Emiliania huxleyi* (Haptophyceae) under phosphorus limitation. Phycologia 33: 324-330

Paerl HW, Tucker J, Bland PT (1983) Carotenoid enhancement and its role in maintaining blue-green algal (*Microcystis aeruginosa*) surface blooms. Limnology and Oceanography 28: 847-857

Palenik B, Henson SE (1997) The use of amides and other organic nitrogen sources by the phytoplankton *Emiliania huxleyi*. Limnology and Oceanography 42: 1544-1551

Peperzak L, Brussaard CPD (2011) Flow cytometric applicability of fluorescent vitality probes on phytoplankton. Journal of Phycology 47: 692-702

Petasne RG, Zika RG (1997) Hydrogen peroxide lifetimes in south Florida coastal and offshore waters. Marine Chemistry 56: 215-225

Peters E (1996) Prolonged darkness and diatom mortality: II. Marine temperate species. Journal of Experimental Marine Biology and Ecology 207: 43-58

Peters E, Thomas DN (1996) Prolonged darkness and diatom mortality I: Marine antarctic species. Journal of Experimental Marine Biology and Ecology 207: 25-41

Piazena H, Perez-Rodrigues E, Häder DP, Lopez-Figueroa F (2002) Penetration of solar radiation into the water column of the central subtropical Atlantic Ocean—optical properties and possible biological consequences. Deep Sea Research Part II: Topical Studies in Oceanography 49: 3513-3528

Plane JMC (1989) Gas-phase atmospheric oxidation of biogenic sulfur compounds Biogenic Sulfur in the Environment. American Chemical Society, pp 404-423

Popels LC, MacIntyre HL, Warner ME, Zhang Y, Hutchins DA (2007) Physiological responses during dark survival and recovery in *Aureococcus anophagefferens* (pelagophyceae). Journal of Phycology 43: 32-42

Porter KG, Feig YS (1980) The use of DAPI for identifying and counting aquatic microflora. Limnology and Oceanography 25: 943-948

Putaud J-P, Nguyen BC (1996) Assessment of dimethylsulfide sea-air exchange rate. Journal of Geophysical Research 101: 4403-4411

Qiao J, Mitsuhara I, Yazaki Y, Sakano K, Gotoh Y, Miura M, Ohashi Y (2002) Enhanced resistance to salt, cold and wound stresses by overproduction of animal cell death suppressors Bcl-xL and Ced-9 in tobacco cells - their possible

contribution through improved function of organella. Plant Cell Physiology 43: 992-1005

Quinn PK, Bates TS (2011) The case against climate regulation via oceanic phytoplankton sulphur emissions. Nature 480: 51-56

Raffi I, Backman J, Fornaciari E, Pälike H, Rio D, Lourens L, Hilgen F (2006) A review of calcareous nannofossil astrobiochronology encompassing the past 25 million years. Quaternary Science Reviews 25: 3113-3137

Ragni M, Airs RL, Leonardos N, Geider RJ (2008) Photoinhibition of PSII in *Emiliania huxleyi* (Haptophyta) under high light stress: The roles of photoacclimation, photoprotection, and photorepair. Journal of Phycology 44: 670-683

Rautio M, Tartarotti B (2010) UV radiation and freshwater zooplankton: damage, protection and recovery. Freshwater Reviews 3: 105-131

Riegman R, Noordeloos AAM, Cadée GC (1992) *Phaeocystis* blooms and eutrophication of the continental coastal zones of the North Sea. Marine Biology 112: 479-484

Ross C, Santiago-Vazquez L, Paul V (2006) Toxin release in response to oxidative stress and programmed cell death in the cyanobacterium *Microcystis aeruginosa*. Aquatic Toxicology 78: 66-73

Roth BL, Poot M, Yue ST, Millard PJ (1997) Bacterial viability and antibiotic susceptibility testing with SYTOX Green nucleic acid stain. Applied and Environmental Microbiology 63: 2421-2431

Rykaczewski RR, Dunne JP (2011) A measured look at ocean chlorophyll trends. Nature 472: E5-E6

Sakshaug E, Holm-Hansen O (1977) Chemical composition of *Skeletonema costatum* (Grev.) Cleve And *Pavlova* (*monochrysis*) *Lutheri* (droop) green as a function of nitrate-, phosphate-, and iron-limited growth. Journal of Experimental Marine Biology and Ecology 29: 1-34

Scaduto RC (1995) Oxidation of DMSO and methanesulfinic acid by the hydroxyl radical. Free Radical Biology and Medicine 18: 271-277

Segovia M, Berges JA (2009) Inhibition of caspase-like activities prevents the appearance of reactive oxygen species and dark-induced apoptosis in the unicellular *Chlorophytedunaliella Tertiolecta*. Journal of Phycology 45: 1116-1126

Segovia M, Haramaty L, Berges JA, Falkowski PG (2003) Cell death in the unicellular chlorophyte *Dunaliella tertiolecta*. A hypothesis on the evolution of apoptosis in higher plants and metazoans. Plant Physiology 132: 99-105

Selye H (1956) The Stress of Life. McGraw-Hill, New York

Shaw GE (1983) Biocontrolled thermostasis involving the sulfur cycle Climatic Change 5: 297

Shenoy DM, Patil JS (2003) Temporal variations in dimethylsulphoniopropionate and dimethyl sulphide in the Zuari estuary, Goa (India). Marine Environmental Research 56: 387-402

Shifrin NS, Chisholm SW (1981) Phytoplankton lipids: Interspecific differences and effects of nitrate, silicate and light-dark cycles. Journal of Phycology 17: 374-384

Sieburth JM (1960) Acrylic acid, an "Antibiotic" principle in phaeocystis blooms in Antarctic waters. Science 132: 676-677

Sigee DC, Bahrami F, Estrada B, Webster RE, Dean AP (2007) The influence of phosphorus availability on carbon allocation and P quota in *Scenedesmus subspicatus*: A synchrotron-based FTIR analysis. Phycologia 46: 583-592

Simó R (2001) Production of atmospheric sulfur by oceanic plankton: Biogeochemical, ecological and evolutionary links. Trends in Ecology and Evolution 16: 287-294

Simó R, Grimalt JO, Albaigés J (1997) Dissolved dimethylsulphide, dimethylsulphoniopropionate and dimethylsulphoxide in western Mediterranean waters. Deep-Sea Research Part II: Topical Studies in Oceanography 44: 929-950

Simo R, Pedros-Alio C (1999) Role of vertical mixing in controlling the oceanic production of dimethyl sulphide. Nature 402: 396-399

Sinha RP, Häder D-P (2008) UV-protectants in cyanobacteria. Plant Science 174: 278-289

Sinha RP, Klisch M, Gröniger A, Häder DP (1998) Ultraviolet-absorbing/screening substances in cyanobacteria, phytoplankton and macroalgae. Journal of Photochemistry and Photobiology B: Biology 47: 83-94

Slezak D, Herndl GJ (2003) Effects of Ultraviolet and visible radiation on the cellular concentrations of dimethylsulfoniopropionate (DMSP) in *Emiliania huxleyi* (strain L). Marine Ecology Progress Series 246: 61-71

Slezak D, Puskaric S, Herndl GJ (1994) Potential role of acrylic acid in bacterioplankton communities in the sea. Marine Ecology Progress Series 105: 191-197

Smayda TJ, Mitchell-Innes B (1974) Dark survival of autotrophic, planktonic marine diatoms. Marine Biology 25: 195-202

Smetacek V (2001) A watery arms race. Nature 411

Smith RC, Prezelin BB, Baker KS, Bidigare RR, Boucher NP, Coley T, Karentz D, Macintyre S, Matlick HA, Menzies D, Ondrusek M, Wan Z, Waters KJ (1992) Ozone depletion - Ultraviolet-radiation and phytoplankton biology in antarctic waters. Science 255: 952-959

Smith SV (1984) Phosphorus versus nitrogen limitation in the marine environment. Limnology and Oceanography 29: 1149-1160

Smyth TJ (2011) Penetration of UV irradiance into the global ocean. Journal of Geophysical Research 116

Sperandio S, de Belle I, Bredesen DE (2000) An alternative, nonapoptotic form of programmed cell death. Proceedings of the National Academy of Sciences of the United States of America 97: 14376-14381

Stefels J (2000) Physiological aspects of the production and conversion of DMSP in marine algae and higher plants. Journal of Sea Research 43: 183-197

Stefels J, Steinke M, Turner S, Malin G, Belviso S (2007) Environmental constraints on the production and removal of the climatically active gas dimethylsulphide (DMS) and implications for ecosystem modelling. Biogeochemistry 83: 245-275

Stefels J, Van Leeuwe MA (1998) Effects of iron and light stress on the biochemical composition of antarctic Phaeocystis sp. (Prymnesiophyceae). I. Intracellular DMSP concentrations. Journal of Phycology 34: 486-495

Steinke M, Brading P, Kerrison P, Warner ME, Suggett DJ (2011) Concentrations of dimethylsulfoniopropionate and dimethyl Sulfide are strain-specific in symbiotic dinoflagellates (*Symbiodinium* sp., Dinophyceae). Journal of Phycology 47: 775-783

Steinke M, Malin G, Liss PS (2002) Trophic interactions in the sea: an ecological role for climate relevant volatiles? Journal of Phycology 38: 630-638

Steinke M, Malin G, Turner SM, Liss PS (2000) Determinations of dimethylsulphoniopropionate (DMSP) lyase activity using headspace analysis of dimethylsulphide (DMS). Journal of Sea Research 43: 233-244

Steinke M, Wolfe GV, Kirst GO (1998) Partial characterisation of dimethylsulfoniopropionate (DMSP) lyase isozymes in 6 strains of *Emiliania huxleyi*. Marine Ecology Progress Series 175: 215-225

Sterner RW, Elser JJ, Fee EJ, Guildford SJ, Chrzanowski TH (1997) The light: nutrient ratio in lakes: the balance of energy and materials affects ecosystem structure and process. American Naturalist 150: 663-684

Stevens B, Feingold G (2009) Untangling aerosol effects on clouds and precipitation in a buffered system. Nature 461: 607-613

Stevenson RJ, Stoermer EF (1982) Luxury consumption of phosphorus by five *Cladorphora* epiphytes in Lake Huron. Transactions of the American Microscopical Society 101: 151-161

Stoecker D, Gifford DJ, Putt M (1994) Preservation of marine planktonic ciliates: losses and cell shrinkage during fixation. Marine Ecology Progress Series 110: 293-299

Strom S, Gordon W, Holmes J, Stecher H, Shimeneck C, Lambert S, Moreno E (2003) Chemical defense in the microplankton I: Feeding and growth rates of heterotrophic protists on the DMS-producing phytoplankter *Emiliania huxleyi*. Limnology and Oceanography 48: 217-229

Strom SL, Bright KJ (2009) Inter-strain differences in nitrogen use by the coccolithophore *Emiliania huxleyi*, and consequences for predation by a planktonic ciliate. Harmful Algae 8: 811-816

Strom SL, Wolfe GV (2001) Phytoplankton chemical signals influence herbivory by protist grazers. Journal of Phycology 37: 47-48

Suggett DJ, Le Floc'H E, Harris GN, Leonardos N, Geider RJ (2007) Different strategies of photoacclimation by two strains of *Emiliania huxleyi* (Haptophyta). Journal of Phycology 43: 1209-1222

Suggett DJ, Moore CM, Hickman AE, Geider RJ (2009) Interpretation of fast repetition rate (FRR) fluorescence: signatures of phytoplankton community structure versus physiological state. Marine Ecology Progress Series 376: 1-19

Sukhanova I, Flint MV (1998) Anomalous coccolithophorid bloom over the eastern Bering Sea shelf. Oceanology 38: 502-505

Sunda W, Hardison R, Kiene R, Bucciarelli E, Harada H (2007) The effect of nitrogen limitation on cellular DMSP and DMS release in marine phytoplankton: climate feedback implications. Aquatic Sciences - Research Across Boundaries 69: 341-351

Sunda W, Kieber DJ, Kiene RP, Huntsman S (2002) An antioxidant function for DMSP and DMS in marine algae. Nature 418: 317-320

Suttle CA (2005) Viruses in the sea. Nature 437: 356-361

Suylen GMH, Stefess GC, Kuenen JG (1986) Chemolithotrophic potential of a *Hyphomicrobium* species, capable of growth on methylated sulphur compounds. Archives of Microbiology 146: 192-198

Sylvan JB, Dortch Q, Nelson DM, Brown AF, Morrison W, Ammerman JW (2006) Phosphorus limits phytoplankton growth on the Louisiana shelf during the period of hypoxia formation. Environmental Science and Technology 40: 7548-7553

Takahashi H, Kopriva S, Giordano M, Saito K, Hell R (2011) Sulfur assimilation in photosynthetic organisms: Molecular functions and regulations of transporters and assimilatory enzymes. Annual Review of Plant Biology 62: 157-184

Taylor BF, Kiene RP (1989) Microbial metabolism of dimethyl sulfide. In: Saltzman ES, Cooper WJ (eds) Biogenic Sulfur in the environment. American Chemical Society, Washington D.C., pp 202-221

Tedetti M, Sempere R (2006) Penetration of ultraviolet radiation in the marine environment. A review. Photochemisty and Photobiology 82: 389-397

Thierstein HR, Geitzenauer KR, Molfino B, Shackleton NJ (1977) Global synchroneity of late quaternary coccolith datum levels validation by oxygen isotopes. Geology 5: 400-404

Thingstad TF, Krom MD, Mantoura RFC, Flaten GAF, Groom S, Herut B, Kress N, Law CS, Pasternak A, Pitta P, Psarra S, Rassoulzadegan F, Tanaka T, Tselepides A, Wassmann P, Woodward EMS, Riser CW, Zodiatis G, Zohary T (2005) Nature of phosphorus limitation in the ultraoligotrophic eastern Mediterranean. Science 309: 1068-1071

Timmermans KR, Leeuwe MAv, Jong JTMd, McKay RML, Nolting RF, Witte HJ, Ooyen Jv, Swagerman MJW, Kloosterhuis H, Baar HJWd (1998) Iron stress in the Pacific region of the Southern Ocean: evidence from enrichment bioassays. Marine Ecology Progress Series 166: 27-41

Torres MA, Jones JDG, Dangl JL (2006) Reactive oxygen species signaling in response to pathogens. Plant Physiology 141: 373-378

Tsiatsiani L, Van Breusegem F, Gallois P, Zavialov A, Lam E, Bozhkov PV (2011) Metacaspases. Cell Death Differentiation 18: 1279-1288

Turner SM, Malin G, Bågander LE, Leck C (1990) Interlaboratory calibration and sample analysis of dimethyl sulphide in water. Marine Chemistry 29: 47-62

Turner SM, Malin G, Liss PS (1989) Dimethyl sulfide and (dimethylsulfonio)propionate in european coastal and shelf waters Biogenic Sulfur in the Environment. American Chemical Society, pp 183-200

Turner SM, Malin G, Liss PS, Harbour DS, Holligan PM (1988) The Seasonal Variation of Dimethyl Sulfide and Dimethylsulfoniopropionate Concentrations in Nearshore Waters. Limnology and Oceanography 33: 364-375

Turner SM, Nightingale PD, Spokes LJ, Liddicoat MI, Liss PS (1996) Increased dimethyl sulphide concentrations in sea water from in situ iron enrichment. Nature 383: 513-517

Turpin DH (1991) Effects of inorganic N availability on algal photosynthesis and carbon metabolism. Journal of Phycology 27: 14-20

Tyrrell T, Merico A (2004) *Emiliania huxleyi*: Bloom observations and the conditions that induce them. In: Thierstein HR, Young JR (eds) Coccolithophores: From molecular processes to global impact, pp 75-97

Tyrrell T, Taylor AH (1996) A modelling study of *Emiliania huxleyi* in the NE atlantic. Journal of Marine Systems 9: 83-112

Uren AG, O'Rourke K, Aravind L, Pisabarro MT, Seshagiri S, Koonin EV, Dixit VM (2000) Identification of paracaspases and metacaspases: Two ancient families of

caspase-like proteins, one of which plays a key role in MALT Lymphoma. Molecular Cell 6: 961-967

Vairavamurthy A, Andreae MO, Iverson RL (1985) Biosynthesis of dimethylsulfide and dimethylpropiothetin by *Hymenomonas carterae* in relation to sulfur source and salinity variations. Limnology and Oceanography 30: 59-70

Vallina SM, Simó R, Anderson TR, Gabric A, Cropp R, Pacheco JM (2008) A dynamic model of oceanic sulfur (DMOS) applied to the Sargasso Sea: Simulating the dimethylsulfide (DMS) summer paradox. Journal of Geophysical Research G: Biogeosciences 113

Van Alstyne KL, Wolfe GV, Freidenburg TL, Neill A, Hicken C (2001) Activated defense systems in marine macroalgae: evidence for an ecological role for DMSP cleavage. Marine Ecology Progress Series 213: 53-65

Van Boekel WHM, Hansen FC, Riegman R, Bak RPM (1992) Lysis-induced decline of a *Phaeocystis* spring bloom and coupling with the microbial foodweb. Marine Ecology Progress Series 81: 269-276

Van De Poll WH, Eggert A, Buma AGJ, Breeman AM (2001) Effects of UV-B-induced DNA damage and photoinhibition on growth of temperate marine red macrophytes: habitat-related differences in UV-B tolerance. Journal of Phycology 37: 30-38

Van Diggelen J, Rozema J, Dickson DMJ, Broekman R (1986) β-3-Dimethylsulphoniopropionate, proline and quaternary ammonium compounds in *Spartina anglica* in relation to sodium chloride, nitrogen and sulphur. New Phytologist 103: 573-586

Van Rijssel M, Buma AGJ (2002) UV radiation induced stress does not affect DMSP synthesis in the marine prymnesiophyte *Emiliania huxleyi*. Aquatic Microbial Ecology 28: 167-174

Van Valen L (1973) A new evolutionary law. Evolutionary Theory 1: 1-30

Vardi A, Berman-Frank I, Rozenberg T, Hadas O, Kaplan A, Levine A (1999) Programmed cell death of the dinoflagellate *Peridinium gatunense* is mediated by CO2 limitation and oxidative stress. Current Biology 9: 1061-1064

Vass I, Kirilovsky D, Perewoska I, Mate Z, Nagy F, Etienne AL (2000) UV-B radiation induced exchange of the D1 reaction centre subunits produced from the psbA2 and psbA3 genes in the cyanobacterium Synechocystis sp. PCC 6803. European Journal of Biochemistry 267: 2640-2648

Veldhuis M, Kraay G, Timmermans K (2001) Cell death in phytoplankton: correlation between changes in membrane permeability, photosynthetic activity, pigmentation and growth. European Journal of Phycology 36: 167-177

Veldhuis MJW, Cucci TL, Sieracki ME (1997) Cellular DNA content of marine phytoplankton using two new fluorochromes: taxonomic and ecological implications. Journal of Phycology 33: 527-541

Ventura M, Liboriussen L, Lauridsen T, SØndergaard M, SØndergaard M, Jeppesen E (2008) Effects of increased temperature and nutrient enrichment on the stoichiometry of primary producers and consumers in temperate shallow lakes. Freshwater Biology 53: 1434-1452

Vercammen D, Declercq W, Vandenabeele P, Van Breusegem F (2007) Are metacaspases caspases? Journal of Cell Biology 179: 375-380

Vernet M (2000) The effects of UV radiations in the marine environment. Cambridge University Press, Cambridge

Vernet M, Smith RC (1997) Effects of ultraviolet radiation on the pelagic Antarctic ecosystem. In: Häder DP (ed) Effects of ozone depletion on aquatic ecosystems. Academic Press and Landes Co., Austin, Texas, pp 247–265

Vetter Y-A, Sharp JH (1993) The influence of light intensity on dimethylsulfide production by a marine diatom. Limnology and Oceanography 38: 419-425

Vincent WF, Neale PJ, Richerson PJ (1984) Photoinhlbition: algal responses to bright light during diel stratification and mixing in a tropical Alpine lake. Journal of Phycology 20: 201-211

Vincent WF, Roy S (1993) Solar ultraviolet-B radiation and aquatic primary production: damage, protection and recovery. Environmental Reviews 1: 1-12

Vogt R, Crutzen PJ, Sander R (1996) A mechanism for halogen release from sea-salt aerosol in the remote marine boundary layer. Nature 383: 327-330

Wakeham SG, Howes BL, Dacey JWH, Schwarzenbach RP, Zeyer J (1987) Biogeochemistry of dimethylsulfide in a seasonally stratified coastal salt pond. Geochimica et Cosmochimica Acta 51: 1675-1684

Walsh JJ (1983) Death in the sea : enigmatic phytoplankton losses. . Progress in oceanography 12: 1-86

Watanabe S, Yamamoto H, Tsunogai S (1995) Dimethyl sulfide widely varying in surface water of the eastern North Pacific. Marine Chemistry 51: 253-259

Welsh DT (2000) Ecological significance of compatible solute accumulation by micro-organisms: from single cells to global climate. FEMS Microbiology Reviews 24: 263-290

Westbroek P, Brown CW, Bleijswijk Jv, Brownlee C, Brummer GJ, Conte M, Egge J, Fernández E, Jordan R, Knappertsbusch M, Stefels J, Veldhuis M, van der Wal P, Young J (1993) A model system approach to biological climate forcing. The example of *Emiliania huxleyi*. Global and Planetary Change 8: 27-46

Wilkinson F, Helman WP, Ross AB (1995) Rate constants for the decay and reactions of the lowest electronically excited singlet state of molecular oxygen in solution. An Expanded and Revised Compilation. Journal of Physical and Chemical Reference Data 24: 663-677

Wilson WH, Tarran G, Zubkov MV (2002a) Virus dynamics in a coccolithophore-dominated bloom in the North Sea. Deep Sea Research Part II: Topical Studies in Oceanography 49: 2951-2963

Wilson WH, Tarran GA, Schroeder D, Cox M, Oke J, Malin G (2002b) Isolation of viruses responsible for the demise of an *Emiliania huxleyi* bloom in the English Channel. Journal of the Marine Biological Association of the United Kingdom 82: 369-377

Wilson WH, Turner S, Mann NH (1998) Population dynamics of phytoplankton and viruses in a phosphate-limited mesocosm and their effect on DMSP and DMS production. Estuarine, Coastal and Shelf Science 46: 49-59

Winter A, Henderiks J, Beaufort L (2008) Implications of coccolithophores expanding to polar waters American Geophysical Union, Fall Meeting

Winter A, Jordan R, Roth P (1994) Biogeography of living coccolithophores in ocean waters. In: Winter A, Siesser WG (eds) Coccolithophores, Cambridge University Press, Cambridge, UK.

Wolfe GV, Steinke M (1996) Grazing-activated production of dimethyl sulfide (DMS) by two clones of *Emiliania huxleyi*. Limnology and Oceanography 41: 1151-1160

Wolfe GV, Steinke M, Kirst GO (1997) Grazing-activated chemical defence in a unicellular marine alga. Nature 387: 894-897

Wolfe GV, Strom SL, Holmes JL, Radzio T, Olson MB (2002) Dimethylsulfoniopropionate cleavage by marine phytoplankton in response to mechanical, chemical, or dark stress. Journal of Phycology 38: 948-960

Wollman F-A (2001) State transitions reveal the dynamics and flexibility of the photosynthetic apparatus. European Molecular Biology Organization Journal 20: 3623-3630

Wu J-T, Chou T-L (2003) Silicate as the limiting nutrient for phytoplankton in a subtropical eutrophic estuary of Taiwan. Estuarine, Coastal and Shelf Science 58: 155-162

Wu Z, Song L, Li R (2007) Different tolerances and responses to low temperature and darkness between waterbloom forming cyanobacterium *Microcystis* and a green alga *Scenedesmus*. Hydrobiologia 596: 47-55

Xue L, Zhang Y, Zhang T, An L, Wang X (2005) Effects of enhanced ultraviolet-B radiation on algae and cyanobacteria. Critical Reviews in Microbiology 31: 79-89

Yang M, Blomquist BW, Fairall CW, Archer SD, Huebert BJ (2011) Air-sea exchange of dimethylsulfide in the Southern Ocean: Measurements from SO GasEx compared to temperate and tropical regions. Journal of Geophysical Research 116

Yentsch CS, Reichert CA (1963) The effects of prolonged darkness on photosynthesis, respiration, and chlorophyll in the marine flagellate, *Dunaliella euchlora*. Limnology and Oceanography 8: 338-342

Yocis BH, Kieber DJ, Mopper K (2000) Photochemical production of hydrogen peroxide in Antarctic Waters. Deep Sea Research Part I: Oceanographic Research Papers 47: 1077-1099

Young JR (1987) Possible functional interpretations of coccolith morphology. Abhandlungen Geologischen Bundensanstalt 39: 305-313

Young JR (1994) Functions of coccoliths. In: Winter A, Siesser WG (eds) Coccolithophores. Cambridge University Press, Cambridge, UK, pp 63-82

Yuan J, Shiller AM (2001) The distribution of hydrogen peroxide in the southern and central Atlantic ocean. Deep Sea Research Part II: Topical Studies in Oceanography 48: 2947-2970

Yuan J, Shiller AM (2005) Distribution of hydrogen peroxide in the northwest Pacific Ocean. Geochemistry Geophysics Geosystems 6: Q09M02

Zafiriou OC (1990) Chemistry of superoxide ion-radical ($O2-$) in seawater. I. pKasw∗ (HOO) and uncatalyzed dismutation kinetics studied by pulse radiolysis. Marine Chemistry 30: 31-43

Zuppini A, Andreoli C, Baldan B (2007) Heat stress: an inducer of programmed cell death in *Chlorella saccharophila*. Plant Cell Physiology 48: 1000-1009